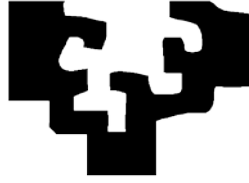eeman ta zabal zazu

University of the Basque Country
Universidad del País Vasco
Euskal Herriko Unibertsitatea

# Modelling, experimental characterization and simulation of Stirling engine-based micro-cogeneration plants for residential buildings

Iker González Pino

(Mechanical Engineer)

Dissertation presented at the University of the Basque Country (UPV/EHU) in fulfillment of the requirements for the degree of PhD of the Energy Efficiency and Sustainability in Engineering and Architecture PhD program of the Department of Thermal Engineering.

Under the supervision of:

Dr. Álvaro Campos Celador

Dr. Estíbaliz Pérez Iribarren

Bilbao, March 2019

# Resumen

La presente tesis doctoral trata la evaluación técnica, energética, ambiental y económica de la utilización de la tecnología Stirling en instalaciones de micro-cogeneración para satisfacer las necesidades térmicas y eléctricas del sector de la edificación, centrándose en las viviendas unifamiliares.

La tesis tiene su origen e interés en la actual situación energética en la que más del 40 % del consumo energético total de la Unión Europea corresponde al sector de la edificación residencial. En el caso de España, este sector de la edificación es responsable del 17 % del consumo total de energía final, correspondiendo aproximadamente un 60 % a la demanda de calefacción y agua caliente sanitaria.

Es precisamente la demanda de calefacción la que, debido entre otros aspectos a la necesidad de conseguir unas condiciones de salubridad y confort en el interior de los edificios de acuerdo a unos estándares cada vez más exigentes, se presenta como el principal motivo de que el consumo en el sector de la edificación haya mantenido una tendencia creciente durante los últimos años. Además, la creciente preocupación por reducir este consumo, así como el impacto medioambiental que éste implica, ha dado lugar a diversas modificaciones del marco legislativo, enfocadas a conseguir una mayor eficiencia energética en los edificios y, junto con ello, al empleo de tecnologías de origen renovable o de alta eficiencia.

De entre estas tecnologías, la Unión Europea y todos sus Estados Miembro reconocen el importante papel que la cogeneración ha de jugar en la transición energética y en la consecución de los objetivos definidos en el Protocolo de Kyoto. Así, de acuerdo a la Directiva 2004/8/CE inicialmente, así como a su correspondiente revisión y actualización plasmada en la Directiva 2012/27/UE, se reconoce que la cogeneración presenta un gran potencial en todas aquellas aplicaciones en las que se tiene un importante consumo de energía térmica, como es el caso del sector residencial.

La micro-cogeneración o cogeneración de pequeña escala engloba unidades de cogeneración de potencias inferiores a 50 kW eléctricos. Por sus características –

pequeñas potencias, compacidad y conexiones – la micro-cogeneración está orientada a la generación in situ en pequeñas aplicaciones residenciales y terciarias.

De entre las distintas tecnologías de micro-cogeneración, el motor Stirling ofrece unas características que lo hacen muy idóneo para su integración en aplicaciones domésticas. Además de las ventajas propias de la cogeneración, la tecnología Stirling posee la capacidad de funcionar con diversas fuentes de energía, desde la combustión hasta el aprovechamiento de calor residual o energía solar. Asimismo, tratándose de motores con pocas partes móviles y cuya fuente de calor es externa ofrecen bajos niveles de emisiones de dióxido de carbono y ruido.

Sin embargo, es un hecho que se trata de una tecnología muy poco extendida para este tipo de aplicaciones, y su comportamiento y adecuación es insuficientemente conocido. De este modo, resulta esencial abordar el estudio de esta tecnología para poder mejorar su diseño y operación, así como conocer su comportamiento una vez integrado en una instalación térmica doméstica. A tal efecto, resulta necesario desarrollar modelos de simulación que, más allá de ayudar a mejorar su diseño, permitan analizar y evaluar el comportamiento técnico, ambiental y económico de esta tecnología.

De esta forma, el desarrollo de esta tesis afronta los pasos necesarios para poder llevar a cabo un análisis completo del impacto que tendría la instalación de equipos de micro-cogeneración en base a motor Stirling en edificios de viviendas unifamiliares en España, tanto desde el punto de vista energético como medioambiental y económico.

La tesis comienza analizando las diferentes tecnologías que permiten obtener mejoras de eficiencia energética así como medioambientales para, posteriormente, analizar la tecnología Stirling y su aplicabilidad al campo de la micro-cogeneración residencial. Después, se presenta el estado actual de la micro-cogeneración Stirling: evolución y situación comercial actual de los motores Stirling, análisis técnico-económicos realizados hasta la fecha, en términos metodológicos y de resultados obtenidos, así como modelos matemáticos desarrollados y los diferentes enfoques existentes a tal efecto.

Una vez contextualizada la tesis, y en base a los objetivos definidos previamente, se plantea el desarrollo de un modelo matemático que permite representar el

comportamiento de las pequeñas unidades de motor Stirling aplicables a viviendas unifamiliares. Dentro de las posibilidades existentes, en base a la aplicabilidad del modelo, se decide utilizar un enfoque de caja gris. Con el modelo propuesto se pretende mejorar los ya existentes, supliendo las carencias de los mismos, así como fortalecer los puntos fuertes que estos poseen.

Así pues, el capítulo 2 de la tesis se centra inicialmente en definir las ecuaciones matemáticas que rigen el comportamiento general de las unidades de micro-cogeneración Stirling, atendiendo a la arquitectura de las mismas así como a los diferentes modos de funcionamiento en los que éstas pueden operar. Posteriormente, una vez definido el modelo matemático propuesto, se particulariza para la unidad de cogeneración Remeha eVita. De esta forma, se describe en detalle a continuación el modo de funcionamiento y lógica de operación de esta unidad cuyo comportamiento energético se caracteriza mediante la ejecución de una rutina de ensayos adecuadamente diseñada. A tal efecto, se diseña y ejecuta en el Laboratorio de Control de Calidad del Gobierno Vasco una instalación experimental, en la que se integra el motor Stirling seleccionado, que permite ensayar tanto individual como de forma integrada equipos de generación térmica. De este modo, se caracteriza el comportamiento en diferentes condiciones de operación, tanto en estado estacionario como en régimen transitorio, de tal forma que, a partir de los datos obtenidos y de una metodología de identificación de parámetros, permite calibrar el modelo y así particularizarlo para el caso del motor seleccionado. Se plantean tres enfoques diferentes, de menor a mayor nivel de sofisticación, para proceder con la identificación de parámetros, concluyendo que las técnicas avanzadas en base a algoritmos de optimización, si bien pueden hacer perder el sentido físico de las variables a cuantificar, permiten reducir al máximo el error cometido y así obtener la combinación que proporciona los mejores resultados posibles.

Una vez calibrado el modelo, se comprueba la validez del mismo. Para ello, se valida tanto el comportamiento estacionario como transitorio comparando las predicciones del modelo tanto con resultados reales medidos en el laboratorio como con un modelo previamente validado, confirmando que el modelo posee la capacidad de predecir tanto el consumo de combustible como los subproductos de la unidad de micro-cogeneración

fehacientemente. Este modelo matemático se programa en lenguaje Fortran y se implementa en el software de simulación energética de edificios TRNSYS.

Uno de los principales problemas que surge a la hora de implementar una unidad de micro-cogeneración en una vivienda es, por un lado, la alta variabilidad de la demanda térmica del sector residencial y, por otro, la dificultad de predecirla. Entre las distintas alternativas para hacer frente a estas particularidades, el almacenamiento térmico ofrece la posibilidad de mejorar la operatividad de estas plantas, otorgando un mayor protagonismo al equipo de micro-cogeneración y permitiendo asimismo independizar en cierta manera la producción de energía y la demanda o consumo de la misma. En este sentido, con el fin de maximizar la explotación del equipo de micro-cogeneración se analiza la integración de sistemas de almacenamiento térmico en base a calor sensible en instalaciones del tipo descrito.

Para ello, en base a simulaciones anuales a partir del modelo previamente desarrollado, se analiza el efecto de la configuración del almacenamiento térmico dentro de la instalación térmica, así como su dimensionamiento. En base a un análisis heurístico, se analizan diversas configuraciones de planta y tamaños de almacenamiento, tanto inercial como de agua caliente sanitaria, y se definen una serie de indicadores para su posterior análisis. En base a esos indicadores – energéticos, ambientales y económicos – se concluye que, por un lado, es recomendable prescindir de depósitos de acumulación de agua caliente sanitaria para pequeñas instalaciones de viviendas unifamiliares en base a micro-cogeneración y que, por otro, los depósitos de acumulación térmica están tradicionalmente sobredimensionados. Asimismo, si bien energéticamente la disposición en serie del almacenamiento térmico proporciona unos resultados energéticamente ligeramente más favorables, se comprueba que económicamente la configuración en paralelo permite amortizar la inversión asociada al depósito de acumulación en plazos inferiores.

Por otra parte, tal y como se recoge en el estado del arte presentado inicialmente, España es uno de los países de la Unión Europea en los que la utilización de la micro-cogeneración en general y de la tecnología Stirling en particular se encuentra menos extendida, y hasta la fecha no se han llevado a cabo estudios significativos que analicen

el comportamiento de esta tecnología. En este sentido, la tesis contempla una metodología de análisis, aplicada a un caso de estudio representativo, que permite profundizar en el impacto técnico-económico de una instalación de micro-cogeneración doméstica en España. Para ello, se lleva a cabo un análisis comparativo frente a una instalación de referencia compuesta por una caldera convencional y una instalación solar térmica para satisfacer los requisitos de aporte renovable mínimo a la demanda de agua caliente sanitaria.

La primera parte del estudio se centra en analizar los principales factores que afectan al diseño de la instalación solar térmica que constituirá el caso de referencia con el que la micro-cogeneración ha de competir. De esta forma, se comprueba que, tanto para la zona climática de Vitoria-Gasteiz donde la vivienda se ubica originalmente, así como para otras zonas climáticas de España, desde el punto de vista económico ha de disponerse de la superficie solar mínima que permita alcanzar la contribución exigida. Además, también se determina, dentro del rango indicado por el Código Técnico de la Edificación, el tamaño de depósito solar necesario por unidad de superficie de colector dispuesta. Una vez diseñado el caso de referencia, y establecida la configuración óptima para la instalación de micro-cogeneración, se analiza el comportamiento técnico, energético, ambiental y económico de esta última. Para ello, se plantea un análisis paramétrico que tiene en consideración, en primer lugar, la influencia climatológica. Dicha influencia se analiza en términos de zonas climáticas representativas a nivel nacional. Se comprueba que, si bien en las condiciones actuales no es económicamente justificable la disposición de un equipo de micro-cogeneración en base a motor Stirling que sustituya a la instalación típica de referencia, los resultados técnicos y energéticos reflejan que se pueden obtener importantes ahorros de energía primaria.

Para analizar la influencia de los factores que afectan a la viabilidad económica de la tecnología, se plantea en segundo lugar un análisis paramétrico que tiene en consideración, por un lado, diferentes escenarios de costes de combustible y electricidad, así como de conste inicial del equipo y tasa de retorno, y por otro lado, la influencia del marco regulatorio. Los resultados muestran que, si bien variaciones realistas en los precios energéticos no consiguen por sí mismos rentabilizar la inversión, en combinación con una reducción moderada del coste inicial del equipo, que podría

lograrse con una introducción masiva de esta tecnología que abaratase los costes, se podría recuperar la inversión a lo largo de la vida útil en zonas climáticas frías. Asimismo, en lo que a marco normativo se refiere, se comprueba que, en comparación con las normativas inglesa y alemana, cuyos incentivos se muestran altamente efectivos, en el caso de España se ha retrocedido notablemente en este sentido.

# Abstract

This PhD Thesis deals with the technical, energetic, environmental and economic evaluation of the potential utilization of Stirling engine-based micro-cogeneration installations for meeting the thermal and electric requirements of the building sector, focusing on single family dwellings.

The interest of the thesis was awoken by the current energy situation, where the construction sector is responsible for the 40 % of the total energy consumption of the European Union. In the case of Spain, this sector accounts for the 17 % of the total final energy consumption, corresponding about 60 % to heating and domestic hot water demands.

It is the heating demand which, due to health and comfort requirements established by the standards amongst other factors, represents one of the main causes for the building sector consumption to maintain an increasing tendency during the last years. Furthermore, the growing concern about reducing this consumption, together with the environmental impact it implies, have given raise to numerous modifications in the regulatory framework, directed towards getting higher energy efficiency in buildings and employing renewable or high efficiency technologies.

Amongst these latter technologies, the European Union and all its Member States recognize the important role cogeneration can play in the energy transition, as well as in the consecution of the objectives defined from the Kyoto Protocol on. This way, according to the Directive 2004/8/EC and its corresponding revision settled through the Directive 2012/27/EU, cogeneration possesses a great application potential in all those activities where high thermal energy consumption exists, as it is the case of the residential sector.

Micro-cogeneration or small-scale cogeneration encompasses cogeneration units with electric power outputs below 50 kW. Its features – small power, compactness and disposed connections – make micro-cogeneration be oriented to in-situ generation in small residential and tertiary applications.

Among the different micro-cogeneration technologies, the Stirling engine offers some features that make its utilization very suitable for domestic applications. Besides the intrinsic advantages micro-cogeneration offers, the Stirling technology can be fed with different energy sources, from combustion to residual heat recovery or solar energy. Likewise, since it has low number of moving parts and its heat source is external, the Stirling engine offer low noise and dioxide carbon emissions levels.

Nevertheless, it is a fact that it is a little spread technology within these applications, and its performance and suitability is not sufficiently known yet. Thus, it is essential to study this technology in order to improve its design and operation, as well as to know the way it behaves when integrated in a domestic thermal installation. For that purpose, it becomes necessary to develop simulation models that, besides improving the design, allow analysing and evaluating the technical, environmental and economic performance of this technology.

This way, this thesis faces the necessary steps to perform a complete analysis of the implications installing these Stirling engine-based micro-cogeneration units in Spanish single family dwellings have. The analysis is carried out both from energy and environmental and economic points of view.

The thesis starts with an analysis of the different technologies that enable obtaining energy efficiency and environmental improvements. Then, the Stirling technology and its applicability in the residential cogeneration field is assessed. Afterwards, the current state of the Stirling micro-cogeneration is presented: evolution and commercial situation of the Stirling engines, techno-economic research carried out so far, both methodologically and in terms of results achieved, as well as mathematical models developed and the different approaches existing.

Once defined the context of the thesis, based on the objectives previously defined, the development of a mathematical model that is able to reproduce the performance of small Stirling engines applicable to single family buildings is assessed. Amongst the existing alternatives, taken into consideration the field where it is to be applied, a grey-box modelling approach is used. The main objective of the model is to overcome some of the weaknesses of previous models, as well as to boost their strong points.

This way, the second chapter of the thesis focuses on defining the mathematical equations that govern the general performance of Stirling micro-cogeneration units, taking into consideration their architecture and the different modes they can operate on. Then, once defined the mathematical model proposed, it is specifically applied to the Remeha eVita micro-cogeneration unit. Thus, the different operation modes and logic of this unit is conscientiously described next, in order to design an appropriate testing routing that allows fully characterizing its performance. For that purpose, and experimental installation is developed in the Laboratory for the Quality Control in Buildings of the Basque Government, where the Stirling engine is integrated and can be tested both individually or integrated with other components of thermal plants. This way, the performance of the unit, submitted to different operation conditions, both steady and transient, is characterized. Using data obtained together with a parameter identification procedure allows calibrating the model and so adapt the model to the engine selected. Three different approaches were contemplated when identifying parameters, from lower to higher level of sophistication. It is concluded that advanced techniques based on optimization algorithms, even though they can make the variables to be quantified lose their physical sense, allow reducing to a greater extent the error committed and so obtain the combination that provides the best results.

Once calibrated the model, its validity is checked. For that, both steady and transient performances were validated, by comparing values predicted by the model with those measuring in laboratory tests. Additionally, results provided by the model were also compared to those predicted by a model already validated. Both approaches confirm that the proposed model possesses the capacity to successfully predict both the fuel consumption and the by-products of the micro-cogeneration unit. This mathematical model is programmed in Fortran language and is implemented in TRNSYS building energy simulation tool.

One of the main problems to come up when implementing a micro-cogeneration unit in buildings lies in the high variability of thermal demands in the residential sector and the difficulty to predict them. Amongst the different alternatives existing to face these features, thermal energy storage offers the possibility to improve effectiveness of these plants, awarding the micro-CHP unit with a more important role and allowing

separation of energy production and demands. In this sense, in order to maximise the exploitation of the micro-CHP device, the integration of sensible heat thermal energy storage systems within this kind of installations is approached.

For that purpose, based on annual simulations using the previously developed model, the effect of both the size and the way thermal energy is arranged within the thermal plant is analysed. By means of a heuristic analysis, different plant configurations and thermal energy storage sizes are analysed, both in terms of inertial and domestic hot water storage. Taking into account results obtained from the energy, environmental and economic indicators defined to face the analysis, it is concluded that, on the one hand, it is desirable to dispense with domestic hot water storage. On the other hand, it is also concluded that sensible thermal energy storage systems are traditionally oversized. Likewise, even though series arrangement of the thermal storage systems provides slightly better energy results, it is also verified that parallel arrangement enables a faster recovery of the purchase of the tank.

On the other hand, as summarized in the state-of-the-art initially presented, Spain is one of the countries in the European Union where micro-cogeneration in general and that based on Stirling engines in particular is less extended, and no significant research analysing its behaviour has been carried out so far. In this sense, this thesis considers an analysis methodology, applied to a representative case-study, that allows going in depth in the techno-economic impact of such a residential installation in Spain. For that purpose, a comparative analysis with a reference installation made up of a conventional boiler and a solar thermal installation that satisfies the renewable contribution requirements in relation with domestic hot water.

The first part of the study focuses on analysing the main factors related to the design of the solar thermal installation that constitutes the reference scenario the micro-cogeneration has to compete with. This way, it is verified that, whatever the climatic zone is, if the economic aspect is exclusively considered, the minimum solar surface that enables reaching the requirements established should be disposed. Besides this, within the broad range defined by the Technical Building Code, the desirable capacity of the solar tank per square meter of collector disposed is also determined. Once the reference

scenario is defined, together with the optimum configuration obtained for the micro-cogeneration installation, the technical, energetic, environmental and economic performance of the latter is assessed. To do so, a parametric analysis where the influence of climatic conditions is taken into consideration is presented. This influence is analysed by means of representative climatic zones. It is evinced that, even though under current conditions substituting the reference installation with Stirling micro-cogeneration is not economically justified, technical and energy results show that important primary energy savings can be achieved.

For analysing the influence of the main factors that affect the economic viability of this technology, a parametric analysis is then considered. This analysis takes into consideration different scenarios in terms of energy (fuel and electricity) and investment costs and, on the other hand, the influence of the regulatory framework. Results show that, even though realistic variations in energy prices do not allow reaching profitability by themselves, if combined with a moderate decrease of the initial cost of the unit – which could be achieved with a major introduction of the technology in the market –, the extra investment could be recovered during the lifetime of the plant in dwellings sited in cold climatic zones. Likewise, as far as the regulatory framework is concerned, it is confirmed that, in comparison with British and German normative, whose incentives seem highly effective, Spain has gone backwards in this sense.

# Agradecimientos / Acknowledgements

Viniendo de donde vengo, subir cuestas es algo a lo que me he ido acostumbrando a lo largo de los años. Sin embargo, hasta el más grande de los ciclistas necesita rodearse de un gran equipo para encarar el ascenso de grandes cotas. El desarrollo de esta tesis, en cierta manera, ha supuesto una de las mayores pendientes a las que he tenido que hacer frente. No habría podido culminarla de no contar con el apoyo de las personas a las que en estas próximas líneas trato de transmitir mi más sincero agradecimiento.

En primer lugar a mis directores de tesis. A Álvaro por ser un director diferente, cercano; por su bendita locura plagada de grandes ideas y sencillas soluciones. A Esti por toda la ayuda prestada durante el desarrollo de la tesis; por ejercer como directora pero también como ejecutora en muchas fases. A ambos, gracias por el día a día, por su dedicación, implicación y ayuda en todos estos años.

A José Mari por animarme y brindarme la oportunidad de asumir el reto de realizar esta tesis. Por su dedicación, apoyo y confianza, así como por aportar soluciones cuando las he necesitado. Por ejercer de director durante tanto tiempo.

A la gente del departamento por su apoyo, implicación y buena disposición. Por hacer que, con el buen ambiente que se respira, los momentos duros sean más livianos. A los que han dedicado parte de su valioso tiempo a atender mis numerosas consultas, mil gracias. Gracias también a Jon y Gonzalo por sus sabios consejos y por todos los momentos compartidos. A todos aquellos ilustres que nos inspiraron.

Al Laboratorio de Control de Calidad en la Edificación (LCCE) del Gobierno Vasco por los medios técnicos y humanos proporcionados. En especial a Dani, por sus innumerables idas y venidas a la cueva; eskerrik asko. Cómo olvidarme asimismo de los compañeros de la Universidad de la Rioja, sin cuya dedicación y saber hacer no habría sido posible que funcionase el transatlántico que teníamos entre manos.

To people of the Institute for Energy Economy and Application Technology of the Technical University of Munich. To Dr. Peter Tzscheutschler for being and extraordinary host; for all his knowledge and for those helpful conversations and queries which shed

light on some aspects of the thesis. To all the guys that made me part of those pull-ups sessions on Friday afternoons. A Manu, por hacerme sentir como en casa durante los meses que estuve de estancia. Por su amistad. Gracias.

Asimismo, agradecer también la colaboración altruista de Beitia Viteri Arkitektura S.C.P., encargados de la redacción y ejecución material del proyecto de la vivienda unifamiliar de referencia, por toda la información proporcionada para la definición y modelado de la misma.

A mis aitas, por otorgarme la oportunidad de ser quien soy, por darme todo aquello que ellos no pudieron tener. Por aguantarme, junto con mi hermano Iván, durante tantos y tantos años. A toda la familia y amigos que, de una manera u otra, han mostrado interés y han contribuido a que el trabajo llegara a buen puerto.

A María, por su paciencia y apoyo durante todo este laborioso proceso. Por todo el tiempo sacrificado.  Por ser la luz que alumbra mi camino.

A todos los grandes músicos que, sin saberlo, han amenizado tantas y tantas horas para que esta tesis vea la luz.

A todos ellos queda dedicado este trabajo.

Para Paula

*Caerse está permitido,*

*levantarse es obligatorio*

# Table of contents

## CHAPTER 1: INTRODUCTION AND OBJECTIVES OF THE THESIS

## CHAPTER 3: INTEGRATION OF THERMAL ENERGY STORAGE WITHIN STIRLING ENGINE-BASED RESIDENTIAL MICRO-CHP INSTALLATIONS

## CHAPTER 4: TECHNO-ECONOMIC FEASIBILITY OF STIRLING ENGINE-BASED RESIDENTIAL MICRO-CHP INSTALLATIONS

## APPENDICES

# Index of figures

# Index of tables

# Nomenclature

## Abbreviations

| | |
|---|---|
| AB | Auxiliary burner |
| AC | Alternating current |
| CFC | Chlorofluorocarbon |
| CFP | Carbon footprint |
| CHP | Cogeneration |
| CS | Climatic severity |
| CTE | Technical Building Code |
| CVRMSE | Normalized root mean square error |
| DHW | Domestic hot water |
| ECBCS | Energy Conservation in Buildings and Community Systems Programme |
| ECU | Electronic control unit |
| EED | Energy Efficiency Directive |
| EPBD | Energy Performance in Buildings Directive |
| EU | European Union |
| GHG | Greenhouse gas |
| GWP | Global Warming Potential |
| HHV | Higher heating value |
| ICE | Internal combustion engine |
| IEA | International Energy Agency |
| IPCC | Intergovernmental Panel on Climate Change |
| LCCE | Laboratory for the Quality Control in Buildings |
| LFPSE | Linear free piston Stirling engine |
| LHTES | Latent heat thermal energy storage |
| LHV | Lower heating value |
| NMBE | Normalized mean bias error |
| NPV | Net present value |
| ORC | Organic Rankine cycle |
| PE | Primary energy |
| PEFC | Polymer electrolyte membrane fuel cell |
| PEMFC | Polymer electrolyte membrane fuel cell |

| | |
|---|---|
| PES | Primary energy savings |
| PLC | Programmable logic controller |
| PVPC | Voluntary price for the small consumer |
| RD | Royal Decree |
| RDL | Royal Decree-Law |
| REE | Equivalent electric efficiency |
| RMSE | Root mean square error |
| SCADA | Supervisory control and data acquisition |
| SE | Stirling engine |
| SHTES | Sensible heat thermal energy storage |
| SOFC | Solid oxide fuel cell |
| TES | Thermal energy storage |
| TUR | Last resource tariff |
| UK | United Kingdom |
| $\mu$CHP | Micro-cogeneration |

# Nomenclature

| | |
|---|---|
| a | Generic index |
| A | Surface |
| Adj-$R^2$ | Adjusted coefficient of determination |
| c | Specific heat |
| C | Cost |
| $c_{dh}$ | Complement for hourly discrimination |
| $c_{eff}$ | Complement for efficiency |
| $c_{reac}$ | Complement for reactive energy |
| E | Electricity (the "·" above indicates power) |
| $E_{demand}$ | Electricity demand |
| $E_{grid}$ | Electricity exported to the grid |
| EP | Electricity price |
| $E_{purchase}$ | Electricity purchased from the grid |
| Ex | Exergy |
| F | Fuel energy (the "·" above indicates power) |
| FP | Fuel price |
| h | Specific enthalpy (the "-" above indicates enthalpy of formation) |
| H | Enthalpy (the "·" above indicates power) |

| | |
|---|---|
| i | Generic index |
| I | Income |
| $i_e$ | Specific income associated to electricity |
| Inc | Incentives |
| Inv | Investment cost |
| j | Generic index |
| k | Constant |
| LT | Lifetime |
| m | Mass (the "·" above indicates flow) |
| M | Molar mass |
| Maint | Maintenance costs |
| MC | Thermal mass |
| $m_{CO2\text{-}eq}$ | Equivalent carbon dioxide emissions |
| n | Generic index |
| $NC_e$ | Net electric coverage |
| $NO_X$ | Nitrogen oxides |
| NS | Net savings |
| P | Pressure |
| PESR | Primary energy savings ratio |
| $P_M$ | Mean pressure behind the piston |
| p-value | Probability |
| Q | Heat (the "·" above indicates power) |
| r | Rate of discount |
| $R^2$ | Coefficient of determination |
| $RC_e$ | Relative electric coverage |
| Ref $E_\eta$ | Harmonised efficiency for electricity production |
| Ref $H_\eta$ | Harmonised efficiency for heat production |
| $R_{inv}$ | Retribution to investment |
| $R_o$ | Retribution to operation |
| $Rt_e$ | Electric regulated tariff |
| $SC_e$ | Self consumed electricity |
| SG | Spark gap |
| SS | Spark spread |
| T | Temperature |
| $t_j$ | Updating rate |

| u | Uncertainty |
|---|---|
| UA | Effective heat transfer coefficient |
| v | Specific volume |
| V | Volume (the "·" above indicates flow) |
| V/A | Volume-to-surface ratio |
| VNA | Net active value |
| VR | Residual lifetime |
| y | Molar fraction |
| YT | Full-year time |

## Greek symbols

| $\partial$ | Partial derivative |
|---|---|
| $\alpha$ | Part-load ratio |
| $\Delta$ | Increment |
| $\eta$ | Energy efficiency |
| $\lambda$ | Air excess |
| $\rho$ | Density |
| $\Psi$ | Exergy efficiency |
| $\boldsymbol{\mu}$ | Specific emission factor |

## Superscripts

| ° | Relative to normal conditions |
|---|---|
| ab | Relative to the auxiliary burner |
| e | Relative to electricity |
| f | Relative to fuel |
| max | Relative to maximum values |
| ref | Relative to reference values |
| se | Relative to the Stirling engine |
| sp | Set-point |

## Subscripts

| 0 | Relative to reference conditions |
|---|---|

| | |
|---|---|
| ab | Relative to the auxiliary burner |
| ac | Relative to avoided costs |
| air | Oxidizing air |
| amb | Relative to indoor ambient conditions |
| boiler | Relative to the conventional boiler |
| C | Relative to the heat sink |
| CHP | Relative to a cogeneration unit |
| comb | Relative to the combustion |
| cond | Relative to condensing water vapor |
| cw | Relative to the cooling water |
| cw,i | Relative to the inlet cooling water |
| cw,o | Relative to the outlet cooling water |
| e | Relative to electricity |
| eng | Relative to the engine-block |
| exh | Relative to the exhaust gases |
| f | Relative to fuel |
| g | Overall |
| gross | Relative to gross output |
| H | Relative to the external heat source |
| head | Relative to the head of the engine |
| HX | Relative to the heat exchanger |
| loss | Relative to heat losses |
| m | Relative to maintenance |
| net | Relative to net output |
| nom | Relative to nominal conditions |
| plant | Relative to the thermal installation |
| r | Relative |
| ref | Relative to reference values |
| reg,i | Relative to the inlet of the regenerator |
| reg,o | Relative to the outlet of the regenerator |
| se | Relative to the Stirling engine |
| shut-down | Relative to shut-down process |
| sol | Relative to the solar installation |
| standby | Relative to standby-mode |
| surf | Relative to the surface of the engine-block |

t   Relative to heat

TES  Relative to thermal energy storage

# CHAPTER 1

## INTRODUCTION AND OBJECTIVES OF THE THESIS

# 1. Introduction to micro-CHP

Residential and commercial buildings are responsible of 40% of the total final energy consumption and 36% of the green house gas (GHG) emissions in the European Union (EU) (Eurostat, 2012). In Spain this sector represents the third largest consumption value of final energy with a 17% (IDAE, 2011b), whilst in the Basque Country this value comes to 14%, 8% of which corresponds to residential buildings and the remaining 6% to the tertiary sector. Energy consumed in households is distributed so that 39.4% corresponds to heating and 19.6% to domestic hot water (DHW) (EVE, 2013).

In this context, the EU recognizes the need for high-efficiency electricity production units for complementing the energy transition, highlighting cogeneration as a key technology for contributing to EU's energy and climate objectives with respect to delivering low-carbon heat and power to citizens and reaching the 2020 objectives (20% increase of the energy efficiency and 20% reduction of the $CO_2$ emissions).

Cogeneration or CHP (Combined Heat and Power) is the combined production of electric or mechanical and useful thermal energies from the same fuel (ASHRAE, 1996). For its application in buildings, CHP is commonly based on replacing conventional heating systems by electricity generators equipped with heat exchangers that allow recovering waste heat with space heating and DHW purposes.
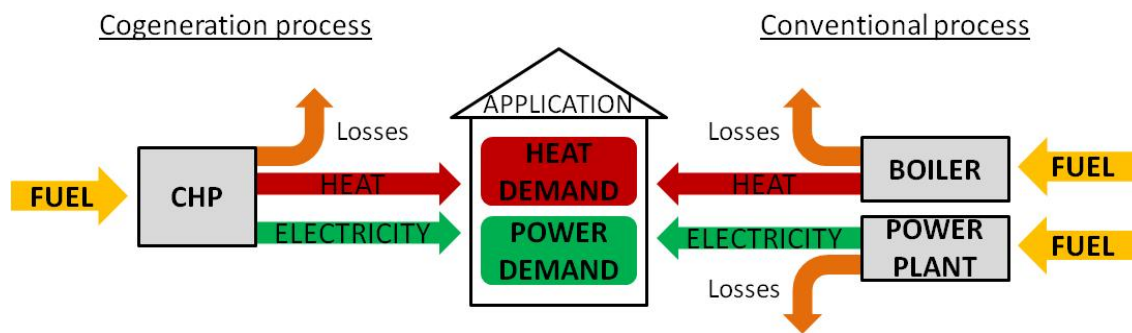
Figure 1.1 – Schematic comparison between CHP and conventional production processes.

Diagram in Figure 1.1 shows the advantages of cogeneration over traditional separate heat and power production processes. Domestic CHP produces heat and power in-situ, with efficiencies close to 100%; consequently, transmission and distribution losses to homes over long distances are significantly reduced.

Micro-CHP or µCHP, according to the cogeneration directive published in February 2004 (Official Journal of the European Union, 2004), comprises cogeneration units with electric power below 50 $kW_e$. However, in the literature several authors limit domestic µCHP to those units with powers below 15 $kW_e$, supporting this definition by the following arguments:

i.     Systems with outputs <15 $kW_e$, unlike district heating systems, are oriented to single buildings (small hotels, apartment houses, small enterprises, etc.).

ii.    Systems with outputs <15 $kW_e$ have a particular typology; they are compact in volume and provided with connections to be integrated as a domestic device.

iii.   Systems with outputs <15 $kW_e$ substantially differ from those larger with respect to electricity distribution, ownership models, restructuring of supply relationships and consumer behaviour. Generally, the implementation barriers for small scale CHP systems are more pronounced that for the larger ones.

## 1.1. Micro-CHP in residential buildings

Micro-CHP units are typically sized and run as conventional heating appliances, providing space heating and warm water in residential, suburban, or rural buildings like conventional boilers. Nevertheless, unlike boilers, micro-cogeneration units also generate electricity together with the heat, so achieving very high efficiencies and therefore providing fuel savings and reductions in greenhouse gas emissions and electricity costs.
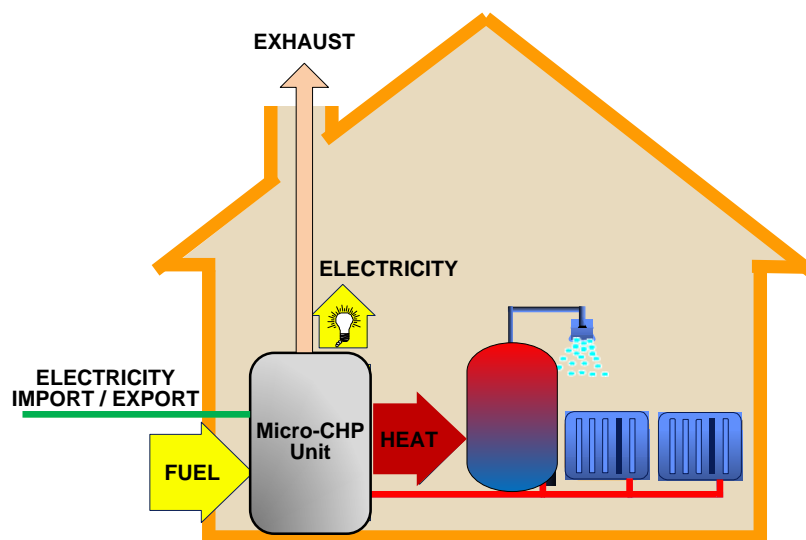


Figure 1.2 –Schematic energy flows in domestic micro-CHP (adapted from SAVE (2002)).

Most units operate in grid-parallel mode, i.e., the building continues receiving some of its electrical needs from the electrical network and may also export some electricity to the grid (Figure 1.2).

Table 1.1 – Evaluation of existing problems and potential solutions for residential cogeneration (Diarce, 2017).

| Existing problems | Potential solutions | | | | |
|---|---|---|---|---|---|
| | Part load operation | Advanced control systems | Centralize thermal production | Micro-CHP | TES |
| Variable thermal demand | √ | | | | √ |
| Unpredictable thermal demand | √ | √ | | | √ |
| Low specific power | | | √ | √ | √ |

Micro-CHP units are normally installed together with thermal energy storage (TES) systems, so that the mismatch between production and consumption sides can be decoupled by storing energy when there is overproduction and afterwards delivering it back, and the system can operate for longer periods and at full load, so increasing its lifetime and efficiency.

Even though there are commercially available products running on light oil gas or renewable sources such as biogas and biodiesel, inter alia, these are few in number, and most of the micro-CHP units work burning natural gas.

A number of different conversion technologies have been developed for the application in micro-CHP systems, as defined below.

**Internal combustion engines** (ICE) are conventional reciprocating engines coupled with a generator and heat exchangers to recover the heat of the exhaust gas and the cooling cycle. It is a quite efficient technology for producing electricity, with large power ranges and various fuels. The main drawbacks are their relatively noisy operation, and the high maintenance their several moving parts require, which turns into a large contribution to the carbon footprint (CFP) (Mikalsen, 2011).

**Stirling engines** (SE) are reciprocating thermal engines where heat is generated externally in separate chambers. Like ICEs, they are also equipped with a generator and heat exchangers. SE are characterised by rather low emissions and lower noise levels. External combustion also requires less maintenance which favourably influences the CFP of the technology. These devices are usually quiet because the combustion is not explosive and, it can use almost any combustible fuel and any source of heat, including biomass. This type of CHP has rather low electrical efficiency; nevertheless the total efficiency is not significantly lower than that of other cogeneration technologies. The electricity-to-heat ratio of Stirling engines makes of them a suitable technology for applications in residential buildings (Harrison and E.ON, 2011).

**Micro gas turbines** are small gas turbines, run with gas or liquid fuels, belonging to the group of turbo machines up to an electric power output of 300 kW. In order to raise the electrical output, micro turbines are equipped with a heat recuperator. They are also

equipped with a regular heat exchanger in order to use the waste heat from the exhaust gases. Such a plant generally consists of a generator, a compressor, a combustion chamber, and a turbine connected to each by a shaft. The high exhaust gas outlet temperature (450-500 °C) enables considerable heat generation. Their main advantages are low noise levels, compactness and lower emissions level (especially $NO_x$) compared to reciprocating engines (Soares, 2007). In contrast, they have low electrical efficiency, especially when working at part-load, and high investment and maintenance costs. This latter aspect makes them rather inapplicable for residential purposes (Kuhn et al., 2008).

The **Organic Rankine Cycle** (ORC) is similar to the conventional steam turbine cycle, except for the fluid that drives the turbine, which is a high molecular mass organic fluid. The selected working fluid allows exploiting efficiently low temperature heat sources to produce electricity in a wide range of power outputs (from few kW up to 3 MW of electric power per unit). Several ORC-based micro-CHP systems suitable for residential applications (up to 10 $kW_e$) driven by solar thermal, biomass-fired boilers and waste heat resource have been researched in the last years, but the lack of commercially available expanders applicable to this technology has hindered its development (Qiu et al., 2011).

**Fuel cells** are electromechanical energy converters similar to primary batteries. Fuel cell micro-CHP systems are either based on the low temperature polymer electrolyte membrane fuel cells (PEFC or PEMFC) which operate at about 80 °C, or on high temperature solid oxide fuel cells (SOFC) working at around 800-1000 °C (Pehnt, 2006). This technology has brought a lot of research attention, but there are still very few commercial solutions, which still have to prove their long-time reliability.

## 1.2. Normative background

Buildings are currently responsible for 40% of the total final energy consumption and 36% of the greenhouse gas (GHG) emissions in the European Union (EU) (Eurostat, 2012). Consequently, the European Commission highlights that substantial energy savings and emissions reductions are needed in the residential and commercial sectors

if the EU is to fulfill its 2020 and longer-term climate and energy objectives. Within this background, electricity demand is expected to significantly increase, doubling its share in final energy demand by 2050 (EU Commission, 2011), which, as stated by COGEN Europe (2013), will raise the profile of security of supply issues related to electricity.

Against this backdrop, the integration of multiple renewable electricity sources is essential, since large-scale intermittent renewable are not conceived to react to peak demand. This fact could lead to mismatch between supply and demand, and the inevitable volatility in pricing as it is currently the case of Denmark due to the great wind power capacity (Lund et al., 2013).

In this context, the EU recognizes the need for high-efficiency electricity production units for complementing the energy transition, highlighting micro-CHP as a key technology for reaching the 2020 objectives. This move is consequently endorsed by two Directives which have been subsequently transposed to the legal framework of each Member State: Directive 2010/31/EU on Energy Performance in Buildings (EPBD) (Official Journal of the European Union, 2010) and Directive 2012/27/EU on Energy Efficiency (EED) (Official Journal of the European Union, 2012).

The EPBD 2010/31/EU, which replaced the preceding EPBD 2002/91/EC (Official Journal of the European Communities, 2002), recasting the objectives of the former in order to get adapted to the new scenario and so strengthening the energy performance requirements to meet the established objectives, aims to promote the energy efficiency of buildings in the EU, taking into consideration outdoor climatic conditions and local conditions, as well as indoor climatic requirements and cost-effectiveness. Meanwhile, the EED 2012/27/EU replaced Directive 2004/8/CE on the promotion of cogeneration based on useful heat demand (Official Journal of the European Union, 2004), as the European Commission recognized that this Directive failed to successfully promote CHP in the last years, and there was a gap emerging between its energy savings target and progress on energy savings in the EU Member States. The EED establishes a common framework of measures for the promotion of energy efficiency within the EU in order to ensure the achievement of the 2020 headline target on energy efficiency.

Since micro-CHP generates both heat and electricity precisely when and where they are required, its contribution to the EU's energy and climate objectives with respect to delivering low-carbon heat and power to residential and commercial buildings is regarded as fundamental. As a dispatchable technology, micro-CHP can help balancing the electricity grid flexibility and thus ease the integration of a higher share of variable renewable energies into the energy mix. In consequence, a significant development of micro-CHP would reduce emissions attributed to the residential and commercial sectors, while increasing the energy performance of existing buildings as required in the EPBD, and contributing to reaching EU's energy savings target as mandated in the EED.

The EED has significantly improved the European legislative landscape for CHP, with positive implications for micro-CHP technologies. This European Directive gives Member States the opportunity to assess current legislation and develop an appropriate policy structure that is supportive of micro-CHP technologies. Stimulating the market with the tools established in the EED will help to realize the significant potential for energy savings and $CO_2$ emission reductions that micro-CHP holds. In the case of Spain, this Directive was partially transposed by Royal Decree 56/2016 (Ministerio de Industria, Energía y Turismo, 2016), where energy audits and aspects related to energy service companies, as well as the promotion of efficiency of the energy supply, are assessed.

As micro-CHP is recognized to be a tool with potential to deliver significant primary energy savings until 2020 and beyond, Member States must develop every five years an analysis of the potential for high-efficiency CHP, as well as a climatic conditions, economic viability and technical feasibility-based cost-to-benefit analysis, in order to promote high efficiency micro-CHP and adopt appropriate measures to let infrastructure for micro-CHP for heating purposes getting developed. In the case of Spain, the former "Informe de potencial de cogeneración de alta eficiencia en España 2010-2015-2020" report was updated and published by the IDAE (Institute for Energy Diversification and Saving) under the title "Evaluación completa del potencial de uso de la cogeneración de alta eficiencia y de los sistemas urbanos de calefacción y refrigeración eficientes".

## 1.3.  Situation of micro-CHP in Spain

As expounded in the so-called "Boletín de Estadísticas Energéticas de la Cogeneración para el año 2015" (IDAE, 2017), the total power of small-scale cogeneration ($\leq$ 1 MW) installed in Spain was 156.9 MW, 95.3% of which is based on ICEs and 76.5% employs natural gas as fuel.

Amongst these, 35.8 MW corresponded to the residential-commercial sector (distributed in 90 independent units), which is only 4 MW more than the capacity installed by 2013 consisting of 31.9 MW (57 independent units). This step-back might be understood as a result of legislative, economic, administrative and technical barriers that obstructed the potential development of cogeneration since 2012.
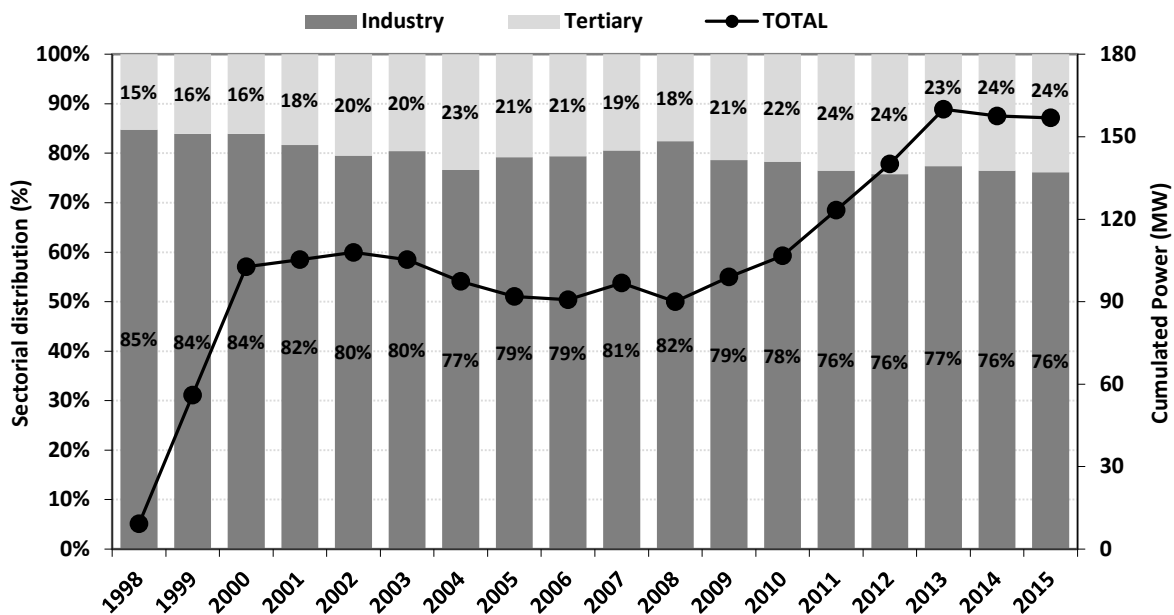


Figure 1.3 – Evolution of small-scale CHP in Spain (IDAE, 2017).

The major part of the potential in small-scale CHP applications consists of domestic and tertiary activities, with an expected potential power of 7,682 MW by year 2015 (IDAE, 2005). This makes the small-scale CHP in general, and micro-CHP in particular, to have a very low breakthrough rate, below 0.48% of its potential.

Despite the enormous potential that currently exists, the development of small cogeneration in the residential sector is absolutely disenchanting. The large gap between expectations and reality makes it important to analyze and identify the main barriers which are responsible for these discrepancies.

In this sense, the transience and complexity of the economic and legal frameworks, amongst other factors, constitute an important barrier for small-scale cogeneration systems, which is reinforced by the lack of technical assessments of the potential of low-power domestic CHP. Example of this fact is that, as reported by many cogeneration associations, the aforementioned "Evaluación completa del potencial de uso de la cogeneración de alta eficiencia y de los sistemas urbanos de calefacción y refrigeración eficientes", apart from being published with huge delay, no demand and energy savings prediction during the following 10 years was included. In addition, there was lack of actuations in some areas that enable achieving the detected potential and it did not contain any estimation of the public support, with its corresponding budget, neither the local and regional actuation plans.

# 2. Stirling cycle engine

Amongst the micro-CHP technologies exposed in the previous section, it is the Stirling engine the one that, taking into account its particular features and current degree of development, shows the highest potential for improving energy efficiency in residential and commercial buildings. Thus, it is this technology, deeply described below, the one that is assessed along this thesis.

## 2.1. Evolution of the Stirling engine development

The Stirling engine was patented in 1816 by reverend Robert Stirling (Figure 1.4), in Scotland (Stirling Robert, 1816). It was the first regenerative cycle heat engine.

As mentioned by Kongtragool and Wongwises (2003) and Thombare and Verma (2008), despite its unattractive thermal efficiency and power-to-weight ratio, and because of its simplicity and safety to operate, as well as its silent, clean and efficient operation on any

combustible fuel compared to steam engines, Stirling engine had substantial commercial success, and engines based upon his invention were built in many forms and sizes until the early 1900s, when the internal combustion engines and the electrical machine entered the scene. However, due to the high potential the Stirling engine could achieve, its development was picked up again some years later.
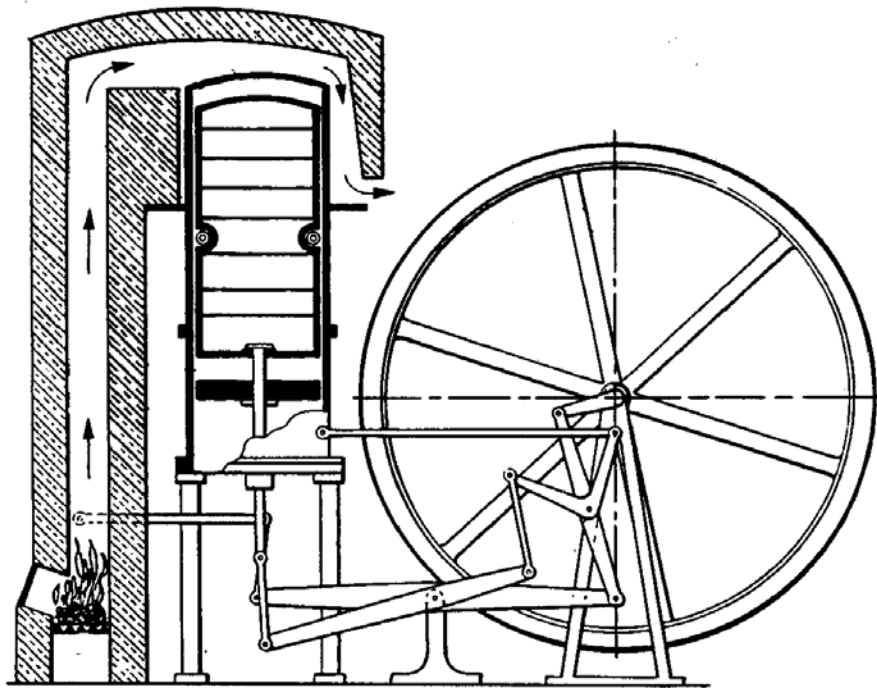


Figure 1.4 – The original patent of the Stirling engine of Rev. Robert Stirling.

Early Stirling engines were coal-burning, low-pressure air engines built to compete with saturated steam engines for providing auxiliary power for manufacturing and mining. These engines were small and the power produced from the engine was low, from 100 W up to 4 kW.

In 1853, John Ericsson built a large marine Stirling engine having four 4.2 m-diameter pistons with a stroke of 1.5 m producing a brake power of 220 kW at 9 rpm (Walker G., 1980).

The second era of the Stirling engine began around 1937, when the Stirling engine was brought to a high state of technological development by the Philips Research Laboratory in Eindhoven, Netherlands, and has progressed continuously since then. Initial work was

focused on the development of small thermal-power electric generators for high-power-consuming vacuum tube electronic devices used in remote areas (Senft JR., 1993).

In the 1940 to 1980 period, research and development works were conducted towards creation of Stirling engines covering a broad range of purposes, such as small generator units, automotive, marine and space applications (Walker G., 1980; West CD., 1988).

Meanwhile, even though the possibility of implementing the Stirling cycle with cooling purposes was known by 1873, it was not until the 1950's when the Stirling refrigerators were commercialized. However, by that time Rankine cycle-based refrigerators utilizing CFCs were firmly entrenched in the most refrigeration applications. Consequently, Stirling refrigerators were only commercialized in very low temperature ranges hardy achievable with the Rankine cycle, such as cooling military infrared detectors or liquefying industrial gases (Bowman, 1993).

New materials were one of the keys to Stirling engine success. The Philips research team used new materials, such as stainless steel. Another key to success was a better knowledge of thermal and fluid physics than in the first era. Thus, the specific power of the small '102 C' engine of 1952 was 30 times that of the old Stirling engines (West CD., 1988).

The progress in further development made by Philips and many other industrial laboratories, together with the need for more energy resources as a result of the fuel crises of 1980, as well as subsequent restrictions on the manufacture and use of CFC and other refrigerants which reopened opportunities for Stirling refrigeration in warmer food preservation and air conditioning applications, has sustained the second era of Stirling engine development until today (Senft JR., 1993).

Nowadays, interest in Stirling engines has been renewed due to the necessity of reducing the impact of fossil fuels and so contribute to mitigate the global warming, mainly focused on electricity and heat generation applications through the usage of solar or biomass sources, as well as conventional fuels. Besides their ability to utilize environmentally benign heat sources, modern free-piston Stirling engines also offer high efficiency, high reliability, low maintenance, long life, and quiet operation. However,

there is still a long way to go, since its full potential have not been reached due to design challenges related to seals, materials, heat transfer, size and weight.

## 2.2. Stirling cycle

The Stirling is a reciprocating externally heated engine, where heat is continuously transferred to the working gas, at a constant temperature, and is then converted to work by expanding the working gas inside the cylinder. In theory, the Stirling cycle engine can be the most efficient device for converting heat into work, as, in fact, the efficiency of the Stirling cycle can be equal to that of the Carnot cycle, the most efficient thermodynamic cycle.

External combustion engines separate the combustion process (which is the energy input to the engine) from the working fluid, which undergoes pressure fluctuations and hence does useful work. Thus, they allow providing continuous heat input to the working gas, with a more controllable combustion, potentially resulting in low pollutant emissions, high combustion efficiency, clean and quiet. It can operate without valves or an ignition system, thus permitting long service intervals and low running costs.

In a Stirling cycle engine a confined volume of gas is repeatedly expanded in the so-called hot end at a constant temperature, while absorbing heat continuously from the environment, and recompressed at another constant temperature in the cold end, when heat is rejected. The difference between the energy absorbed and that rejected appears as the useful energy obtained.

Since heat is supplied externally to the Stirling engine, it can be designed based upon a wide variety of heat sources: heat from combustion of any gaseous, liquid or solid fuels, solar irradiation, waste heat… Such flexibility, however, is not needed generally for an individual unit; therefore, a Stirling system will normally be designed for only one or two types of heat sources.

To complete the thermodynamic cycle, the Stirling engine must be externally cooled to relieve the pressure on the piston and thus allow it to return it its original position. This can be accomplished in a variety of ways: forced or free convection cooling; water,

ethylene glycol, or a mixture of both, circulated through a cooling jacket surrounding the cold end of the engine...

In addition, the Stirling engine is "reversible"; that is, mechanical power input can be used to provide cooling.

## 2.2.1. Mechanical configurations

Over the years, innumerable Stirling engine designs, embodying the basic thermodynamic concept, have been developed. All these designs can be classified according to their mechanical configurations, which determine the way the necessary timing of the expansion, cooling, compression and heating processes is achieved. This fact leads to kinematic and free-piston arrangements (EPRI, 2002):

Kinematic engines have a crankshaft and a mechanical linkage to the power piston. Electricity is generated with a rotating synchronous, permanent magnet, or induction generator. The amplitude of the power-piston motion is constrained by mechanical linkages. The amplitude and phasing of the displacer (a component unique to Stirling engines) may also be constrained by mechanical linkages. Since the performance of Stirling cycle machines is proportional to the mean pressure of the working gas, leakage of high pressure working gas out of the machines through seals where the shaft penetrates the pressure vessel progressively degrades performance. Kinematic machines also require frequent maintenance of heat exchangers fouled by oil lubricating the mechanism. The piston and cylinder in a kinematic machine also suffer wear due to the side-loads imposed by the mechanical linkage. Kinematic machines are generally mechanically complex, but relatively simple to analyze.

By contrast, free-piston engines, deeply described afterwards, typically generate electric power with a linear alternator formed by the oscillatory travel of the power piston in a magnetic field. The displacer and power piston typically move as tuned spring-mass-damper systems in response to pressure differences. The frequency and phase of these oscillations is controlled through precise understanding by the physics of the inertial, spring, and damping forces acting on these parts. Free piston machines are mechanically simple but dynamically and thermodynamically complex. For power generation

applications, electricity is transferred from a linear alternator connected directly to the power piston; for cooling applications, the power piston is driven by an integral linear motor. This is done without dynamic seals that may leak or fail. The absence of the kinematic mechanism also eliminates the side-loads on the piston and displacer so that wear can be completely eliminated by gas bearings that levitate the piston and displacer off of the cylinder surface. As a result, free-piston Stirling cycle machines offer the potential for long life and high reliability without maintenance.

Stirling engines can also have alpha, beta, or gamma arrangements:

• Alpha engines (see Figure 1.5) have two or more separate pistons mechanically linked to oscillate with constant phase lag. The working gas passes through a cooler, a regenerator, and a heater as it moves back and forth between the cylinders. Each piston requires its own seals to contain the working gas. All alpha engines are kinematic engines. Although the Alpha configuration is conceptually the simplest one, it suffers from the disadvantage that both pistons need to have seals to contain the working gas.
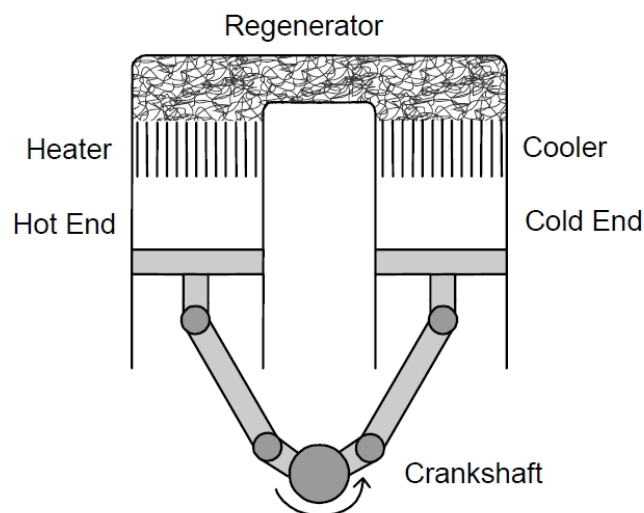


Figure 1.5 – Alpha configuration (EPRI, 2002).

• Beta engines (see Figure 1.6) have a displacer-piston arrangement in which both the displacer and the power piston are accommodated in the same cylinder, in line with each other. The displacer shuttles the working gas back and forth between the hot and cold ends of the engine. The hot end is the expansion space, and the cold end is the

compression space. As the working gas moves back and forth, it passes through a cooler, regenerator, and heater. Beta engines can be either kinematic or free-piston engines.
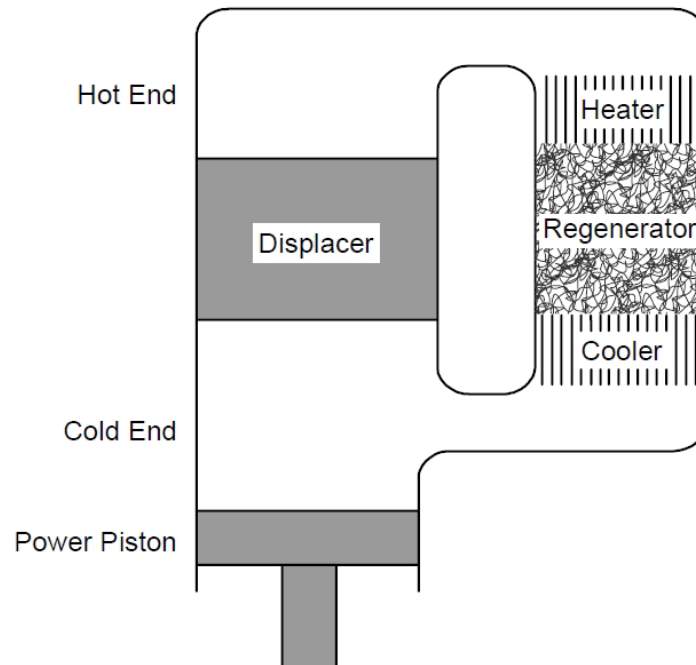


Figure 1.6 – Beta configuration (EPRI, 2002).
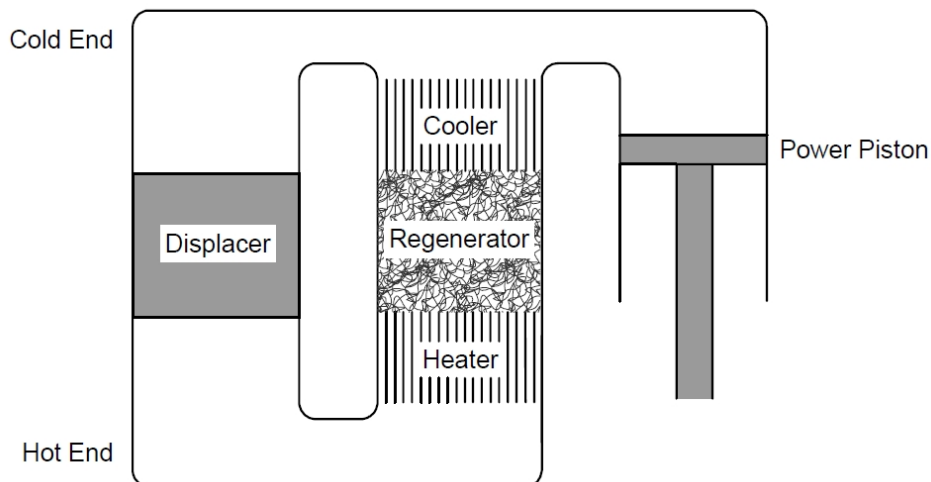


Figure 1.7 – Gamma configuration (EPRI, 2002).

• Gamma engines (see Figure 1.7) have a displacer-piston arrangement where the displacer and power pistons are in separate cylinders. The displacer shuttles the working gas back and forth between the hot and cold ends of the engine. The cold end

space includes the cold side of the displacer as well as the power piston. As the working gas moves back and forth, it passes through a cooler, a regenerator, and a heater. Gamma engines can be either kinematic or free-piston engines.

## 2.2.2. Principle of operation

As illustrated in Figure 1.5 to Figure 1.7, the displacer and power piston reciprocate in sealed cylinders filled with a fixed charge of the working gas, typically helium, nitrogen, hydrogen or air.

The working fluid in a Stirling engine must present the following thermodynamic, heat transfer and gas dynamic properties (Thombarse, 2008): i) high thermal conductivity, ii) high specific heat, iii) low viscosity, and iv) low density. Additionally, availability, cost, safety and storage requirements should also be taken into consideration.

The use of hydrogen or helium leads to higher efficiencies than the use of heavier working gases, due to the low viscosities and high thermal conductivities of these gases. On the other hand, the high diffusivity of hydrogen and helium molecules makes sealing more difficult. The lower diffusivity of nitrogen and air allow using more conventional sealing techniques, whereas hermetic seals are often required on engines that employ hydrogen or helium. The higher viscosity and lower thermal conductivity of air and nitrogen tend to reduce the ability to achieve high cycle efficiencies.

All external heat is transferred to the working gas at the cycle maximum temperature and rejected at the cycle minimum temperature. The regenerator absorbs heat from the working fluid as the gas passes through it from the hot end to the cold end. The heat stored in the regenerator is the returned to the working gas on its return from the cold end to the hot end, with minimal thermal loss.

As the displacer reciprocates, it shuttles the working gas through the regenerator between the hot and cold spaces of the engine. The pressure oscillations created by varying the average working gas temperature in a fixed volume are applied to the power piston, thus reciprocating it. The displacers and power pistons are phased so that more work is put into the power piston in the expansion stroke, when most of the working gas

is in the hot space, than the work that the piston returns to the working gas a half cycle later, to compress the mostly cold working fluid. The net surplus of expansion work less compression work is extracted as useful work by the power piston.
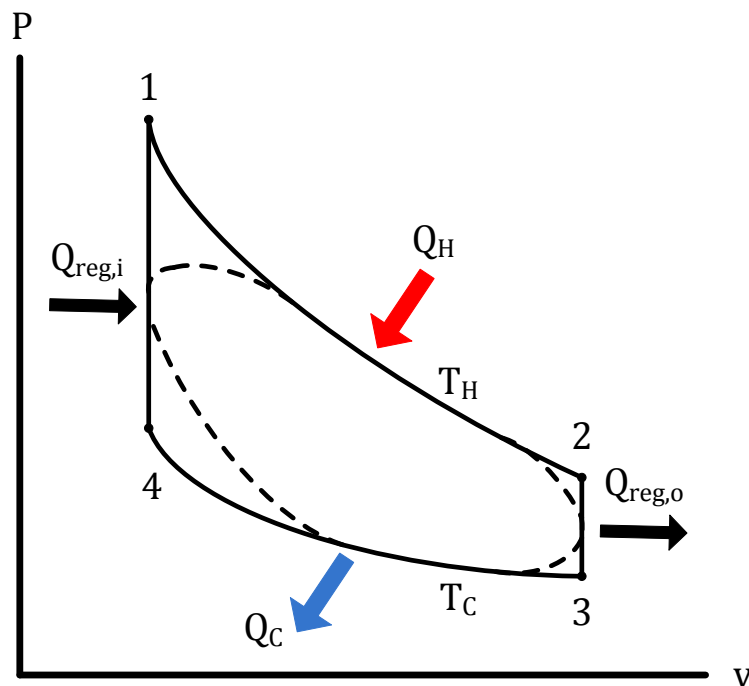


Figure 1.8 – P-v diagram for the theoretical and actual Stirling thermodynamic cycles.

The Stirling cycle is constituted by the four following processes, as represented in the pressure-volume diagram of Figure 1.8:

• Process 1-2: Isothermal expansion. Heat ($Q_H$) is added from an external source.

• Process 2-3: Isochoric cooling. Internal heat transfer from the working gas to the regenerator.

• Process 3-4: Isothermal compression. Heat is rejected to an external sink.

• Process 4-1: Isochoric heating. Internal heat transfer from the regenerator to the working gas.

During the regeneration process, heat is transferred to a thermal storage device, called regenerator, during one part of the cycle and it is transferred back to the working fluid in another part of the cycle. The regenerator can be a wire of ceramic mesh or any kind of porous plug with a high thermal mass. The regenerator is ideally assumed to be a reversible heat transfer device, since heat stored during isochoric cooling process is returned to the working gas during its return from the cold to the hot end, with minimal thermal losses.

The efficiency of the ideal Stirling cycle, calculated according to Equation 1.1, coincides with that of the Carnot cycle, i.e. the maximum thermodynamically possible. For the ideal Stirling engine cycle with a heat absorption of $Q_H$ and a heat rejection of $Q_C$, the difference $Q_H - Q_C$ is the useful product. Therefore, the efficiency of the ideal Stirling engine is:

$$\eta_{engine} = \frac{Q_H - Q_C}{Q_H} = 1 - \frac{Q_C}{Q_H} = 1 - \frac{T_C}{T_H} \qquad \text{Equation 1.1}$$

However, actual Stirling cycle engines do not achieve these ideal theoretical efficiencies, due to losses associated with temperature drops across heat exchangers, regenerator inefficiency, mechanical friction, viscous dissipation etc. In practice, compression and expansion processes are not isothermal, i.e., a temperature gradient exists between the source/sink and the fluid. In addition, when a piston and displacer reciprocate sinusoidally, the corners of the P-v diagram are rounded off, reducing the associated areas, so representing an ellipse as illustrated Figure 1.8.

### 2.2.3.  Free piston Stirling engine

Amongst the different mechanical configurations presented, free piston beta engines offer long life and high reliability, smooth, silent and maintenance-free operation and compactness, which make them very suitable for domestic applications.

The typical linear free piston Stirling engine (LFPSE), shown in Figure 1.9, is comprised of two oscillating unconnected pistons, the displacer and the power piston, which are contained within a hermetically sealed casing.
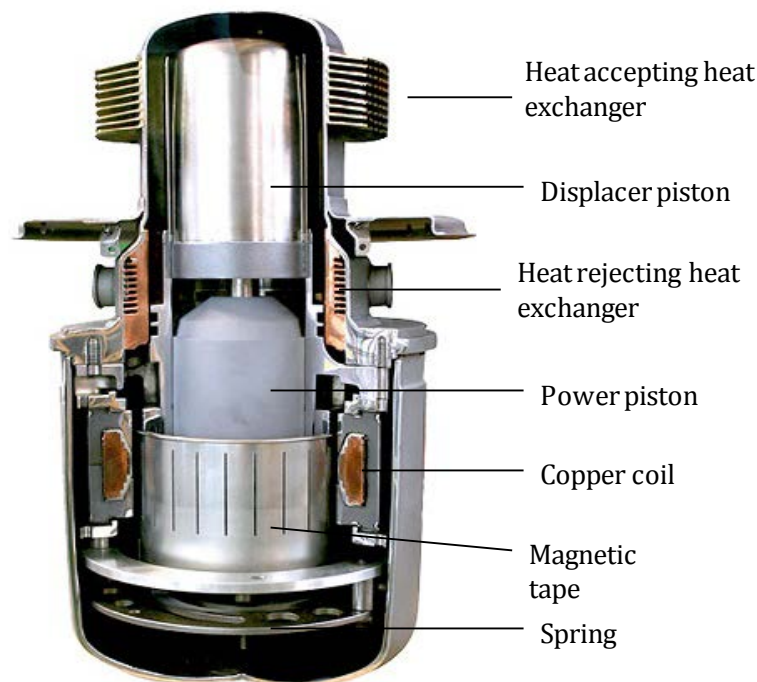
Figure 1.9 – Main components of a LPFSE (ÖkoFEN International, 2015).

The displacer, which is connected to a rod that is attached to a planar spring at the closed end of the cylinder, reciprocates along a central axis within a displacer cylinder and extends between an expansion space, hot end, and a compression space, cold end. The displacer cylinder extends within a heat accepting heat exchanger, a regenerator, and a heat rejecting heat exchanger, all of which surround the displacer cylinder and permit working gas to be shuttled between the expansion and compression spaces serially through the heat exchanger, regenerator, and heat exchanger.

The working space of the Stirling engine is bounded by a piston that reciprocates in a piston cylinder and is connected to magnets of an electromagnetic linear alternator. The time varying pressure within the working gas space drives the reciprocation of the piston and the displacer.

By definition, a displacer is a reciprocating system with a temperature difference across it, but at constant pressure. This absence of a pressure difference, as depicted in Figure 1.9 and Figure 1.10, is due to the canal where the heat exchangers are disposed, through which the working gas flows from one end to the other of the working space of the cylinder. Thus, when the displacer is at the hot end of its travel, the pressure of the gas

drops as a consequence of its temperature fall and, conversely, when the displacer reaches the cold end, the pressure of the gas raises due to the temperature increment.

On the other hand, a piston is defined as a reciprocating system whose working principle, contrary to the displacer, is not based in a temperature difference but a pressure difference, since it is tightly fit to the cylinder where it is contained. Thus, when the displacer is placed at the hot end, the resulting fall in the gas pressure pulls the piston toward the displacer while, on the contrary, when the displacer is at the cold end, the resulting rise in the gas pressure pushes the piston away from the displacer.

The mass of the displacer is very small compared to that of the power piston, and its oscillation is damped by the gas flowing through the regenerator. The power piston reciprocates undamped, except for the forces from the magnetic field of the linear alternator at the bounce space, due to the fixed magnetic coil with copper windings responsible of generating alternating current.

The planar spring on the opposite casing, connected to the displacer through the disposed rod, provides the forces necessary to initiate harmonic oscillations of the low mass piston and pushes it back upwards. The temperature difference across the displacer maintains those oscillations, and the system operates at the natural frequency of the mass-spring system.

Free piston Stirling engines, with respect to the kinematic ones, present the following advantages:

• No cranks or rotating parts which generate lateral forces and require lubrication.

• Fewer moving parts, so allowing longer time periods between maintenance operations.

• The engine is generally built as a hermetically-sealed unit, so preventing losses of the working gas and allowing operation in various kinds of environments.

With respect to the basic thermodynamics of a free-piston Stirling engine, as previously done by Bowman (1993) for instance, its working principle is conceptually illustrated in Figure 1.10 and Figure 1.11, where positions of the piston and displacer, with labels for

the relevant pressures and heat flows at four distinctive states during an ideal engine cycle are represented. Each ideal Stirling cycle is a repetitive sequence of four heat transfer processes, two at constant temperature and two at constant volume.

The gas is displaced from end to end by the reciprocation of an internal part called displacer. By definition, a displacer is a reciprocating part that has a temperature difference, but not a pressure difference, across it. When the displacer is at the cold end of the cylinder, the resulting rise of the temperature of the gas makes its pressure go up, so pushing the piston away from the displacer. Conversely, when the displacer is at the hot end of the cylinder, the pressure of the gas, which is then at the cold end, goes down because its temperature drops, so pulling the piston back toward the displacer. Sinusoidal reciprocation of the displacer causes the gas pressure in the cylinder to vary sinusoidally with the time.
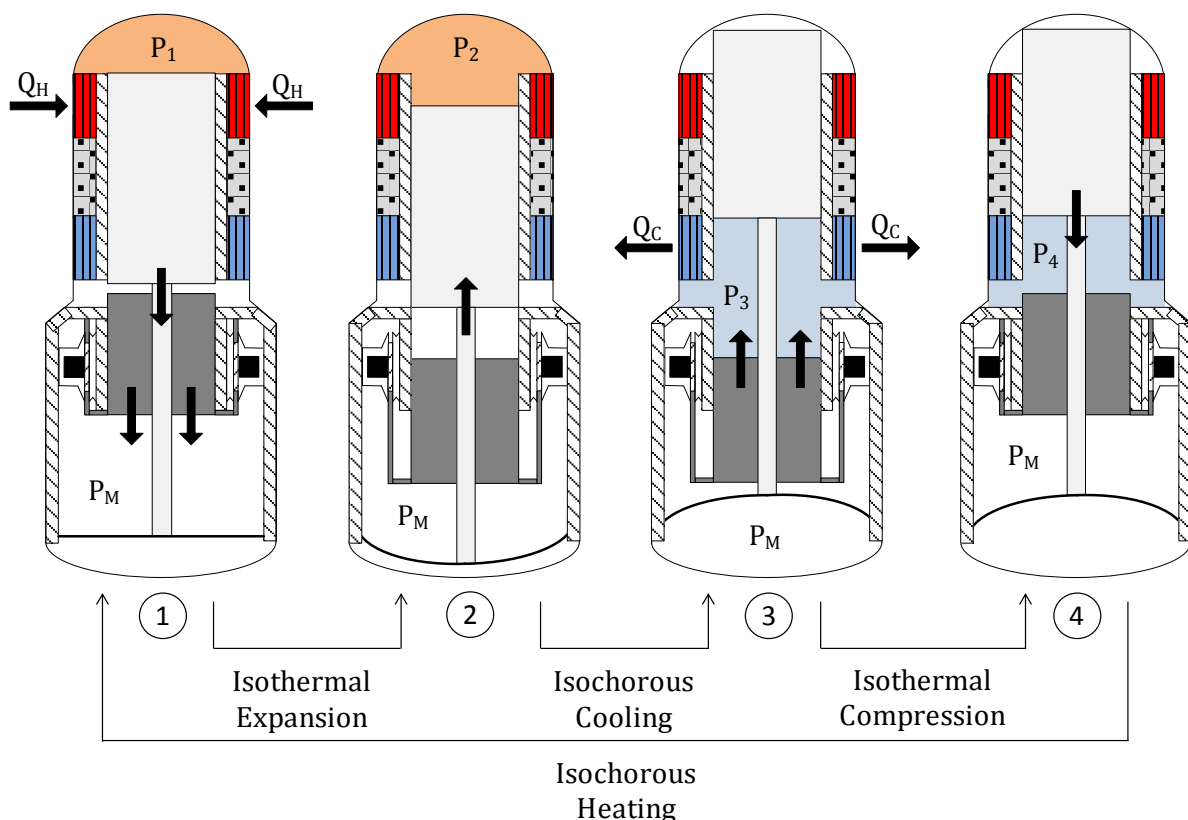


Figure 1.10 – Stirling cycle for a free-piston engine.

A rod attached to the displacer passes through a hole in the piston to expose the face of the rod to the pressure behind the piston. The piston fits tightly to the rod as well as the cylinder.

At state 1, the whole working gas is hold at the hot end, at high pressure and temperature. The resulting pressure difference between the pressure of the gas at the hot end (P₁) and the mean pressure behind the piston (P$_M$), also known as bounce space, drives both the displacer and the piston out away from the expansion space. During this isothermal expansion of the working gas, whose temperature remains constant due to the heat absorption from an external source at temperature T$_H$, the displacer is nearing the bottom while the power piston is just starting down. As the workspace volume is expanded by the outward displacement of the piston and the displacer from state 1 to 2, the pressure of the working gas falls below the mean pressure behind the piston.
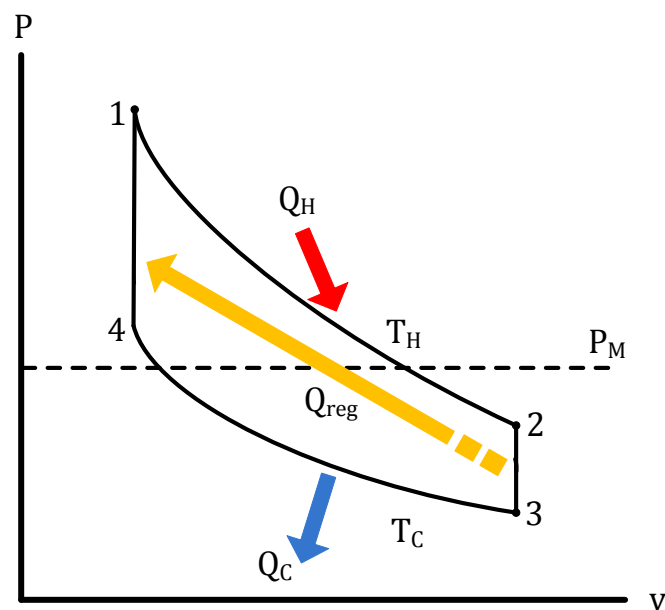


Figure 1.11 – P-v diagram for the theoretical Stirling thermodynamic cycle of a free piston engine.

A force due to the pressure difference between P₂ and P$_M$ acts on the displacer, pulling it in toward the hot end, and on the piston, stopping its outward motion. During this process, the displacer is starting up, while the power piston is at the bottom. The resulting motion of the displacer from state 2 to 3 shuttles the working gas from the hot

end to the cold end of the engine without changing its volume, as the pressure keeps decreasing down to $P_3$. The isochoric cooling is regenerative in that the heat removed from the gas, which makes the average temperature of the gas drop quickly as it passes through the regenerator, is stored in the walls of the passageway around the displacer.

At state 3, while the displacer is at the top, the resulting pressure difference between $P_3$ and $P_M$ makes the piston draw rapidly in toward the displacer, reducing the work space volume and raising the pressure of the working gas from $P_3$ to $P_4$. During this isothermal compression, the temperature of the working gas remains constant by rejecting heat to the heat sink at temperature $T_C$.

Once the system reaches state 4, a net force proportional to the pressure difference $P_4$-$P_M$ pushes the displacer out toward the piston, while the piston is set at a stop. The resulting motion of the displacer from state 4 to 1 shuttles the working gas from the cold to the hot end of the engine, without changing its volume. This isochoric regenerative heating of the working gas increases its pressure to $P_1$. The heating process is regenerative, so that the heat that raises the temperature of the gas comes from the walls of the passageway around the displacer. Ideally, the regenerative process is perfect, so that all the heat stored during the cooling is returned to the gas during the subsequent heating.

This cycle is generally repeated 50 times per second, so generating AC power at 50 Hz.

## 3. Stirling engines in micro-CHP

Micro-CHP is seen as a replacement for traditional gas boiler systems; it must therefore perform at least as well as this technology it attempts to displace. This implies that the micro-CHP device must achieve long life, long service intervals, low noise and vibration, low emissions and high efficiency, and constitute a cost-effective solution.

Stirling engines are, at least in theory, well suited to fulfil these requirements when supplying heating, DHW and electric power in the household sector; hence the emerging interest in its use in residential appliances.

Even though there have been a wide variety of Stirling engine models for small-scale cogeneration applications in the last years, the main effort has been focused on developing low-powered residential devices suitable for covering most thermal and electric demands in single-family houses, as summarized right after in Section 3.1.

However, there are still technical, economic and regulatory barriers for a massive market entrance, and this kind of equipment is only commercially available in a few countries. The impact this technology can have on electricity and gas networks when applied on a large scale, the need for further development for reducing manufacturing costs and strengthening on-site performance, together with the evolution of energy prices and the lack of incentives and support policies for micro-CHP, as well as the country-dependant regulation complexity and instability in some cases, are some of the main obstacles that should be overcome (Six et al., 2009).

## 3.1. Review of existing units

As previously mentioned, Stirling engine-based micro-CHP units are still not a mature technology in the marketplace when compared, for instance, to reciprocating internal combustion engines, as the technology is not fully assessed yet. Nevertheless, advantages outlined in previous sections have made this technology to attract significant interest. Thus, as collected by Roselli et al. (2011) and Harrison (2013), there are different small scale Stirling-based micro-cogenerators available in the market or under development which may be available in the next few years, mainly targeted to markets in Germany, UK and Netherlands, although some other countries may be involved as well.

In this section, based on the review carried out by Harrison and E.ON (2011) and Harrison (2013), a summary of the evolution and commercial status of the main micro-CHP Stirling devices is presented, introducing their main features.

**Whisper Tech LTD**

WhisperTech, created in 1995 in New Zealand, was the first company to make commercially available a Stirling micro-CHP unit in 2004, with an alpha-type 4-cylinder

Stirling engine-based micro-CHP unit. This device, named Whispergen, supplies an electrical power of 1 kW and a thermal power of 8 kW, up to 14 kW with the incorporated auxiliary burner. The unit can be fuelled by diesel oil, kerosene, petrol and natural gas. This device, massively manufactured and marketed in Europe by the Spanish brand EHE from 2008, and afterwards also launched in the UK by E.ON (formerly Powergen) late in 2012, is currently unavailable, as the Spanish company is now in receivership, and E.ON abandoned the product as it no longer fitted their core strategy.
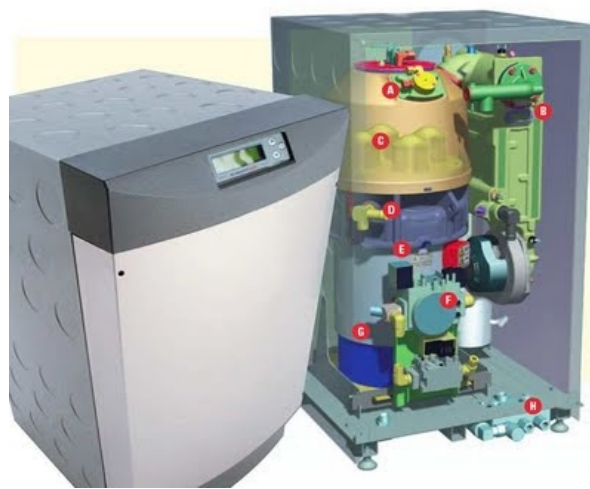


Figure 1.12 – Whispergen EU1 micro-CHP unit (EHE, 2008).

### Stirling Danmark

Stirling Danmark, in cooperation with the Danish Technical University, developed an 8.1 kW$_e$ and 24.9 kW$_t$ beta-type Stirling cogenerator (Carlsen and Fentz, 2004). The unit, not commercially available, used helium as working gas and could be fuelled both by natural gas or biogas.

### Sunmachine

A German manufacturer produced a biogas, wood pellet and solar-fuelled Stirling cogeneration unit called Sunmachine, with electric and thermal power productions rated at 3 kW and 10.5 kW, respectively. However, the company had to start insolvency proceedings due to technical problems.

Figure 1.13 – Sunmachine wood pellet micro-CHP unit (Sunmachine, 2009).

### Microgen Engine Corporation

Microgen Engine Corporation (MEC) has been working on the development of free-piston Stirling engines since 1995. As a result, the company has become the world's only successful mass producer of Stirling engines since 2010, when they first became a commercial viability. The Microgen unit, developed by BG Group from a US (Sunpower) design, is a LFPSE which is intended for wall-mounting. It contains a supplementary burner which enables it to meet the full heating requirements.
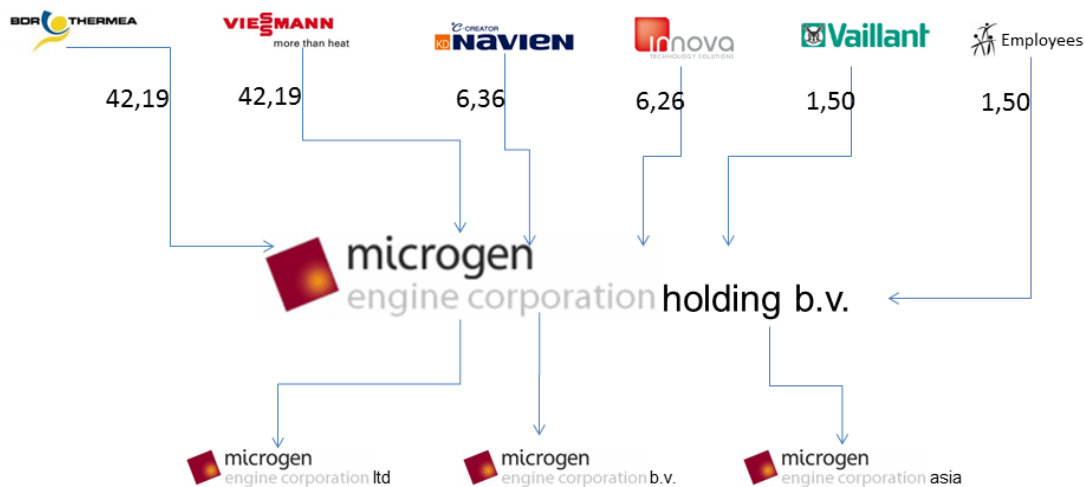


Figure 1.14 – Microgen Engine Corporation shareholder and company structure (MEC, 2010).

Following disposal by BG Group in 2007, development of the Microgen unit was taken over by MEC, a consortium of gas boiler companies (see Figure 1.14). As a result of this work, boiler manufacturer BDR Thermea – company formed by Remeha, de Dietrich and Baxi's merger – launched two Microgen Stirling engine-based micro-CHP units, eVita and Ecogen. Other world-renowned companies, such as Vaillant and Viessman, as well as Navien in Korea, have also relied on the Microgen Stirling engine to develop their products. All these products are built around the same 1 kW electric power gas-powered MEC Stirling engine, although each of the boiler company has developed its own variant of the micro-CHP unit.

In 2015, using its Pellematic Smart boiler, Ökofen developed a 1 $kW_e$ MEC engine-based wood pellet micro-CHP unit, also proposing integrated solutions with batteries and photovoltaic. Currently, the unit is ready for series production in Austria, while there are several pilot projects being implemented in other European countries.



Figure 1.15 – From left to right: Remeha eVita (Remeha, 2010), Viessmann Vitotwin (Viessmann, 2011) and Baxi Ecogen (Baxi, 2010).

### ENATEC / Infinia

ENATEC micro-cogen BV was founded in 1997 as result of the consortium by ENECO (Dutch energy supplier), ATAG Heating (Dutch boiler manufacturer) and ECN (Energy Research Centre of the Netherlands), with the objective of developing domestic CHP technology based on free piston Stirling engine. Their initial design was an adaptation of

the Stirling Technology Company's (STC) RemoteGen.

In 2005, under the leadership of Infinia (formerly STC), owner of the patent of the Stirling generator, ENATEC entered into cooperation with European boiler manufacturers Bosch Thermotechnik and Ariston Thermogroup, as well as the Japanese engine manufacturer Rinnai, to develop a natural gas-fired micro-CHP unit, based on the Infinia LPFSE generator, for cogenerative applications in single-family dwellings.

The Infinia engine was developed and adapted by ENATEC for its implementation in micro-CHP products manufactured by Junkers and Buderus (Bosch Thermotechnik) and Elco (Ariston Thermogroup) in Europe, as well as Rinnai in Japan, which was at the same time in charge of producing the Stirling module for integration into the micro-CHP packages by the other European partners.



Figure 1.16 –Buderus (left) (Bosch Thermotechnik, 2010) and Elco (right) (Pfannstiel, 2010) Stirling micro-CHP systems.

Even though the LFPSE core was virtually identical to that of the MEC derivatives, with similar electrical output (1 kW$_e$) but lower claimed efficiency, this unit was subsequently housed within an integrated floor-mounted package, incorporating a supplementary burner and a hot water storage cylinder, so being able to obtain heat outputs of 3-7 kW$_t$, up to 24 kW$_t$ when the extra condensing boiler was activated.

In 2013, Infinia was acquired by Qnergy (2013).

## Qnergy

Formed by Ricor, the Israeli company best known for its cryogenic Stirling as well as solar conversion technologies, Qnergy, in November 2013, acquired the US based Infinia.

Qnergy commercialises two 3.5 kW$_e$ and 7.5 kW$_e$ dual-opposed LFPSE products, for residential and commercial applications respectively, fuelled by natural gas or propane, as well as wood pellets or bio-fuel (Qnergy, 2013). This configuration should provide even more power output even than single piston configurations, reducing vibration and engine stress, leading to enhanced reliability.



Figure 1.17 – Qnergy 7.5 kWe micro-CHP system (Qnergy, 2013).

## Inspirit

The Inspirit micro-CHP unit arose from the Disenco kinematic beta-type Stirling engine. The product originated in the Swedish TEM SCP Stirling engine was subsequently developed by Sigma Elektroteknisk AS in Norway, before being taken up by Disenco in the UK (Harrison, 2013).

In early 2010 Disenco was placed in receivership, and the design was taken over by Inspirit Energy. The initial trial unit, rated at 3 kW$_e$ and 12-18 kW$_t$ lead to two different versions of the product, available from early 2017 on: Inspirit Charger 2.0, with outputs

of 1-2 kW$_e$ and 5-10 kW$_t$, and Inspirit Charger 3.0, capable of producing 1-3 kW$_e$ and 5-15 kW$_t$ (Inspirit Energy, 2016).



Figure 1.18 – Inspirit Charger micro-CHP system (Inspirit Energy, 2016).

## Cleanergy AB

The Cleanergy cogeneration unit started life in the 1980's, when the Stirling Power Systems company was created in Sweden and started its development based on previous works by Philips.

After several reincarnations, in 2004, a German company, Solo Stirling GmbH, started selling massively a 2-cylidner alpha-type Stirling engine, using helium as working gas in the micro-CHP unit and hydrogen in the solar-based system. The device was designed for varying working gas pressure between 35 and 150 bar, which afterwards turned into a modulation between 2 and 9 kW$_e$ and 8 and 26 kW$_t$.

In 2008, after the failure of the Swiss Stirling Systems AG and the Swiss energy supplier EBM in taking over Solo Stirling to allow a capital increase, Swedish Cleanergy AB becomes the new owner, launching the first units of Cleanergy Stirling V161 (afterwards renamend Cleanergy C9G) in 2010 for gas-fired micro-CHP and solar power generation applications.

Figure 1.19 – Cleanergy Gas Box 901CHP system (Cleanergy, 2014).

It is an alpha-type Stirling engine, meaning that the working gas shuttles between two cylinders, one containing the displacer and the other the working piston. Somewhat unusually, it is not a hermetically sealed package and thus faces the challenge of helium leakage from the high working pressure cylinders to atmosphere. This is overcome partly by means of highly efficient piston seals (which result in relatively high frictional losses). However, the significant helium leakage which still occurs is continuously replaced from a cylinder of the gas which must be periodically replenished (Harrison, 2013).

The unit is able to modulate power from 2 to 9 $kW_e$, achieving electrical and overall efficiencies at nominal power rating and a flow temperature of 40 °C of up to 25% and 95%, respectively (Cleanergy, 2014). For more realistic flow temperatures, electrical efficiency falls by 2-3% (Harrison, 2013).

Nowadays, Cleanergy commercialises a unit called Gas Box 901, based on the same Stirling engine, that can be fed with any gas with methane gas concentrations over 18%.

All the above-described Stirling engine-based micro-CHP units, together with their main features, are summarized in Table 1.2.

Table 1.2 – Recently available Stirling micro-CHP units[1].

| Manufacturer & Model | Engine type | Fuel | Power (kW) | | | Efficiencies (%) | | |
|---|---|---|---|---|---|---|---|---|
| | | | Input Power | Electric Power | Thermal Power | Electric efficiency | Thermal efficiency | Overall efficiency |
| Cleanergy Gas Box 901 | Alpha | Any gas / Solar energy | 36 | 9 | 25 | 25 | 70 | 95 |
| Qnergy QB-3500 | Linear free piston | Natural gas / Propane / Wood pellet / Biogas | 15 | 3.5 | 10 | 23 | 67 | 90 |
| Sunmachine | Alpha | Wood pellet / Solar energy | 15 | 3 | 10.5 | 20 | 70 | 90 |
| Inspirit Charger 2.0 | Beta | Natural gas | 13.5 | 2 | 10 | 15 | 75 | 90 |
| Whispergen EU1 | Alpha | Natural gas | 8.3 | 1 | 7 | 12 | 84.3 | 96.3 |
| Bosch Thermotechnik | Linear free piston | Natural gas | 7.8 | 1 | 6.4 | 13 | 82 | 95 |
| Baxi Ecogen | Linear free piston | Natural gas / Biogas | 7.4 | 1 | 6 | 13.5 | 81.1 | 94.6 |
| Senertec Dachs Stirling | Linear free piston | Natural gas / LPG | 7.5 | 1 | 5.8 | 13.3 | 77.3 | 90.6 |
| De Dietrich Hybris Power | Linear free piston | Natural gas | 7.3 | 1 | 5.8 | 13.7 | 77.3 | 91 |
| Viessmann Vitotwin 350-F | Linear free piston | Natural gas | 6.5 | 1 | 5.3 | 15.3 | 81.5 | 95.8 |
| Remeha eVita | Linear free piston | Natural gas / LPG | 6.3 | 1 | 5 | 15.9 | 79.4 | 95.3 |

[1] All data collected within this table correspond to information published by the different manufacturers.

## 3.2. Review of existing experimental and simulation-based assessments

There is an emerging interest in using Stirling engine-based micro-CHP systems in residential applications due to their potential for achieving the aforementioned benefits. However, this technology is not widely used in this kind of applications, owed to the fact that it is not fully developed, amongst others. Consequently, there is a need for developing experimental and simulation-based researches in order to improve design, operation and analysis of these residential micro-CHP systems, so that their technical, environmental and economic performances can be assessed.

Over the years, Stirling engines for micro-CHP have been researched from different perspectives. There are studies aimed at deepening in the thermodynamics of the Stirling cycle itself, such as that developed by Rogdakis et al. (2012). Other investigations, for its part, focus on analysing certain components of the units (Costa et al., 2014), so that the global performance of the engine can be improved when upgrading such components.

On the contrary, others researches approach laboratory testing for characterizing thermal, electric and environmental features of the devices under certain conditions. For instance, Thomas carried out a laboratory tests-based research of the performance of, amongst others, two Stirling micro-CHP units commercially available in Germany and another one in development state (Thomas, 2008; Thomas, 2014). Results obtained indicated that commercial units showed not only suitable characteristics for satisfying thermal demands of residential users, but also reasonable emission levels concerning to $CO_2$ and $NO_x$, as well as to noise and vibration. Data obtained through this kind of tests can be afterwards utilized, as done by Babaelahi and Sayyaadi (2014) for instance, to validate simulation models focused on predicting the building-integrated performance of such units, as reviewed in Section 3.3.

Additionally, many experimental and simulation-based building-integrated researches on this technology have been conducted in various countries, demonstrating that satisfactory results can be achieved within small-scale domestic applications, enabling

potential reductions in primary energy consumption.

Ren and Gao (2010) affirmed that Japan, Germany, United Kingdom, Netherlands and United States have been the most actively involved countries in researching and introducing these gas-fired reciprocating engine-based systems in the market. In this sense, Kuhn et al. (2008) presented results of field tests carried out with different Stirling micro-cogeneration devices in various regions of Germany, as well as in other countries such as United Kingdom, France and the Netherlands, reaching satisfactory results for small-scale applications. Lipp (2013) worked on a field-test measurement campaign of four gas-fired Stirling engine-based micro-combined heat and power Remeha eVita units installed in four different single family houses in southern Bavaria. After monitoring the dwellings over a year, the author affirmed that the Stirling μCHP units, which showed a steady-state overall efficiency above 90%, are capable of supplying these small residential buildings with thermal and electric power.

Concerning simulation-based researches, Peacock and Newborough (2005) studied the consequences of utilizing Stirling micro-CHP units in single-family houses in the United Kingdom, using annual thermal and electric demand data in 1-minute intervals. Results showed that the Stirling engine contributed to fulfill most of the daily heat and power demands, while achieving cutbacks of GHG emissions in the range of 9-16%.

De Paepe et al. (2006) focused on analysing the performance of two Stirling engines. They developed a simplified simulation-based comparative study of the use of Stirling units in a dwelling in Belgium with respect utilizing a conventional gas natural boiler and purchasing electricity from the grid. Results showed that if correctly dimensioned, micro-CHP units allowed obtaining important reductions in primary energy. In this sense, Six et al. (2009) and Van Bael et al. (2011) estimated the economic viability and potential of SE-based micro-CHP devices, amongst other technologies, in the Belgian region of Flanders, concluding that with current princes Stirling-based units are not economically viable yet.

Alanne et al. (2010) carried out a simulation-based techno-economic assessment of a Stirling micro-CHP device installed in a single-family house located in Finland, achieving 3-5% decrease in primary energy consumption and $CO_2$ emissions compared to a

traditional heating system, and obtaining substantial economic savings.

In Italy, Barbieri et al. (2012) evaluated the feasibility of different micro-CHP technologies with low electrical outputs to meet the household energy demands of single family users. Results showed that, from an energy point of view, the systems satisfied almost most of the thermal and electric requirements while achieving important savings. Economic results, however, were not satisfactory. Magri et al. (2012) developed an economic and energetic performance analysis of a Stirling engine with an electric output of 1 kW, installed in a detached house in Italy. Results show that installing the studied system leads to reducing primary energy consumption and greenhouse gas emissions, as well as obtaining economic benefits. Rosato et al (2013) developed a dynamic performance assessment of a number of micro-CHP systems fuelled by natural gas integrated within Italian multi-family houses. Compared to a traditional reference system, primary energy consumption, carbon dioxide equivalent emissions, as well as operating costs were notably reduced.

Other country-specific energy, economic and environmental assessments, such as that developed by Conroy et al. (2014) in Ireland or Teymourihamzehkolaei and Sattari (2011) in various climatic zones of Iran subscribe those energy savings and emissions reductions previously mentioned.

In the case of Spain, some studies on a 1 kW$_e$ micro-CHP Stirling engine were carried out for applications such as caravans (Ulloa et al., 2013b) and recreational sailing boats (Ulloa et al., 2013c). However, in the small residential area where, according to data extracted from the Spanish Statistical Office (INE) database (INE, 2011), in 2011 there were more than 90,000 houses in the coldest regions of Spain with surfaces above 180 m$^2$, no significant research has been carried out so far. Consequently, the building-integrated actual performance of this technology is rather unknown.

## 3.3. Review of existing combustion-based cogeneration device models

Before tackling the modelling of the combustion-engine based cogeneration for the

Stirling unit which is the subject of this work, a review of existing cogeneration device models was undertaken, in order to study general modelling approaches used and identify existing simulation models that might be suitable or adaptable for the use within the framework of this thesis.

As cited by Kelly and Beausoleil-Morrison (2007), the modelling review reveal that, whereas the literature is rich with respect to Stirling engine (SE) and internal combustion engine (ICE) models developed for general analysis (e.g. Dochat (1993); Heywood (1998)), there have not been many attempts to model combustion engine-based small-scale cogeneration in building simulation tools.

### 3.3.1. Modelling approaches

Urieli and Berchowitz (1984) classified combustion engine-based models into three categories: first-order, second-order and third-order models.

First-order models use thermodynamic principles to characterize engine performance in steady-state operation. Second-order models divide an engine's working fluid into one or more control volumes, and characterize the system's dynamic performance at discrete, sub-cycle time-steps. Finally, third-order models further divide the piston-cylinder configuration into additional control volumes suitable for finite-element analysis.

However, as mentioned by Kelly and Beausoleil-Morrison, Urieli and Berchowitz omitted a fourth class of engine model from their categorization: parametric or zero-order models. This sort of model relies entirely on empirical data and makes no attempt to characterize thermo-physical processes occurring within the system (Kelly N., 2007).

Chen and Griffin published in 1983 a modelling review where various numerical methods among the aforementioned classification were described (Chen and Griffin, 1983).

Likewise, Shultz and Schwendig (1996) became the first in building a simulation model of the general Stirling cycle, which was afterwards optimized by Kongtragool and Wongwises (2003).

In this sense, Valenti et al. (2014) developed a numerical model taking the work of Urieli and Berchowitz as a reference. They calibrated and validated the model by means of experimental tests carried out with a specific commercial micro-CHP device, where extra instrumentation was installed inside the engine. However, the model was not implemented in building simulation software and, on the other hand, this model was hardly applicable to other commercially available micro-CHP units, as invasive instrumentation was also required. The authors mentioned that an accurate numerical model is especially useful for improving designs of generation devices, by evaluating the major sources of energy waste and optimizing geometries of both the engine and the heat exchangers, which is not actually the final goal of building simulation.

As concluded by Kelly and Beausoleil-Morrison (2007), it has been corroborated that the majority of the engine models available in the literature fall into the last two categories of model-types, and were developed for the analysis of engine phenomena occurring over very short time scales (between microseconds and milliseconds), while building simulation operates using time scales many orders of magnitude longer. This explicit approach, only focusing on the Stirling engine, requires a very detailed modelling of the combustion process and thermodynamic cycle of the engine (Qvale and Smith, 1968; Organ, 1987; Kawajiri et al., 1989; Kongtragool and Wongwises, 2006).

This sort of model generally requires a huge amount of data related to the physic phenomena of the engine, which is sometimes hard and technically unviable to obtain. Thereby, this approach is considered to be over-detailed for charactering micro-cogeneration units in building applications and, furthermore, the combination of these two groups of models is also considered to be impractical from the computational point of view, as solving the resulting set of excessively stiff equations results extremely difficult using the numerical solution techniques employed in simulation tools.

Furthermore, many of the processes characterized by this kind of engine models reviewed, such as the variation of thermodynamic properties within a cylinder during a single engine stroke (Abd Alla, 2002), are not relevant within the context of building simulation assessed in this work, where the different aspects related to energy performance of the device when implemented in a building installation is of interest.

Thus, the need to rigorously model complex internal processes is less important, except when this has a direct bearing on the output of the model.

Finally, it is concluded that modelling of such devices need to focus on the development of system-simulation-compatible engine models that adequately represent thermal, chemical and electrical phenomena necessary for dynamic simulations involving models of cogeneration, balance of plant and the building itself.

### 3.3.2.   Building-integrated combustion engine-based CHP modelling

McRorie et al. (1996) described a partial model of an internal combustion engine that might be used in system level simulations; however the paper recognized that the model required a huge effort for it to being integrated into building simulation codes.

Pearce et al. (1996; 2001) studied the annual performance of Stirling engines in comparison to measured and calculated residential heating loads by assuming constant seasonal efficiencies. This modelling approach neglected the effects of different control strategies and thermal storage, which are of great interest when investigating the integration of this technology in residential buildings.

Kelly (1998) incorporated a multi-component small-scale engine model into ESP-r building simulation tool. The parameters derived for the model were taken from tests on an atypical two-cylinder diesel engine unit. However, it was not considered to be appropriate for the modelling of domestic cogeneration.

Kelly and Beausoleil-Morrison (2007) took a step forward in this area with the modelling carried out within the IEA/ECBCS Annex 42 framework. This cogeneration model, which intended to accurately predict the thermal and electrical outputs of the residential CHP device, was developed with the aim of being used in conjunction with the capabilities existing simulation tools offer – building envelope and performance, other plant components, electrical systems – in order to perform simulations for assessing technical, environmental and economic performance of these residential cogeneration technologies, and their explicit interaction with the aforementioned subsystems. Essentially, this means that the device models must interact with the other

technical domains of the building simulation tool on a time-step basis.

This grey-box empirical model, which relied partially on experimental data and consisted of 3 blocks as represented in Figure 1.20, was implemented within global energy dynamic simulation tools.
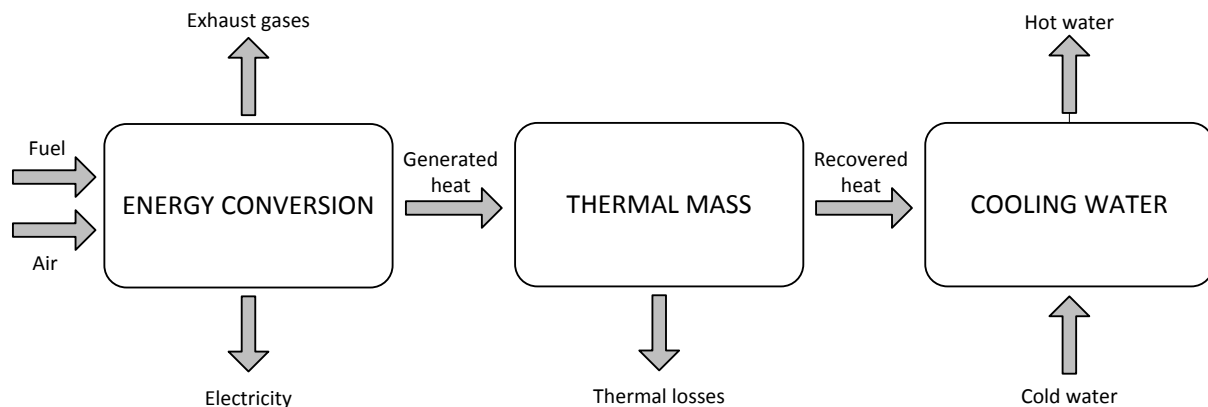


Figure 1.20 – Control volumes associated to the Annex 42 model.

This model contemplated four main modes of operation: stand-by, start-up, full-load operation and shut-down. Its modular structure permitted its appliance to both ICE and SE-based micro-CHP units. Nevertheless, the model, which was calibrated and validated using non-specific experimental tests over a Whispergen unit which only worked at full load, besides not considering part-load operation, had a number of weaknesses, as discussed by Lombardi et al. (2010), susceptible of being improved.

Thiers et al. (2010) developed a model for a wooden pellets-fuelled 3 kW$_e$ Stirling unit. Their approach, based on hourly intervals, was very schematic, consisting of a simplified parametric model using the information obtained through steady and dynamic tests carried out. Its quasistatic nature and, especially, the impossibility of calibrating the model for other Stirling units, void the use of this approach for the current research work.

Conroy et al. (2013) developed and carried out a field trial data-based validation of an easily customizable dynamic energy model for a 1 kW$_e$ and 8 kW$_t$ Stirling engine. The model developed was based on empirical equations which were specific to the engine

under study. Thus, one of the main purposes of the work was providing installers of the aforementioned engine a tool for predicting both thermal and electric outputs using the heat demand profile of a given dwelling, as well as for policy makers to explore sustainability of the micro-CHP unit in different house types for larger scale deployment.

Bouvenot et al. (2014), based on the work carried out by Andlauer (2011), developed an experimental data driven model for a gas-fed Stirling micro-CHP boiler. The modelling approach was based on an energy balance on the device and on empirical expressions for the main inputs and outputs, where start-up and shut-down processes were modelled through time constants instead of trying to define the physical phenomena taking place. The aim of this model was to reduce the number of parameters with respect to other models while maintaining an acceptable compromise between the accuracy and simplicity required in energy simulation in buildings environments. While the former version of the model contemplated the part-load operation, it was not validated in this sense since the engine used for this purpose could not modulate its load. Anyway, the modelling approach by Andlauer overlooked transient effects taking place when changing between different part-load points of operation, and did not take into consideration the fuel overshooting which takes place during the start-up phase in order to quickly achieve normal operation temperature of the hot side of the engine.

Cacabelos et al. (2014), as a continuation of the work previously carried out by the authors (Ulloa et al., 2013a), developed a one-dimensional dynamic model of a commercial micro-CHP unit, consisting of two lumped masses and a heat exchanger, based on components from the Trnsys libraries. Even though their modelling approach was very interesting, some geometrical and operation parameters proposed are generally hard to get from the manufacturers. The main weaknesses of the model were the lack of modelling of the fuel input, the neglect of heat losses to the surroundings, and the dynamic nature of the data sets used for calibration and validation.

A summary of the main building-integrated Stirling engine-based micro-CHP models that can be found in the bibliography is presented in Table 1.3, where the main aspects susceptible of being improved are highlighted.

Table 1.3 – Main building-integrated Stirling engine-based micro-CHP models.

| Author & year | Model order | Modelling approach | Validation | Main weakness |
|---|---|---|---|---|
| Kelly, 2007 | 0, 1 and 2 | Dynamic | √ | Weak steady-state validation<br>No part-load operation<br>Huge number of parameters |
| Lombardi et al., 2010 | 0, 1 and 2 | Dynamic | X | Incomplete model<br>No full validation |
| Thiers et al.,2010 | 0 | Quasistatic | √ | No transient operation<br>Engine-specific model |
| Andlauer, 2011 | 0 and 1 | Dynamic | √ | No part-load validation<br>Time-based transients |
| Conroy et. al, 2013 | 0 | Dynamic | √ | Engine-specific model<br>No steady-state data |
| Ulloa et al., 2013 | 1 | Dynamic | √ | Weak steady-state validation<br>No fuel input modeling<br>No part-load operation |
| Bouvenot et al., 2014 | 0 and 1 | Dynamic | √ | No part-load operation<br>Time-based transients<br>No start-up fuel overshooting |
| Cacabelos et al, 2014 | 1 | Dynamic | √ | Weak steady-state validation<br>No fuel input modeling<br>Complex parameters |

# 4. Objectives and structure of the Thesis

Whilst in Europe, as previously mentioned, residential and commercial buildings are responsible of 40% of the energy consumed, in Spain this sector represents the third largest consumption value of final energy with a 17% (IDAE, 2011b). In the Basque Country, this value comes to 14%, 8% of which corresponds to residential buildings and the remaining 6% to the tertiary sector. Energy consumed in households is distributed 39.4% corresponds to heating and 19.6% to DHW (EVE, 2013).

With these data in mind, as well as the intrinsic potential micro-CHP in general and Stirling engines in particular possess to efficiently supply energy in residential buildings, the main objective of this thesis is to completely evaluate the potential application of

Stirling engine-based micro-CHP systems in the Basque and Spanish households sector, focusing on single family dwellings as the destination with the greatest potential they are. According to the shortcomings and necessities defined in the literature review presented in this chapter, the following specific objectives, classified into primary (O1) and secondary (O2), are sought:

❖ Evaluate the energy, environmental and economic potential of the Stirling engine with application in the Spanish household sector (**O1.1**).

The attainment of this objective, due to its significance, implies using a simulation-based approach. This fact, thus, gives raise to other principal and secondary objectives:

❖ Develop a transient model of a typical Stirling engine-based combi micro-CHP boiler (**O1.2**). This main objective comes with a secondary one: review the current status of the Stirling technology in the micro-CHP field and the commercial solutions available (**O2.1**).

❖ Once methodologically determined the most suitable commercial solution for typical single-family dwellings in northern Spain, experimentally characterize the performance under steady and transient conditions of the selected micro-CHP unit (**O1.3**), so that the model developed can be calibrated, validated and implemented in a transient building-environment simulation tool (**O1.4**). To do so, the design, assembly and start-up of an experimental test-bench are required (**O2.2**).

❖ Optimise the design, dimensioning and operation of the Stirling engine-based residential micro-CHP installation, with special emphasis on analysing the vital role TES plays on it (**O2.3**).

❖ Deeply analyse the influence the country-specific regulation framework has on the feasibility of a Stirling engine-based residential micro-CHP installation (**O2.4**).

All these objectives are achieved through a series of tasks developed along the chapters presented. Each chapter covers one or various specific objectives which, when put all of them together, constitute the final goal. In this section a general description of each chapter is offered, in order to help the reader have a perspective of the work developed.

Chapter 2 comprises the modelling, experimental characterization and validation of a Stirling engine-based micro-CHP unit. This chapter constitutes the base on which the subsequent chapters are hold up. More specifically, in this chapter a mathematical model, amending the weaknesses of the main models described in Section 3.3.2 of Chapter 1, is developed and programmed for its later implementation in simulation environments, so that the technical, environmental and economic performance of these micro-CHP units can be evaluated in subsequent chapters.

In Chapter 3, known the vital role TES plays on the performance of a micro-CHP plant, its integration within such an installation is assessed. Different arrangements and TES sizes are proposed and, by means of transient simulations utilizing the previously developed model to a representative case study, they are analysed using diverse criteria. This way, the plant design was optimised taking into consideration various aspects previously overlooked in the bibliography.

Once the installation is optimized, its techno-economic feasibility is assessed in Chapter 4. On it, results achieved with the micro-CHP installation, taking into consideration key aspects such as climatic conditions, are studied and compared to those achievable with a traditional installation, previously designed and optimized according to some criteria exposed throughout this chapter. Economic results are put down to hypothetical variations in the main economic parameters, so constituting the sensibility analysis through which the long-term performance of the installation can be kept in mind.

Chapter 4 also focuses on analysing the influence the normative and economic frameworks have on the feasibility previously analysed. Thus, the evolution of the normative conditions regulating micro-CHP in Spain is overviewed, and afterwards, the translation of this evolution to economic terms is carried out by means of a case study. Additionally, results are compared to those achievable in pioneering countries when introducing micro-CHP in residential applications. In short, the reality of the micro-CHP and renewable energies in Spain is deeply analysed and the main obstacles to overcome are discussed.

Finally, Chapter 5 contains a summary of the results and main conclusions of the PhD

thesis and establishes the future works and research lines. The structure of the thesis in chapters is graphically presented in Figure 1.21.
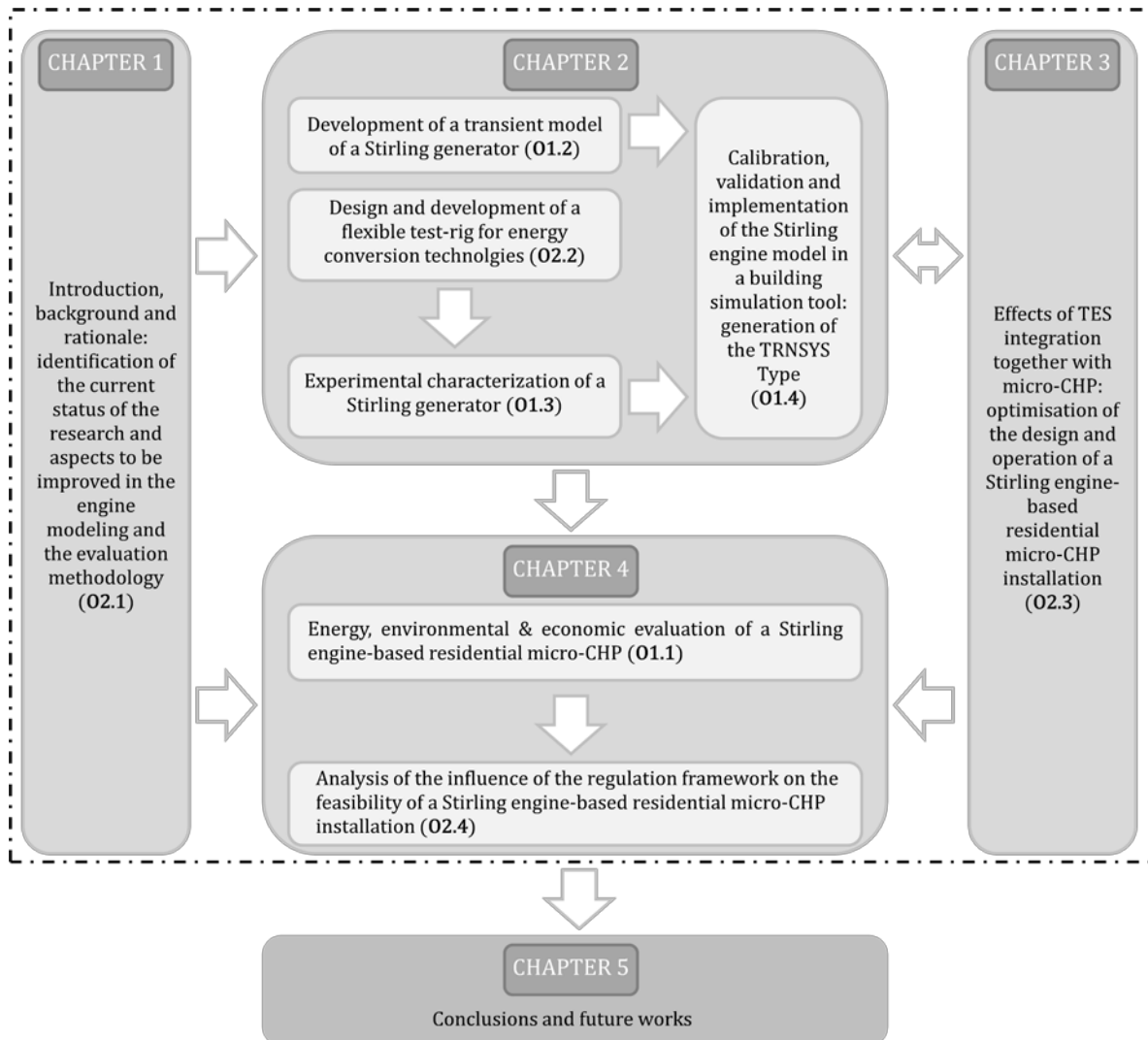


Figure 1.21 – Flow diagram of the structure of the PhD thesis.

# CHAPTER 2

## MODELLING AND EXPERIMENTAL CHARACTERIZATION OF A NATURAL GAS STIRLING ENGINE-BASED DOMESTIC MICRO-CHP DEVICE

# 1. Introduction and objectives

In this chapter a dynamic model for a small-scale natural gas-run micro-CHP boiler, whose primary mover is a Stirling engine, is developed, calibrated and validated experimentally. For this purpose, the development of an experimental test-bench where the tested device could be implemented for its individual testing, but also for getting integrated in more complex hybrid energy plants, was one of the main objectives to overcome during the development of this PhD Thesis.

As presented in Chapter 1, Stirling engines are considered to possess an inherent potential for contributing to the fulfilment of energy efficiency improvement and cutback of primary energy consumption and pollutant emissions in the household sector. However, there is still a huge potential to exploit and for getting competitive in the small residential sector, both from technical and economic points of view. Thus, beyond laboratory and field-test-based experimental researches, simulation-based studies turn out essential for improving design and optimizing control in the development phase, as well as when assessing the energy, environmental and economic performance both individually and when integrated in thermal more complex installations.

Based on the preliminary literature review on modelling presented in Chapter 1, and the purpose for which this model is to be used, a semi-empirical grey box approach is proposed. Thus, the model consists of general mass and energy conservation principles,

supported by empirical expressions that rely on parametric factors that must be determined experimentally. Consequently, the test-rig used for the evaluation is presented, describing the experimental characterization procedure. Unlike some other previous models, the one developed throughout this PhD Thesis takes into account both the dynamics that occur during the start-up and cool-down periods, as well as the partial load performance of the engine.

The chapter comprises three main blocks: in the first part of the chapter the model developed is presented and described in detail. The second part focuses on describing conscientiously the tested unit and the experimental set-up where it is integrated, as well as the experimental tests carried out for the subsequent calibration and validation of the model, which is presented in the third part of the chapter.

# 2. Model Topology

A Stirling engine-based system for domestic micro-CHP is a primary energy conversion system which produces a simultaneous output of electricity and heat for domestic usage.
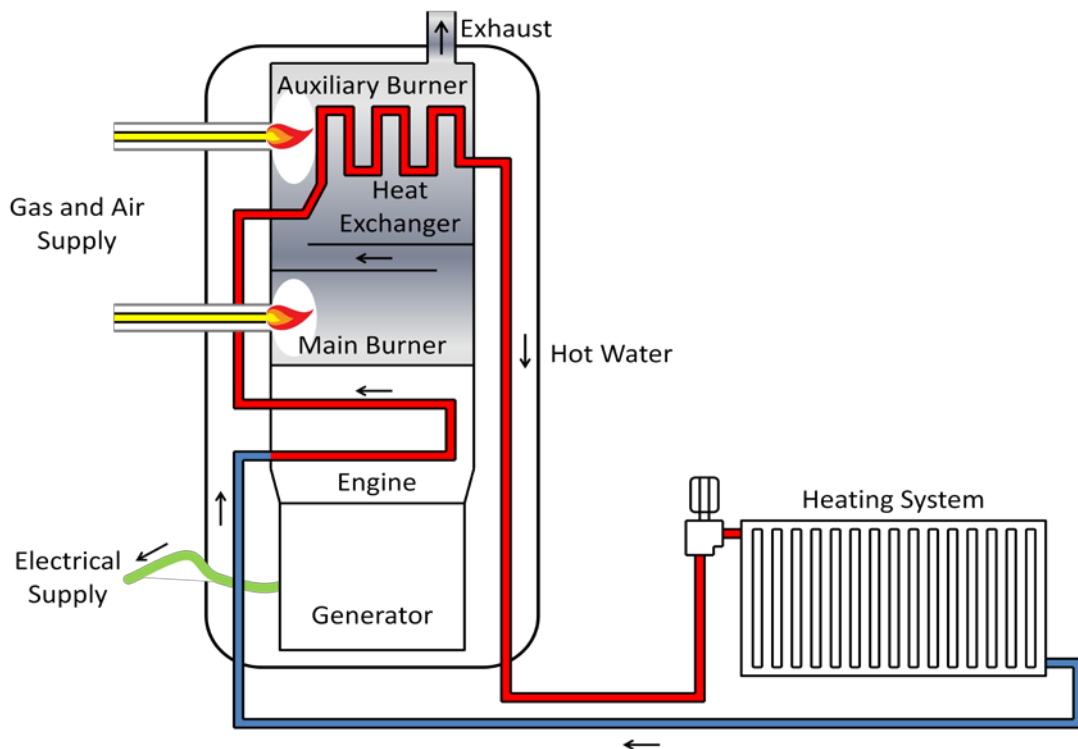


Figure 2.1 – Basic layout of a Stirling micro-CHP unit.

The energy conversion from fuel to electric power is carried out by a Stirling engine (SE), i.e. the prime mover, which drives a generator that produces electrical power, while useful heat for space heating and DHW is obtained through a heat exchanger which recovers waste heat from the engine casing and the combustion exhaust gases. Additionally many of the manufacturers of these micro-CHP units do also include an auxiliary burner (AB), mounted on the heat exchanger, which operates when the heating demand is increased above the capacity of the main burner, as depicted in Figure 2.1.

In this way, the main objective of the model is to predict semi-empirically the main energy flows of Stirling engine-based micro-CHP devices – fuel consumption and electric and thermal productions – utilizing the same approach for both generators, the Stirling engine and the auxiliary boiler, separately.

Actual mass and energy flows taking place through an engine are schematized in Figure 2.2 and described next.
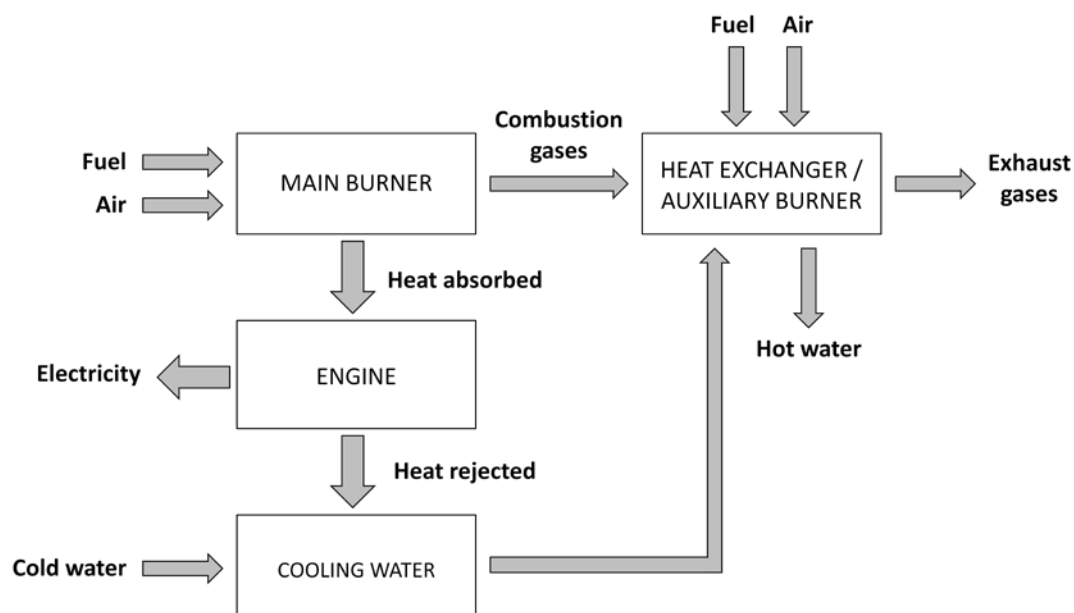


Figure 2.2 – Actual main mass and energy flows of the Stirling micro-CHP unit.

Once combustion takes place (fuel + air[1]), part of their energy content is transferred to the thermodynamic cycle (heat absorbed) while, afterwards, these gases flow through a heat exchanger before being expelled, where heat is transferred to the cooling water

[1] Terms in brackets correspond to mass and energy fluxes represented in Figure 2.2 and Figure 2.3.

coming from the casing of the engine in order to heat it up. Meanwhile, heat absorbed by the working fluid – normally helium or nitrogen – is partially converted into electric energy by means of an alternator, whilst the remaining heat is transferred to the cold reservoir (heat rejected), constituted by both the cooling water flowing through the casing of the engine (useful heat) and the ambient air in the room where the engine is located (heat losses).

For modelling purposes, these processes are reordered and the energy balance is posed as depicted in Figure 2.3. This way, heat absorbed from the engine, on the one hand, and that absorbed from the exhaust gases in the heat exchanger on the other, are lumped together within an effective heat transfer process between the engine and the heat exchanger (recoverable heat).
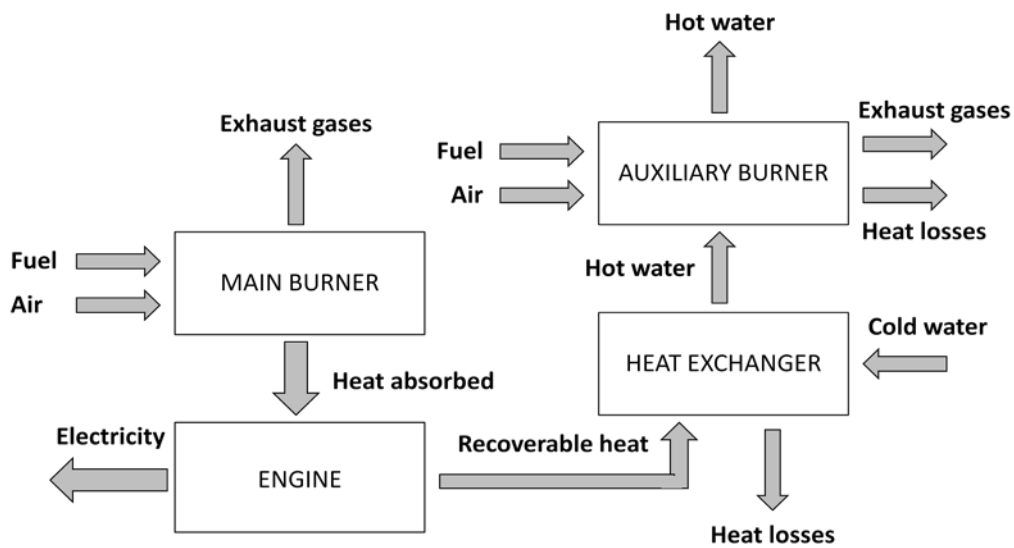


Figure 2.3 – Simplified mass and energy flows of the Stirling micro-CHP unit.

According to the aforementioned arrangement, as depicted in Figure 2.4, three control volumes and a control mass were set out for modelling the dynamic thermal performance of the micro-CHP combi-boiler: the head of the engine (burner) control volume, the engine block control mass and the heat exchanger control volume corresponding to the Stirling engine operation, and the additional boiler block when extra heat is required. All the components are supposed to be thermally defined by a unique mean temperature.

The head control volume represents the energy conversion of the energy contents of the external source (fuel) into gross heat in the form of exhaust gas, some of which is recovered and transferred to the engine control mass where electricity is produced in the alternator.
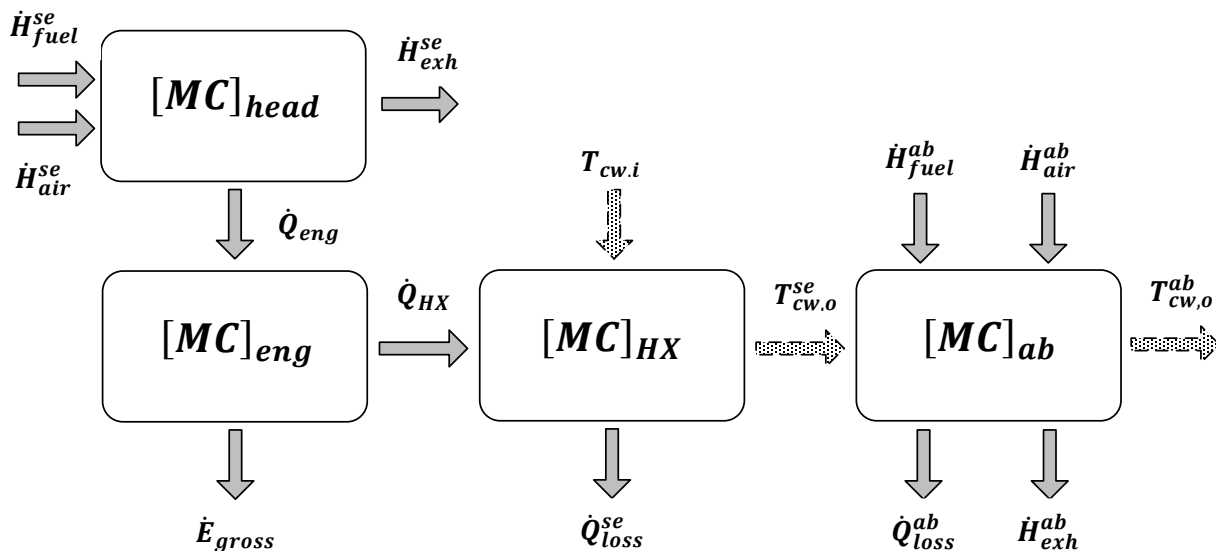


Figure 2.4 – Control mass and volumes used in the dynamic thermal performance modelling of the Stirling micro-CHP unit.

The heat exchanger control volume represents the heat transfer fluid flowing through the engine and the elements of the heat exchanger in direct thermal contact that take part on the heat fraction recovered from the exhaust gases. This way, the thermal mass of this block considers both the capacitance of the heat exchanger itself as well as that of the heat exchanger body associated to the engine block.

Meanwhile, the auxiliary boiler block considers both the energy conversion of the energy contents of the second energy source and the thermal capacitance of such element and its associated heat exchange between the exhaust and the cooling water. Since the thermal mass of the back-up boiler is already contained in the term of the heat exchanger, it is not taken into consideration when the auxiliary burner is off.

The general energy balance of the engine-head control volume can be written as follows:

$$[MC]_{head} \cdot \frac{dT_{head}}{dt} = \dot{H}_{fuel}^{se} + \dot{H}_{air}^{se} - \dot{H}_{exh}^{se} + \dot{H}_{cond}^{se} - \dot{Q}_{eng} \qquad \text{Equation 2.1}$$

where $[MC]_{head}$ is the thermal capacitance of the engine-head control volume – where the main energy conversion takes place –, $T_{head}$ is the mean temperature of the hot-side of the engine, $\dot{H}_{fuel}^{se}$ is the total enthalpy of the fuel input of the main burner, i.e. the higher heating value (HHV) brought to the ambient conditions at which fuel is supplied, $\dot{H}_{air}^{se}$ is the enthalpy of the humid air used for the main combustion, $\dot{H}_{exh}^{se}$ is the enthalpy, both including the sensible and the latent, of the exhaust gas associated to the main burner, $\dot{H}_{cond}^{se}$ is the enthalpy of the recoverable latent heat of the exhaust gas, and $\dot{Q}_{eng}$ is the gross amount of heat rate recovered from the exhaust gases and transferred to the engine-block.

On the other hand, the energy balance of the engine-block control mass can be written as follows:

$$[MC]_{eng} \cdot \frac{dT_{eng}}{dt} = \dot{Q}_{eng} - \dot{E}_{gross} - \dot{Q}_{HX} \qquad \text{Equation 2.2}$$

where $[MC]_{eng}$ is the thermal capacitance of the engine control mass, where heat is converted into electricity, $T_{eng}$ is the mean temperature of the engine, $\dot{E}_{gross}$ is the gross electric power output of the engine, and $\dot{Q}_{HX}$ is the net amount of heat rate recovered from the engine casing and the exhaust gases and transferred to the heat exchanger.

With respect to the heat exchanger, the energy balance corresponding to its control volume can be written as follows:

$$[MC]_{HX} \cdot \frac{dT_{cw,o}^{se}}{dt} = \dot{Q}_{HX} - \dot{Q}_{loss}^{se} - \dot{Q}_{net}^{se} \qquad \text{Equation 2.3}$$

where $[MC]_{HX}$ is the thermal capacitance of the heat exchanger control volume, where the thermal recovery takes place; $T_{cw,o}^{se}$ is the mean temperature of the heat exchanger,

which is considered to be representative of that of the cooling water at the outlet due to the logarithmic increase of the temperature of a cold fluid flowing through a heat exchanger; $\dot{Q}_{loss}^{se}$ is the heat loss rate through the skin of the micro-CHP engine, which is considered to occur from the cooling water to the surroundings, and $\dot{Q}_{net}^{se}$ is the net main thermal output of the micro-CHP unit.

As far as the backup boiler (auxiliary burner) control volume is considered, its energy balance corresponds to the following:

$$[MC]_{ab} \cdot \frac{dT_{cw,o}^{ab}}{dt} = \dot{H}_{fuel}^{ab} + \dot{H}_{air}^{ab} - \dot{H}_{exh}^{ab} + \dot{H}_{cond}^{ab} - \dot{Q}_{loss}^{ab} - \dot{Q}_{net}^{ab}$$

Equation 2.4

where $[MC]_{ab}$ is the thermal capacitance of the auxiliary burner control volume, where the additional energy conversion takes place, $T_{cw,o}^{ab}$ is the mean temperature inside the additional boiler, $\dot{H}_{fuel}^{ab}$ is the total enthalpy of the fuel input of the additional burner, $\dot{H}_{air}^{ab}$ is the enthalpy of the humid air used for the additional combustion, $\dot{H}_{exh}^{ab}$ is the enthalpy, both including the sensible and the latent, of the exhaust gas associated to the additional burner, $\dot{H}_{cond}^{ab}$ is the enthalpy of the recoverable latent heat of the exhaust gas associated to the auxiliary burner, $\dot{Q}_{loss}^{ab}$ is the heat loss rate through the skin of the unit associated to the backup boiler, and $\dot{Q}_{net}^{ab}$ is the net additional thermal output of the micro-CHP unit.

As previously mentioned, the model does not attempt to physically model the actual heat transfer phenomena taking place in micro-CHP units but substitutes exhaust gas by heat transfer-rates between the main control mass and volumes. This approach considers that all heat obtained from the combustion process is first addressed to the hot-side of the engine and, afterwards, it is the head of the engine which transfers heat to the engine-block. Finally, heat not absorbed by the thermodynamic power cycle, as well as that rejected, is transferred from the engine-block to the cooling water.

Heat transfer between the different control mass and volumes are modelled as the product between an effective UA coefficient and the temperature difference of the

control mass and volumes. This way, heat transferred from the combustion chamber to the engine block and that from the engine to the heat exchanger is modelled as follows:

$$\dot{Q}_{eng} = [UA]_{eng} \cdot \left(T_{head} - T_{eng}\right)$$

<div align="right">Equation 2.5</div>

$$\dot{Q}_{HX} = [UA]_{HX} \cdot \left(T_{eng} - T_{cw,o}^{se}\right)$$

<div align="right">Equation 2.6</div>

When the micro-CHP unit only works with the main burner, heat losses are exclusively those corresponding to the engine. Since cooling water flows by the outer side of the engine block, the model considers that it is the water who receives heat corresponding to losses of the engine and therefore, it is the cooling water control volume the one that undergoes heat losses:

$$\dot{Q}_{loss}^{se} = [UA]_{loss}^{se} \cdot \left(T_{cw,o}^{se} - T_{amb}\right)$$

<div align="right">Equation 2.7</div>

Finally, concerning heat losses when the auxiliary burner is running, $\dot{Q}_{loss}^{ab}$, it is considered that losses to the surroundings correspond to the cooling water as well. Additionally, since the auxiliary burner will not normally operate unless the main burner is on, no losses through the jacket of the engine and towards the head of the engine are explicitly associated to the additional boiler:

$$\dot{Q}_{loss}^{ab} = [UA]_{loss}^{ab} \cdot \left(T_{cw,o}^{ab} - T_{amb}\right)$$

<div align="right">Equation 2.8</div>

## 2.1. Steady operation

### 2.1.1. Thermal power

In general terms, the thermal output of the Stirling engine, once steady conditions are reached, depends on three operational stretches. First, when the thermal demand exceeds the maximum heat output of the unit at some given mass flow and return temperature conditions, i.e. when the temperature of the cooling water at the outlet of

the engine, $T_{cw,o}^{se}$, is below the generation set-point temperature, $T_{cw,o}^{sp}$, the engine will work at full load, in order to reach that set-point.

Once the set-point temperature is reached, the engine's burner will start modulating so that the thermal production can be adapted to the demand. Consequently, a part-load ratio, $\alpha_t^{se}$, defined as the relation between the instantaneous thermal power and the nominal full-load power at those mass flow and cooling water return conditions, must be obtained, which is used afterwards for modelling the electric and fuel performances.

Additionally, the model must also take into consideration the maximum modulation rate, i.e. the minimum thermal power the engine can provide, below which, with the corresponding hysteresis, the engine will turn off.

$$\dot{Q}_{net}^{se} = \begin{cases} \dot{Q}_{net,full}^{se} & \text{for } T_{cw,o}^{max} \leq T_{cw,o}^{sp} \\ \dot{Q}_{net,part}^{se} & \text{for } T_{cw,o}^{min} - \Delta T < T_{cw,o}^{sp} < T_{cw,o}^{max} \\ 0 & \text{for } T_{cw,o}^{min} \geq T_{cw,o}^{sp} + \Delta T \end{cases}$$

Equation 2.9

where $T_{cw,o}^{max}$ and $T_{cw,o}^{min}$ are the outlet temperature of the cooling water at full load and minimum load operation, respectively, and $\Delta T$ is the internally controlled temperature hysteresis for the outlet cooling water before the engines turns off. This fact makes the engine turn out once the actual outlet temperature exceeds the set-point on certain pre-fixed degrees.

The net heat recovery of the cooling water can be determined by means of the thermal energy transport equation:

$$\dot{Q}_{net}^{se} = \dot{m}_{cw} \cdot c_{cw} \cdot \left( T_{cw,o}^{se} - T_{cw,i} \right)$$

Equation 2.10

where $\dot{Q}_{net}^{se}$ is the net thermal production of the micro-CHP unit, $\dot{m}_{cw}$ is the cooling water mass flow, $c_{cw}$ is the specific heat of the cooling water, and $T_{cw,o}^{se}$ and $T_{cw,i}$ are the

respective temperatures of the cooling water at the outlet and the inlet of the micro-CHP unit.

The cooling water specific heat is to be calculated using a temperature-dependant self-tailored polynomial expression, developed with data extracted from Engineering Equation Solver (EES) database (S. A. Klein and Alvarado, 1992):

$$C_{cw} = \alpha + \beta \cdot T_{cw} + \gamma \cdot T_{cw}^2 + \delta \cdot T_{cw}^3 + \varepsilon \cdot T_{cw}^4 + \zeta \cdot T_{cw}^5 + \theta \cdot T_{cw}^6 \qquad \text{Equation 2.11}$$

where $\alpha$, $\beta$, $\gamma$, $\delta$, $\varepsilon$, $\zeta$ and $\theta$ are regression coefficients with values indicated in Table 2.1 for the case of water.

Table 2.1 – Values of the regression coefficients for the cooling water specific heat.

| $\alpha$ | $\beta \cdot 10^3$ | $\gamma \cdot 10^4$ | $\delta \cdot 10^5$ | $\varepsilon \cdot 10^7$ | $\zeta \cdot 10^9$ | $\theta \cdot 10^{12}$ |
|---|---|---|---|---|---|---|
| 4.22513 | 6.83202 | 4.15888 | 1.22124 | 1.83099 | 1.34516 | 3.87190 |

Simultaneously solving Equation 2.1, Equation 2.2 and Equation 2.3, the cooling water outlet temperature ($T_{cw,o}^{se}$) is obtained. If the set-point temperature ($T_{cw,o}^{sp}$) exceeds the value of $T_{cw,o}^{se}$, the thermal load fraction will be equal to 1 and the engine will be operating at full load; otherwise, the burner will start modulating and the part-load operation will start.

The thermal load fraction, $\alpha_t^{se}$, which is dependent on the production set-point temperature, is obtained as the quotient of the actual heat demand, calculated from Equation 2.10, and the maximum heat producible at the same cooling water mass flow and inlet temperature conditions:

$$\alpha_t^{se} = \frac{\dot{Q}_{net,sp}^{se}}{\dot{Q}_{net,max}^{se}} \qquad \text{Equation 2.12}$$

where $\dot{Q}_{net,sp}^{se}$ is the net thermal output when the temperature of the cooling water at the outlet is at the set-point and $\dot{Q}_{net,max}^{se}$ is the maximum net heat power to be transferred

to the cooling water at certain cooling water temperature and flow conditions. The determination of $\dot{Q}_{net,max}^{se}$ can be assessed by means of a multiple linear regression parametric equation.

$$\dot{Q}_{net,sp}^{se} = \dot{m}_{cw} \cdot c_{cw} \cdot \left(T_{cw,o}^{sp} - T_{cw,i}\right)$$ 

<div align="right">Equation 2.13</div>

$$\dot{Q}_{net,max}^{se} = \dot{Q}_{net,ref}^{se} + a_1^{se} \cdot \left(T_{cw,i} - T_{cw,i}^{ref,se}\right) + a_2^{se} \cdot \left(\dot{m}_{cw} - \dot{m}_{cw}^{ref,se}\right)$$

<div align="right">Equation 2.14</div>

where $a_1^{se}$ and $a_2^{se}$ are empirically determined regression coefficients and $\dot{Q}_{net,ref}^{se}$ is the full-load thermal power value measured when the respective temperature and mass flow of the cooling water are $T_{cw,i}^{ref,se}$ and $\dot{m}_{cw}^{ref,se}$.

The multiple linear approach, based on the regression philosophy and considerations first proposed by Lombardi et al. (2010) and later on modified by Bouvenot et al. (2014), evinces that an energy exchange or efficiency can be expressed as a function of a reference value, with its correspondent cooling water inlet temperature and mass flow, and the actual water temperature and mass flow. So, equations obtained through this approach, contrary to the multiple polynomial regression approach used by Kelly and Beausoleil-Morrison (2007), for instance, are somehow related to thermo-physical phenomena.

Due to the architecture of this kind of micro-CHP boilers, which generally, as mentioned, include the Stirling engine and an additional boiler, both modulating, as well as a variable-speed pump, independent nominal values for the reference variables of the engine are not always available in the manufacturers' data sheets. Consequently, the proposed reference conditions are those obtained by experimental evaluation under nominal volumetric flow conditions, which normally are the corresponding to the first stage of the internal pump at which the Stirling engine operates. For full load reference values, as later on proposed for fuel and electricity flows, the nominal power is measured at the most favourable return temperature, i.e. 30 °C.

Since the auxiliary burner is also modulating, these modelling fundamentals can be applied to both the Stirling engine and the additional boiler. This way, its thermal load fraction, $\alpha_t^{ab}$, can be expressed as follows:

$$\alpha_t^{ab} = \frac{\dot{Q}_{net,sp}^{ab}}{\dot{Q}_{net,max}^{ab}} \qquad \text{Equation 2.15}$$

where the actual heat demand, $\dot{Q}_{net,sp}^{ab}$, and the maximum heat producible by the auxiliary burner at some given cooling water temperature and flow conditions, $\dot{Q}_{net,max}^{ab}$, are determined as follows:

$$\dot{Q}_{net,sp}^{ab} = \dot{m}_{cw} \cdot c_{cw} \cdot \left(T_{cw,o}^{sp} - T_{cw,o}^{se}\right) \qquad \text{Equation 2.16}$$

$$\dot{Q}_{net,max}^{ab} = \dot{Q}_{net,ref}^{ab} + a_1^{ab} \cdot \left(T_{cw,o}^{se} - T_{cw,i}^{ref,ab}\right) + a_2^{ab} \cdot \left(\dot{m}_{cw} - \dot{m}_{cw}^{ref,ab}\right) \qquad \text{Equation 2.17}$$

### 2.1.2. Electric power

Concerning the exchange of electric energy of the engine, since this kind of engine is typically regulated in order to reach and maintain a certain level of electric output, the modelling is tackled in terms of net power by a multiple linear regression correlation. Since the performance of any power cycle depends on the temperature of a hot and a cold reservoir, the correlation proposed considers the net power variation as a function of the temperature of the head of the engine (hot reservoir) and the inlet temperature and mass-flow of the cooling water(cold reservoir).

This way, since once the firing rate is reduced the temperature of the hot side will diminish inevitably, using this temperature makes both full and part load operation modes get encompassed through a unique correlation. The temperature of the head of the engine is typically reported by its control and monitoring system.

$$\dot{E}_{net}^{se} = \dot{E}_{net,ref}^{se} + b_1^{se} \cdot \left(T_{head} - T_{head}^{ref}\right) + b_2^{se} \cdot \left(T_{cw,i} - T_{cw,i}^{ref,se}\right) +$$

Equation 2.18

$$+b_3^{se} \cdot \left(\dot{m}_{cw} - \dot{m}_{cw}^{ref,se}\right)$$

where $\dot{E}_{net}^{se}$ is the actual net electric power at full load, $\dot{E}_{net,ref}^{se}$ is the reference net electric power, $T_{head}$ is the temperature of the burner and $T_{head}^{ref}$ is the reference temperature of the head of the engine which constitutes the hot reservoir of the cycle.

While the net electric power can be measured through an external electricity meter, the gross electric power, $\dot{E}_{gross}$, can generally be obtained through an internal measurement reported by its control and monitoring system. Thus, the electric consumption requirements of the device can be determined, as a difference of both:

$$\dot{E}_{gross} = \dot{E}_{net}^{se} + \dot{E}_{standby} + \dot{E}_{fan}^{se} + \dot{E}_{pump}^{se}$$

Equation 2.19

The electric consumption considers on the one hand the standby consumption ($\dot{E}_{standby}$) mainly due to the electronic control board and, on the other hand, the energy required by the auxiliaries, i.e. the intake air fan ($\dot{E}_{fan}^{se}$) and the cooling water circulation pump ($\dot{E}_{pump}^{se}$).

However, as the final purpose of the modelling presented in this PhD Thesis is to implement it in a building simulation tool, the pump consumption is excluded from these parasitic losses. So, when a simulation is faced, if an external pump is to be used instead of the internal one, its energy consumption can be accounted independently and then, put it together with the net power production extracted from Equation 2.19. Additionally, since the engine may operate together but the auxiliary burner, accounting for the energy consumption of the pump separately permits distributing this consumption between the two generators.

This way, concerning the auxiliary burner, since it does not produce any electricity but only consumes, its net electricity exchange is expressed as follows:

$$\dot{E}_{net}^{ab} = -\dot{E}_{fan}^{ab} - \dot{E}_{pump}^{ab}$$

Equation 2.20

where $\dot{E}_{fan}^{ab}$ and $\dot{E}_{pump}^{ab}$ stand for the respective electricity consumption of the fan and the pump that is directly related to the operation of the auxiliary burner.

## 2.1.3.  Fuel power

The fuel input, in terms of power, is related to the fuel volumetric as follows:

$$\dot{F} = \dot{V}_f \cdot LHV_f$$

Equation 2.21

where $\dot{V}_f$ is the volumetric fuel flow, in m³/h, and $LHV_f$ is the lower heating value of the fuel, in kWh/m³.

The lower heating value of the fuel at normalized conditions, $LHV_f^{\circ}$, can be determined from the enthalpies of formation of all the reactants and products of the complete stoichiometric combustion, known the fuel composition, and considering that all the water content of the products appears in vapour phase.

$$LHV_f^{\circ} = \frac{\left(\sum_{reactants} y_i \cdot \overline{h}_i - \sum_{products} y_i \cdot \overline{h}_i\right)}{\sum_{reactants} M_i}$$

Equation 2.22

where $y_i$ is the molar fraction of each constituent, $\overline{h}_i$ is the enthalpy of formation of each constituent at normalized conditions, i.e. 0 °C and 1 atm, in kJ/kmol, and $M_i$ is the molar mass of each reactant, in kg/kmol. The higher heating value $HHV_f$ is obtained in the same way but considering all the water content of the products in liquid phase.

The enthalpies of the different components of reactants and products at the given conditions are determined as follows:

$$\bar{h}_i(T) = \bar{h}_i^{\circ}(T_0) + \left[\bar{h}(T) - \bar{h}(T_0)\right] =$$

$$= R \cdot T \cdot \left(\alpha_1 + \alpha_2 \cdot \frac{T}{2} + \alpha_3 \cdot \frac{T^2}{3} + \alpha_4 \cdot \frac{T^3}{4} + \alpha_5 \cdot \frac{T^4}{5} + \frac{\alpha_6}{T}\right)$$

Equation 2.23

where coefficients $\alpha_1$ to $\alpha_6$, specific for each substance, are provided by the NASA 7 term polynomials (McBride et al., 1993), and $T_0$ is the temperature at standard conditions, 25 °C.

As $LHV_f$ is usually given at normal conditions ($LHV_f^{\circ}$ in kWh/Nm³), a conversion factor, $V_0/V$, in Nm³/m³, must be applied for its conversion to the desired conditions:

$$LHV_f = LHV_f^{\circ} \cdot \frac{V_0}{V}$$

Equation 2.24

$$\frac{V_0}{V} = \frac{T_0}{T} \cdot \frac{P}{P_0}$$

Equation 2.25

where $T_0$ and $P_0$ are the temperature and pressure under normal conditions, 0 °C and 1 atm, respectively, and $T$ and $P$ are the temperature and absolute pressure conditions at which fuel is supplied.

$$\dot{m}_f = \dot{V}_f \cdot \rho_f$$

Equation 2.26

where $\dot{m}_f$ is the mass flow rate of fuel input and $\rho_f$ is the density of the fuel, which is obtained as follows:

$$\rho_f = \left(\rho_{r,f} \cdot \rho_0\right) \cdot \frac{V_0}{V}$$

Equation 2.27

where $\rho_{r,f}$ is the specific density of the fuel and $\rho_0$ is the density of air at normal conditions, i.e. 0 °C and 1 atm.

Usually, the hourly composition of the fuel required by building energy simulation is not known, but the daily higher and lower heating values, as well as the specific density, are usually given by gas distribution companies. In this case, the enthalpies of all the terms concerning to fuel and air inputs ($\dot{H}_{fuel}$ and $\dot{H}_{air}$) and the exhaust enthalpy ($\dot{H}_{exh}$), as well as the corresponding condensed fraction of the exhaust gases ($\dot{H}_{cond}$), can be joint together within a combustion efficiency term, so avoiding an exhaustive analysis of the combustion. This combustion efficiency, $\eta_{comb}$, together with the fuel power input related to the LHV, $\dot{F}$, takes into consideration the power fluxes which also imply some mass transfer (fuel input, air, exhaust, condensate):

$$\dot{H}_{fuel} + \dot{H}_{air} - \dot{H}_{exh} + \dot{H}_{cond} = \eta_{comb} \cdot \dot{F} \qquad \text{Equation 2.28}$$

This efficiency can be modelled by a multiple linear regression approach, as that used for the maximum thermal power output, so avoiding the necessity to know the variations in the fuel composition. This approach considers that the efficiency can be expressed as a function of a reference efficiency value, $\eta_{comb}^{ref}$, associated to the correspondent cooling water inlet reference temperature ($T_{cw,i}^{ref}$) and mass flow ($\dot{m}_{cw}^{ref}$), and the actual water temperature and mass flow, as follows:

$$\eta_{comb}^{se} = \eta_{comb,ref}^{se} + c_1^{se} \cdot \left(T_{cw,i} - T_{cw,i}^{ref}\right) + c_2^{se} \cdot \left(\dot{m}_{cw} - \dot{m}_{cw}^{ref}\right) \qquad \text{Equation 2.29}$$

Considering all this, the gross heat obtained from the combustion, under steady-state conditions, can be obtained as follows:

$$\dot{Q}_{comb} = \eta_{comb} \cdot \dot{F} \qquad \text{Equation 2.30}$$

where $\dot{Q}_{comb}$ is the gross heat obtained from the combustion, which accounts for the difference between the enthalpies of the input flows (fuel and combustion air) and that of the exhaust gases.

These engines are generally regulated to maintain some preset temperature conditions at the hot-side of the engine, i.e. the head of the engine, which enable reaching the electric output desired. To do so, the intake air mass flow is regulated by the fan rotation speed and the fuel mass flow accordingly. Therefore, the fuel flow can vary depending on the LHV, and it is a certain power input what is required for reaching the desired operation point. Thus, the fuel consumption in nominal conditions under steady operation, $\dot{F}_{nom}^{se}$ is related to the net electrical power by means of the electric efficiency:

$$\dot{F}_{nom}^{se} = \frac{\dot{E}_{net}^{se}}{\eta_{e,nom}^{se}} \qquad \text{Equation 2.31}$$

where $\eta_{e,nom}^{se}$ and $\dot{E}_{net}^{se}$ are the nominal electric efficiency and the net electric output when the engine operates at full load, respectively.

For its part, the nominal net electric efficiency is modelled in terms of a multiple linear regression correlation:

$$\eta_{e,nom}^{se} = \eta_{e,ref}^{se} + d_1^{se} \cdot \left(T_{cw,i} - T_{cw,i}^{ref,se}\right) + d_2^{se} \cdot \left(\dot{m}_{cw} - \dot{m}_{cw}^{ref,se}\right) \qquad \text{Equation 2.32}$$

Combining Equation 2.18 and Equation 2.32 as established in Equation 2.31 the fuel nominal power at full load is determined.

On the other hand, when the micro-CHP unit works at part load, since the burner modulates its firing rate in order to take back the generation set point temperature, a linear relationship between the thermal load and the firing rate is proposed:

$$\alpha_f^{se} = 1 - e^{se} \cdot (1 - \alpha_t^{se}) \qquad \text{Equation 2.33}$$

where $\alpha_f^{se}$ is the firing rate of the burner and $c^{se}$ is an empirical coefficient.

Finally, in order to impose the modulation limits of the devices, a minimum firing rate must be defined that makes the device switch off once this limit is overtaken. This

minimum firing rate, for the case of the Stirling engine, is generally related to the temperature of the head of the engine, so that, when this temperature drops below a certain prefixed minimum value, $T_{head,min}$, the unit will shut-down.

Taking all this into account, the actual fuel power of the Stirling engine, $\dot{F}_{se}$, is determined as follows:

$$\dot{F}_{se} = \begin{cases} \alpha_f^{se} \cdot \dot{F}_{nom}^{se} & \text{for } T_{head} \geq T_{head,min} \\ \\ 0 & \text{for } T_{head} < T_{head,min} \end{cases}$$

Equation 2.34

With respect to the auxiliary burner, due to the difference between its control and that of the Stirling engine, the modelling of the fuel consumption is approached in a different way except for the combustion efficiency.

In this sense, the fuel input power in nominal conditions is related to the maximum heat output achievable (previously defined through Equation 2.17):

$$\dot{F}_{nom}^{ab} = \frac{\dot{Q}_{net,max}^{ab}}{\eta_{t,nom}^{ab}}$$

Equation 2.35

where $\eta_{t,nom}^{se}$ is the nominal thermal efficiency when the auxiliary burner operates at full load. This nominal net thermal efficiency is modelled in terms of a multiple linear regression correlation:

$$\eta_{t,nom}^{ab} = \eta_{t,ref}^{ab} + d_1^{ab} \cdot \left(T_{cw,i} - T_{cw,i}^{ref,ab}\right) + d_2^{ab} \cdot \left(\dot{m}_{cw} - \dot{m}_{cw}^{ref,ab}\right)$$

Equation 2.36

On the other hand, analogous to the Stirling engine, a linear relationship between the thermal load and the firing rate is proposed for defining the part-load performance:

$$\alpha_f^{ab} = 1 - e^{ab} \cdot \left(1 - \alpha_t^{ab}\right)$$

Equation 2.37

where $\alpha_f^{ab}$ is the firing rate of the auxiliary burner and $e^{ab}$ is an empirical coefficient.

Additionally, concerning the part-load performance, contrary to the main burner, the auxiliary burner does not have a control temperature signal that limits modulation. In this case, the maximum modulation rate is defined with respect to the thermal output, as follows:

$$\alpha_{t,min}^{ab} = \frac{\dot{Q}_{net,min}^{ab}}{\dot{Q}_{net,nom}^{ab}}$$

Equation 2.38

where $\dot{Q}_{net,min}^{ab}$ and $\dot{Q}_{net,nom}^{ab}$ are the minimum and maximum thermal power provided by the auxiliary burner in steady operation, respectively, which are experimentally determined.

Taking all this into account, the fuel power of the auxiliary burner, $\dot{F}_{ab}$, is determined as follows:

$$\dot{F}_{ab} = \begin{cases} \alpha_f^{ab} \cdot \dot{F}_{nom}^{ab} & \text{for } \alpha_t^{ab} \geq \alpha_{t,min}^{ab} \\ 0 & \text{for } \alpha_t^{ab} < \alpha_{t,min}^{ab} \end{cases}$$

Equation 2.39

## 2.2. Transient operation

Transient thermal behaviour of the generator is characterized by the thermal capacity of the engine block and the working fluid within, the internal heat exchanger, and the external combustor. The energy exchanges that take place during the operation modes described next can be determined by solving the specific equations defined for each mode together with Equation 2.1, Equation 2.2 and Equation 2.3.

### 2.2.1. Stand-by

Since Stirling engine-based micro-CHP units are generally thermally driven devices, when no heat is requested no activation signal is transferred to the electronic control unit (ECU) and the unit remains stand-by. Under this mode of operation, the unit does not consume any fuel nor produces any heat and electricity. Nevertheless, since the ECU is permanently active in order to respond to any activation request, some electricity is

required for these electronic controllers. Thus, during the standby-mode, the following equations govern the performance of the unit:

$$\dot{m}_{fuel} = \dot{m}_{fuel,standby} = 0$$

<div style="text-align: right">Equation 2.40</div>

$$\dot{Q}_{net} = \dot{Q}_{net,standby} = 0$$

<div style="text-align: right">Equation 2.41</div>

$$\dot{E}_{gross} = \dot{E}_{gross,standby} = 0$$

<div style="text-align: right">Equation 2.42</div>

$$\dot{E}_{net} = \dot{E}_{gross,standby} - \dot{E}_{net,standby}$$

<div style="text-align: right">Equation 2.43</div>

where $\dot{E}_{net,standby}$ is the power required by the ECU while awaiting activation during the stand-by mode.

These four equations are applicable to both the prime mover (Stirling engine) and the auxiliary burner.

Since under standby mode the fan and the pump are switched off, the effective heat transfer coefficients (Equation 2.5, Equation 2.6 and Equation 2.7) correspond only to natural convection. This way, they will significantly differ from those associated to steady operation, where forced convection is the predominant heat transfer mechanism.

$$UA_{eng} = UA_{eng\,standby}$$

<div style="text-align: right">Equation 2.44</div>

$$UA_{HX} = UA_{HX\,standby}$$

<div style="text-align: right">Equation 2.45</div>

$$[UA]_{loss}^{se} = [UA]_{loss\,stanby}^{se}$$

<div style="text-align: right">Equation 2.46</div>

Concerning the auxiliary burner, the model is structured so that, whenever it is off, no losses or thermal mass exist, and all the losses and inertia of the heat exchanger is exclusively associated to the heat exchanger control volume of the engine.

## 2.2.2.  Warm-up

The warm-up process differs from one energetic vector to another. Once the engine receives the activation signal and it is switched on, the fan starts introducing air into the burner and the head of the Stirling engine is heated up until its temperature is high enough to make the piston move and, therefore, the generator starts producing electricity. As this process must be as fast as possible, the fuel consumption during this phase grows exponentially and exceeds the nominal value required during the steady-state operation.

During this period, three phases can be distinguished. First, when the combustion process starts, in order to raise the temperature of the head of the engine, no effective heat or electricity production takes place. Then, once the thermal mass of the heat exchanger reaches a temperature broad enough to warm up the cooling water, heat production starts. It is not until the head of the Stirling engine gets a preset set-point temperature when the electricity production begins.

Concerning the fuel consumption, two main phases can be distinguished. First, as previously mentioned, once the engine switches on, the fuel consumed grows exponentially until the head of the engine gets a preset temperature, achieving a peak. Then, the consumption drops smoothly until its value achieves that of the steady operation.

As stated before, the start-up fuel consumption during the warm-up period, on a mass basis, is modelled as a function of the steady-state value and the relationship between the actual head temperature and the nominal head temperature at which the fuel peak occurs:

$$\dot{m}_{f,warmup}^{se} = \begin{cases} \dot{m}_{f,max}^{se} \cdot \left( 1 - e^{-\frac{T_{head}}{k_{f,1} \cdot T_{head,nom}^{start}}} \right) & \text{for } \boldsymbol{T_{head}} < \boldsymbol{T_{head,nom}^{start}} \\[4em] \dot{m}_{f,warmup,2}^{se} & \text{for } \boldsymbol{T_{head}} \geq \boldsymbol{T_{head,nom}^{start}} \end{cases}$$

Equation 2.47

where $\dot{m}_{f,max}^{se}$ is the maximum fuel mass flow during the warm-up, i.e. the nominal fuel flow at the given cooling water mass flow and temperature conditions multiplied by an overshooting factor, $k_{f,1}$ is an empirical coefficient indicative of the sensitivity of the fuel power to the temperature of the head of the engine, and $\dot{m}_{f,warmup,2}^{se}$ is the fuel consumption from the moment the peak consumption is achieved until the warm-up phase ends. This latter term, which tries to reproduce the typically underdamped control of the gas valve, is determined as follows:

$$
\begin{aligned}
\dot{m}_{f,warmup,2}^{se} = \dot{m}_{f,nom}^{se} + & \left[ \left( \dot{m}_{f,max}^{se} - \dot{m}_{f,nom}^{se} \right) + k_{f,2} \cdot \frac{T_{eng} - T_{eng}^{start}}{T_{eng,nom} - T_{eng}^{start}} \right] \\
& \cdot exp \left( -k_{f,3} \cdot \frac{T_{eng} - T_{eng}^{start}}{T_{eng,nom} - T_{eng}^{start}} \right)
\end{aligned}
$$

<div align="right">Equation 2.48</div>

where $k_{f,2}$ and $k_{f,3}$ are empirical coefficients indicative of the sensitivity of the fuel power to the temperature of the engine control mass.

Since the objective of such control is to adapt the electric power output to its nominal value while maintaining security conditions, the fuel mass flow was related to the temperature of the engine control mass, which is responsible of determining whether the warm-up phase is completed or not.

With respect to the net electricity production during the warm-up phase:

$$
\dot{E}_{net}^{se} =
\begin{cases}
-\left( \dot{E}_{standby} + \dot{E}_{fan}^{se} \right) & \text{for } \boldsymbol{T_{head}} < \boldsymbol{T_{start}^{e}} \\
\\
\dot{E}_{net,nom}^{se} \cdot \left[ 1 - k_{e,1} \cdot \left( T_{eng,nom} - T_{eng} \right) \right] & \text{for } \boldsymbol{T_{head}} \geq \boldsymbol{T_{start}^{e}}
\end{cases}
$$

<div align="right">Equation 2.49</div>

where $\dot{E}_{net,nom}^{se}$ is the net electricity power production at steady operation and $k_{e,1}$ is an empirical coefficient indicative of the sensitivity of the electric power during warm-up to the temperature of engine control volume.

Regarding the effective heat transfer coefficients, no distinction is made between steady operation and warm-up periods because the phenomena behind these heat transfer processes between control volumes can be treated in similar terms.

With respect to the auxiliary burner, once switched on the fuel power rises to nominal conditions, while the net electric energy consumption is the same that in steady-state conditions.

### 2.2.3.    Shut-down

Once the stop signal is transferred to the device, the fuel supply is immediately cut off. However, the device keeps on producing both electric and thermal energy during the shut-down period. In this period, different stages can be distinguished.

$$\dot{m}_f = \dot{m}_{f\,shutdown} = 0 \qquad\qquad \text{Equation 2.50}$$

Concerning the electricity production, once the engine is switched off, even though its value drops quickly, it keeps on active due to the inertia of the engine until the temperature of the hot side of the engine falls below certain value. This way, the electricity output during this period is modelled through a 3-stretches equation:

$$\dot{E}_{net}^{se} = \begin{cases} \dot{E}_{net,shut-down} & \text{for } T_{head} > T_{stop}^e \\[2mm] -\left(\dot{E}_{standby} + \dot{E}_{fan} + \dot{E}_{pump}\right) & \text{for } T_{stop}^q < T_{head} \leq T_{stop}^e \\[2mm] -\dot{E}_{standby} & \text{for } T_{head} \leq T_{stop}^q \end{cases} \qquad \text{Equation 2.51}$$

where the net electricity production during the first part of the shut-down, $\dot{E}_{net,shutdown}$, can be calculated through Equation 2.52:

$$\dot{E}_{net,shutdown} = \dot{E}_{gross,shutdown} - \left(\dot{E}_{standby} + \dot{E}_{fan} + \dot{E}_{pump}\right) \qquad \text{Equation 2.52}$$

The gross electricity production during the first part of the shut-down, $\dot{E}_{gross,shutdown}$, is modeled through a linear equation, as follows:

$$\dot{E}_{gross,shutdown} = k_{e,2} \cdot \left(T_{head} - T_{stop}^e\right)$$

The thermal production during the shut-down period takes place due to the fact that, even though the fuel supply is cut off, the fan of the device keeps on working and introducing air to the burner. So, it continues being heated up with the heat stored within the body of the engine and transferring such heat to the heat transfer fluid through the heat exchanger, prior to its expulsion through the exhaust duct.

Generally, these devices are provided with an internal control that, once the temperature of the hot side of the engine drops below certain pre-fixed value, makes both the fan and the circulation pump stop and so cease the heat production. However, if an external pump is employed, the recovery of the heat stored within the engine can be stretched on but, since the fan is already stopped, the heat recovered will be mainly that stored within the heat exchangers. This heat recovery can be determined by simultaneously solving Equation 2.1, Equation 2.2 and Equation 2.3.

On the other hand, micro-CHP units may halt due to high temperature protection. In these cases, as well as in those when the engine gets stopped through an external stop signal but before the engine switches to standby mode an activation signal is transferred to the device, it does not generally restart operation until the whole shut-down process is completed.

As far as effective heat transfer processes between control mass and volumes are concerned, once the shutdown period starts, as mentioned, the fuel consumption is cut off; consequently no exhaust gases flow through the device but only air. During this phase the fan is on and the air-to-fuel ratio is generally very high, i.e. no significant change in the mass flow is appreciated. Nevertheless, since it is the working fluid of the thermodynamic cycle who is responsible of absorbing heat from the hot reservoir (head control volume) and rejecting it to the cold source (heat exchanger control volume), $[UA]_{HX}$ and $[UA]_{eng}$ must necessarily differ from those proposed for warm-up and

steady operation modes. This is mainly due to the speed at which the engine moves in each phase and once the engine is switched off, the velocity of the working fluid of the cycle decreases with respect to the aforementioned modes of operation.

$$UA_{eng} = UA_{eng_{shutdown}}$$ <span style="float:right">Equation 2.54</span>

$$UA_{HX} = UA_{HX_{shutdown}}$$ <span style="float:right">Equation 2.55</span>

In the case of the auxiliary burner, once switched off, the fuel input is cut off, as well as the air-intake fan. In this point, the internal pump keeps on functioning, at a lower speed when internal controlled pumps are used, until the temperature difference between the outlet and the inlet of the cooling water drops below a certain value. However, since the auxiliary burner is usually used as backup of the Stirling engine, once no thermal support of the additional boiler is required, its burner will stop, but the pump and the fan will keep on working normally for the Stirling engine operation.

## 2.3. Switching between modes of operation

The mathematical model developed, according to the current state of the system, the corresponding external control signals and the operation constraints, determines the transition between operation modes. Thus, the logic of the model is schematized in Table 2.2 and Figure 2.5.

Table 2.2 – Main transitions between operating modes of the Stirling engine.

| Current mode | Future mode | Triggering |
|---|---|---|
| Standby | Warm-up: Phase 1 | Activation signal |
| Warm-up: Phase 1 | Warm-up: Phase 2 | $T_{head} \geq T_{start}^e$ |
| Warm-up: Phase 2 | Steady operation: full load | $T_{head} \geq T_{head}^{nom}$ |
| Steady operation: full load | Steady operation: part load | $T_{cw,o}^{se} \geq T_{cw,o}^{sp}$ |
| Steady operation: part load | Shut-down: Phase 1 | $T_{cw,o}^{se} \geq T_{cw,o}^{se} + \Delta T$ |
| Cool-down: Phase 1 | Shut-down: Phase 2 | $T_{head} \leq T_{stop}^e$ |
| Cool-down: Phase 2 | Standby | $T_{head} \leq T_{stop}^t$ |
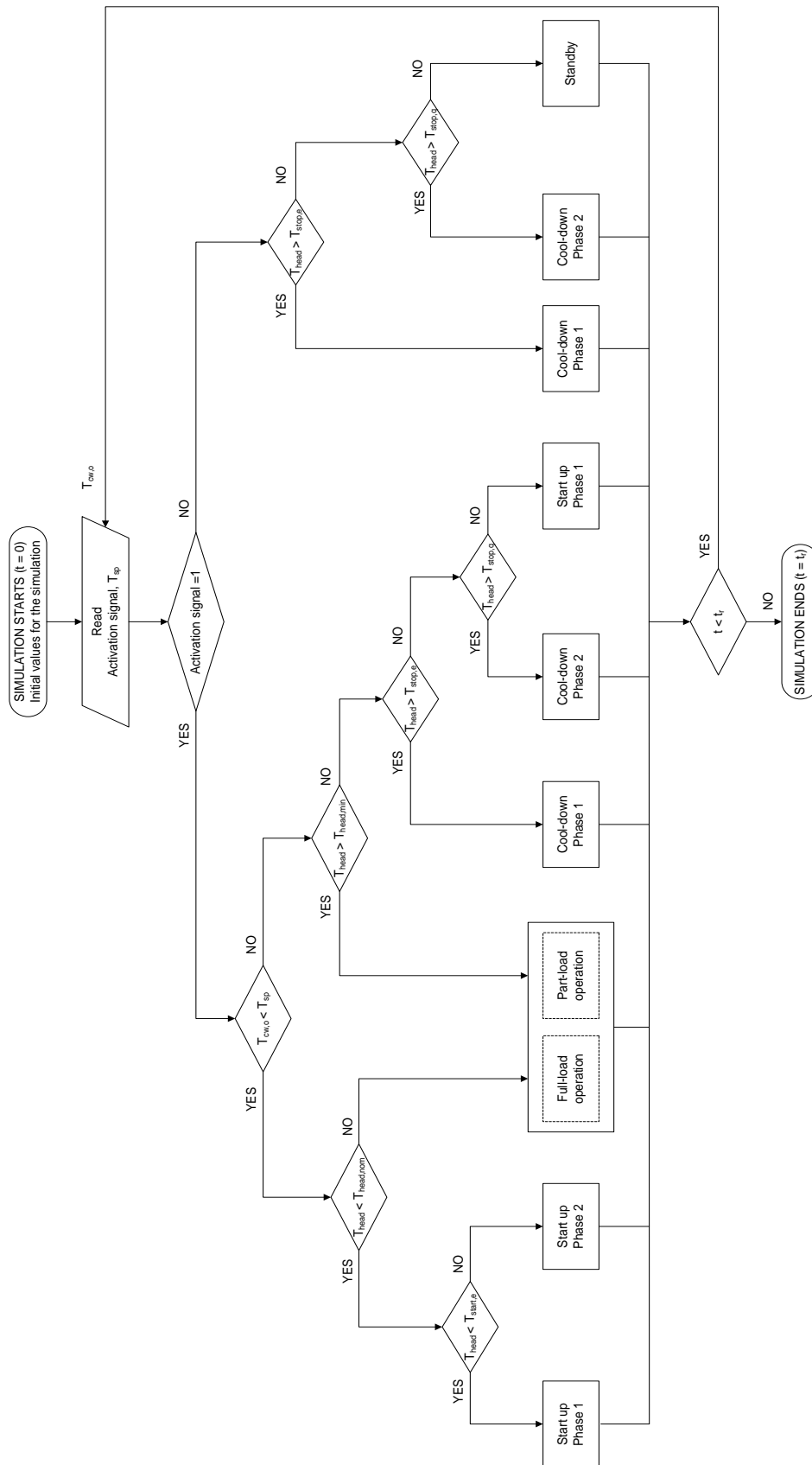
Figure 2.5 – Flow diagram of the resolution scheme of the engine model proposed.

The unit will initially stay uninterruptedly in standby mode as far as no activation signal associated to a heat demand is transferred to the ECU. Once this signal is received, the model must switch and make the operation mode change to warm-up. The warm-up mode, split into two sub-phases, will persist until the nominal engine temperature is reached.

Once the warm-up mode lapses, the engine will start steady operation, initially at full load, which will persist indefinitely unless any of the constraints listed in Table 2.2 are applied. From this state, the model can transit to one out of two different modes of operation: steady operation at part load if the outlet cooling water temperature exceeds the set-point value (this should be the following mode if the control of the installation is defined properly), or shut-down if a deactivation signal is transferred.

If the system changes its firing rate in order to modulate its load, this mode will persist until the flow temperature exceeds the set-point temperature (considering the pre-fixed hysteresis) or the heat demand increases needing for full load operation.

When shut-down mode is reached, this period generally lasts until it lapses, i.e. the model must complete the cool-down period before it can be reactivated again. Once this shut-down period is completed, depending on the on/off signal, it will come into standby mode or, otherwise, the warm-up period will commence.

In Figure 2.5 the flow diagram of the resolution scheme of the model proposed for the SE is presented. Since the model does not include the internal control which governs the auxiliary burner, the operation of both generators is separately treated. This way, the auxiliary burner will operate whenever it receives an external activation signal, and the cooling water outlet temperature, $T_{cw,o}^{ab}$ is obtained by solving Equation 2.4.

# 3. Experimental evaluation

## 3.1. Stirling micro-CHP unit

As presented and argued in detail in the case study of Chapter 3, the Remeha eVita micro-CHP unit was targeted as object of study.

### 3.1.1. Description of the micro-CHP unit

The Remeha eVita is a wall-mounted natural gas-run Stirling engine-based boiler, made of a linear free-piston Stirling engine manufactured by Microgen (MEC), which provides 5 $kW_t$ and 1 $kW_e$ for base loads, and an additional burner for peak loads up to 23 $kW_t$. Both burners are condensing and modular.

Two versions of the unit are available, 25s and 28c, which only differ on that the latter is a combi-boiler that possesses the same heating characteristics than the first but also includes an internal plate heat exchanger and an associated 3 way-valve for instantaneous DHW production, as described later on. The main technical characteristics of both versions are summarized in the data sheet attached in Appendix B.

For developing the work of this PhD Thesis, the 28c version was installed, but the DHW exchanger was put out of service since, in order to maximise the operation time of the engine and as discussed in Chapter 3, no direct DHW production was contemplated along the PhD Thesis.
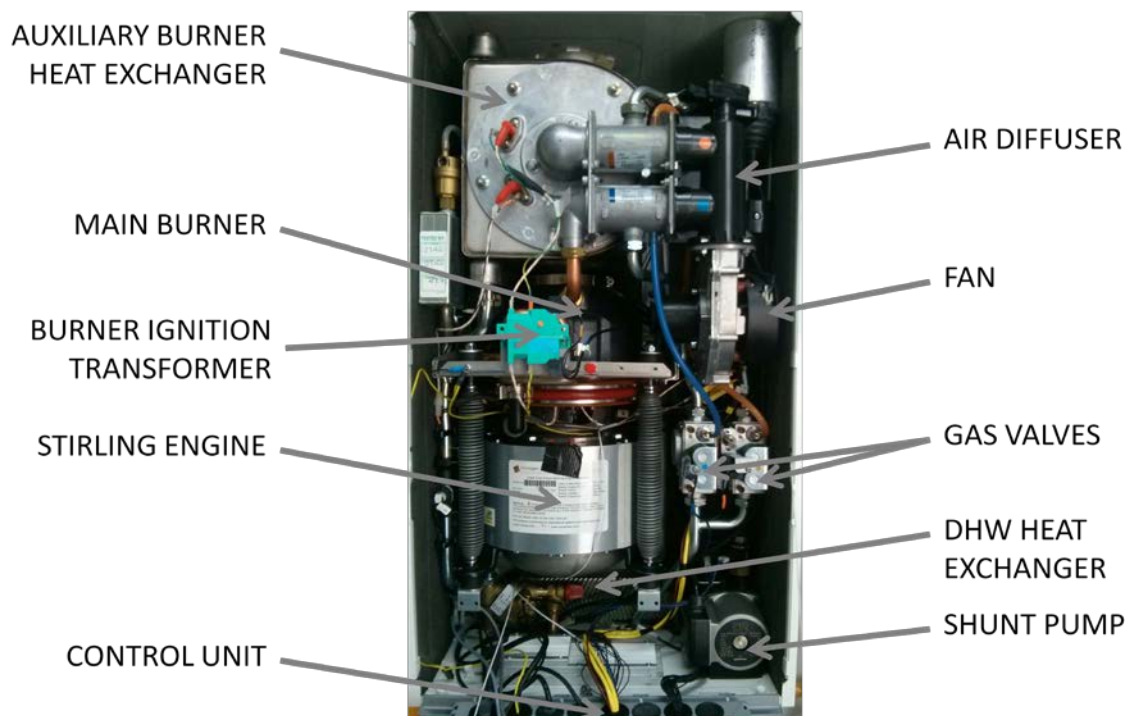


Figure 2.6 – Main subsystems of the Remeha eVita 28c Stirling micro-CHP unit.

This kind of systems, as described by Thombarse (Thombarse, 2008) in detail, is generally composed of the subsystems represented in Figure 2.6 and described next.

### 3.1.1.1. Energy input

The unit is fitted with two burners, as represented in Figure 2.6 and Figure 2.7: a main burner, which is the first to come into service and acts as the hot reservoir of the Stirling cycle, and an auxiliary burner, which operates as backup of the main burner when heating demand gets increased. Both burners are managed by an automatic control integrated within the ECU (7)[2].

While the main burner assembly is a single nozzle and induced-draught type, the auxiliary burner, for its part, is a cylindrical pre-mix gas burner sited at the heat exchanger (3). Fuel flows through the gas intake (19) to the combined gas valves of the engine-burner (28) and the auxiliary-burner (29). These units contain the gas supply solenoid valve of each burner, responsible of controlling the air-to-fuel ratio, and a gas pressure measuring device. Fuel is then sucked into the Venturi burners (23 and 25) where, once mixed with the oxidizing air, the mixture is supplied to the head of the Stirling engine (10) and the heat exchanger (3) where both main and auxiliary burners are sited, respectively.

Both burners are installed inside an enclosure that operates as a sealed air box (2). The disposed suction fan (26) draws air through the outer annular space concentric to the smoke nozzle (1) into the enclosure and makes it circulate through the casing prior to its distribution to both Venturi burners (23 and 25), located on the outlet side of the fan, where air and fuel are mixed.

Combustion takes place in the head of the Stirling engine (10) and the condensing heat exchanger (3) where the auxiliary burner is sited. Heat released by the combustion which takes place in the head of the Stirling engine constitutes the hot reservoir of the thermodynamic cycle. Afterwards, combustion gases pass through the heat exchanger (3) where, together with the combustion gases of the auxiliary burner if this latter operates, exchange sensible heat with the cooling water, as well as latent heat if the

---

[2] Numbers in brackets refer to the different parts of the micro-CHP unit marked in Figure 2.7.

temperature level of the water is below the dew point of the flue gases, before being conducted to the gas evacuation nozzle (8). The condensation water is evacuated through the condensation channel (11) to the evacuation hose (15) located at the siphon outlet.
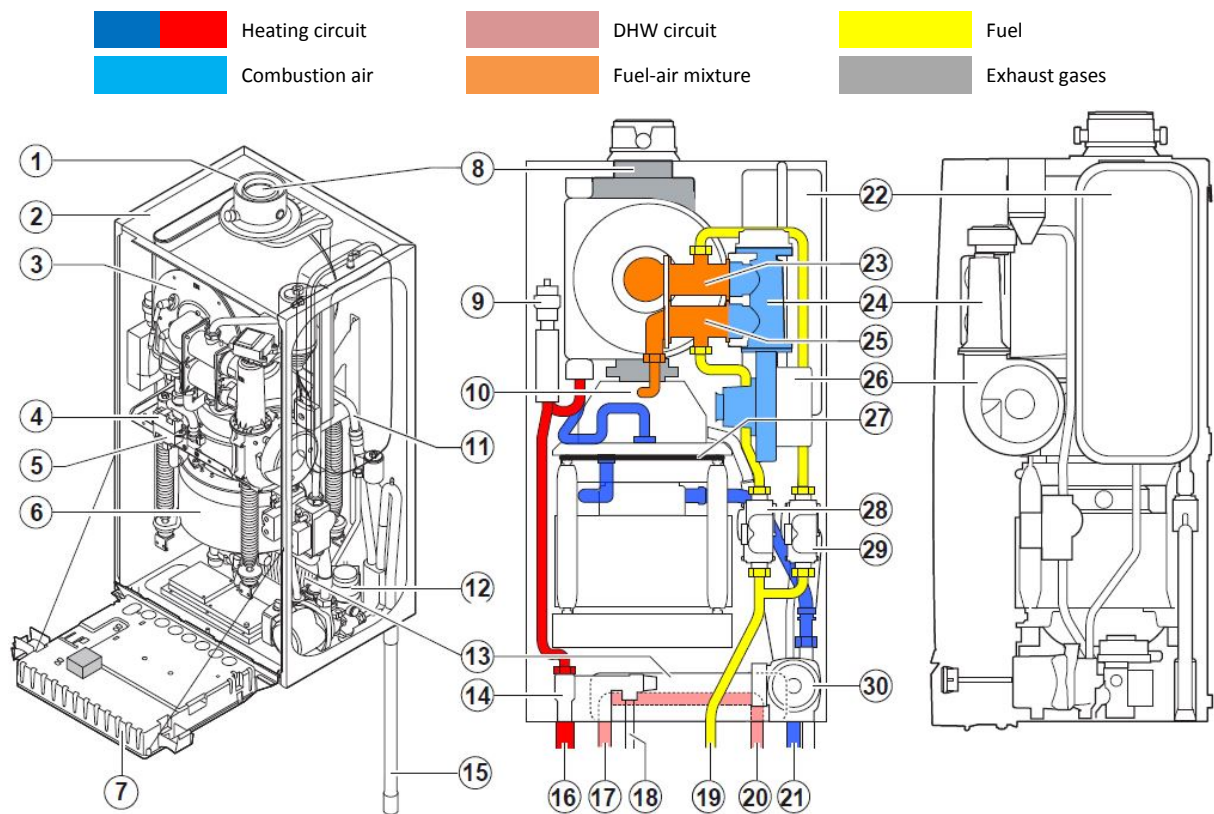
| | Heating circuit | | DHW circuit | | Fuel |
|---|---|---|---|---|---|
| | Combustion air | | Fuel-air mixture | | Exhaust gases |

| | | | | | |
|---|---|---|---|---|---|
| **1** | Air intake | **11** | Condensation channel | **21** | Heating return |
| **2** | Casing / Air box | **12** | Three-way valve[3] | **22** | Expansion vessel |
| **3** | Heat exchanger front plate | **13** | Plate heat exchanger[3] | **23** | Auxiliary Venturi burner |
| **4** | Auxiliary burner ignition transformer | **14** | Hydrobloc | **24** | Air diffuser |
| **5** | Engine burner ignition transformer | **15** | Siphon outlet / Condensate evacuation hose | **25** | Engine's Venturi burner |
| **6** | Stirling engine | **16** | Heating flow | **26** | Fan |
| **7** | Instrument box (ECU) | **17** | DHW outlet | **27** | Water cooled seal |
| **8** | Smoke nozzle | **18** | Safety valve flow pipe | **28** | Combined engine-burner gas valve unit |
| **9** | Automatic air vent | **19** | Gas connection | **29** | Combined auxiliary-burner gas valve unit |
| **10** | Head of the Stirling engine / Main burner | **20** | DHW inlet | **30** | Shunt pump |

Figure 2.7 – Schematic representation of the Remeha eVita 28c Stirling micro-CHP unit[4].

---

[3] Only on the model with DHW production.

### 3.1.1.2. Thermal output

As far as cooling water is concerned, it flows into the unit through the heating inlet (21) to the internal shunt pump (30). The latter conducts the water to the heat exchanger of the Stirling engine block (between 6 and 10), constituting the cold reservoir of the thermodynamic cycle. Then, water flows circularly through a plate in order to keep the silicon joint cool and so guarantee the union of the two sides of the Stirling engine (27). Afterwards, it flows through the tubes of the plate heat exchanger (3) where heat transfer between the exhaust gases and the water occurs. It is in this phase when, by the recovery of sensible and latent heats of the exhaust gas, the water undergoes the greater thermal gradient and, consequently, the majority of the thermal recovery takes place. Finally, after passing through an automatic air vent (9), the heated cooling water flows through a safety hydrobloc (14) before leaving the unit via the heating outlet (16). An internal expansion vessel is connected to the water circuit (22).

On heating and DHW production type boilers, DHW may be instantaneously produced by means of an integrated plate exchanger (13). In such case, the circuit previously described is supplemented by a three-way valve (12) that determines whether the heated water is fed into the heating system or the plate exchanger. When the pick-up sensor detects that a hot water tap is being opened, the signal is transmitted to the control panel (7), which then activates the supplementary burner and switches the three-way valve – controlled on an all or nothing basis – to the hot water position, prioritising its supply and so heating up the counter-flow DHW from the inlet (20) to the outlet (17).

### 3.1.1.3. Electric output

The boiler is fitted with a single-cylinder Stirling engine (6) that functions by the repeated heating and cooling of a quantity of pressured helium inside the cylinder. The gas is heated at the top of the cylinder (10) and cooled by water at the base of the cylinder (between 6 and 10); the pressure difference thus created drives a piston which moves from the top to the bottom, as deeply explained in Section 2.2.3 of Chapter 1. The piston is fitted with magnets which are driven through a fixed coil which convert the

---

[4] Figure adapted from the eVita 25s-28c Installation and Service Manual by Remeha.

reciprocating motion of the piston into an alternating current with a frequency of 50 cycles per second (Hz). It is the alternator who, connected to a 230 $V_{AC}$ electrical circuit, acts as the engine starter.

## 3.1.2. Operation and regulation of the micro-CHP unit

Based upon experimental testing of the micro-CHP unit, together with information obtained from the manufacturer and, principally, from a previous research by Andlauer (2011) over a similar device, the internal control of the unit was deduced, considering the integration of both generators.

It is the ECU who manages the operation and regulation of the system and monitors the different variables and timings of the system. Once the unit gets activated, the main regulation of the unit is based on the hot water supply temperature, established as a set-point. The internal control adjusts the flow temperature based on the comfort temperature set by the user.

When a heat demand signal is received, as depicted in Figure 2.8, the Stirling engine burner is the first to come into service and, through the combustion gases, starts heating up the head of the engine.
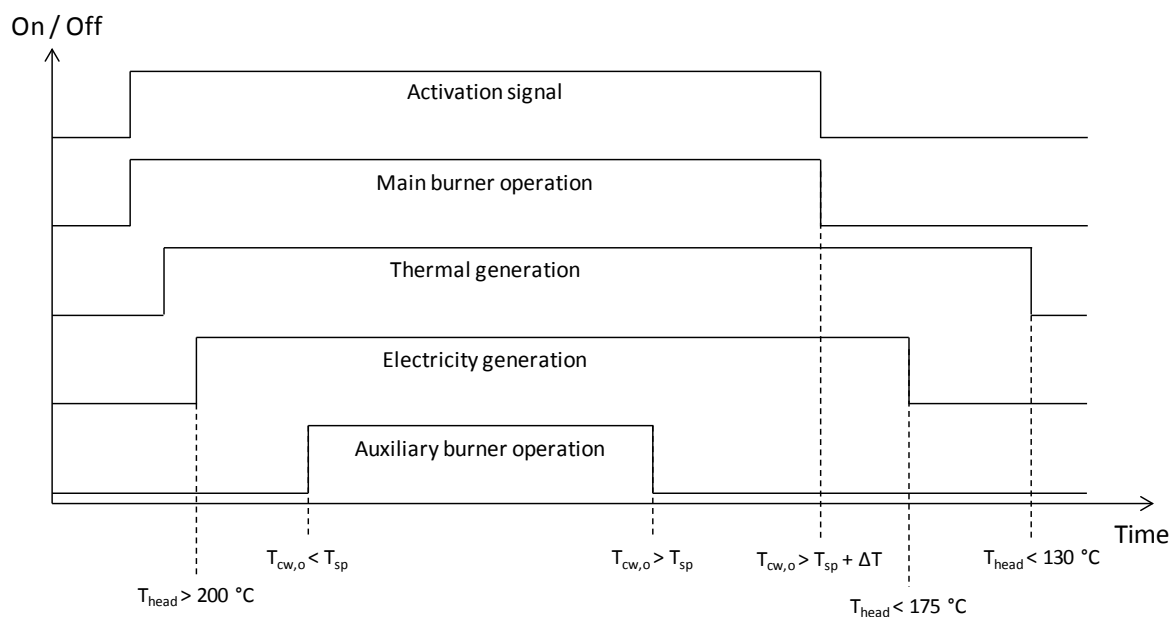


Figure 2.8 – Operation sequence of the Remeha eVita Stirling micro-CHP unit (adapted from Andlauer (2011)).

At a preset temperature of 200 °C, previously defined in the model as $T_{start}^e$, the engine starts running and supplying electricity. In parallel, the unit also supplies heat by means of heat transfer from the exhaust gases to the circulating water, as well as from recovering waste heat from the jacket of the engine.

Depending on the quantity of heat required, directly related to the cooling water temperature, the heat management system can switch on the auxiliary burner to supply additional heat. The auxiliary burner is configured by default in order start working at minimum load, afterwards elevating its firing rate ($\alpha_f^{ab}$) if more heat is required.

The main burner is also modulating, so that when the heat produced equals that demanded the regulation system changes the firing rate of the burner, $\alpha_f^{se}$, in order to adjust the temperature of the water flow to that established as set-point. The burner can be modulated until the temperature of the head of the engine falls below 400 °C ($T_{head,min}$). Once this temperature is reached, the temperature of the cooling water at the outlet of the device will be greater than the set-point, so giving rise to a temperature hystheresis ($\Delta T$), and it will switch off.

On the other hand, whenever the engine receives a deactivation order, both by an external stop signal which is sent to the device or by temperature deactivation, the fuel supply is cut off, but the device keeps on producing electric energy until the temperature of the hot side of the engine falls below 175 °C ($T_{stop}^e$). As far as the thermal production is concerned, once the unit is switched off, the air-intake fan and the internal circulation pump keep on working and thus recovering useful heat until the shut-down process ends and the temperature of the head of the LFPSE falls below 130 °C ($T_{stop}^q$).

On the other hand, the internal pump of the system is regulated in order to maintain the temperature difference between the outlet and the inlet of the heating circuit below 10 °C. For this purpose, this pump is speed-variable with three levels, so that when the temperature difference is to exceed the preset security value the circulator jumps to a greater speed-stage (see Figure 2.9) and when the water flow falls below 7 l/min the pump will return to a higher stage in order to overcome hydraulic pressure losses. Thus, when only the main burner is on, the pump will normally remain on its first stage,

switching to the second one when the auxiliary burner turns on at minimum load, and jumping to the third stage when the auxiliary burner increments its firing rate. Additionally, whenever the volumetric flow is below 3 l/min the unit stops due to security reasons.
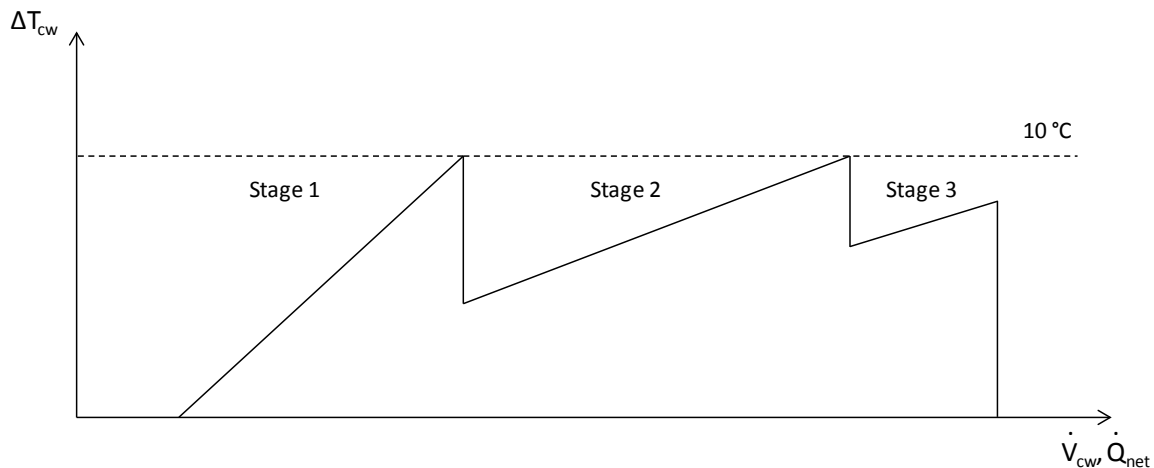


Figure 2.9 – Cooling water flow regulation principle of the Remeha eVita Stirling micro-CHP unit (adapted from Andlauer (2011)).

Finally, concerning the security associated to the electric side of the device, as explained by Andlauer (2011), the engine is permanently regulated in order to maintain an apparent electrical output of 1 kVA. For that purpose, the controllable variable is the air flow, by means of regulating the rotation speed of the air intake fan and the position of the air shutter of the burner. The air flow variation carries variation in the fuel flow entering the premix venture, and, consequently, the temperature of the head of the engine. This way, the temperature of the hot side of the engine is maintained between 400 (at minimum load) and 520 °C (at full load).

## 3.2. Experimental routine

According to the specification and requirements previously defined for the modelling, a testing routine for obtaining the required data for calibrating and validating such model was developed. These tests were developed in an experimental facility sited at the Laboratory for the Quality Control in Buildings (LCCE) of the Basque Government

(Departamento de Medio Ambiente, Planificación Territorial y Vivienda, 2018), so that, all the phenomena and conditions could be controlled and evaluated.

The Stirling micro-CHP unit was integrated within a wide experimental facility developed with the purpose of being able to test energy conversion technologies not only individually but also joint with other components, so giving raise to hybrid installations. The description of the whole installation has been extracted from this chapter for the sake of clarity, and is presented in Appendix C.

As previously defined, the target unit of the study is a wall mounted natural gas-run Stirling engine-based micro-CHP boiler by Remeha. It is made of a free-piston 5 $kW_t$ and 1 $kW_e$ Stirling engine for base loads, and an additional boiler for peak loads up to 25 $kW_t$. Both prime movers, which are condensing and modular, were separately tested and characterized, and their joint performance was afterwards considered in the model developed.

For characterizing both the Stirling engine and the additional condensing boiler, amongst all the modules of the experimental plant described in Appendix C, three were utilized. On the one hand, the high temperature module, where the tested unit is integrated; on the other hand, the external flow pump in the name of the distribution loop and, finally, the heating module, where the produced heat was released in order to maintain the operation conditions required.

In order to maintain a constant return temperature of the cooling water and, consequently, reach steady-state conditions and study the influence this temperature has on the final performance of the micro-CHP unit, a three-way valve was disposed. Additionally, to be able to govern the cooling water mass flow and test different flow-rates, a 3-stage external pump was installed together with the internal one contained in the boiler, which was disabled.

Based upon previous experimental researches and the implicit necessities of the model presented within this chapter, the measure points specified in Table 2.3 and described next were projected.

Table 2.3 – Summary of the main variables measured.

| Variable group | Measure | Symbol | Measuring description | Units |
|---|---|---|---|---|
| Electricity | Net power | $\dot{E}_{net}$ | Input and output power measured with an electricity meter | W |
| | Gross power | $\dot{E}_{gross}$ | Internal measurement | W |
| Natural gas | Volumetric flow | $\dot{V}^{\circ}_{fuel}$ | Fuel flow in normal conditions measured with a gas counter | Nm³ |
| | Temperature | $T_{fuel}$ | Measured with a thermo-hygrometer | °C |
| | Pressure | $p_{fuel}$ | Measured with a manometer | mbar |
| | LHV | $LHV^{\circ}_{fuel}$ | Measurements and information of the gas distributor[5] | kWh/ Nm³ |
| Ambient features | Temperature | $T_{amb}$ | Measured with a thermo-hygrometer | °C |
| | Relative humidity | $p_{amb}$ | | % |
| Water circuit | Inlet temperature | $T_{cw,i}$ | Measured with thermocouples | °C |
| | Outlet temperature | $T_{cw,o}$ | | °C |
| | Volumetric flow | $\dot{V}_{cw,o}$ | Measured with an electromagnetic flow-meter | l/h |
| Exhaust gas | Volumetric flow | $\dot{V}_{exh}$ | | l/min |
| | Temperature | $T_{exh}$ | | °C |
| | Pressure | $p_{exh}$ | | hPa |
| | Air excess | $\lambda_{air}$ | | % |
| | O₂ content | $O_2$ | | % |
| | CO content | $CO$ | Measured with a gas analyzer | ppm |
| | CO₂ content | $CO_2$ | | % |
| | NO content | $NO$ | | ppm |
| | NO₂ content | $NO_2$ | | ppm |
| | NOₓ content | $NO_x$ | | ppm |
| | H₂ content | $H_2$ | | ppm |
| | Combustion efficiency | $\eta_{comb}$ | | % |
| Others | Engine-head temperature | $T_{head}$ | Internal measurement | °C |
| | Engine-block surface temperature | $T_{surf}$ | Internal measurement / Measured with thermocouples | °C |

[5] The natural gas composition was not measured straightaway in the laboratory. Continuous measurements were carried out nearby and the LHV obtained with those compositions was checked and compared to that provided by the gas distribution company for the station which feeds the laboratory.

In order to determine the main energy flows accurately, several low-uncertainty gauges were set up around the Stirling device, as detailed in the simplified hydraulic diagram in Figure 2.10 and its picture in Figure 2.11.

Thus, apart from measuring both gross and net electricity productions, as well as the fuel consumption, PT-100 resistance temperature detectors and electro-magnetic flow meters were installed for calculating the thermal power produced, as follows:

$$\dot{Q}_{net} = \rho_{cw,o} \cdot \dot{V}_{cw,o} \cdot C_{cw} \cdot (T_{cw,o} - T_{cw,i})$$

Equation 2.56

where $\dot{Q}_{net}$ is the net thermal output of the unit, $\rho_{cw,o}$ is the density of the outlet cooling water, and $C_{cw}$ is the specific heat of the cooling water.
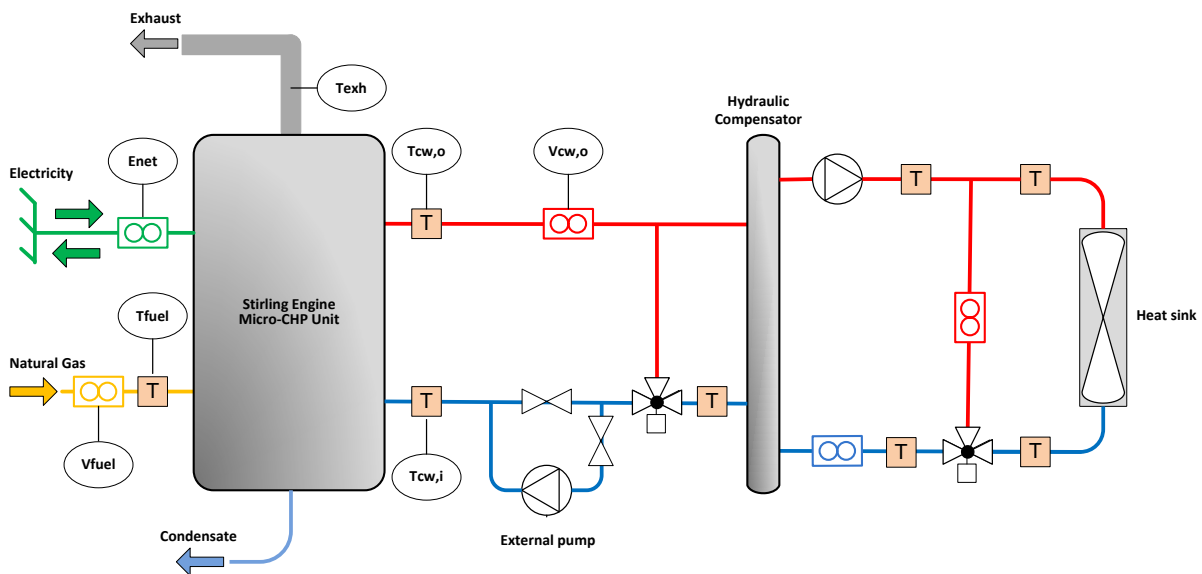


Figure 2.10 – Simplified hydraulic principle diagram of the Stirling engine test rig.

With respect to the fuel consumption, the power required by the device is obtained based on the reading of the experimental dry-system counter disposed and the heating capacity of the fuel, both in normal conditions:

$$\dot{F} = \dot{V}_{fuel}^{\circ} \cdot LHV_{fuel}^{\circ}$$

Equation 2.57
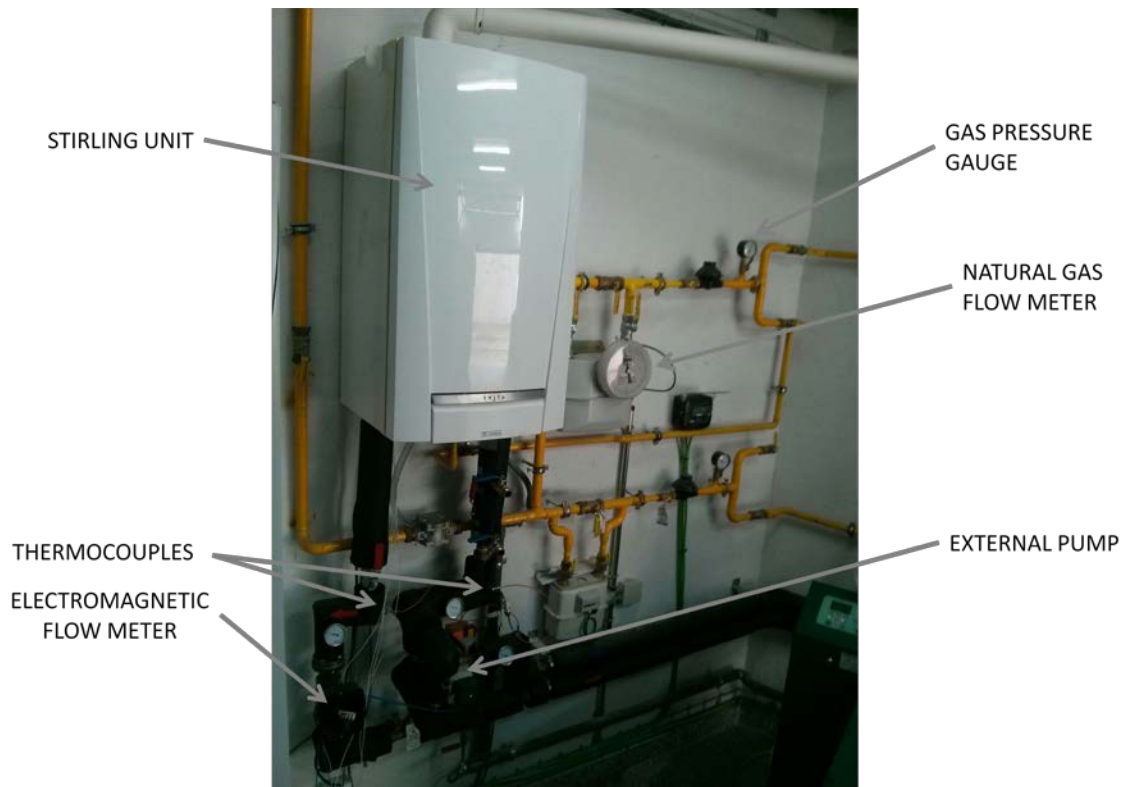
Figure 2.11 – Picture of the Stirling engine test rig.

The fuel components, corresponding to natural gas, obtained from a gas chromatograph operating throughout a whole year, are those given in Table 2.4.

Table 2.4 – Mean fuel volumetric composition measured during 2016.

| Component | Chemical formula | Mean composition (%) |
|---|---|---|
| Nitrogen | $N_2$ | 1.1230 |
| Carbon dioxide | $CO_2$ | 1.2761 |
| Methane | $CH_4$ | 89.1626 |
| Ethane | $C_2H_6$ | 7.1976 |
| Propane | $C_3H_8$ | 0.9923 |
| Isobutane | $C_4H_{10}$ | 0.0960 |
| n-butane | $C_4H_{10}$ | 0.1119 |
| Isopentane | $C_5H_{12}$ | 0.0232 |
| n-pentane | $C_5H_{12}$ | 0.0139 |
| Hexane | $C_6H_{14}$ | 0.0034 |

The electric power was measured by an electricity meter which allows determining the net electricity produced by the Stirling engine, as well as the consumption of the auxiliaries of the unit and the unit in stand-by mode itself.

The determination of the uncertainties of these three measurements, are described in detail in the next section.

Additionally, due to the impossibility of getting some information related to the functioning of the unit by means of external measurements, information of some internal variables measured by the unit for its own regulation were utilized. This information was acquired by using a communication interface by Siemens between the micro-CHP unit and the PC where all other data from the PLC were collected. This way, values of the temperature of hot-side of the engine, as well as the gross electricity output, amongst other, could be obtained.

## 3.3. Propagation of uncertainties

Each of the three aforementioned energy input and output is obtained through the usage of high precision instrumentation. Despite this high precision, every measurement involves an uncertainty that is reflected in the final calculation of energy flows. Such global uncertainty was evaluated according to the Guide to the Expression of Uncertainty in Measurement (Bureau International des Poids et Mesures et al., 1995).

The uncertainty of a magnitude, whose measurement is made of several un-correlated input magnitudes, can be obtained through the law of uncertainty propagation:

$$u_y = \sqrt{\sum_{i=1}^{N} \left(\frac{\partial f}{\partial x_i}\right)^2 \cdot u_{x_i}{}^2} \qquad \text{Equation 2.58}$$

where $u_y$ is the combined uncertainty of the indirect measurement of $y$, $f$ is the function that relates the variable $y$ with the input magnitudes $x_1 \dots x_N$, $u_{x_i}$ is the standard uncertainty of the $x_i$ measurement, and $\frac{\partial f}{\partial x_i}$ is the sensitivity coefficient.

On the other hand, the relative combined uncertainty in percentage, $u_y/y$, is obtained through an equation employed for multiplicative models of uncorrelated measurements:

$$\frac{u_y}{y} = \sqrt{\sum_{i=1}^{N} \left[\frac{u_{x_i}}{x_i}\right]^2}$$

Equation 2.59

### 3.3.1. Electric energy

In the case of electricity, whose power is measured straightaway through the usage of a CIRCUTOR CVM-1D-RS-485-C network analyzer, the uncertainty of this energy flow is directly related to the precision of the instrument, i.e. $\pm1\%$ for the active power in the utilized meter.

### 3.3.2. Fuel consumption

With respect to fuel power consumption, natural gas in the current work, it was calculated as set in Equation 2.21, since the fuel consumption was measured indirectly, based on the measurement of its volumetric flow and LHV (this latter value provided by the gas company):

$$u_{\dot{F}} = \sqrt{\left(\frac{\partial \dot{F}}{\partial \dot{V}_{fuel}}\right)^2 \cdot u_{\dot{V}_{fuel}}{}^2 + \left(\frac{\partial \dot{F}}{\partial LHV_{fuel}}\right)^2 \cdot u_{LHV_{fuel}}{}^2}$$

Equation 2.60

The volumetric flow was determined through a high precision flow meter, whose maximum error is $\pm0.5\%$, which is afterwards transformed into energy by means of the LHV. The relative uncertainty associated to the measurement of the LHV ($u_{LHV_f,\%}$) is typically considered to be of 5% when using the value provided by the local gas carrier (Carotenuto et al., 2005; Dentice d'Accadia and Musto, 2011).

$$\frac{u_{\dot{F}}}{\dot{F}} = \sqrt{\left(\frac{u_{\dot{V}_{fuel}}}{\dot{V}_{fuel}}\right)^2 + \left(\frac{u_{LHV_{fuel}}}{LHV_{fuel}}\right)^2}$$

Equation 2.61

All this turns into an uncertainty value for the fuel power consumption of 0.958%.

### 3.3.3. Thermal energy

Concerning the thermal power of the micro-CHP unit, it is obtained as the product of the cooling water mass flow rate and its enthalpy variation between the outlet and the inlet:

$$\dot{Q}_{net} = \dot{m}_{cw} \cdot \Delta h_{cw} = \rho_{cw,i} \cdot \dot{V}_{cw,i} \cdot \Delta h_{cw}$$

Equation 2.62

Thus, the uncertainty of the thermal power is calculated as the standard combined measurement of the volumetric flow, the density, and the enthalpy variation:

$$u_{\dot{Q}_{net}} = \sqrt{\left(\frac{\partial \dot{Q}_{net}}{\partial \dot{V}_{cw,i}}\right)^2 \cdot u_{\dot{V}_{cw,i}}{}^2 + \left(\frac{\partial \dot{Q}_{net}}{\partial \rho_{cw,i}}\right)^2 \cdot u_{\rho_{cw,i}}{}^2 + \left(\frac{\partial \dot{Q}_{net}}{\partial \Delta h_{cw}}\right)^2 \cdot u_{\Delta h_{cw}}{}^2}$$

Equation 2.63

Solving the partial derivatives and rearranging:

$$u_{\dot{Q}_{net}} = \dot{Q}_{net} \cdot \sqrt{\frac{u_{\dot{V}_{cw,i}}{}^2}{\dot{V}_{cw,i}{}^2} + \frac{u_{\rho_{cw,i}}{}^2}{\rho_{cw,i}{}^2} + \frac{u_{\Delta h_{cw}}{}^2}{\Delta h_{cw}{}^2}}$$

Equation 2.64

The relative combined uncertainty of the heat produced by the micro-CHP unit is, consequently:

$$\frac{u_{\dot{Q}_{net}}}{\dot{Q}_{net}} = \sqrt{\left(\frac{u_{\dot{V}_{cw,i}}}{\dot{V}_{cw,i}}\right)^2 + \left(\frac{u_{\rho_{cw,i}}}{\rho_{cw,i}}\right)^2 + \left(\frac{u_{\Delta h_{cw}}}{\Delta h_{cw}}\right)^2}$$

Equation 2.65

The volumetric flow was measured through a MJK MagFlux flow meter, with an uncertainty of $\pm 0.1\%$. The uncertainty of the enthalpy variation of the cooling water was calculated taking into consideration that it is the result of the product of the specific heat and the temperature of the cooling water.

The typical pressure range in domestic heating and DHW applications does not show any dependence on the density and the specific heat of the cooling water on the working pressure; thus, it can be considered to be negligible. Consequently, while the specific heat of the water was modelled through Equation 2.11, the density was calculated according to the following equation:

$$\rho_{cw} = 14.9 \cdot 10^{-6} \cdot T_{cw}{}^3 - 57.2 \cdot 10^{-4} \cdot T_{cw}{}^2 + 68.3 \cdot 10^{-4} \cdot T_{cw} + 1000.22$$

<div align="right">Equation 2.66</div>

Due to the low variation of the specific heat throughout the temperature jump suffered by the cooling water within the micro-CHP unit, enthalpy variation was calculated by means of constant specific heats for outlet and inlet conditions:

$$\Delta h_{cw} = \int_{T_{cw,i}}^{T_{cw,o}} c_{cw} \cdot dT_{cw} = c_{cw} \cdot \left(T_{cw,o} - T_{cw,i}\right)$$

<div align="right">Equation 2.67</div>

Accordingly:

$$u_{\Delta h_{cw}} = \sqrt{\left(\frac{\partial \Delta h_{cw}}{\partial c_{cw}}\right)^2 \cdot u_{c_{cw}}{}^2 + \left(\frac{\partial \Delta h_{cw}}{\partial T_{cw,o}}\right)^2 \cdot u_{T_{cw,o}}{}^2 + \left(\frac{\partial \Delta h_{cw}}{\partial T_{cw,i}}\right)^2 \cdot u_{T_{cw,i}}{}^2}$$

<div align="right">Equation 2.68</div>

$$u_{\Delta h_{cw}} = \Delta h_{cw} \sqrt{\frac{u_{c_{cw}}{}^2}{c_{cw}{}^2} + \frac{u_{T_{cw,o}}{}^2}{T_{cw,o}{}^2} + \frac{u_{T_{cw,i}}{}^2}{T_{cw,i}{}^2}}$$

<div align="right">Equation 2.69</div>

The uncertainty of the temperature depends on the uncertainty of the temperature sensors employed: PT100 1/10 with ±0.1% uncertainty in the tests presented in this paper. Meanwhile, those uncertainties associated to specific heats and densities can be considered to be negligible (Rosato and Sibilio, 2013). Consequently, the uncertainty due to the indirect measurement of the enthalpy variation:

$$\frac{u_{\Delta h_{cw}}}{\Delta h_{cw}} = \sqrt{\frac{u_{T_{cw,o}}{}^2}{T_{cw,o}{}^2} + \frac{u_{T_{cw,i}}{}^2}{T_{cw,i}{}^2}}$$

Equation 2.70

### 3.3.4. Efficiencies

On the other hand, uncertainties of both electric and thermal efficiencies of the micro-CHP device are respectively calculated as follows:

$$u_{\eta_Q} = \sqrt{\left(\frac{\partial \eta_Q}{\partial \dot{F}}\right)^2 \cdot u_F{}^2 + \left(\frac{\partial \eta_Q}{\partial \dot{Q}}\right)^2 \cdot u_Q{}^2} = \sqrt{\left(-\frac{\dot{Q}}{\dot{F}^2}\right)^2 \cdot u_F{}^2 + \left(\frac{1}{\dot{F}}\right)^2 \cdot u_Q{}^2} =$$

$$= \eta_Q \cdot \sqrt{\frac{u_F{}^2}{\dot{F}^2} + \frac{u_Q{}^2}{\dot{Q}^2}}$$

Equation 2.71

$$u_{\eta_E} = \eta_E \cdot \sqrt{\frac{u_F{}^2}{\dot{F}^2} + \frac{u_E{}^2}{\dot{E}^2}}$$

Equation 2.72

Additionally, taking into consideration that the overall efficiency of the micro-CHP unit is indirectly measured, its uncertainty must be calculated from the combination of the individual standard uncertainties of the fuel consumption, and the electricity and heat productions of the device. Since no correlation exists among the measurement of these magnitudes, the uncertainty of the overall efficiency of the production device is determined with the error propagation method:

$$u_\eta = \sqrt{\left(\frac{\partial \eta}{\partial \dot{F}}\right)^2 \cdot u_F{}^2 + \left(\frac{\partial \eta}{\partial \dot{Q}}\right)^2 \cdot u_Q{}^2 + \left(\frac{\partial \eta}{\partial \dot{E}}\right)^2 \cdot u_E{}^2}$$

Equation 2.73

As the overall efficiency is the sum of the electric and thermal efficiencies, its relative uncertainty can be calculated as follows:

$$u_{\eta_{global},\%} = \sqrt{u_{\eta_Q,\%}{}^2 + u_{\eta_E,\%}{}^2}$$

Equation 2.74

Thus, relative uncertainties calculated for fuel, electric and thermal powers give raise to uncertainties of 5.02%, 5.12% and 7.17% for thermal, electric and overall efficiencies, respectively. These uncertainties are mainly due to the high uncertainty associated to the natural gas LHV measurement.

Table 2.5 – Uncertainties associated to the main energy measurements.

| Magnitude | Type of measurement | Uncertainty (%) |
|---|---|---|
| Fuel power | Indirect | $\pm 5.02$ |
| Electric power | Direct | $\pm 1.00$ |
| Thermal power | Indirect | $\pm 0.17$ |
| Electric efficiency | Indirect | $\pm 5.12$ |
| Thermal efficiency | Indirect | $\pm 5.03$ |
| Overall efficiency | Indirect | $\pm 7.18$ |

# 4. Model calibration

In this section characterization results of experimental tests carried out over the previously described Remeha eVita device are presented, for the subsequent calibration and validation of the model. Most of these experimental tests took place from July 2016 to January 2017 in the experimental facility of the LCCE.

The main methodology chosen for validating the model is by comparison of the model predictions with the experimental performance of the tested device, both for under transient and steady-state conditions. Thus, the model must be first calibrated using such experimental data.

## 4.1. Parameter identification of the Stirling engine

The identification procedure encompasses the four main operating modes previously defined: steady operation, warm-up, shutdown and standby. Calibration tests were both steady and transient, depending on the parameter to be identified.

The parameters to be identified, previously introduced in the description of the model, can be classified into three main categories:

- Parameters of the performance map, which are related to the normal steady operation of the device and are calibrated by means of steady-state tests.
- Dynamic parameters, which are responsible of making outputs vary over the time and are calibrated through dynamic tests.
- Control logic parameters, which are responsible of switching between operation modes.

Whilst steady and dynamic parameters are those summarized from Table 2.6 to Table 2.8, control logic parameters encompass the following: $T_{start}^{e}$, $T_{head,nom}^{start}$, $T_{head,min}$ $T_{stop}^{e}$ and $T_{stop}^{t}$.

Table 2.6 – Main parameters of the performance map of the micro-CHP boiler.

| Dependent variable | Parameters | | | | | |
|---|---|---|---|---|---|---|
| | Coefficients | | | Reference values | | |
| $\dot{Q}_{net,max}^{se}$ | $a_1^{se}$ | | $a_2^{se}$ | $\dot{Q}_{net,ref}^{se}$ | | $T_{cw,i}^{ref,se}$ |
| $\dot{E}_{net}^{se}$ | $b_1^{se}$ | $b_2^{se}$ | $b_3^{se}$ | $\dot{E}_{net,ref}^{se}$ $T_{head}^{ref}$ | | |
| $\eta_{comb}^{se}$ | $c_1^{se}$ | | $c_2^{se}$ | $\eta_{comb,ref}^{se}$ | | |
| $\eta_{e,nom}^{se}$ | $d_1^{se}$ | | $d_2^{se}$ | $\eta_{e,ref}^{se}$ | | $\dot{m}_{cw}^{ref,se}$ |
| $\alpha_f^{se}$ | | $e^{se}$ | | | | |
| $\dot{Q}_{net,max}^{ab}$ | $a_1^{ab}$ | | $a_2^{ab}$ | $\dot{Q}_{net,ref}^{ab}$ | | $T_{cw,i}^{ref,ab}$ |
| $\eta_{comb}^{ab}$ | $c_1^{ab}$ | | $c_2^{ab}$ | $\eta_{comb,ref}^{ab}$ | | |
| $\eta_{t,nom}^{ab}$ | $d_1^{ab}$ | | $d_2^{ab}$ | $\eta_{e,ref}^{ab}$ | | $\dot{m}_{cw}^{ref,ab}$ |
| $\alpha_f^{ab}$ | | $e^{ab}$ | | | | |

Table 2.7 – Main heat transfer coefficients of the micro-CHP boiler.

| Dependent variable | Parameters | | |
|---|---|---|---|
| $\dot{Q}_{eng}$ | $[UA]_{eng,1}$ | $[UA]_{eng,2}$ | $[UA]_{eng,3}$ |
| $\dot{Q}_{HX}$ | $[UA]_{HX}$ | $[UA]_{HX,shutdown}$ | $[UA]_{HX,standby}$ |
| $\dot{Q}_{loss}^{se}$ | $[UA]_{loss}^{se}$ | $[UA]_{loss,shutdwon}^{se}$ | $[UA]_{loss,standby}^{se}$ |
| $\dot{Q}_{loss}^{ab}$ | $[UA]_{loss}^{ab}$ | | $[UA]_{loss,shutdown}^{ab}$ |

Table 2.8 – Main parameters of the dynamics of the micro-CHP boiler.

| Dependent variable | Dynamic parameters |
|---|---|
| - | $[MC]_{head}$ |
| - | $[MC]_{eng}$ |
| - | $[MC]_{HX}$ |
| - | $[MC]_{ab}$ |
| - | $T_{eng,nom}$ |
| $\dot{E}^{se}_{net,warmup}$ | $k_{e,1}$ |
| $\dot{E}^{se}_{net,shutdown}$ | $k_{e,2}$ |
| $\dot{m}^{se}_{f,warmup}$ | $k_{f,1}, k_{f,2}, k_{f,3}$ |

## 4.1.1.    Steady operation

For a full characterization of the Stirling engine device, tests at full load as well as at part load were run. The steady state experimental set comprises tests in function of both cooling water inlet temperature and volumetric flow, as well as the generation set-point temperature, so that their influence on the energy performance can be determined. The main results of the test are depicted and summarized from Figure 2.12 to Figure 2.21.

It was considered that the unit was operating under steady-state conditions provided that two conditions, evaluated on a 10 seconds basis, were met during at least 10 consecutive minutes:

▪ the cooling water return temperature variation with respect to the inlet set-point was lower than $\pm 0.5$ °C:

$$T^{sp}_{cw,i} - 0.5 \leq T_{cw,i} \leq T^{sp}_{cw,i} + 0.5 \qquad \text{Equation 2.75}$$

▪ the maximum deviation of the electric power with respect to the mean value of the measured interval was lower than 2%:

$$0.98 \cdot \dot{E}^{mean}_{gross} \leq \dot{E}_{gross} \leq 1.02 \cdot \dot{E}^{mean}_{gross} \qquad \text{Equation 2.76}$$

As it can be observed in figures presented next, the three main energy flows, i.e. fuel input and electrical and thermal outputs, are strongly dependent on the cooling water return temperature, while the cooling water flow has a lower influence.
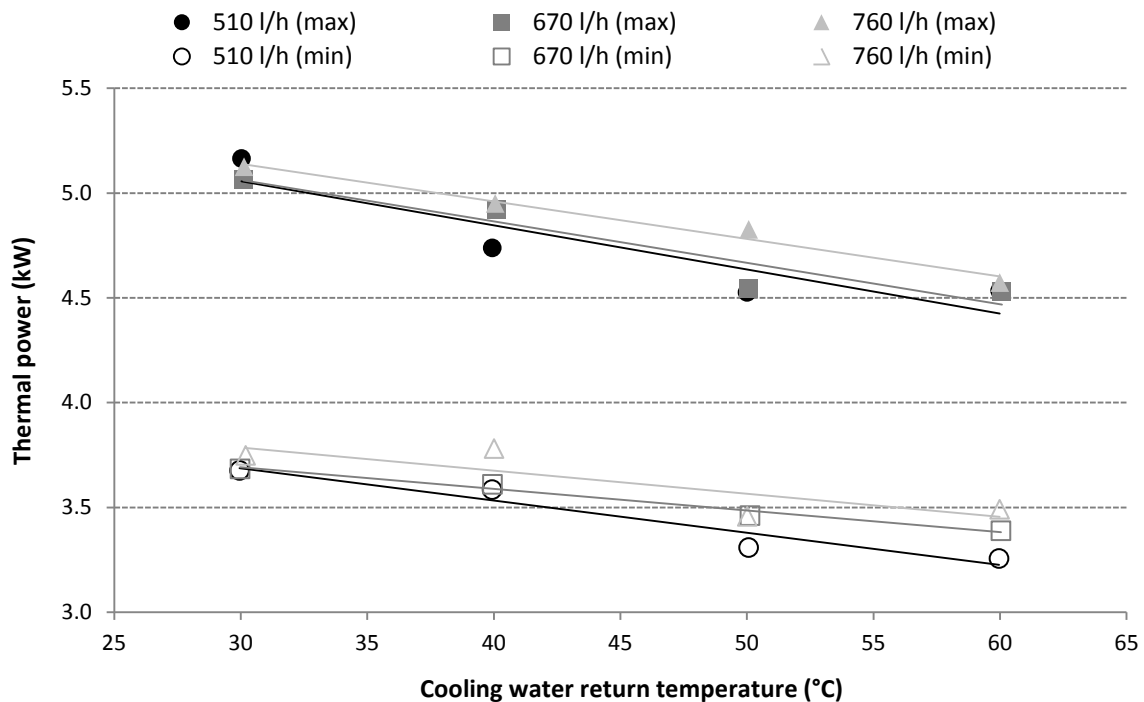


Figure 2.12 – Thermal power of the Stirling engine in function of the cooling water inlet temperature.

First, concerning the thermal output, represented in Figure 2.12, the lower the return temperature is, the higher the thermal production will be, following a linear correlation. This is mainly due to condensation gains since, once lowered the return temperature below the condensing temperature (around 50°C - 55°C for natural gas), a higher part of the latent heat content of the exhaust gases is recovered when condensing their vapor water content. This gets increased even more as circulating water flow grows, as depicted in Figure 2.13.

The net thermal power output at full load presents a linear trend which mainly lies in variations on the cooling water inlet temperature. Accordingly, taken into consideration experimental data obtained in laboratory tests, the regression equation (Equation 2.14) was adjusted.
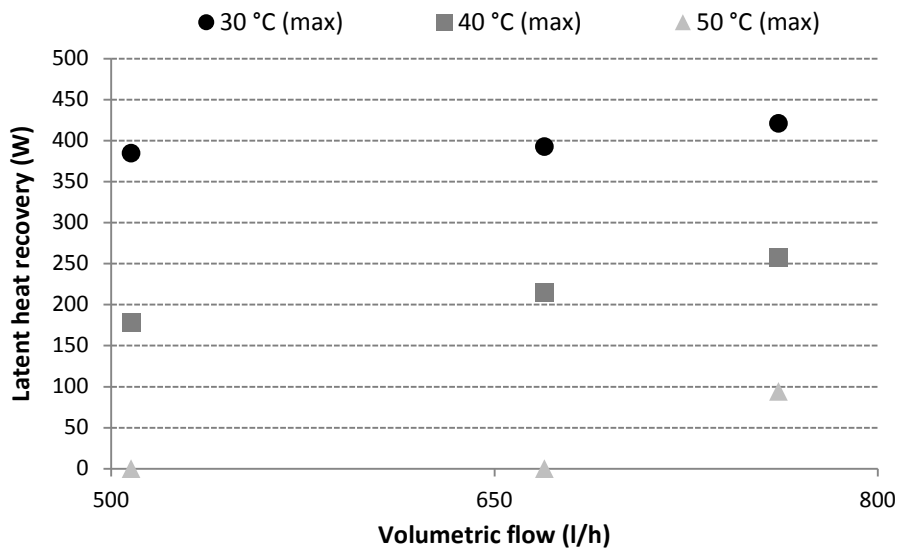
Figure 2.13 – Condensation gains of the Stirling engine

When analyzing the quality of a regression different statistical parameters can be taken into consideration:

❖ The multiple correlation coefficient, **R**, or Pearson's R, indicates how strong the linear relationship between the dependent variable ($y$) and the independent variables ($x_1, x_2 \ldots x_n$) is. A value of one means a perfect positive relationship, while a value of zero means that no linear relationship exists at all.

❖ The coefficient of determination, R-squared (**R²**), gives an indication about how many experimental points fall on the regression line proposed. For instance, a value of 0.9 indicates that 90% of the values of the correlated variable are explained by the independent variables utilized.

❖ The adjusted R-squared (**Adj-R²**) is a parameter that adjusts the aforementioned $R^2$ to the number of terms in the modeling regression. This is the parameter that should be employed when more than one dependent variable are used to describe variations on the independent one, as it is the case in the correlations proposed in this PhD Thesis. While $R^2$ considers that every single independent variable explains the variation of the dependent variable, the Adj-R² indicates the percentage of variation explained just by those variables that actually affect the dependent variable, thus penalizing the addition of independent variables that do not fit the model and so helping to identify which variables are significant and which are not.

❖ The standard error represents the average distance that the observed values fall from the regression line. The smaller the values are, the better the model will be, since experimental observations will be closer to the regression line.

❖ The probability, called **p-value**, defined as the lowest significance level at which a null hypothesis can be rejected, allows evaluating the statistical significance of each independent variable included in the regression equation. Thus, for a confidence interval of 95%, a probability value lower than 0.05 indicates that the null hypothesis for that independent variable can be rejected and, therefore, that the variable has statistical significance. The lower the probability value of a coefficient is, the more meaningful its associated variable will be, since changes on that term are strongly related to changes in the response variable.

According to the afore-defined parameters, the adjusted R-squared and the probability were utilized to statistically analyze the proposed regression equations.

This way, results of the regression equation for the net thermal output at full load, $\dot{Q}_{net,max}^{se}$, used to determine the part-load ratio, the term which accounts for the influence of the cooling water mass flow presents a p-value of 0.124, which means that variations of this dependent variable will not affect significantly the heat output. Thus, this coefficient, $a_2^{se}$, was set to zero. Main coefficients for the regression equations are summarized in Table 2.9.

Once the maximum net thermal output at some given cooling water conditions is determined (Equation 2.14), the thermal load fraction, $\alpha_t^{se}$, can be calculated (Equation 2.12). In order to adjust the thermal production to that requested, the burner will adjust its firing rate, $\alpha_f^{se}$, in consequence. Both load fractions can be related through a linear regression equation, as presented in Equation 2.33 and depicted in Figure 2.14. The p-value of the thermal load fraction term in the proposed correlation, whose value is gathered in Table 2.9 presented next, shows that the selected independent variable is very significant on changes of the firing rate.
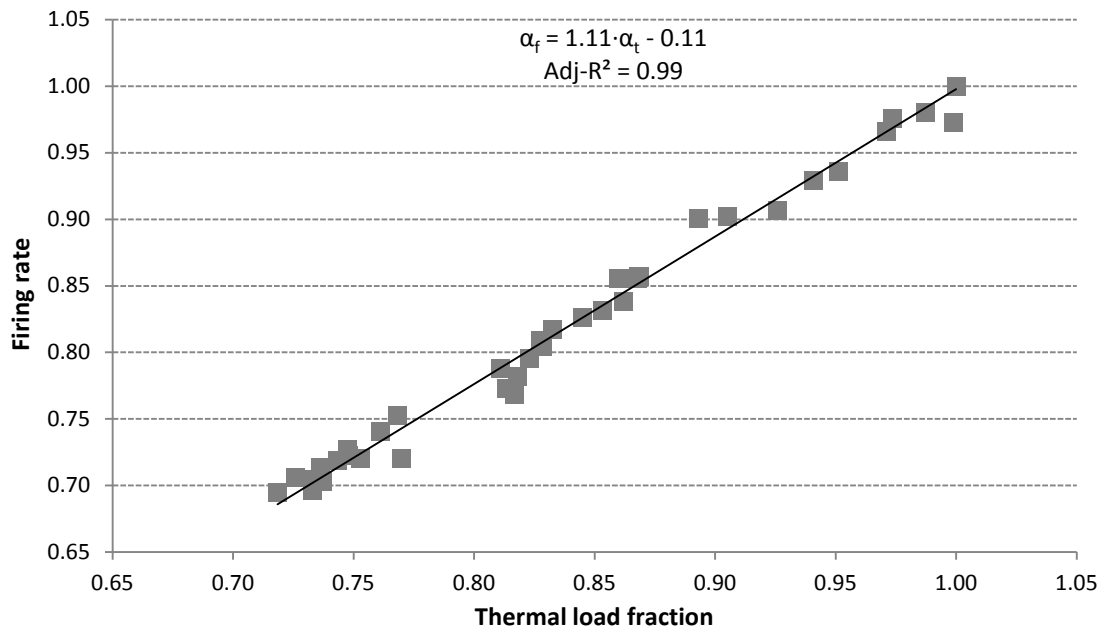
Figure 2.14 – Relationship between the firing rate and the thermal load fraction.
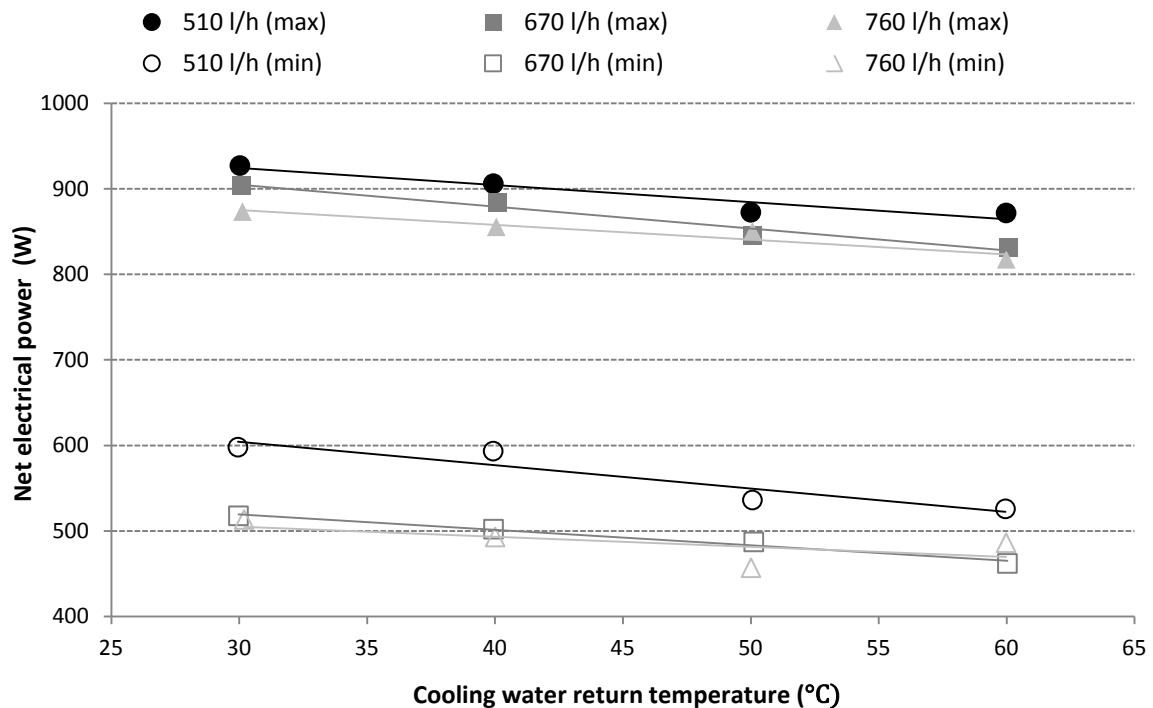


Figure 2.15 – Net electrical power of the Stirling engine in function of the cooling water inlet temperature.

As far as the electric side of the engine is considered, as depicted in Figure 2.15 and Figure 2.16, while the gross electrical output of the engine is weakly dependent on the

volumetric flow of the cooling water, its dependency when working in net terms of power raises slightly (Figure 2.15).
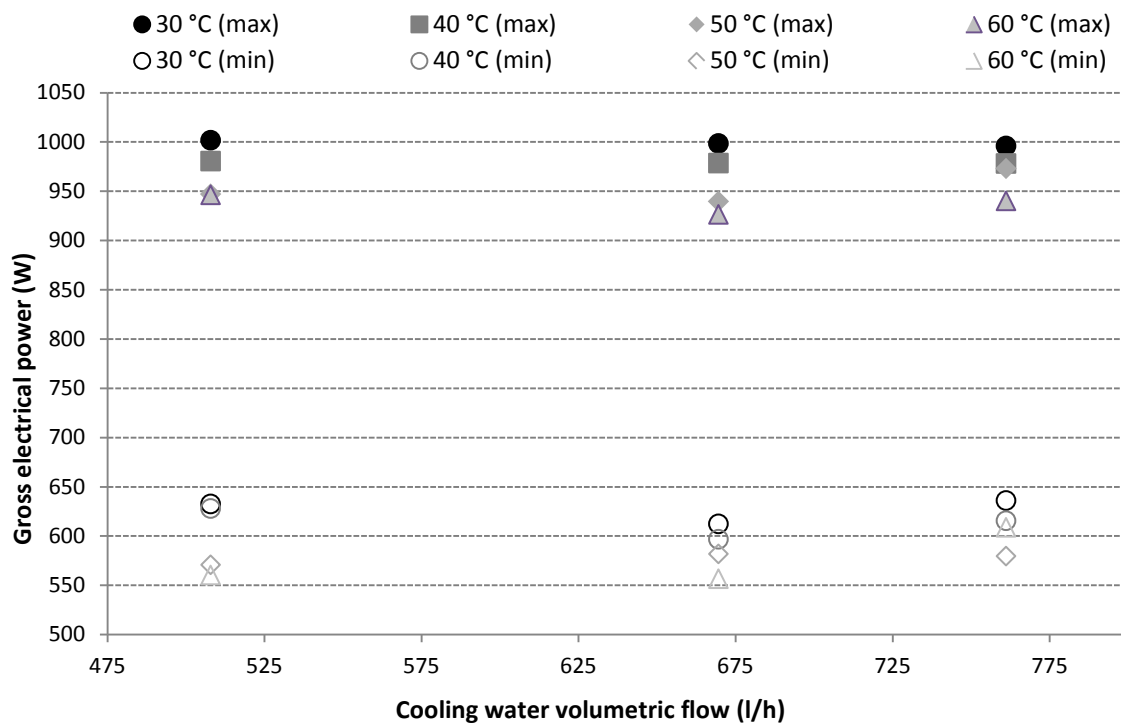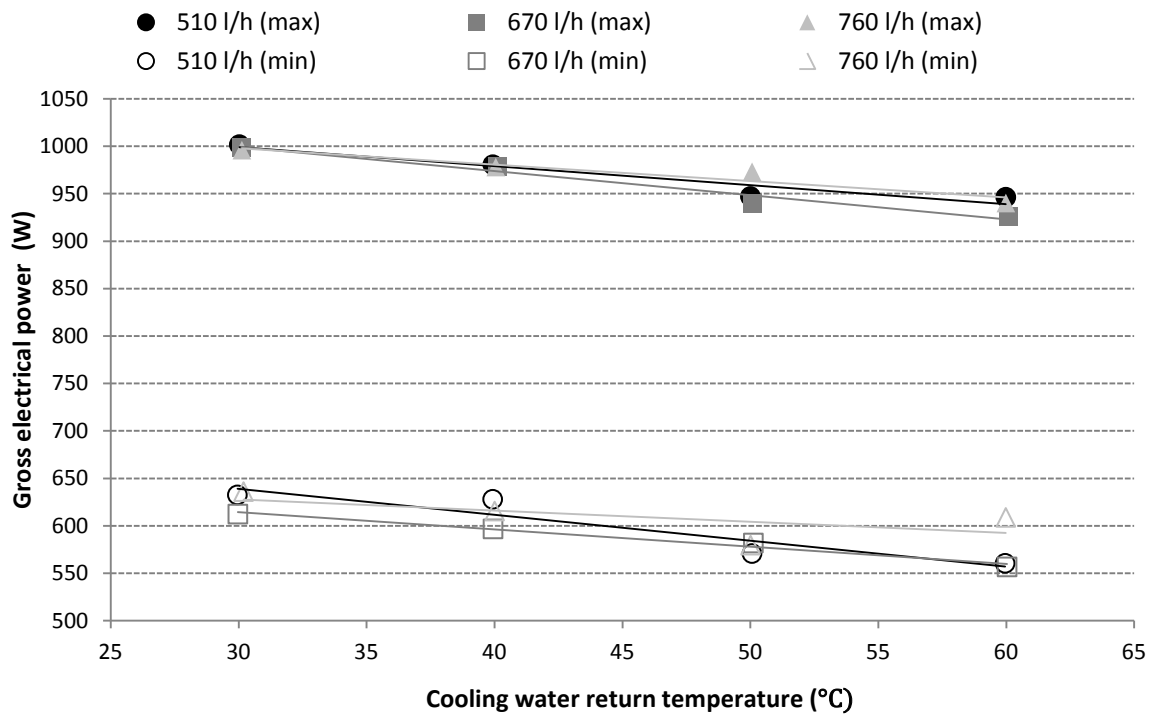


Figure 2.16 – Gross electrical power of the Stirling engine in function of the cooling water inlet temperature (top) and the cooling water volumetric flow (bottom).

When analyzing the effect of the cooling water return temperature on the electricity production (both net and gross), it can be observed that as the engine works with higher cooling water temperatures, the electric output suffers substantial reductions. These variations, as reported in the model definition, have a clear linear trend.

On the other hand, the engine energy input is regulated in order to maintain the temperature of the hot source in a range between 400 °C and 520 °C, as described in Section 3.1.2 and corroborated in Figure 2.17. This regulation lies in the adjustment of the thermal power produced to that demanded.
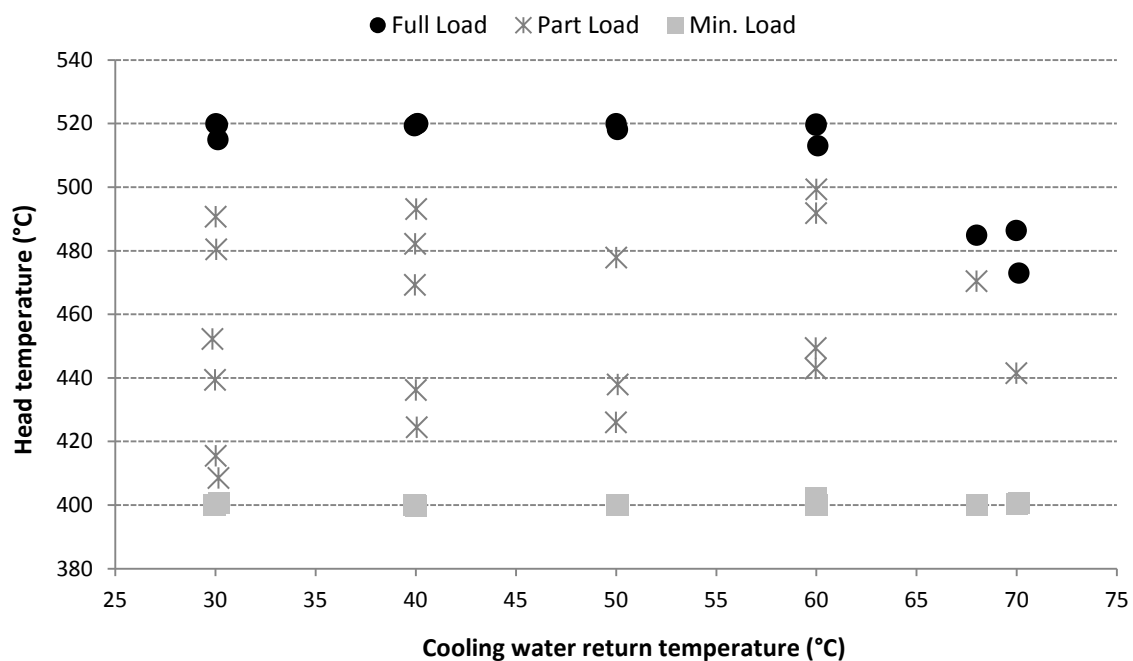


Figure 2.17 – Temperature of the head of the Stirling engine.

These temperature variations in the hot reservoir of the power cycle, as it is the case with the cold reservoir (represented by the cooling water), have direct influence on the electric power produced by the engine, as shown in Figure 2.18, where results associated to tests involving different cooling water return temperatures and a constant water flow of approximately 500 l/h are presented. This graph evinces once again that the dependency of the dependent variable, $\dot{E}_{net}^{se}$, and this independent variable, $T_{head}$, is clearly linear, so confirming the suitability of Equation 2.18.
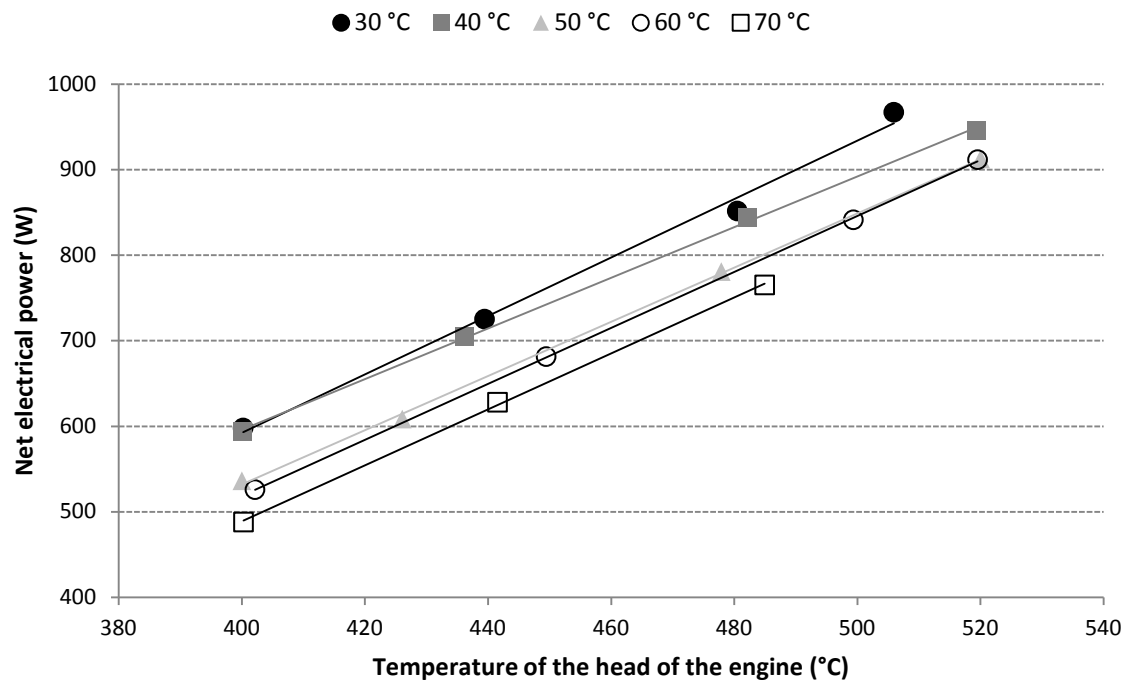
Figure 2.18 – Net electrical power of the Stirling engine in function of the head temperature.

As previously mentioned, the engine is regulated in order to maintain a pre-fixed temperature value at the hot side of the engine and, in consequence, an apparent electric power. This regulation is achieved by varying the air mass flow introduced through the fan and, consequently, the fuel mass flow. Nevertheless, due to the fact that the LHV of the tests did not show large variations on its daily value, fuel variations remained bounded.

In this sense, attending to the fuel input, as expected and shown in Figure 2.19, its consumption in a volumetric basis, brought to normal conditions, presents very low variations. When the engine works at full load, once fixed the air flow, the gas valve remains at a completely open position; consequently, in normal conditions where pressure and temperature conditions are fixed, the volumetric input must also remain virtually constant. Something similar happens when the analysis is tackled in terms of power (Figure 2.20).

However, when working with cooling water temperatures over 60 °C the engine's internal overheating control makes the fuel input reduce and, consequently, the temperature of the head of the engine, as evinced in Figure 2.17. This way, in order to

include the range of cooling water temperatures from 60 °C to 70 °C in the modeling and avoid defining the fuel input with a two stretches equation, the modeling was linearly related to the net electric power (Equation 2.31 and Equation 2.32).
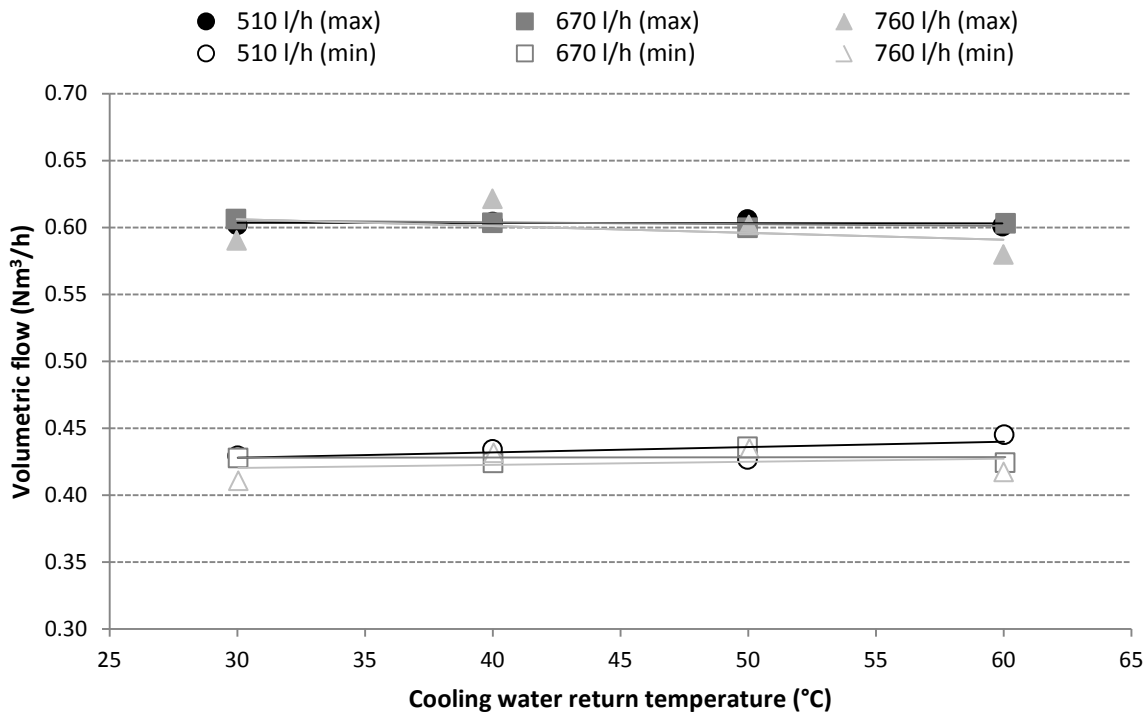


Figure 2.19 – Fuel volumetric flow input of the Stirling engine.

On the other hand, as proposed in the modeling, combustion efficiency, defined as the ratio between the recoverable heat obtained from the combustion and the LHV-based fuel power input, as well as net electric efficiency shows a linear trend which mainly lies in variations on the cooling water inlet temperature (Figure 2.21). Accordingly, taking into consideration experimental data obtained in laboratory tests, the regression equation (Equation 2.29) was adjusted.

This way, results, in terms of combustion efficiency, show that the probability associated to the term which accounts for the cooling water mass flow is 0.048 (very close to 0.05), which, as appreciated in Figure 2.21, evinces that variations of the mass flow are less significant than those of the cooling water temperature.
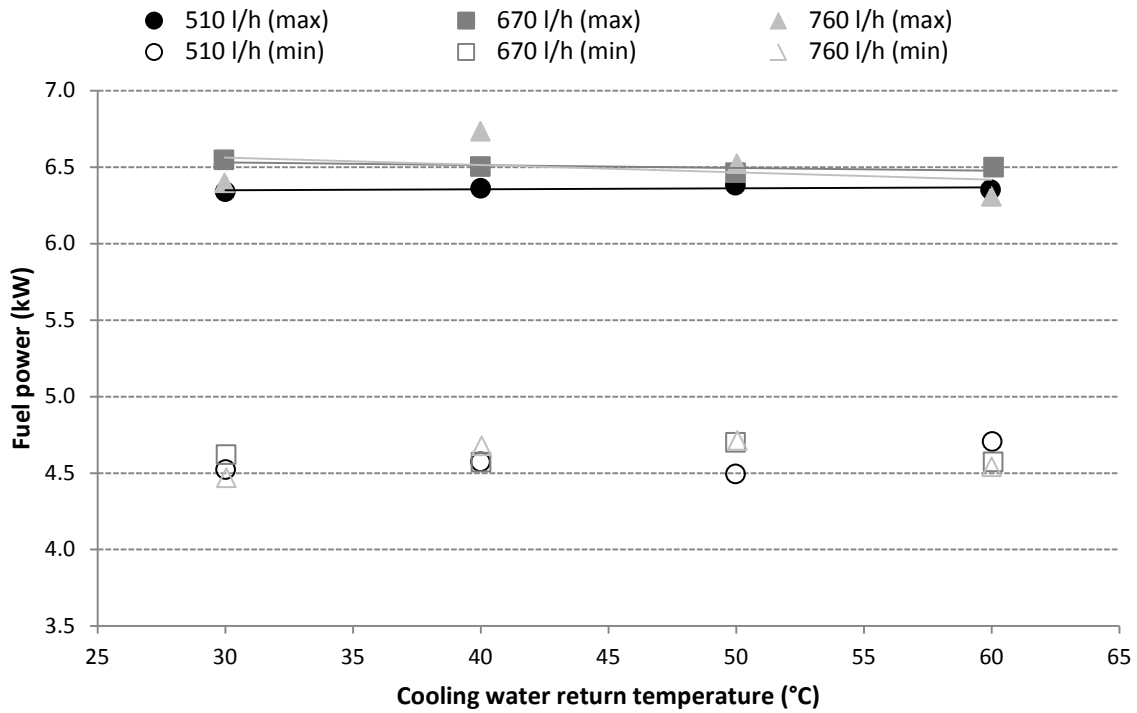
Figure 2.20 – Fuel power input of the Stirling engine.
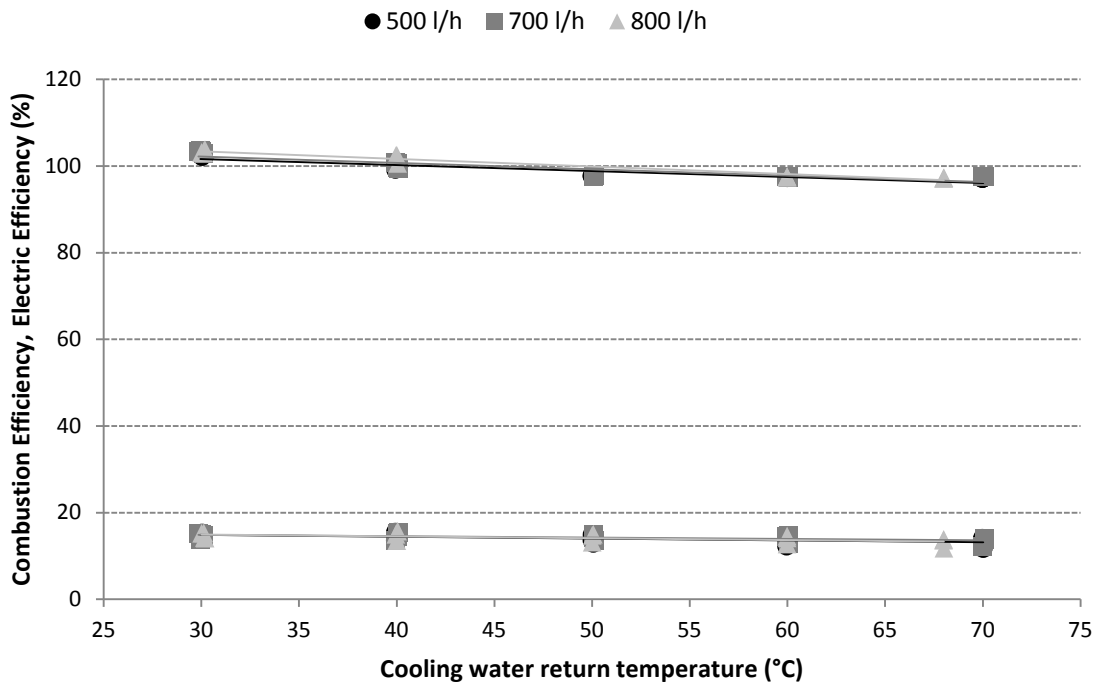


Figure 2.21 – Combustion and electric efficiencies of the Stirling engine.

Since the model is to be used in dynamic simulations where a constant fuel composition or LHV is set, this approach is considered to describe satisfactorily the fuel input modeling.

Table 2.9 – Summary of steady-state calibration coefficients of the SE.

| Dependent variable | Coefficient | Value | Adj-R$^2$ | p-value |
|---|---|---|---|---|
| $\dot{Q}^{se}_{net,max}$ | $a^{se}_1$ | -26.817 | 0.89 | 7.199E-10 |
| $\dot{E}^{se}_{net}$ | $b^{se}_1$ | 3.071 | 0.98 | 4.419E-51 |
| | $b^{se}_2$ | -2.189 | | 1.221E-19 |
| $\eta^{se}_{comb}$ | $c^{se}_1$ | -16.089E-5 | 0.91 | 1.257E-24 |
| | $c^{se}_2$ | 82.214E-4 | | 0.048 |
| $\eta^{se}_{e,nom}$ | $d^{se}_1$ | 58.526E-5 | 0.81 | 2.022E-06 |
| $\alpha^{se}_f$ | $e^{se}$ | 1.118 | 0.98 | 5.418E-69 |

## 4.1.2. Transient operation

Concerning dynamic phases, three different procedures for identifying the main parameters of the model were proposed, according to different levels of sophistication: basic calibration, intermediate calibration, and advanced calibration. This calibration process was applied to an experimental test were the volumetric flow and temperature of the returning cooling water was 700 l/h and 40 °C, respectively.

### 4.1.2.1. Basic calibration

The model is structured so that each control volume is thermally defined by a unique mean temperature. With respect to the engine control mass, since the inner of the engine where the thermodynamic cycle takes place is in thermal contact with the two reservoirs (the head of the engine and the cooling water on the one hand, and with the case of the engine-block on the other hand), the internal virtual temperature for steady-state performance was defined as follows:

$$T_{eng} = \frac{T_{head} + T_{surf} + T_{cw,i}}{3}$$

Equation 2.77

Additionally, as previously exposed by Andlauer (2011), it was observed that the temperature of the surface of the engine-case in steady-state conditions has a linear relationship with the temperature of the cooling water at the inlet.

$$Q_{eng} = 19.446 \cdot (T_{head} - T_{eng})$$
$$Adj\text{-}R^2 = 0.93$$
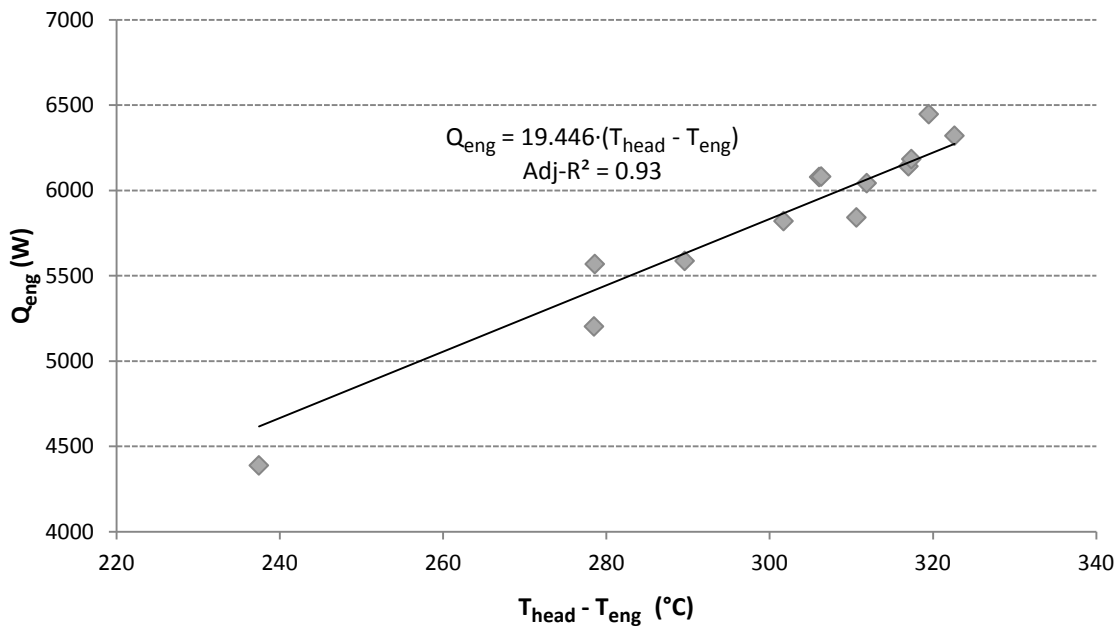
Figure 2.22 – Identification of the effective overall heat transfer coefficient between the head and the block of the Stirling engine ($UA_{eng}$).

$$Q_{HX} = 34.395 \cdot (T_{eng} - T_{cw,o})$$
$$Adj\text{-}R^2 = 0.93$$
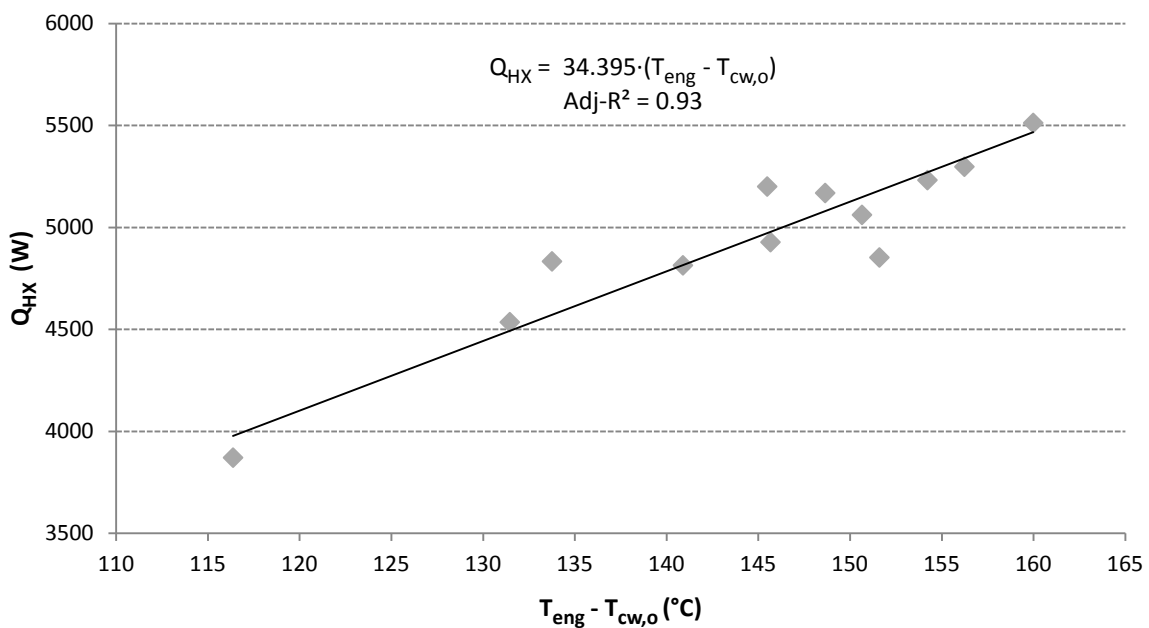
Figure 2.23 – Identification of the effective overall heat transfer coefficient between the engine block and the heat exchanger ($UA_{HX}$).

Under these assumptions, it was observed that both heat transfers between the head of the Stirling engine and the engine-block and between the engine-block and the cooling water control volume can be expressed by means of an effective UA value and the temperature difference between both bodies, as previously set in Equation 2.5 and Equation 2.6, respectively:

$$T_{surf} = 0.6258 \cdot T_{cw,i} + 21.769 \qquad \text{Equation 2.78}$$

$$\dot{Q}_{eng} = 19.446 \cdot \left( T_{head} - T_{eng} \right) \qquad \text{Equation 2.79}$$

$$\dot{Q}_{HX} = 34.395 \cdot \left( T_{eng} - T_{cw,o}^e \right) \qquad \text{Equation 2.80}$$

$$\dot{Q}_{loss}^{se} = 11.245 \cdot \left( T_{cw,o}^e - T_{air} \right) \qquad \text{Equation 2.81}$$
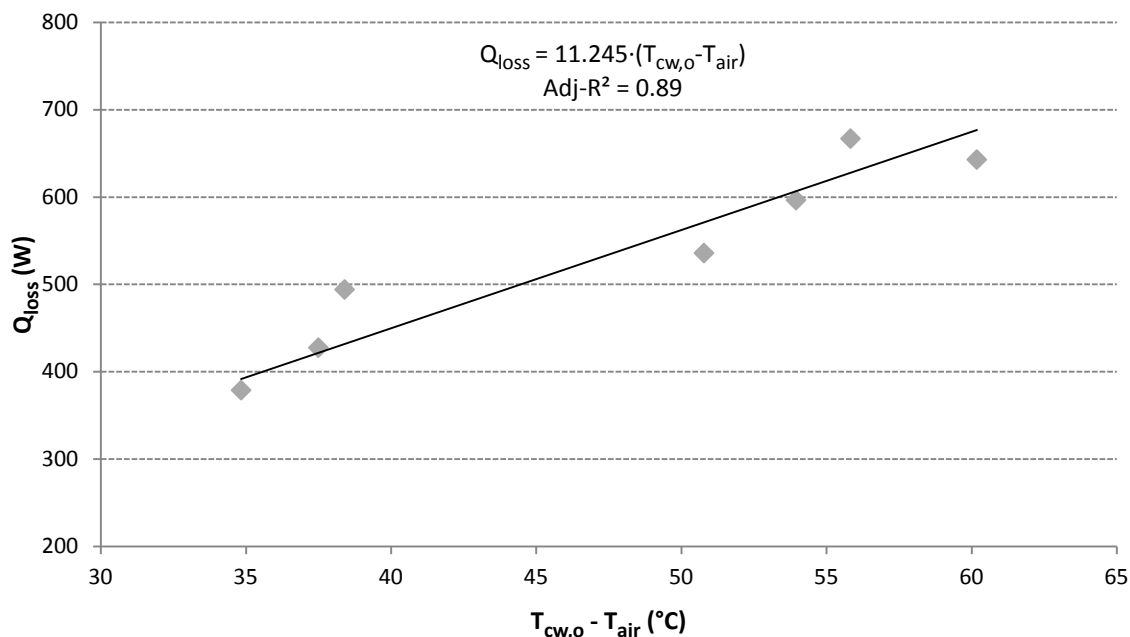


Figure 2.24 – Identification of the effective overall heat transfer coefficient for heat losses of the Stirling engine ($[UA]_{loss}^{se}$).

Effective thermal capacities (MC) of each control volume were then adjusted taking into consideration values obtained in warm-up tests. Warm-up processes were considered instead of considering shut-down processes since, once the stop signal is transferred to

the device, effective UA values change due to the modification of the conditions under which heat transfer processes occur. Thus, as discussed in Section 2.2, effective UA values calculated for steady operation are not valid for both extreme steady-state operation points of the shut-down process.

For estimating the MC value of each control volume defined data once the engine is switched on and once each control volume reaches its steady-state conditions were taken into consideration. For the case of the control volume corresponding to the head of the engine $T_{head}$ was considered as a reference.

$$[MC]_{head} = \frac{Q_{comb}^{se} - Q_{eng}}{\Delta T_{head}}$$

Equation 2.82

where $Q_{comb}^{se}$ is the useful thermal energy obtained from the combustion, calculated by combining Equation 2.28 and Equation 2.30 and integrating all the instantaneous values along the time that lasts the process; $Q_{eng}$ represents the thermal energy transferred to the engine control volume, calculated as indicated in Equation 2.83, and $\Delta T_{head}$ represents the temperature difference of the head of the engine between the initial instant ($\approx T_{air}$ for a cold start) and the moment when it gets stabilized (around 520 °C).

$$Q_{eng} = \sum_{t} [UA]_{eng} \cdot (T_{head} - T_{eng})$$

Equation 2.83

where $[UA]_{eng}$ is the effective UA value for the head-to-engine heat exchange in steady operation conditions, and $T_{head}$ and $T_{eng}$ are the respective instantaneous values of head and engine control volumes.

With respect to the engine block control mass, its MC value can be determined analogously to that of the head control volume:

$$[MC]_{eng} = \frac{Q_{eng} - Q_{HX}}{\Delta T_{eng}}$$

Equation 2.84

where $Q_{HX}$ is the effective thermal recovery of the heat exchanger control volume and $\Delta T_{eng}$ is the temperature variation of the engine control mass until steady-state conditions are reached.

$$Q_{HX} = \sum_t [UA]_{HX} \cdot \left(T_{eng} - T_{cw,o}^{se}\right)$$

<div align="right">Equation 2.85</div>

where $[UA]_{HX}$ is the effective UA value for the engine-to-water heat exchange in steady operation conditions, and $T_{cw,o}^{se}$ is the instantaneous value of the cooling water, which is consider to represent that of the heat exchanger.

Following the same premises, the thermal mass of the heat exchanger control volume, $[MC]_{HX}$, can be determined as follows:

$$[MC]_{HX} = \frac{Q_{HX} - Q_{loss}^{se} - Q_{net}^{se}}{\Delta T_{cw,o}^{se}}$$

<div align="right">Equation 2.86</div>

$$Q_{loss}^{se} = \sum_t [UA]_{loss}^{se} \cdot \left(T_{cw,o}^{se} - T_{air}\right)$$

<div align="right">Equation 2.87</div>

$$Q_{net}^{se} = \sum_t m_{cw} \cdot c_{cw} \cdot \left(T_{cw,o}^{se} - T_{cw,i}\right)$$

<div align="right">Equation 2.88</div>

### 4.1.2.2. Intermediate calibration

The mid-level parameter identification procedure proposed is based on the lumped parameter modelling, which describes the thermal system as an electrical analogue RC network. For this purpose, Logical R-Determination (LORD) software was employed. LORD is a tool for the modelling and calculation of passive thermal systems that calculates, in a stochastic way, data of individual elements of the network by means of parameter identification, known some other data obtained from measurements (Gutschker, 2008).

For the LORD calibration, a test containing warm-up and steady operation data was introduced, so determining UA and MC values which minimize the residual for those operation modes, considering $T_{head}$ and $T_{cw,o}$ as objective functions. Afterwards, the cool-down period of the same test, as well as the standby phase, was utilized, fixed MC values obtained in the previous phase, for calculating those UA representative values of those two periods. All calculated values are summarized in Table 2.10.
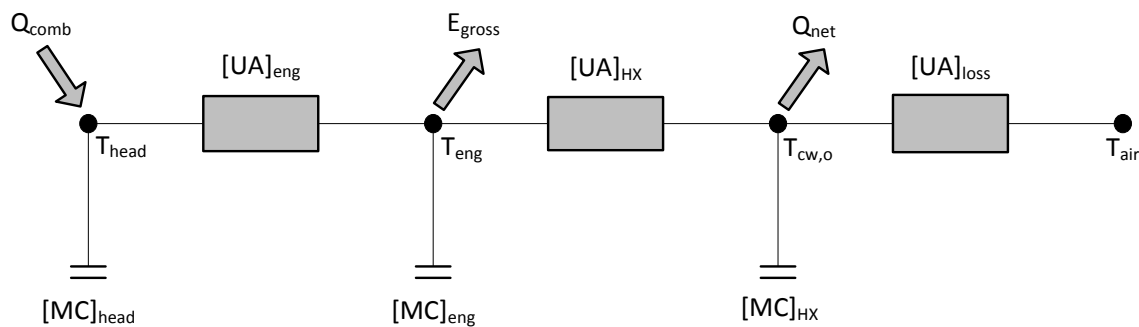


Figure 2.25 – RC model for the Stirling engine.

## 4.1.2.3. Advanced calibration

The advanced parameter calibration method allows calibrating at the same time all the MC and UA values, as well as the sensibility factors for electricity and fuel during transient processes. This process requires programming and implementing the model into the TRNSYS simulation environment and, once put together with an optimization tool such as GenOpt, an iterative process is carried out.

GenOpt (Generic Optimization Program) was developed by the Lawrence Berkeley National Laboratory to be coupled with external simulation programs and thus give solution to computationally complex optimization problems. The objective of such an optimization tool is to identify values of user-selected design and/or operational parameters that minimize the cost function selected.

A cost function is a measure of how bad a model is in terms of its ability to estimate the relationship between independent and dependent variables.

The calibration process, as represented in Figure 2.26, consists of an iterative calling between GenOpt, which reads and writes input/output text files, and TRNSYS. Once the optimization process is started, GenOpt initializes the variables to be calibrated – $\dot{F}_{se}$, $T_{head}$, $T_{cw,o}^{se}$ and $\dot{E}_{net}$ – and provides this information to TRNSYS where, once the model is run and the output values are obtained, the cost function is calculated from simulated and real values. This cost function value is then transmitted to GenOpt in order to adjust the values of the parameters, between user-specified limits, and thus achieve the lowest possible cost function value.
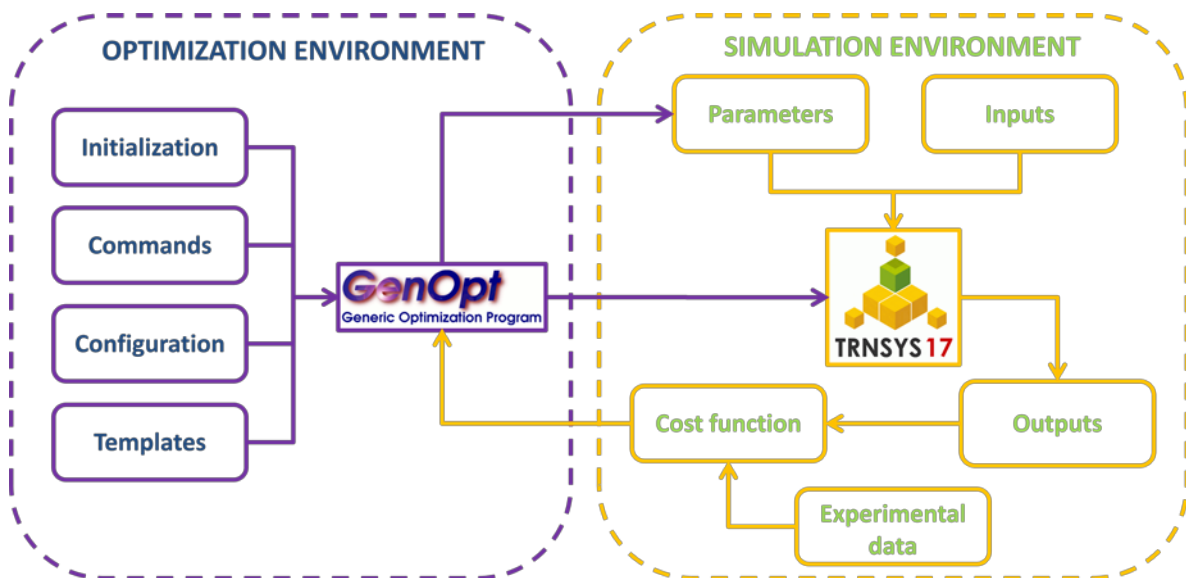


Figure 2.26 – Linking diagram between GenOpt and TRNSYS.

In order to obtain the best result, apart from an adequate optimization function, and appropriate optimization algorithm should be chosen. In this sense, the calibration process was divided into two steps.

Firstly, as an approximation phase, the GPS Hooke-Jeeves algorithm was used in order to reach, with relative low computational cost, to obtain acceptable results. This algorithm, as explained by Fernández et al. (2017), is a hybrid algorithm for global optimization that combines restrictions set by the algorithm developed by Hooke and Jeeves with a global optimization pattern search (GPS).

Since GenOpt allows adding customized minimization algorithms that are not included by default, a genetic algorithm was implemented to complete the second phase of the optimization.

A genetic algorithm is a heuristic search inspired on Charles Darwin's theory of evolution. This algorithm reflects the process of natural selection where the fittest individuals are selected for reproduction and mutation in order to produce offspring of the next generation with more capable individuals. The main advantage of genetic algorithms over other heuristic methods is their capability to simultaneously operate various solutions and that are less affected by local maximums or minimums.

In this case, the Java Genetic Algorithms Package (JGAP) 3.6.2 has been used. This package incorporates a robust and mature uni-objective simple genetic algorithm which has been used for optimizing thermal systems (Machairas et al., 2014; A. T. D. Perera and M. P. G. Sirimanna, 2014; Pérez-Iribarren, 2016).

This way, in the second optimization step, results obtained with the Hooke-Jeeves method were utilized to narrow de range of values and the optimization process was improved while avoiding local optimums.

### 4.1.3. Calibration results

Results for the parameters identified through the three calibration approaches are summarized in Table 2.10. In this table, the difference amongst the values of the effective heat transfer coefficients should be noted. This difference lies in the fact that both intermediate and advanced calibration approaches do not take into consideration the physical nature of the heat transfer processes, but aim to determine the combination of values that make the results of the model fit best with the reality. On the contrary, the basic calibration approach, whose values are determined from thermodynamic mass and energy balances, fails to quantify some of the values due to the complexity, mostly, of the transient processes of warm-up and shutdown. Furthermore, in order to physically approximate these processes, more detailed information should be obtained from the laboratory tests.

Table 2.10 – Calibration values for thermal masses and global heat transfer coefficients.

| Parameter | Basic Calibration | Intermediate Calibration | Advanced Calibration | Units |
|---|---|---|---|---|
| $[UA]_{eng,1}$ (W/K) | 19.446 | 37.815 | 19.650 | W/K |
| $[UA]_{eng,2}$ (W/K) | 8.244 | 54.110 | 11.435 | W/K |
| $[UA]_{eng,3}$ (W/K) | 0.807 | 0.1851 | 0.5925 | W/K |
| $[UA]_{HX,1}$ (W/K) | 34.395 | 15.765 | 31.470 | W/K |
| $[UA]_{HX,2}$ (W/K) | 24.664 | 3.135 | 47.343 | W/K |
| $[UA]_{HX,3}$ (W/K) | 2.865 | 15.765 | 19.950 | W/K |
| $[UA]_{loss,1}$ (W/K) | 11.245 | 18.745 | 11.538 | W/K |
| $[UA]_{loss,2}$ (W/K) | 10.773 | 18.745 | 44.981 | W/K |
| $[UA]_{loss,3}$ (W/K) | 10.773 | 0.1000 | 3.025 | W/K |
| $[MC]_{head}$ (J/K) | 1492.803 | 629.94 | 1026.25 | J/K |
| $[MC]_{eng}$ (J/K) | 3621.974 | 3268 | 6741.25 | J/K |
| $[MC]_{HX}$ (J/K) | 76775.142 | 6029.3 | 20826 | J/K |
| $T_{eng,nom}$ | 202.5 | 356.5 | 206.9 | °C |

As previously mentioned, a cost function is a measure of how bad a model is in terms of its ability to estimate the relationship between independent and dependent variables.

The cost function selected for the calibration process is the coefficient of variation of the root mean square error, CV(RMSE). The root mean square error (RMSE) accounts for differences between values predicted by a model and those observed or measured experimentally, calculated as follows:

$$RMSE = \sqrt{\frac{1}{n} \cdot \sum_{i=1}^{n} (\hat{y}_i - y_i)^2}$$

Equation 2.89

where $n$ is the number of measurement points of the sample, $\hat{y}_i$ stands for the predicted values – simulated temperatures and energy exchanges in the current case – and $y_i$ stands for the actual values of the variables.

Meanwhile, the CV(RMSE), which is the normalized value of the RMSE, measures the variability of the errors between measured and simulated values.

$$CV(RMSE) = \frac{RMSE}{\bar{y}}$$

where $\bar{y}$ is the mean value of the observed data.

Additionally, in order to compare the three calibration approaches proposed, apart from the CV(RMSE), a statistical index which allows quantifying the error committed during a complete test was also used, in terms of normalized mean bias error (NMBE):

$$NMBE\ (\%) = \frac{\sum_{i=1}^{n}(\hat{y}_i - y_i)}{\sum_{i=1}^{n}(\hat{y}_i)} \cdot 100$$

Table 2.11 – NMBE for the full test with the three calibration methods.

| NMBE | Basic Calibration | Intermediate Calibration | Advanced Calibration |
|---|---|---|---|
| Fuel Power | 2.15 % | 2.44 % | -0.27 % |
| Net Electric Power | 1.90 % | 0.00 % | -0.22 % |
| Thermal Power | -2.01 % | -1.16 % | -1.18 % |
| Overall | 2.02 % | 1.20 % | 0.56 % |

Table 2.12 – CV(RMSE) for the full test with the three calibration methods.

| CVRMSE | Basic Calibration | Intermediate Calibration | Advanced Calibration |
|---|---|---|---|
| Fuel Power | 7.16 % | 7.51 % | 5.54 % |
| Net Electric Power | 9.30 % | 6.43 % | 3.11 % |
| Thermal Power | 18.94 % | 18.68 % | 7.58 % |
| Overall | 11.81 % | 10.87 % | 5.41 % |

For the case of the basic calibration, the error, besides the fact that when calculating NMBE positive and negative forecast errors can offset each other, is due to the duration of each mode of operation, since the error committed in the warm-up phase is somehow diluted within the duration of the whole test (3.1 hours), which fits better. This way, if only the warm-up period is taken into consideration (see Figure 2.27), overall NMBE goes up to 3.4 %, with a total CVRMSE of 3.9 %. This effect is mainly due to the bad adjustment of the thermal power during the first phase of this operating period where,

due to the big inertia of the heat exchanger control volume, thermal power turns positive much later than when the engine actually starts heating water up. However, this mismatch in the prediction is obscured since the initial underestimation gets compensated by a later overestimation once the thermal production becomes positive.
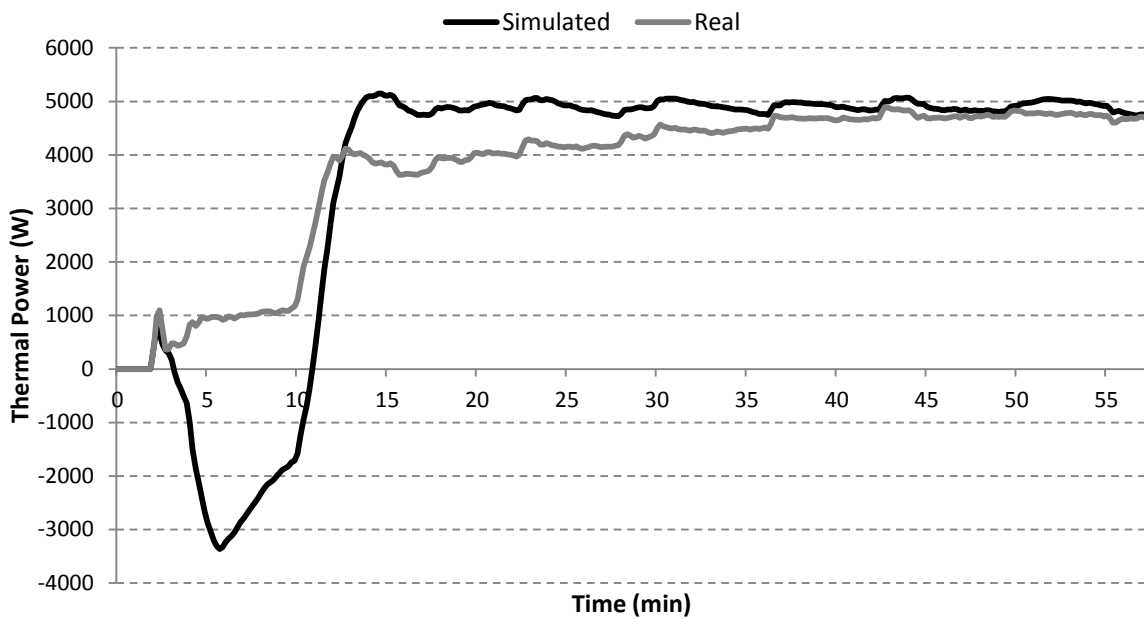


Figure 2.27 – Thermal power during the warm-up period: basic calibration.
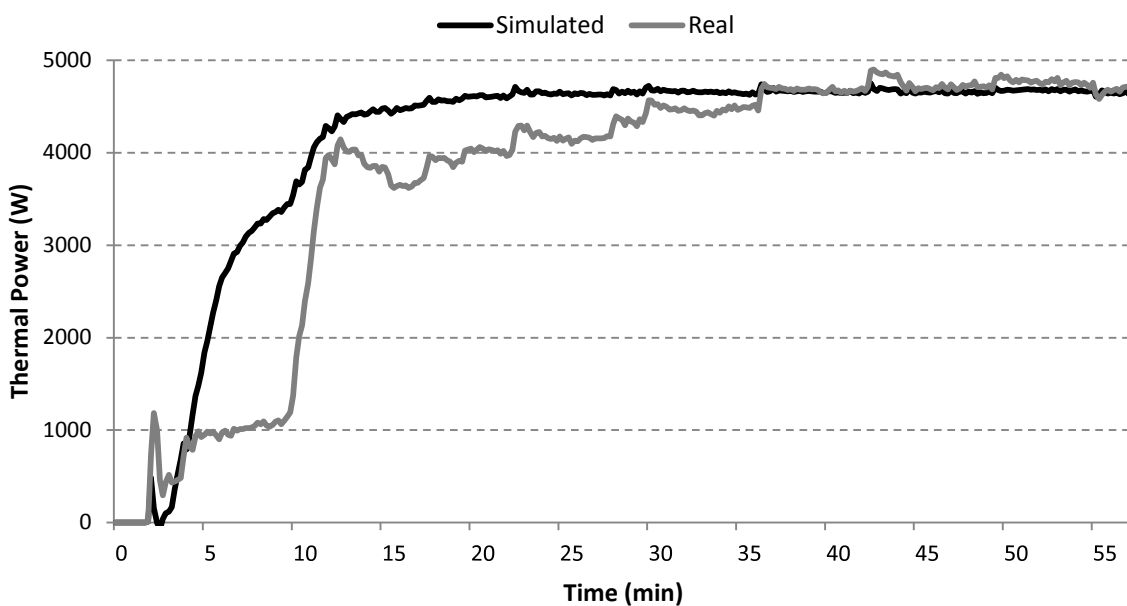


Figure 2.28 – Thermal power during the warm-up period: intermediate calibration.

Concerning the Lord-based calibration, better results than those of the previous case were obtained. However, thermal power, does not show a good agreement during the warm-up period, as represented in Figure 2.28. This is due to the fact that it is the most difficult variable to guess since it is calculated from the differential equations that represent the energy balances over the three mass and control volumes. Thus, the simulation overestimates (by 10%) the heat output of the micro-CHP device, so giving raise to overall NMBE and CVRMSE values of 6.8 and 3.2 %, respectively. Even though the NMBE value is higher than that of the manual calibration, the CVRMSE decreases slightly with respect to the previous case, which evinces the existence of an offset effect in the basic calibration case, as previously alerted and as depicted in Figure 2.28.
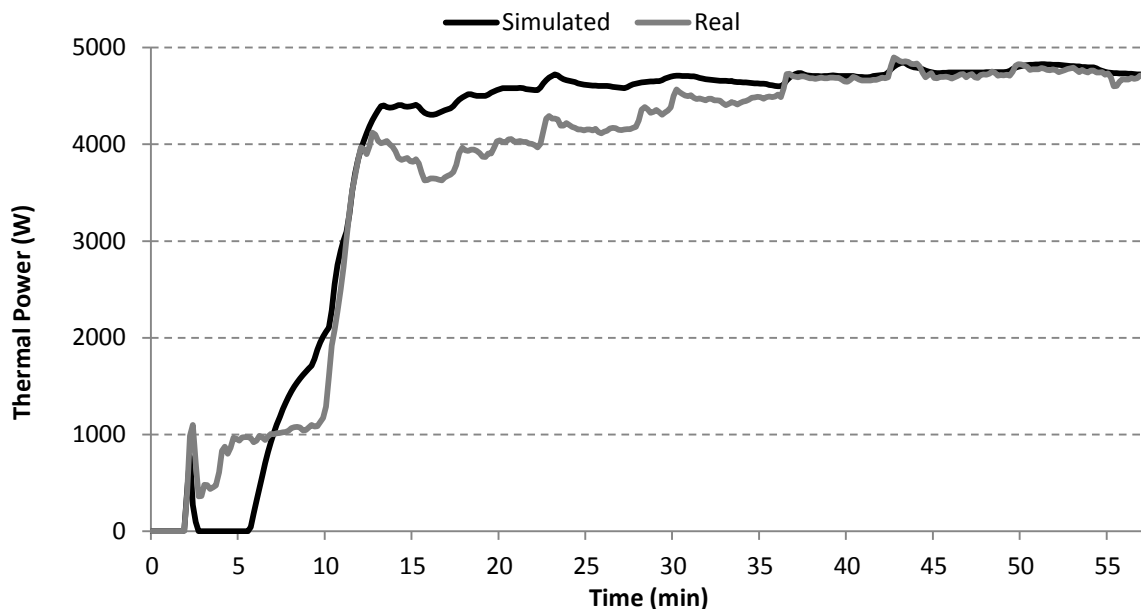


Figure 2.29 – Thermal power during the warm-up period: advanced calibration.

Lastly, the GenOpt-based calibration provides the best results. Both in the dynamic phases, depicted in Figure 2.29 and Figure 2.30, as well as in a full-test analysis, as summarized in Table 2.11 and Table 2.12, it is observed that statistical results are widely better than those of the two other calibration methods proposed. Thus, the model was calibrated taking into consideration these last values. However, this calibration approach, as well as the Lord-based one, omits the physical sense of the processes that take place during the operation of the engine, and is exclusively focused

on obtaining a combination of the parameters to be identified that enables minimizing the error committed.
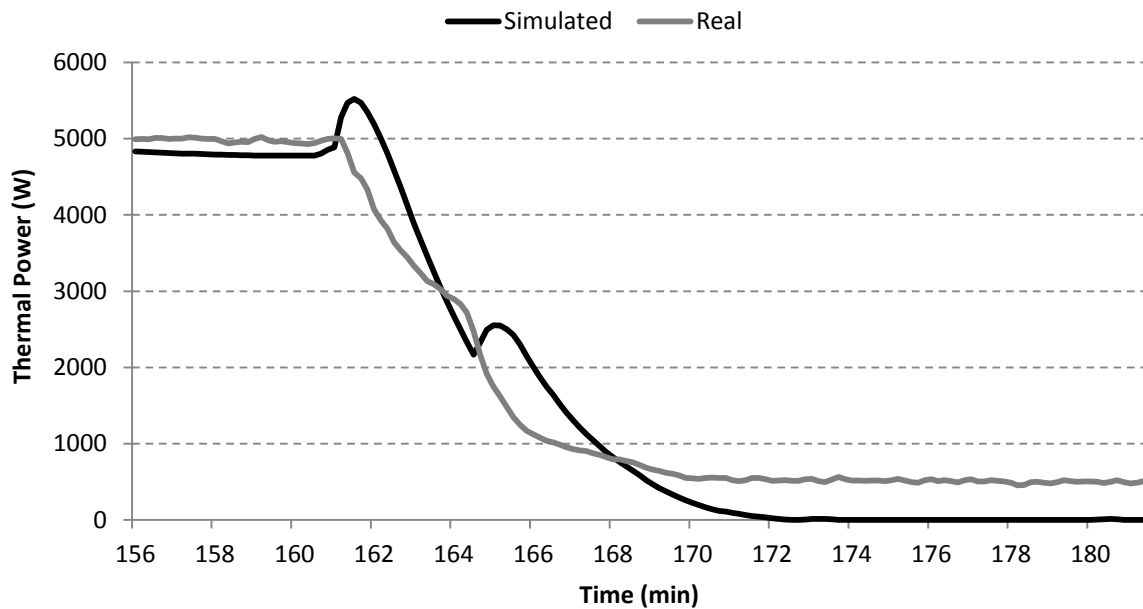


Figure 2.30 – Thermal power during the shutdown period: advanced calibration.

It must be pointed out that the mismatch existing in both warm-up and shut-down periods is mainly due to the stochastic nature of these transient processes. Thus, the description of the phenomena occurring during these periods is hardly improvable taking into consideration the level of detail of the modelling approach used.

## 4.2. Parameter identification of the auxiliary burner

As far as the auxiliary burner is concerned, its nominal thermal power oscillates significantly as a function of the the return water temperature. This is mostly due to the latent heat recovery from the exhaust gases, as evinced in Figure 2.31.

These condensation gains were calculated from a complete combustion analysis which enables obtaining the condensed mass flow of the flue gases, and the vaporization heat of water at the exhaust temperature. For that purpose, the composition of the fuel, as well as the temperature and humidity of the combustion air were taken into consideration, together with the analysis of the exhaust gases obtained with the gas analyzer: unburned hydrocarbons, temperature of the exhaust gases, and air excess.
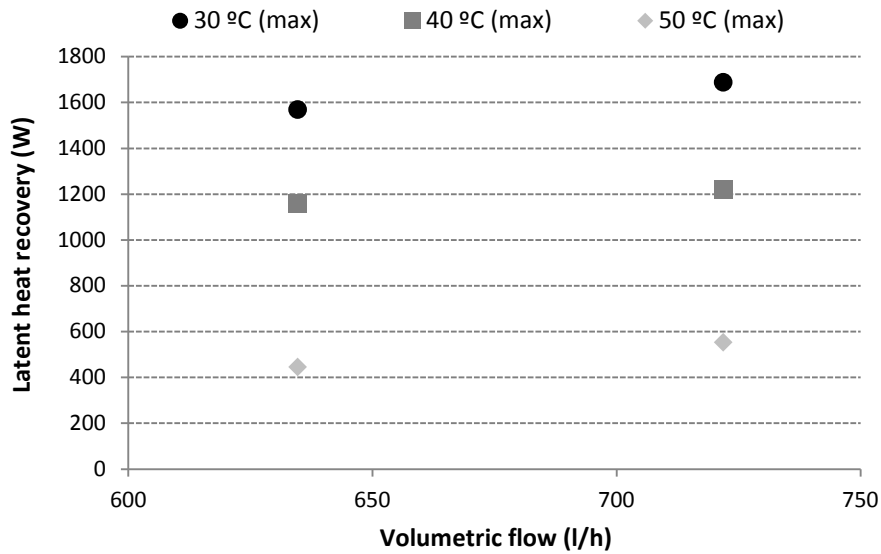
Figure 2.31 – Condensation gains of the auxiliary boiler.

Additionally, full-load tests presented in Figure 2.32 and Figure 2.33 evince that, when the thermal energy put into play is elevated, the higher the cold water flow is, the higher the thermal recovery will be.
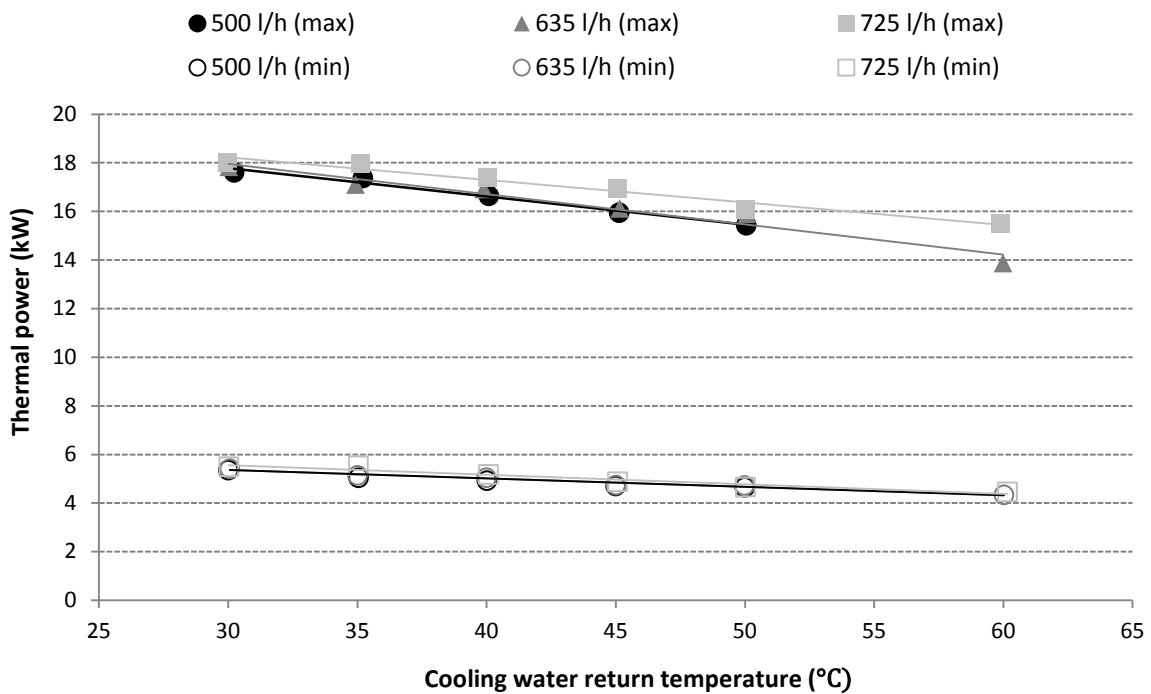


Figure 2.32 – Thermal power of the additional boiler.

Meanwhile, if the part-load operation is to be attended, no appreciable difference in the afore-commented sense is detected when the auxiliary burners works at the minimum load. The minimum part-load ratio achievable, independent of the cooling water temperature or mass flow imposed, is 0.3.
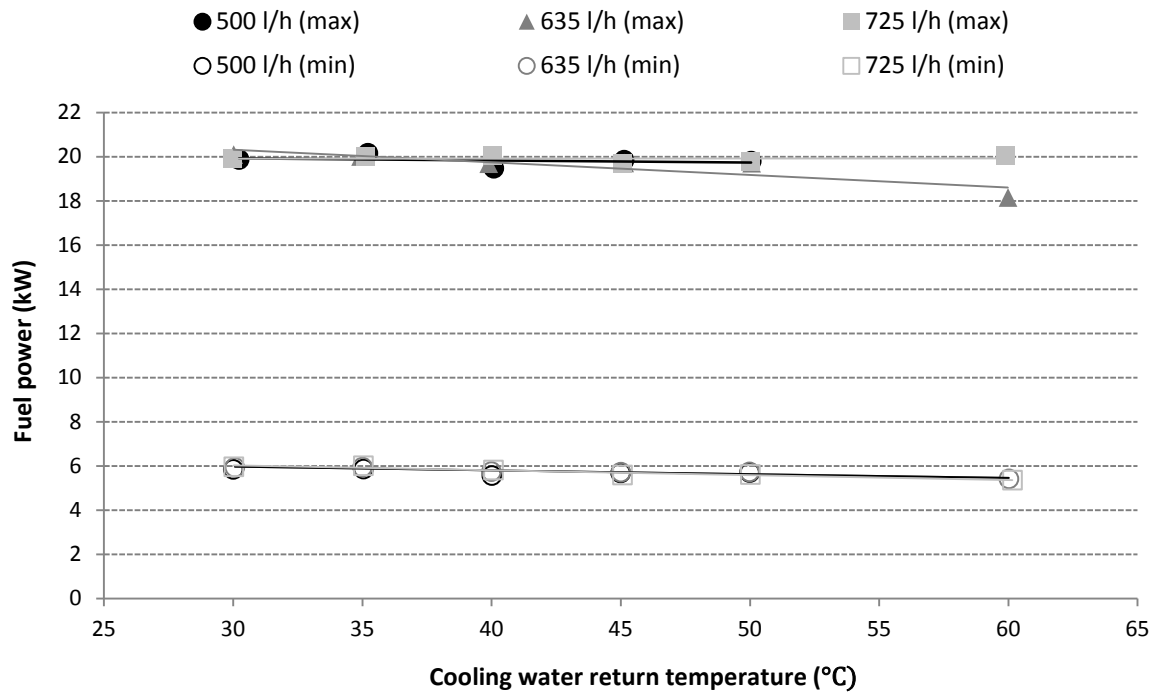


Figure 2.33 – Fuel power of the additional boiler.

As exposed in the modelling definition, the fuel power at full load is calculated from the thermal efficiency (Equation 2.35 and Equation 2.36), which, as presented in Figure 2.34, shows a clear linear trend with respect to the inlet temperature and flow of the cooling water. This way, as summarized in Table 2.13, all the steady-state calibration values show good statistical indicators.

Furthermore, it was also observed that the electricity consumption of the auxiliaries when operating the auxiliary burner at full load raised up to 29.5 W approximately.
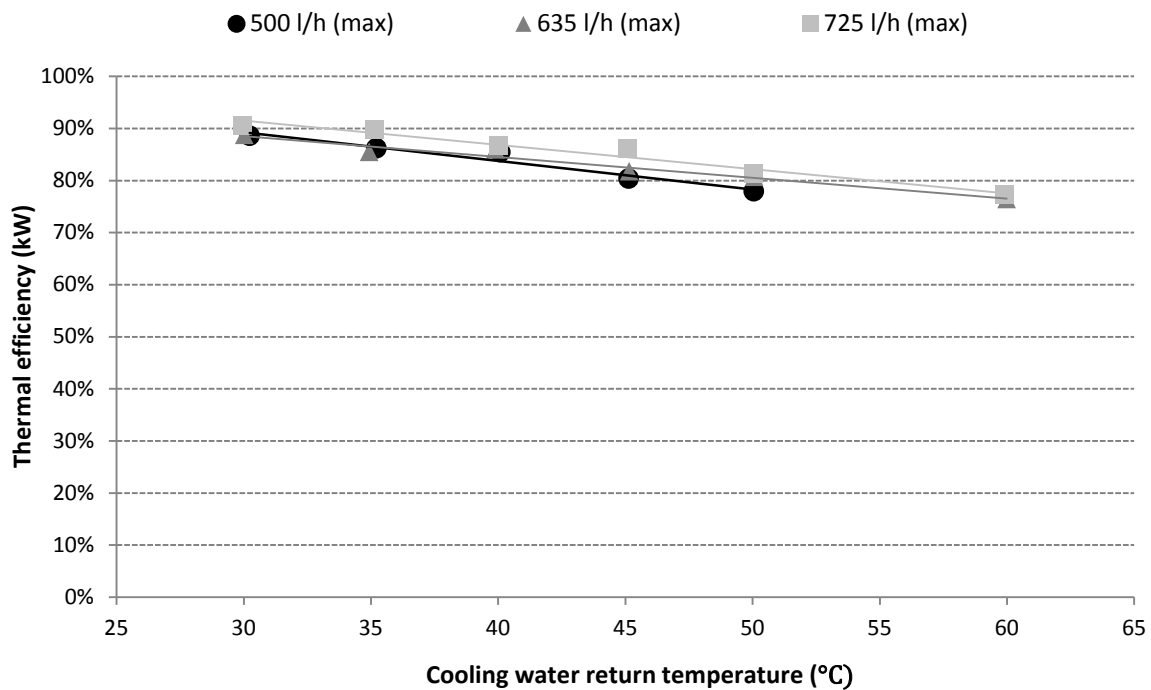
Figure 2.34 – Full-load thermal efficiency of the additional boiler.

Table 2.13 – Summary of steady-state calibration coefficients of the AB.

| Dependent variable | Coefficient | Value | Adj-R² | p-value |
|---|---|---|---|---|
| $\dot{Q}^{se}_{net,max}$ | $a^{ab}_1$ | -97.770 | 0.88 | 5.131E-11 |
| | $a^{ab}_2$ | 8601.963 | | 1.723E-02 |
| $\eta^{ab}_{comb}$ | $b^{ab}_1$ | -2.372E-03 | 0.94 | 1.365E-20 |
| $\eta^{ab}_{t,nom}$ | $c^{ab}_1$ | -3.865E-03 | 0.89 | 2.531E-11 |
| | $c^{ab}_2$ | 3.624E-01 | | 9.021E-03 |
| $\alpha^{ab}_f$ | $d^{ab}$ | 1.03 | 0.99 | 1.716E-35 |

Taken into account that, as concluded for the Stirling engine dynamic parameter identification, GenOpt based calibration provides the best results, the auxiliary burner was accordingly calibrated. In this case, due to the low number of dynamic parameters to identify ($[MC]_{ab}$ and $[UA]^{ab}_{loss}$), the calibration was straightaway carried out using the genetic algorithm.

The statistical analysis of the modelling corroborates what it can be appreciated in Figure 2.35: the model of the auxiliary burner, once calibrated, is able to represent its

performance faithfully, with very low deviations with respect to real output values. In this sense, overall NMBE and CV(RMSE), assessed on a 10 seconds basis, are valued at 1.23 % and 10.61 %, respectively, so evincing the accuracy of the predictions of the model. It must be remarked that part of the discrepancy between predictions and reality, in terms of CV(RMSE), is due to the noise that the internal control of the gas valve generates on both thermal and fuel power measurements, as well as to the time of response of the PID control of the three way-valve that controls the set-point of the return temperature of the cooling water. This way, if the model was evaluated on a 1 minute basis, the CV(RMSE) would reduce to 7.59 %.
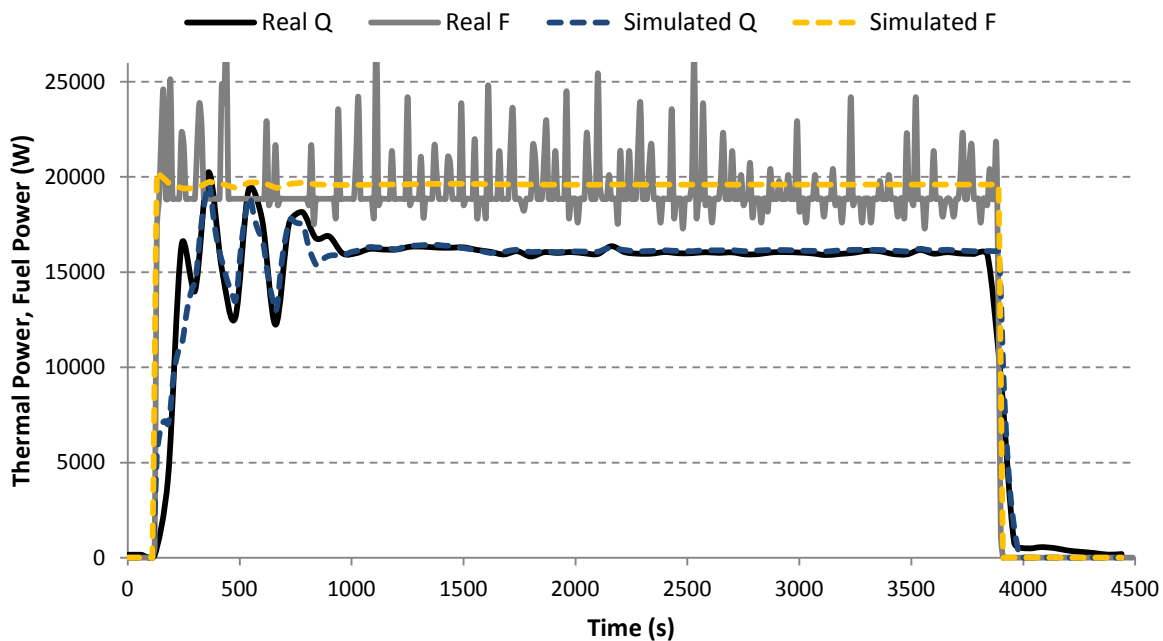


Figure 2.35 – Full-load calibration test of the additional boiler.

Additionally, as previously stated when the SE modelling was analysed, the thermal power does also present some off-set that makes differences slightly higher when the burner is switched off. In this case, since once the auxiliary burner is switched off the main burner will keep on working, this difference will wane within the thermal output of the engine.

# 5. Model validation

In this section the previously defined and calibrated model is validated, by means of comparison with different experimental data sets. Additionally, it is compared with the model proposed by Beausoleil-Morrison (2007) within the Annex 42 framework. The steady-state validation presented in Section 5.1 is carried out from different data-sets that emerge from the combination of different return mass flow and temperatures of the cooling water. Additionally, the dynamic validation and the part-load validation were carried out taking into consideration two tests with different constraints to that of the test used for calibrating the model.

In this sense, whereas the calibration was carried out with a test of 700 l/h and 40 °C of respective volumetric flow and return temperature of the cooling water, in sections 5.2 and 5.3 two other tests were utilized:

- Test A: Full test with 490 l/h and 40 °C (6-hours length)
- Test B: Full test with 540 l/h and 50 °C, including part-load operation (9-hours length)

## 5.1. Steady-state validation

Comparison between the actual experimental values and the two main outputs provided by the model under steady-state conditions are summarized in Table 2.14, for two different mass flow levels and 4 temperature levels.

Table 2.14 – Steady-state validation results for the Stirling engine: comparison with experimental results.

| | $T_{cw,i}$ level | $\dot{E}_{net}$ | | | $T_{cw,o}^{se}$ | | |
|---|---|---|---|---|---|---|---|
| | | Measured (W) | Model (W) | NMBE (%) | Measured (°C) | Model (°C) | NMBE (%) |
| 635 l/h | 30 | 964 | 955 | -0.93 | 37.09 | 36.88 | -0.57 |
| | 40 | 944 | 945 | 0.11 | 46.46 | 46.28 | -0.39 |
| | 50 | 905 | 923 | 1.99 | 55.97 | 56.10 | 0.23 |
| | 60 | 892 | 901 | 1.01 | 65.71 | 65.79 | 0.12 |
| 765 l/h | 30 | 961 | 961 | -0.02 | 36.49 | 36.39 | -0.27 |
| | 40 | 943 | 944 | 0.01 | 45.77 | 45.37 | -0.87 |
| | 50 | 938 | 923 | -1.60 | 55.28 | 55.09 | -0.34 |
| | 60 | 906 | 902 | -0.44 | 64.96 | 65.02 | 0.09 |

Meanwhile results for two tests with lower cooling water mass flows are graphically shown, in terms of power, in subsequent figures, when dynamics of the model are analysed (Test A and Test B).

Results confirm, by comparing outputs in terms of power and on a NMBE basis, that the model is able to reproduce the steady-state performance of the micro-CHP unit faithfully.

When comparing results of the current model with that of the Annex 42 (summarized in Table 2.15), the ability of the model to adequately predict output values is confirmed. The main discrepancy found in this comparison lies in the electricity output. This difference may respond, in part, to the suitability of the correlations employed to model the performance map of the engine, but also to the uncertainty of the measurement of the gross electric power provided by the engine.

Table 2.15 – Steady-state validation results for the Stirling engine: comparison with the Annex 42 model.

| | $T_{cw,l}$ level | $\dot{E}_{net}$ | | | $T^{se}_{cw,o}$ | | |
|---|---|---|---|---|---|---|---|
| | | Measured (W) | Annex 42 (W) | NMBE (%) | Measured (W) | Annex 42 (W) | NMBE (%) |
| 635 l/h | 30 | 964 | 942 | -2.28 | 37.09 | 36.93 | -0.43 |
| | 40 | 944 | 949 | 0.53 | 46.46 | 46.31 | 0.32 |
| | 50 | 905 | 967 | 6.85 | 55.97 | 56.21 | 0.43 |
| | 60 | 892 | 967 | 8.41 | 65.71 | 66.17 | 0.70 |
| 765 l/h | 30 | 961 | 940 | -2.19 | 36.49 | 36.28 | -0.58 |
| | 40 | 943 | 943 | 0.01 | 45.77 | 45.57 | -0.44 |
| | 50 | 938 | 967 | 3.09 | 55.28 | 55.17 | -0.20 |
| | 60 | 906 | 967 | 6.73 | 64.96 | 65.32 | 0.55 |

## 5.2. Dynamic validation (Test A)

The dynamic validation of the model was carried out taking into consideration Test A, and, visually, when assessed the part-load validation, with Test B.

While results corresponding to a complete on-off cycle, when operating at full load (Test A), are presented in Figure 2.36 to Figure 2.38, comparison of results corresponding to

warm-up and shutdown periods of the same test are presented from Figure 2.39 to Figure 2.41 and in Figure 2.42 and Figure 2.43, respectively.
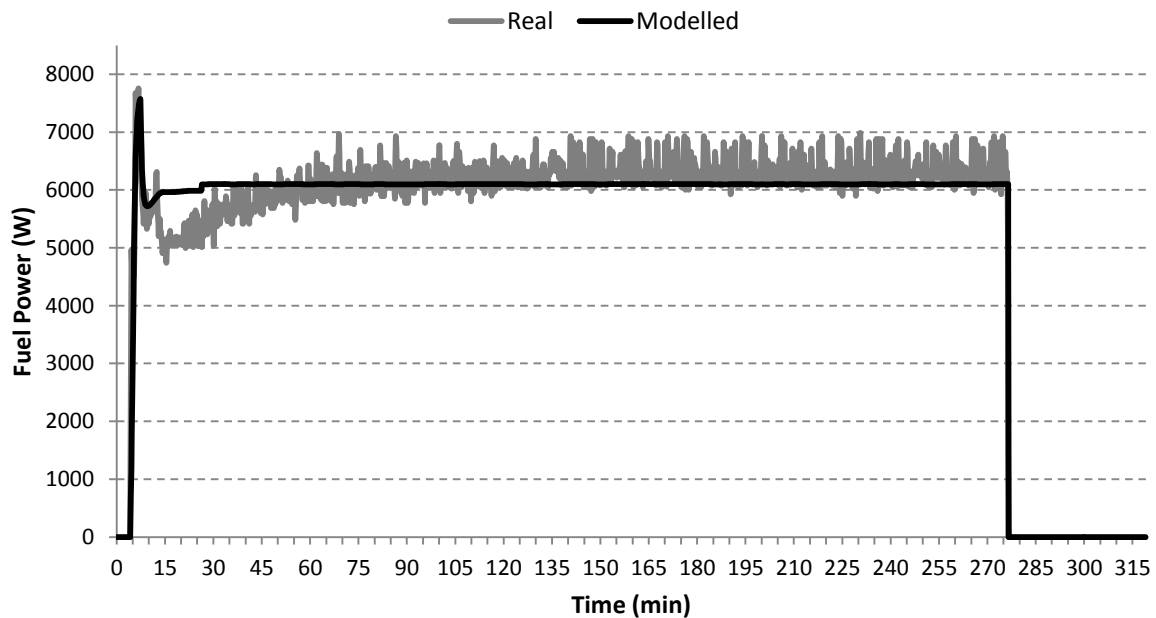


Figure 2.36 – Full-load validation test of the Stirling engine: fuel power (Test A).
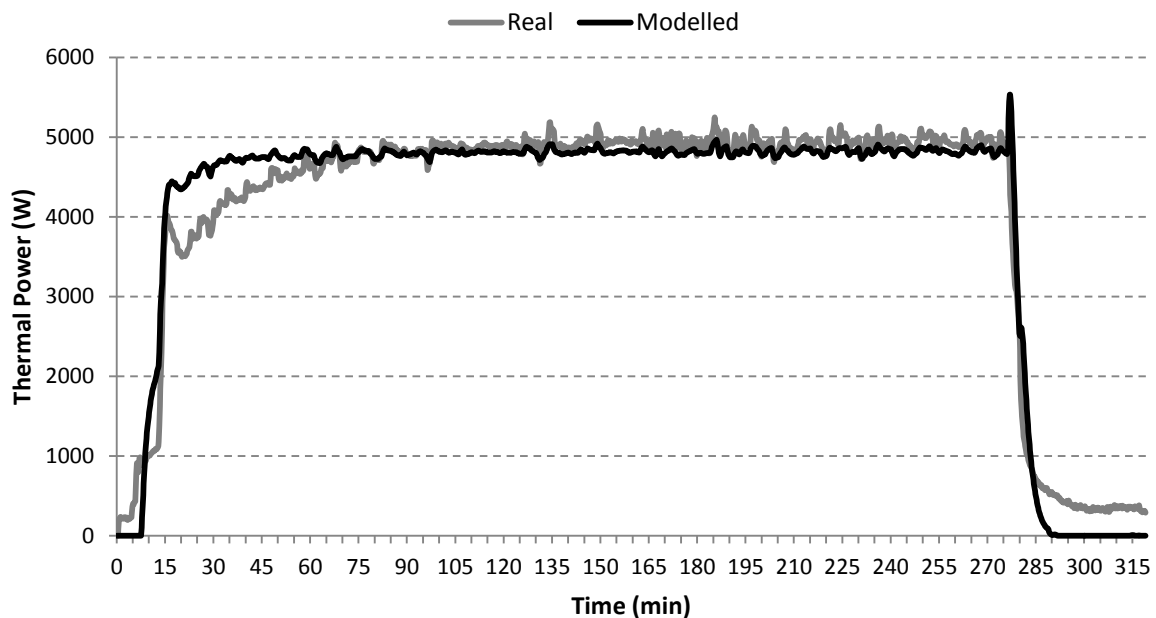


Figure 2.37 – Full-load validation test of the Stirling engine: thermal power (Test A).
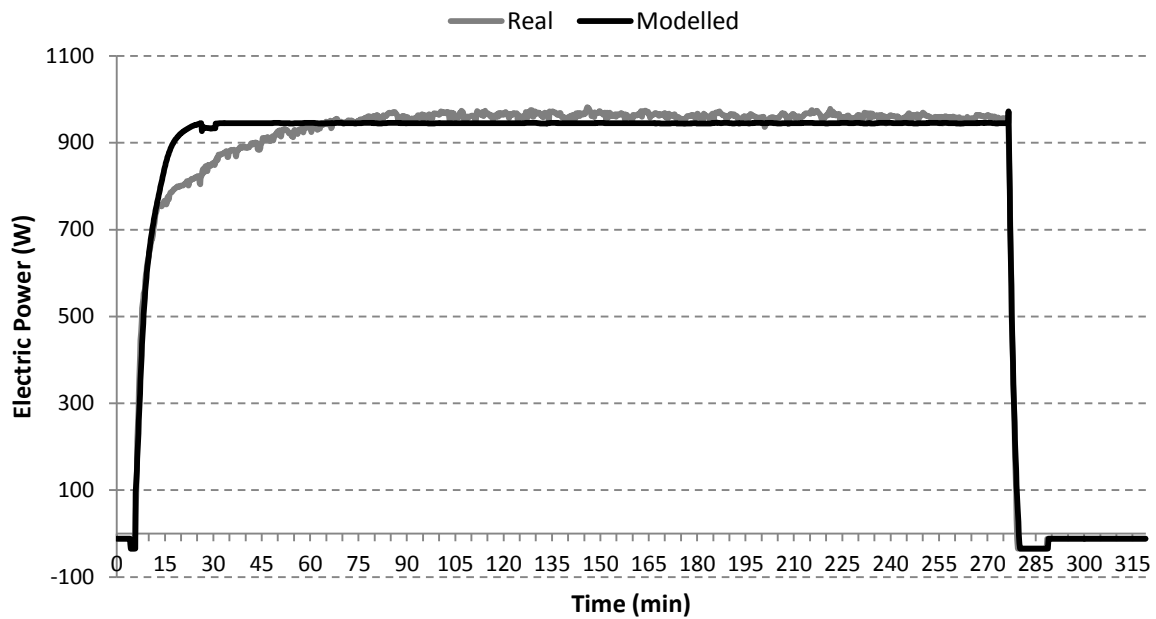
Figure 2.38 – Full-load validation test of the Stirling engine: electric power (Test A).

Additionally, the dynamic phases of Test A were separately analysed, complementing the analysis with a comparison with the model developed in the Annex 42, which was calibrated following the calibration protocol therein presented (Beausoleil-Morrison, 2007) and the same experimental data set employed for calibrating the model developed in this chapter.
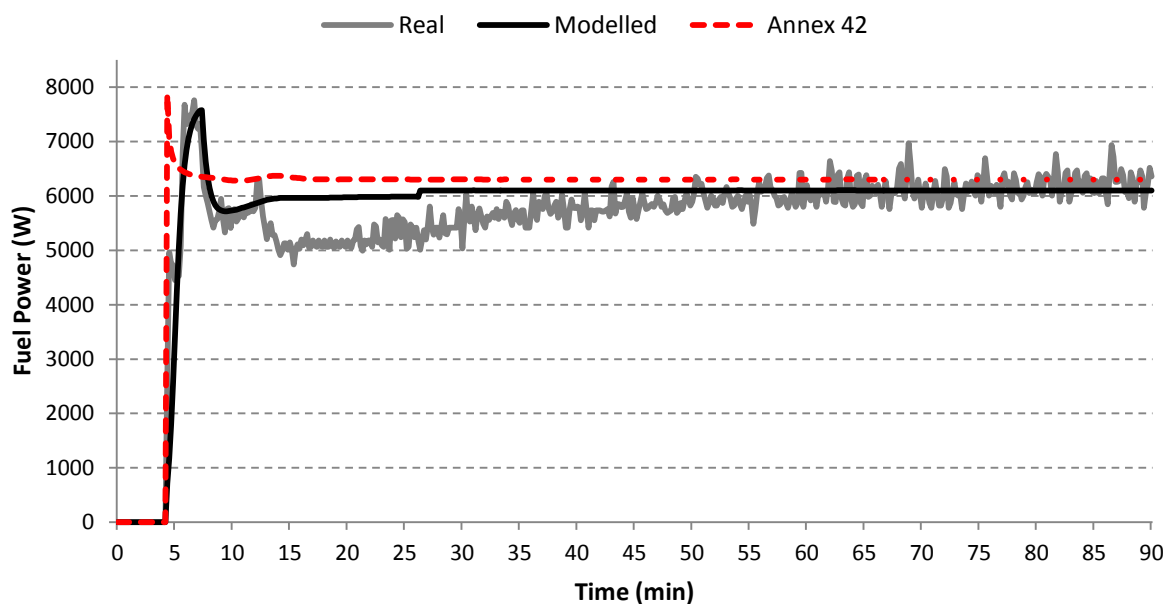


Figure 2.39 – Real and simulated fuel power during the warm-up period (Test A).
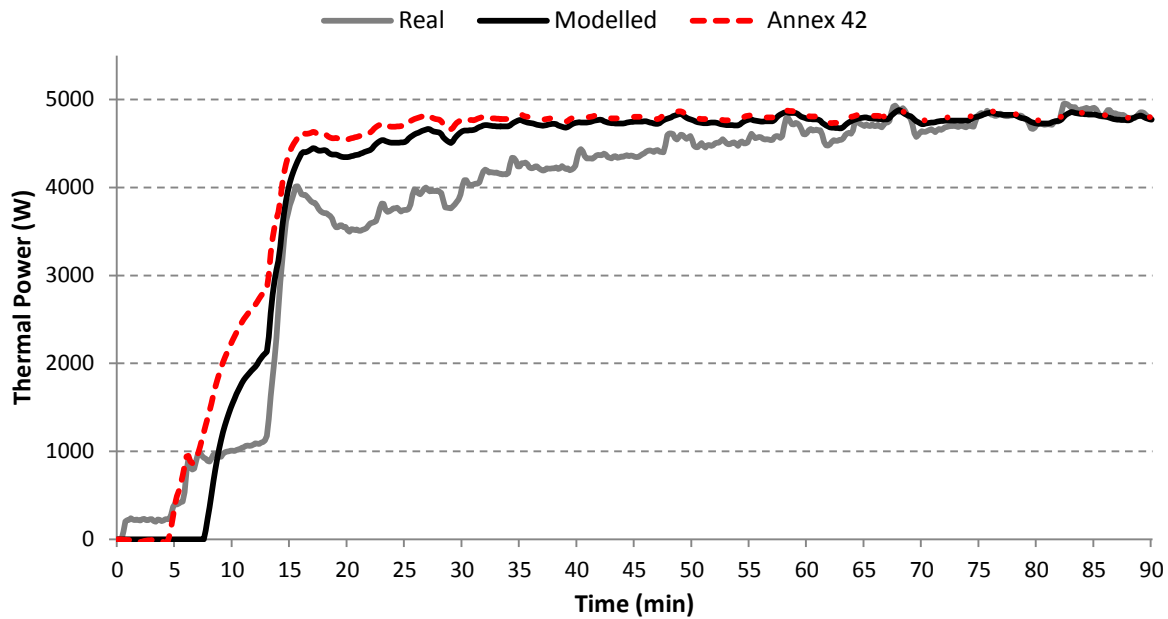
Figure 2.40 – Real and simulated thermal power during the warm-up period (Test A).

As observed, the model has good agreement with the model developed within the Annex 42 context, as well as with the experimental data in both dynamic phases.
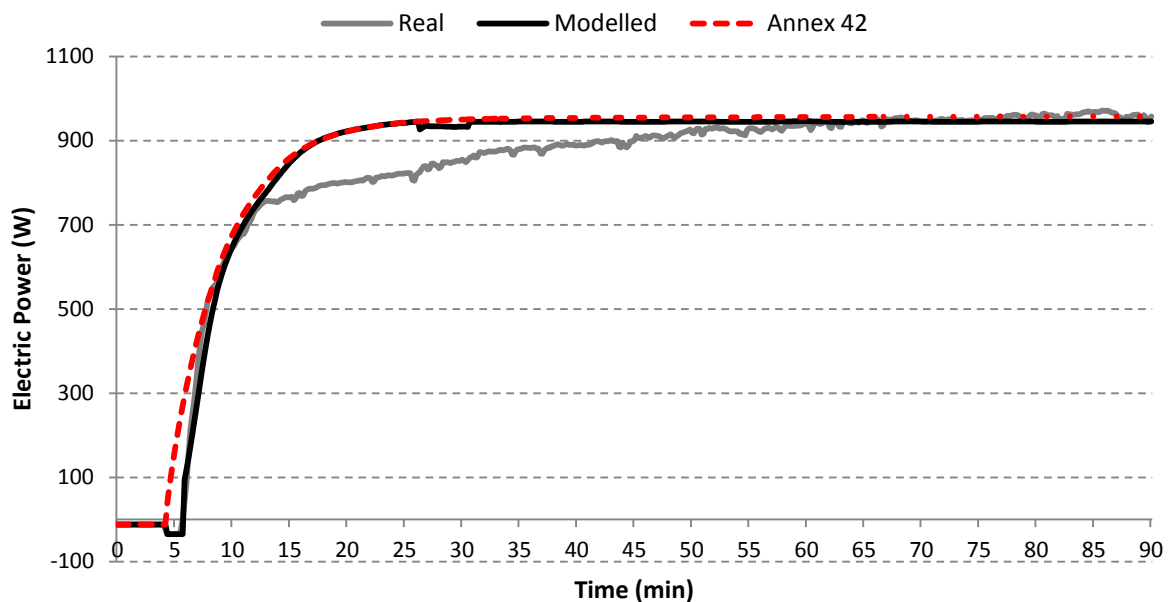


Figure 2.41 – Real and simulated electric power during the warm-up period (Test A).

In the case of the warm-up period, whose results are depicted from Figure 2.39 to Figure 2.41, the main discrepancy, as previously commented in Section 4.1.3, resides in the

second part of the fuel power during this phase. The internal control makes the fuel power drop in two steps from the peak achieved during the overshooting that takes places when the engine switches on before it trends to the nominal value in steady-state conditions. Since the natural gas counter sends out a pulse very frequently (every 10 dm$^3$ while traditional residential gas counters generate a pulse every 100 dm$^3$), this effect is accurately measured, but the model is not able to reproduce such control in all its extension, and only takes into consideration the first decline.

It is this fuel overfeeding considered by the model that makes both thermal and electric outputs be slightly above the measured values. However, provided that the micro-CHP unit should operate during long periods, this fact will not have significant impact in final results. Additionally, if the model is to be used with time-steps greater than the 10-second frequency considered during calibration and validation of the model in this PhD Thesis, as typically done in building energy simulation applications, this difference is drastically reduced.

Even so, the NMBE of the three energy exchanges are 3.6 %, 6.8 % and 3.6 %, respectively, for the fuel power, the thermal power and the electric power.

Concerning the comparison with results achieved with the already validated model of the Annex 42, it is observed that the fuel overshooting of the current model adapts better to reality, while both outputs are very similar for both models. In the case of the electricity output, however, it is observed that, whilst the model developed within this PhD Thesis fits the initialization of the power output, the Annex 42 comes ahead of time to this starting point.

In the case of the shut-down period, while the electric output is almost identical, the model is also capable of following the tendency of the thermal output during the shut-down process. Meanwhile the discrepancy existing during the stand-by phase, which is partially due to the offset existing in the data acquisition, is negligible when the engine is integrated within a thermal installation. This latter aspect responds to the fact that, once the temperature of the head of the engine falls below 130 °C, the pump will stop together with the air intake fan; consequently, the thermal power output will be zero.
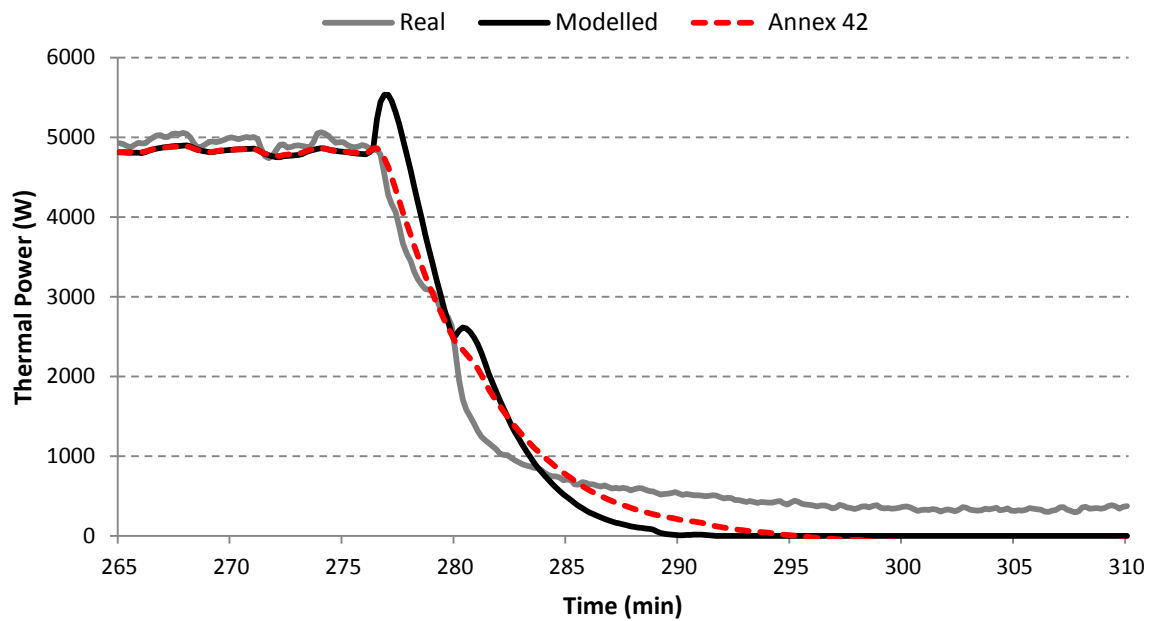
Figure 2.42 – Real and simulated thermal power during shutdown and standby periods (Test A).
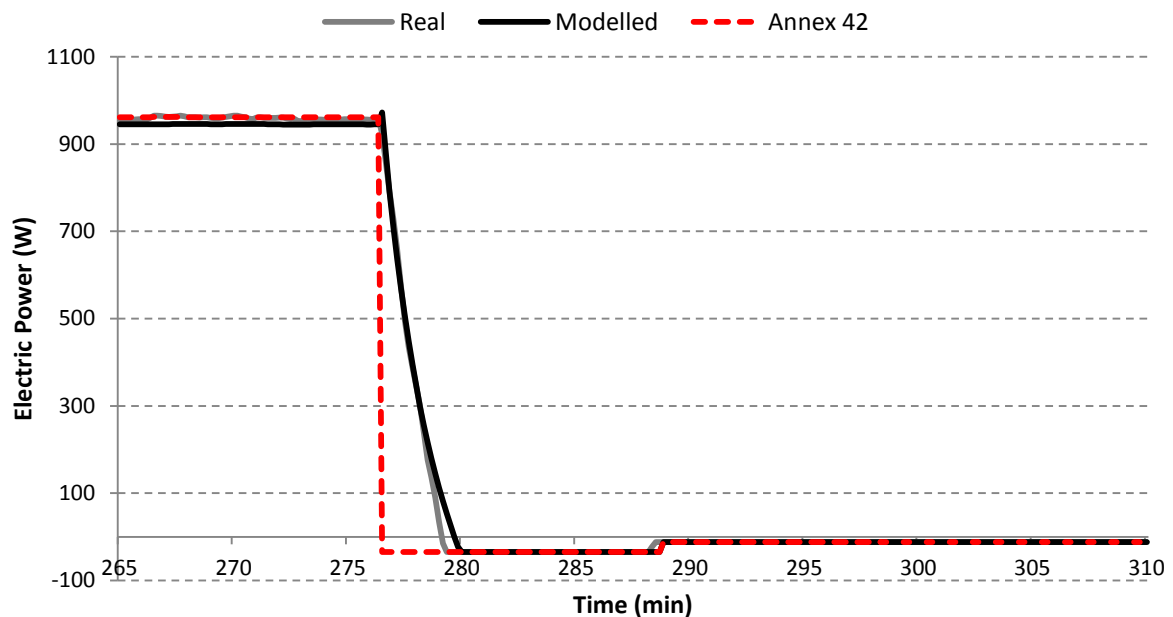


Figure 2.43 – Real and simulated electric power during shutdown and standby periods.

In the case of the shut-down period, while the electric output is almost identical, the model is also capable of following the tendency of the thermal output during the shut-down process, while the discrepancy existing during the stand-by phase, which is partially due to the offset existing in the data acquisition, is negligible when the engine is

integrated within a thermal installation. This latter aspect responds to the fact that, once the temperature of the head of the engine falls below 130 °C, the pump will stop together with the air intake fan; consequently, the thermal power output will be zero.

In both output cases the NMBE is below 10% during this mode of operation, constituting this difference 0.1 % of the energy produced during the whole test in the case of the thermal output, while in the case of the electric production is virtually zero.

Attending to the Annex 42 model, it was checked that the thermal output difference between both models is only 1.6 % (6.3 Wh). Meanwhile, the electric output modelled, contrary to the Annex 42 model, does not overlook the production that takes place once the fuel flow is cut off.

The main results of the two models compared with respect to real data are summarized in Table 2.16. On it, it can be appreciated that both models can predict the performance of the engine with low errors and, additionally, both models fit each other with high precision.

Table 2.16 – Comparison of the results of the experimental test, the proposed model and the Annex 42 model (Test A).

| | Measurements (kWh) | | | NMBE (%) | |
|---|---|---|---|---|---|
| | Experimental | Model | Annex 42 model | Model | Annex 42 model |
| Fuel input | 27.98 | 27.59 | 28.60 | -1.4 | 2.2 |
| Thermal output | 21.39 | 21.48 | 21.72 | 0.4 | 1.5 |
| Electric output | 4.22 | 4.22 | 4.27 | -0.1 | 1.1 |

## 5.3. Part-load validation (Test B)

As far as part load performance is concerned, as depicted in Figure 2.44 for Test B, very good agreement between experimental and modelled data is reached, whatever the part-load ratio is.
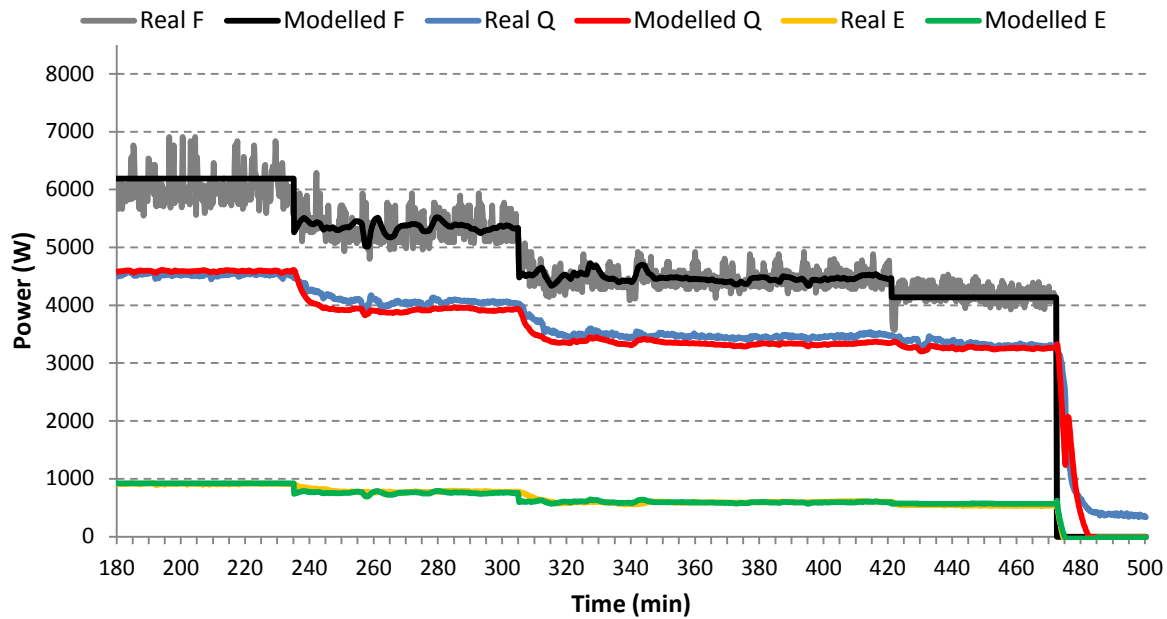
Figure 2.44 – Real and simulated power exchanges during part-load operation (Test B).
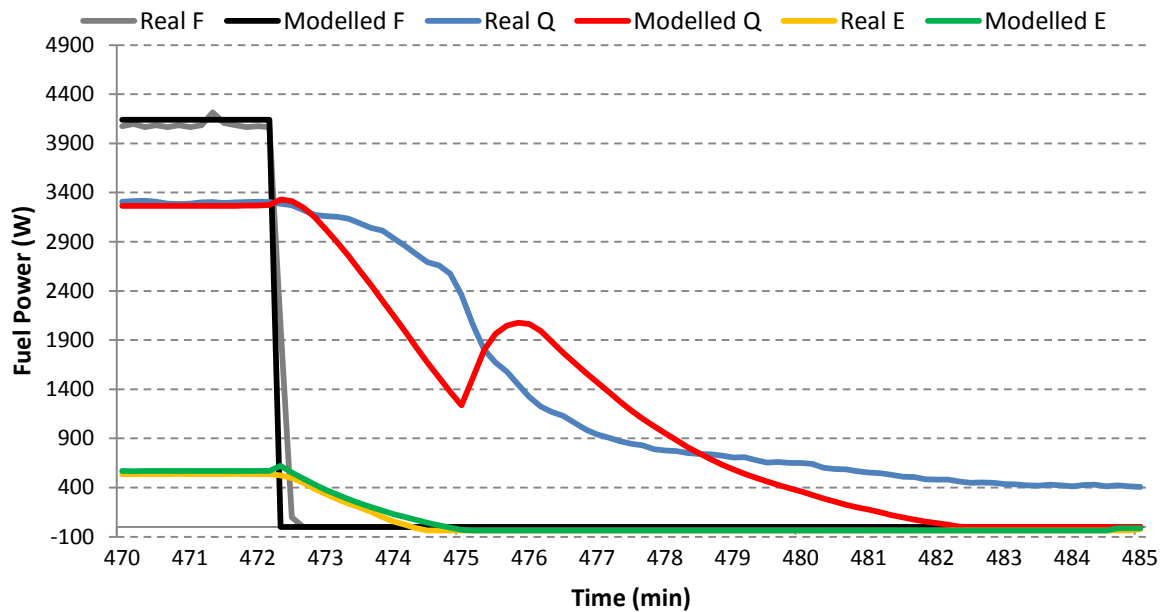


Figure 2.45 – Real and simulated power exchanges during shut-down from part-load operation (Test B).

In this sense, nevertheless, it can be appreciated that the thermal power output predicted by the model at part-load is slightly below the real value. This is due to the fact that the test was carried out with a fixed cooling water temperature at the inlet while, in order to modulate the engine, it was the set-point temperature the one that was

variable. Since the engine is controlled in order to reach the set-point temperature measured by its internal sensor, differences between internal and external measurements make the set-point temperature not be exact to that imposed. Accordingly, the fuel power can also differ slightly, as observed in Figure 2.45 before the engine switches off, due to this discrepancy in the set-point temperature, as well as due to low errors when predicting the temperature of the head of the engine.

On the other hand, it can also be appreciated that the shutdown process, as happened for the full-load validation test, is successfully modelled, both for thermal and electric outputs.

Finally, concerning the auxiliary burner, power-based results summarized in Table 2.17, prove that the model proposed fulfils successfully its objective.

Table 2.17 – Validation results for the auxiliary burner.

| | $T_{cw,i}$ level | Fuel input | | | Thermal output | | |
|---|---|---|---|---|---|---|---|
| | | Measured (W) | Calculated (W) | NMBE (%) | Measured (W) | Calculated (W) | NMBE (%) |
| 635 l/h | 30 | 19463 | 20094 | 3.24 | 17156 | 17910 | 4.39 |
| | 35 | 19676 | 19990 | 1.60 | 17260 | 17599 | 1.96 |
| | 40 | 19407 | 19851 | 2.29 | 16543 | 16829 | 1.73 |
| | 50 | 19738 | 19587 | -0.77 | 16063 | 15873 | -1.18 |
| 720 l/h | 30 | 20618 | 20124 | -2.40 | 18091 | 18442 | 1.94 |
| | 35 | 19740 | 20027 | 1.45 | 17296 | 17869 | 3.31 |
| | 40 | 20231 | 19888 | -1.70 | 17100 | 17105 | 0.03 |
| | 50 | 20069 | 19630 | -2.19 | 15930 | 15761 | -1.06 |

# 6. Conclusions

This chapter deals with the modelling, experimental characterization and validation of Stirling engine-based residential micro-CHP units.

Taking into consideration the literature review about Stirling engine modelling with building energy simulation purposes presented in Chapter 1, this chapter presents a new modelling approach with the objective of relieving the deficiencies associated to previous models, as well as strengthen their strong points.

The so developed model, due to its architecture and topology, is generic and adaptable to most of the Stirling engine-based micro-CHP units available in the market. Due to its scope of application, it is conceived in terms of a grey-box modelling approach, which combines an analytical description of some of the physical phenomena together with empirical data.

The first part of the chapter is exclusively dedicated to presenting the structure of the model, together with the different equations that describe the performance of the Stirling engine, as well as the auxiliary burner this kind of device is typically integrated with, under different modes of operation and constraints.

One of the main strengths of the model lies in the consideration of the part-load operation of this kind of devices, which is generally overlooked in researches previously presented by other authors.

Once the model is defined, the second part of the chapter deals with the experimental characterization of a Stirling micro-CHP unit which is of interest for the subsequent application in the case studies of coming chapters. In this sense, the selected micro-CHP unit and its main features are first conscientiously described, in order to be aware of how the engine works and develop the characterization routine in accordance.

Concerning this experimental characterization of the unit, the description of the test-rig developed at the Laboratory for the Quality Control in Buildings, sited in Vitoria-Gasteiz, has been addressed first, where the engine was integrated. This test-rig, which is part of an ambitious experimental installation designed and developed within the context of this PhD Thesis, fulfils all the necessities derived from the modelling for its calibration and validation.

The testing routine encompasses the evaluation of every operation mode the engine can operate at, according to the previously defined model, and all the measurements and data which must be taken into consideration when developing the characterization tests, necessary for calibrating and validating the model afterwards. Based on an uncertainty analysis, it is verified that the main source of uncertainty when evaluating the different measurements lies in the fuel determination.

Subsequently, using the empirical data obtained, the model proposed is calibrated. Three different calibration approaches are presented, concluding that sophisticate parameter identification techniques based on optimization algorithms allow minimizing the deviation with respect to real data (0.56% overall error during a complete on-off cycle versus 1.20 % and 2.02 % of the intermediate and basic calibration approaches, respectively). However, this approach, contrary to that based on the First Law of Thermodynamics, overlooks the physical sense of the different energy exchanges, and it just looks for the combination of parameters that minimize the difference between actual and simulated values. In order to be able to calibrate the model attending to simple thermodynamic energy balances, more exhaustive information on some heat transfer processes is required.

Finally, the last section of the chapter is focused on validating the model. For the case of the engine, a dual validation is presented, by comparison with both a previous validated model and experimental data obtained through laboratory tests. In the case of the auxiliary burner, its validation is only conducted in terms of comparison with the obtained experimental data. Both validations, even though predicted values can differ slightly from the actual values under some working conditions, present good agreement in general terms, with errors lower than $\pm 1$ % when predicting the cooling water temperature and below $\pm 2$ % when attending to the net electric output. Definitely, being a simplified model whose appliance is aimed at being used in buildings energy simulation tools, the model can be considered to represent the performance of the engine accurately while maintain quite a simple structure in comparison with analytical and numerical approaches.

# CHAPTER 3

# INTEGRATION OF THERMAL ENERGY STORAGE WITHIN STIRLING ENGINE-BASED RESIDENTIAL MICRO-CHP INSTALLATIONS

# 1. Introduction and objectives

When the potential implementation of a cogeneration unit in any application is considered, its performance in terms of economics, energy savings and avoided $CO_2$ emissions must be analysed. This profitability mainly lies in an appropriate dimensioning of the system and the operative strategy of the plant, which becomes more complex as the demands get more variable and the market prices of the energy resources and the normative suffer from significant changes.

In most of industrial applications, selection of the main generator and operative conditions of the cogeneration plant is a relatively simple procedure, since thermal and electric loads of an industrial process are nearly constant throughout the whole year. That is why the optimum sizing of the main components of such a cogeneration plant can be obtained from the annual mean thermal demand (Roncato and Macchi, 2000).

However, design of small-scale applications in tertiary and residential sectors require a more complex approach due to the great fluctuations electrical and thermal demands present, which are related to the climate, occupation and other highly stochastic conditions. Thus, one major concern when implementing micro-CHP systems lies in the mismatch between the electricity and heat provided by the micro-CHP system and the electrical and thermal energy required in the household (Horlock, 1997). Moreover, a micro-CHP system operates more efficiently at a constant full load, but the thermal and electrical energy demands are hardly ever constant and difficult to forecast.

This problem may be reduced when thermal energy storage (TES) is enabled (Petchers, 2003). Thereby, TES will capture thermal energy when there is overproduction and then deliver it back when the micro-CHP system is not able to provide as much energy as the building requires. This fact turns into longer periods and a more beneficial operation of the micro-CHP, consequently avoiding the frequent occurrence of transients during start-up and shutdown (de Wit, 2007b).

TES will also permit to extend the operational time of the micro-CHP facility, which is translated into more energy savings and larger $CO_2$ reductions. Even the installation of a small TES leads to an important increase of the number of hours of operation per year (Haeseldonckx et al., 2007).

Definitely, as affirmed by Sala (2015), TES can be considered as an energy conservation technology, since it allows decoupling production and consumption sides and so, ensuring energy security, efficiency and environmental quality.

Amongst the three main techniques existing for thermal energy storage, sensible heat thermal energy storage (SHTES) systems are the most commercially available. These systems are based on warming up or cooling down a certain quantity of mass, commonly water. Hot water SHTES systems are based on the stratification effect that occurs due to the density difference between the hot and cold water; hot water flows to the top and cold water remains at the bottom, while the intermediate region forms the thermocline (de Wit, 2007a).

In the literature, several works dealing with the feasibility of CHP residential plants including hot water storage have appeared so far. Fragaki et al. (2008) highlighted the importance of properly sizing the thermal storage through the economic study of engine-based cogeneration plants of different size and thermal storage capacities for a district heating in the United Kingdom. Similar conclusions were drawn by Streckienè et al. (2009), who carried out a study of a cogeneration unit participating in the German spot market, which was run during those hours when the electricity price was higher, accumulating the heat excess.

Khan et al. (2004) developed a techno-economic study of a trigeneration plant, concluding that heat storage not only increases the profitability (especially in those cases when the cooling load is also met by cogeneration by means of an absorption chiller), but also allows obtaining a substantial reduction in the peak production. Analogous results were obtained by Bogdan and Kopjar (2006) and Verda and Colella (2011).

Mongibello et al. (2013) analysed, both technical and economically, the integration of a cylindrical hot water tank with a residential micro-CHP system and compared it with the employment of a latent heat thermal energy storage (LHTES) system. The sizing of the TES was estimated based on the operational logic and the thermal and electric loads. Barbieri et al. (2012) presented a model to analyze the effect of the size of the TES on the energy and economic profitability of residential micro-CHP systems in a single-family dwelling, concluding that this effect is not linear and becomes more important as the thermal power of the prime mover is increased.

Other studies are based in mathematical models where the size and operation of the cogeneration plant and the charging and discharging of the thermal storage tank were optimized. Gustafsson and Karlsson (1992) developed a mixed integer program to optimize the running of the plant in order to maximise the economic performance. Ibáñez et al. (2014) presented a simple analytical method for sizing DHW tanks fed by CHP systems. In this line, Katulić et al. (2014) developed a simplified method for optimizing the capacity of a thermal energy storage system so that profits obtained in a cogeneration plant in Croatia could be maximized. Lozano et al. (2010) developed a cost-optimization study for obtaining the optimal design and operation of a trigeneration plant.

All these studies recognize the importance of including thermal storage tanks in these kinds of applications but, on the other hand, they do not deepen on analyzing the importance of the way it is arranged within the plant.

Thereby, focusing on the vital role TES can play, as highlighted in the bibliography, the main objective of this chapter, as a previous step of deeply analysing the feasibility of employing Stirling engines in domestic applications addressed in a subsequent chapter

of the thesis, is to deal with the implications of implementing Stirling engine-based micro-CHP systems into single-family dwellings, focusing on how TES, both considering the capacity of accumulation and the way tanks are integrated, can influence the techno-economic behaviour of the whole system.

This chapter is structured in six sections. After the introduction, fundamentals of SHTES systems are addressed in Section 2, focusing on traditional hot water tanks, the way they can be arranged within an energy plant and the subsequent configurations that should be considered when integrating TES within a micro-CHP plant. Section 3 first introduces the simulation bases and considerations and, afterwards, the methodology employed to analyse those results obtained from the simulations and, consequently, the impact TES has on the micro-CHP performance are described. Section 4 is entirely referred to the particular case study to which the previously described methodology is applied, afterward presenting the main energy, exergy and economic results in Section 5. Finally, the main conclusions and achievements got through the chapter are summarized in Section 6.

The chapter corresponds to an adapted version of the article *Effects of the thermal energy storage integration within a Stirling engine-based residential micro-CHP installation,* currently under review.

## 2. Sensible heat thermal energy storage systems

Traditional SHTES systems are made of a medium which is usually a tank which contains a liquid which is at the same time the storage medium and the heat transfer fluid. Heat is stored and discharged by elevating and lowering the temperature of the substance, generally water, respectively.

The most usual practice is to employ vertical cylindrical hot water tanks as storage medium, with no partitions inside. The heat storage effect is enhanced by the thermal stratification, i.e a thermal gradient across the storage, which is caused by the density difference between the hot and cold layers of the fluid, so maintaining hot water at the top of the tank while cold water, with higher density, sinks to the bottom.

As mentioned by Dincer and Rosen (2002), an effective utilization of a TES tank must imply stratification, that is, separate volumes of water at different temperatures should be hold. In this sense, mixing of the volumes should be minimal, even during charging and discharging periods. Additionally, the effective storage capacity should minimize the thermocline, i.e. the amount of dead water volume in the tank. Consequently, in order to maintain the stratification effect during operation, the hot fluid should be added and removed from the top and the cold fluid from the bottom. This way, high temperatures are available to be sent to the load and lower ones to the heat source, therefore improving the performance of the generator and, as mixing is reduced as well and consequently the destruction of exergy within the tank, the global performance of the plant is improved (Campos Celador, Odriozola et al., 2011).

## 2.1. Integration of SHTES within an energy plant

As previously introduced, TES systems are integrated in micro-CHP installations in order to store the heat produced by the micro-CHP unit when there is no load or when this production exceeds the load. In this integration, the way it is arranged plays a very important role.

As proposed by Campos-Celador (2012), any heat storage system can be classified regarding its connections as: *1 inlet - 1 outlet* or *2 inlets - 2 outlets* configurations.

In 1 inlet - 1 outlet systems, as represented in Figure 3.1, there is a single loop for both the charging and discharging processes, which goes through the storage system from the inlet to the outlet. Likewise, these systems can be implemented by an upstream or a downstream configuration.

The performance of these configurations of the storage depends on the operating mode. In the downstream configuration, the storage capacity is increased during the charging process, as it is connected at the outlet of the cogeneration unit where the temperature of the fluid reaches its maximum. However, this adds priority to the storage over the load, which can cause deficit in meeting the demand. Under the upstream storage configuration, even though the effective storage capacity is reduced, the inlet temperature to the micro-CHP unit is reduced during the charging process, which

results in an increase of the CHP performance. Although the selection and operation of this kind of system is hardly dependent on the operation strategy of the micro-CHP and the nature of the heat loads, in small residential applications, in general, downstream configuration results more suitable.
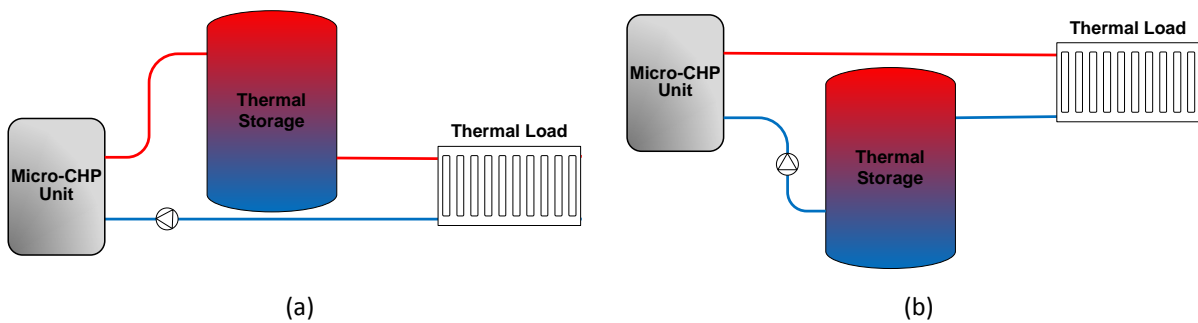


Figure 3.1 – Basic integration of 1 inlet-1 outlet TES system in a micro-CHP plant: (a) downstream integration and (b) upstream integration.

A typical solution for improving the exchanged power and, therefore, the storage efficiency, is to make the heat transfer fluid enter the storage system on opposite sides during the charging and discharging, respectively, as depicted in Figure 3.2. Thus, the temperature gradient between the heat transfer fluid and the storage medium increases and simultaneously the heat transfer ratio. However, this solution requires an active piping system governed by a control system that discerns between charging and discharging which, in fact, turns into a more complex and expensive facility.
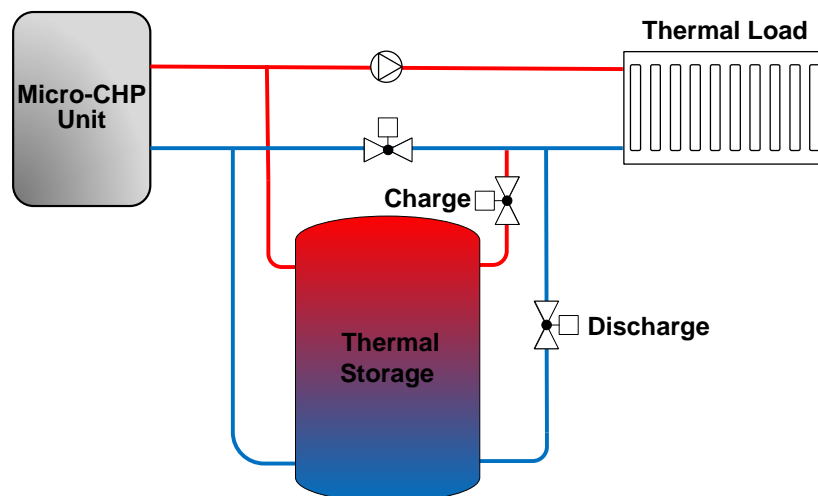


Figure 3.2 – Advanced integration of 1 inlet-1 outlet TES system in a micro-CHP plant.

On the other hand, in 2 inlets - 2 outlets systems, as shown in Figure 3.3, two different loops can cross the storage system at a certain instant.
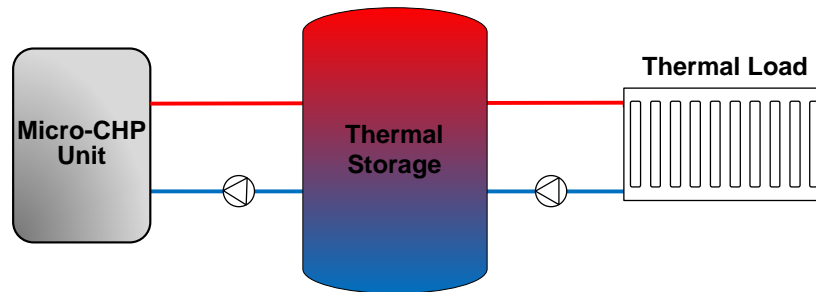


Figure 3.3 – Integration of 2 inlets-2 outlets TES system in a micro-CHP plant.

These systems exhibit two decoupled hydraulic loops, one for the discharging process and the other one for the charging, so being the integration and operation simpler than in the case of the 1 inlet - 1 outlet system. Nevertheless, the management of the energy content of the storage system is less flexible than in the previous case.

## 2.2. Configurations of the micro-CHP installation

Most commercially available small-scale Stirling engine-based micro-CHP units, some of which with thermal outputs of 10 kW and below have been introduced in Chapter 1 and are collected in Table 3.4 presented in Section 4.1, are designed to operate in a similar way as conventional high-performance boilers do but also integrating an engine that covers the base thermal and electric loads. As a consequence of this fact, in the different arrangements of the TES within a micro-CHP installation presented in this section, no external backup heat source was considered.

Therefore, the installation was conceived as a combined system for the joint production of heating and DHW, and all of the selected configurations include certain level of accumulation. The main goal is to make the operation of the micro-CHP unit steadier, so avoiding repeated on-off cycles and efficiency losses due to the transient effects during these cycles.

On the other hand, besides the integration of the TES within the plant, the influence of the configuration of the distribution loop on the final results was also assessed. In this

sense, two different options do exist: parallel distribution (Figure 3.4 (a)) and series distribution (Figure 3.4 (b)). While the parallel distribution makes no distinction between the two thermal demands, in the series distribution priority is given to the DHW demand, afterwards providing heating at a lower temperature.
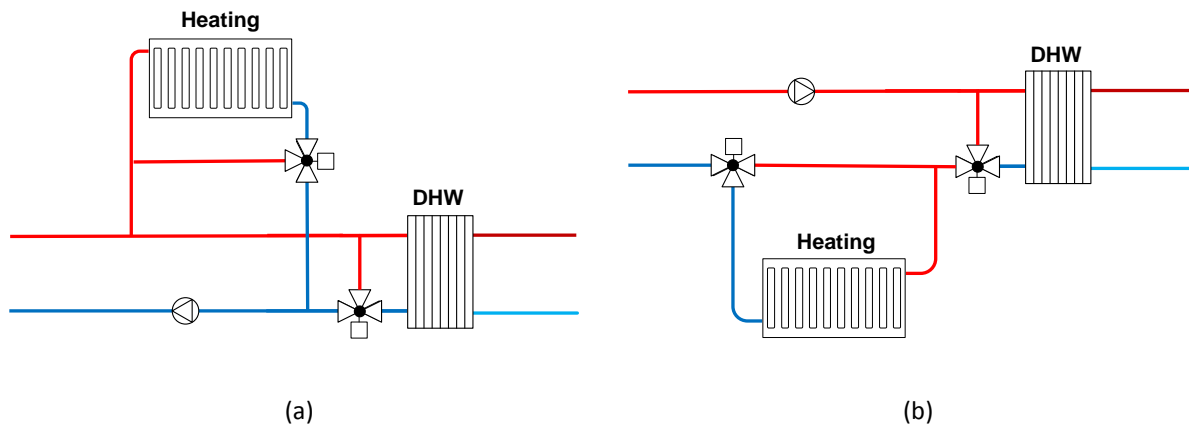


Figure 3.4 – Different configurations of the distribution circuit: (a) parallel connection and (b) series connection.

According to the TES configurations previously presented in Section 1, in combination with the fact that DHW can be instantaneously produced or accumulated, four main designs were considered for the installation to cover the thermal energy demand of the final user. Each of the four main configurations was afterwards split into two different variants, depending on if space heating and DHW circuits are connected in parallel (Figure 3.5 to Figure 3.8) or in series, giving raise to all the cases contemplated and summarized in Table 3.1 once introduced the specific assumptions to the case study in Section 4.2.

Finally, there was one last configuration, consisting on direct heating and DHW production through a tank, that was rejected. As reported in the Annex 54 (Darcovich and Entchev, 2014), with this arrangement, which was implemented in two detached dwellings in Bavaria and presented by Lipp (2013), the Stirling unit presented too many daily on-off cycles, short operating periods, as well as frequent interventions of the auxiliary burner for covering those peaks which could not be met by the engine itself.

This fact was verified when the baseline case[1] was simulated and analysed as mentioned in the economic methodology presented in Section 3.4 of this chapter.

### Configuration 1: parallel arrangement with buffer tank and DHW storage

In the first case, as depicted in Figure 3.5, the micro-CHP device is directly connected to a buffer tank which allows increasing the number of running hours of the unit by providing inertia to the installation. Afterwards, space heating and DHW demands are directly fulfilled with the hot water flowing from the buffer tank. This parallel arrangement requires the installation of two pumps, giving rise to a primary and a secondary loop. Additionally, a third pump is required for the DHW loop.
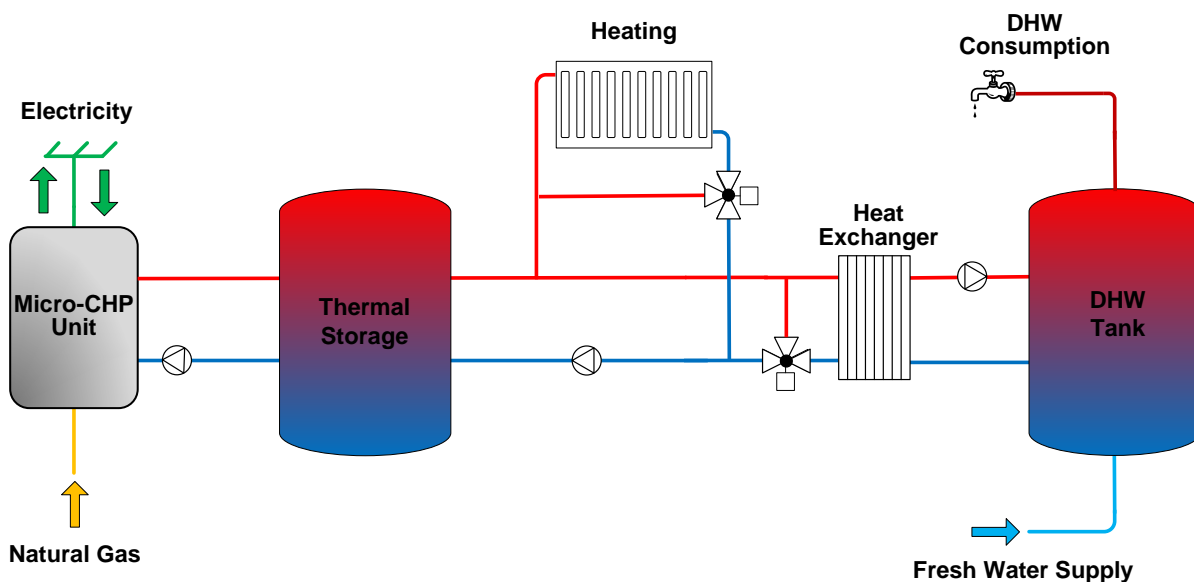


Figure 3.5 – Scheme of the plant installation with the TES system in a parallel arrangement and DHW tank.

### Configuration 2: parallel arrangement with combined heat buffer

The second configuration, shown in Figure 3.6, works in the same way as the first case does, except for the DHW supply, where the demand is directly produced with a heat exchanger, with no tank usage. This arrangement does not require a pump for feeding the DHW tank.

---

[1] The baseline case consists of an installation where the micro-CHP unit directly feeds both heating and DHW demands, without any hot water storage.
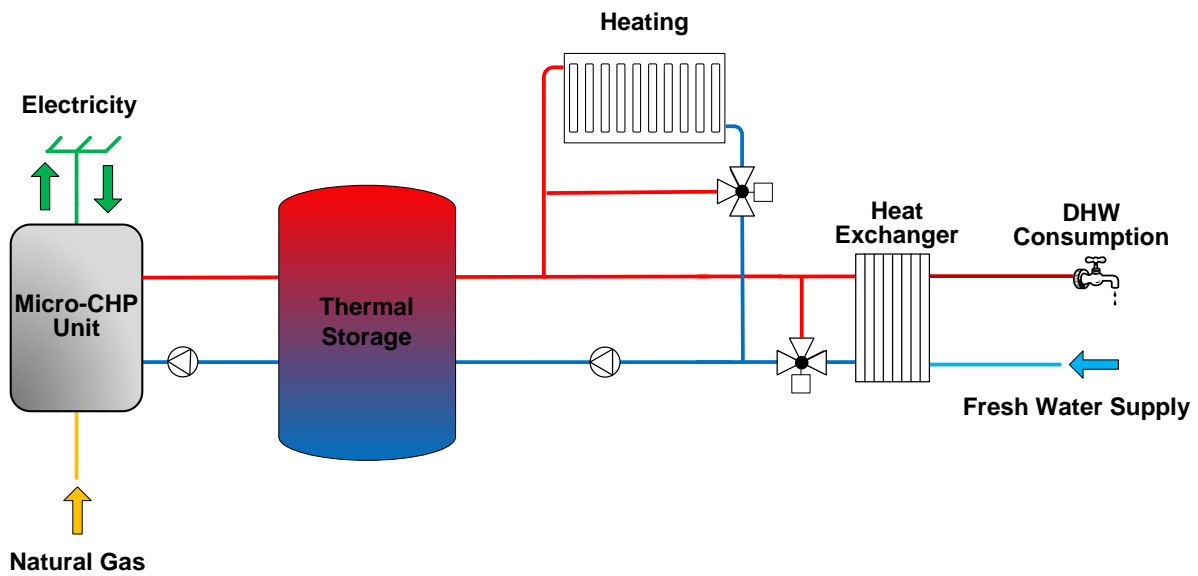
Figure 3.6 – Scheme of the plant installation with the TES system in a parallel arrangement and instantaneous DHW production.

## Configuration 3: series arrangement with thermal storage and DHW tank

The third configuration combines space heating, DHW production and thermal storage, all of them connected in series. Additionally, a hydraulic compensator is installed in between generation and demand sides, as illustrated in Figure 3.7.

Two different operating modes were proposed: in the first, the tank works as it does in configurations 1 and 2, except for it is connected in series, which turns into 1 inlet-1outlet instead of the 2 inlet-2 outlet nature of configurations 1 and 2. In this case, as discussed by Campos-Celador et al. (2011; 2014), the connection should be top-bottom, so that the irreversibility caused by the mixture can be reduced.

In the second variant, in accordance with the sophistication of the control logic introduced in Figure 3.2, the micro-CHP module feeds space heating and DHW generation loops with hot water, and afterwards, if the power produced by the engine is higher than the one demanded, the return of the demand side is used for charging the thermal storage tank (top-bottom). Afterwards, when the tank is charged and there is any thermal energy demand, it will get discharged (bottom-top).
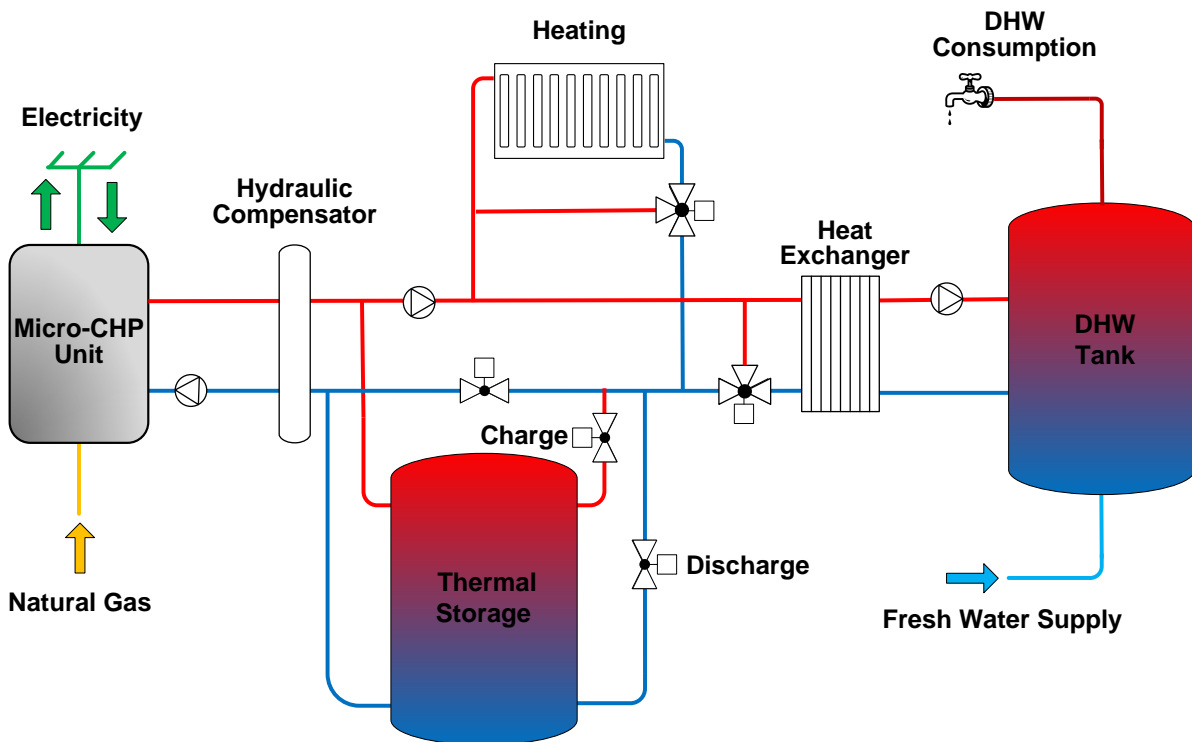
Figure 3.7 – Scheme of the plant installation with the TES system in a serial arrangement and DHW tank.
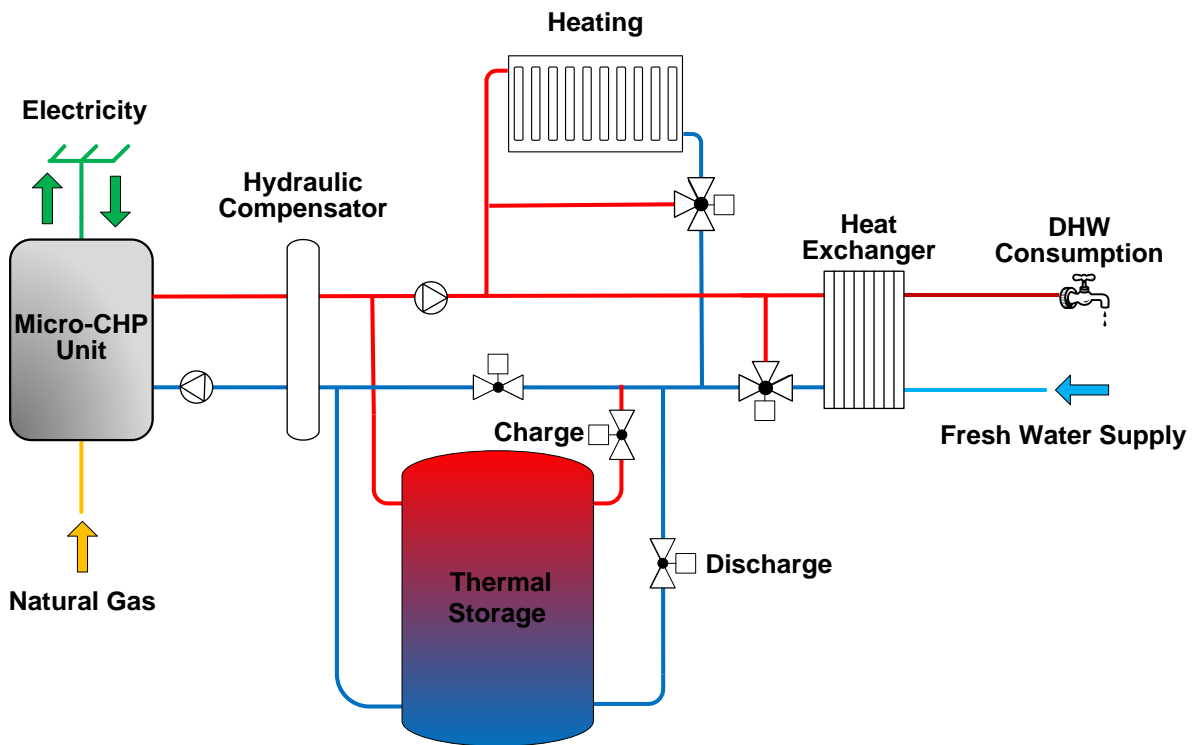


Figure 3.8 – Scheme of the plant installation with the TES system in a serial arrangement and instantaneous DHW production.

**Configuration 4: series arrangement with thermal storage and no DHW tank**

In the fourth configuration, which is outlined in Figure 3.8, thermal storage is integrated as it is in case 3, with the only variation of DHW production, as no tank is utilized.

When analyzing all the resulting scenarios in Sections 4 and 5, each case is named according to the procedure explained next: first, the configuration of the TES is referred to (P: parallel, S: series), second the distribution arrangement is expressed (P: parallel, S: series), then the TES volume is indicated and, last, the DHW tank volume is specified. Thus, for example, case represented in Figure 3.8, with a TES capacity of 500 litres, would correspond to scenario SP500.000. The main configurations considered for the actual analysis are summarized in Table 3.1.

Table 3.1– Summary of the main configurations contemplated.

| Case ID | TES arrangement | Demand distribution | TES volume | DHW accumulation volume |
|---------|-----------------|---------------------|------------|-------------------------|
| PP500.200 | Parallel | Parallel | 500 | 200 |
| PS500.200 | Parallel | Series | 500 | 200 |
| PP500.000 | Parallel | Parallel | 500 | 0 |
| PS500.000 | Parallel | Series | 500 | 0 |
| PP750.000 | Parallel | Parallel | 750 | 0 |
| PS750.000 | Parallel | Series | 750 | 0 |
| SP500.200 | Series | Parallel | 500 | 200 |
| SS500.200 | Series | Series | 500 | 200 |
| SP500.000 | Series | Parallel | 500 | 0 |
| SS500.000 | Series | Series | 500 | 0 |
| SP750.000 | Series | Parallel | 750 | 0 |
| SS750.000 | Series | Series | 750 | 0 |

# 3. Methodology

All the configurations previously set out were analysed in energy, exergy and economic terms by means of dynamic simulations carried out within a building energy simulation tool, as detailed throughout this section.

## 3.1. Modelling and simulation approach

The configurations to simulate were implemented in the Simulation Studio pack contained in TRNSYS 17 energy simulation software. TRNSYS is a widely used transient system simulation software tool, modularly structured, that has been specifically designed for developing complex energy-related systems and their coupling to building modelling and simulation. According to Sousa (2012), which carried out an analysis of some of the most important energy simulation programs, except for certain cases where others can get more appropriated in terms of needs-complexity, TRNSYS is generally the most complete tool for building-scale simulation.

Each simulation case is defined as an ensemble of individual components, called Types, which are subsequently described.

The generation device, i.e. a Stirling engine-base micro-CHP unit, is modelled by a self-tailored Type, based on the model developed in Chapter 2. The modelling also considers the internal control and regulation responsible for determining the operation mode of the system, as well as the auxiliary burner that most of these kinds of units are provided with. Additionally, the generation unit is externally governed by a controller that aims to maintain the temperature of the water delivered to the demand above a certain temperature. This control is implemented by Type 2, providing the installation with a hysteresis that avoids repeated on-off cycles of the generation unit, so helping to get a smoother operation of the Stirling engine.

Hot water tanks, as well as hydraulic compensators, are simulated using the model developed by Klein et al. (1976), implemented in TRNSYS as Type 4. This model, which takes into account all the main effects occurring within a tank, is considered to perform the most realistic behaviour amongst the existing modelling approaches with simplicity and good agreement with the experimental results shown by Klein (1976). The model is based on solving a one-dimensional convection equation.

DHW is produced by a plate heat exchanger modelled by Type 91, whether it is instantaneously or tank-through produced. This zero-capacitance sensible heat exchanger is modelled with constant effectiveness, i.e. the effectiveness is given as an

input parameter, and it is independent of the system configuration. Thus, the maximum possible heat transfer is calculated based on the minimum capacity rate fluid and the cold side and hot side fluid inlet temperatures. Additionally, a three-way valve modelled with Type 11 is disposed so that pumping water through the DHW circuit can be avoided for those cases when there is no need for heating up the DHW tank or the occupants of the dwelling do not demand any DHW.

Meanwhile, heating is supplied to each zone by a radiator system which is modelled by a lumped capacity model which exchanges heat (80% convective/ 20% radiative) with the air nodes modelled by Type 56. The radiator, as detailed in (Terés-Zubiaga et al., 2016), is modelled as a self-tailored Type 211 using the thermo-physical properties of the commercial series StelRad Elite K2. Radiators present a bypass controlled by a three-way valve (Type 11), which reduce the need for pumping water through radiators lines when heating is not required. This control can be performed either with a thermostatic valve which maintains the control room temperature within a temperature range, or based on the outdoor temperature; in both cases it is modelled by Type 2.

Table 3.2 – Main components employed in the TRNSYS simulation.

| Component | Model | Source |
|---|---|---|
| Micro-CHP boiler | Type 159 | Self-tailored |
| Hydraulic compensator | Type 4 | Standard |
| Constant flow pumps | Type 114 | TESS |
| Storage tanks | Type 4 | Standard |
| Flow diverters | Type 11f | Standard |
| Flow mixers | Type 11h | Standard |
| Differential controller | Type 2 | Standard |
| Heat exchanger | Type 91 | Standard |
| Radiators | Type 211 | Self-tailored |

Finally, pumps are modelled by Type 114, and their operation is linked to the Stirling operation and DHW and heating demands. This Type models a single speed pump that maintains a constant fluid outlet mass flow, without considering starting and stopping characteristics, nor pressure drop effects. Additionally, since pipes are located in conditioned spaces, heat losses through them have been ignored, as well as the inner of water circulating within them.

All the main TRNSYS Types employed in the simulations are summarized in Table 3.2, and their mathematical description can be found in (S. Klein, 2012).

## 3.2. Energy analysis

The energy analysis of the installation encompasses an evaluation based on the on-off cycles and the total operation time of the engine, as well as the PES (as shown in Equation 3.1) and reduction of GHG emissions achievable with the different configurations and the corresponding efficiencies.

$$PES = \left( 1 - \frac{F_{CHP}}{\frac{Q_{CHP}}{RefH_\eta} + \frac{E_{CHP}}{RefE_\eta}} \right) \cdot 100 \qquad \text{Equation 3.1}$$

where $F_{CHP}$, $H_{CHP}$ and $E_{CHP}$ are the respective fuel consumption, useful heat produced and electricity output of the micro-CHP installation, and $RefH_\eta$ and $RefE_\eta$ are the harmonized efficiencies for separate heat and electricity productions, respectively (Official Journal of the European Union, 2012).

For determining the useful heat production of the engine, the corresponding heat losses of the TES must be determined and subtracted to the gross production. For that purpose, taking into consideration the previously mentioned fact that Stirling generation devices susceptible of being installed in single-family houses are generally made up of a Stirling engine and a condensing boiler working in series, an exergy-based assignment was considered, so that the influence of the temperature level at which each technology produces on the heat losses of the TES could be taken into account.

With respect to GHG emissions, the Global Warming Potential (GWP) defined in the IPCC 2007 method developed by the International Panel on Climate Change was taken as a basis. The GWP is defined as the potential of global warming in a period of 100 years, in kg of carbon dioxide per kg of emission, comparing the effect of the liberation of any GHG with that caused by the $CO_2$. All emission factors are given in kg of $CO_2$ equivalent. Emissions during the operation of each case were considered, in terms of natural gas

and electricity, while those relative to the extraction and manufacturing of the components were neglected (Pérez-Iribarren et al., 2011).

On the other hand, for evaluating the performance of the TES itself, the charging-discharging process was assessed, by studying the amounts of energy accumulated per unit of volume for each configuration. Additionally, the efficiency, that is, the ratio between the released and the stored energy, was also calculated.

## 3.3. Exergy analysis

As underlined by Bejan (1982), the objective of any TES system is not only to store energy, but also exergy. Thus, when evaluating their performance, the capacity of storing exergy should also be analyzed. Additionally, as pointed out by Campos-Celador et al. (2011), working with stratified tanks has a direct impact in the global performance of any plant, as stratification is not ideal and always implies some mixing. In this sense, an exergy analysis, which takes into consideration the Second Law of Thermodynamics, is considered to be a proper way to analyze this effect.

With data obtained from the simulations, main exergy flows through the micro-CHP plant were obtained and, consequently, as every thermodynamic irreversibility implies an exergy destruction, the effects of the tank volume on the exergy performance of the principal equipment could be assessed, finally calculating the exergy efficiency of the installation, as defined in Equation 3.2:

$$\psi = \frac{Ex_t + Ex_e}{Ex_f}$$

Equation 3.2

where $\psi$ is the exergy efficiency, and $Ex_t$, $Ex_e$ and $Ex_f$ stand for the exergy of the heat supplied, the exergy of the electricity produced, and the exergy of the natural gas, respectively.

On the other hand, the exergy content of the main components of the plant, as indicated by Campos-Celador et al. (2012), can be considered to be negligible.

## 3.4. Economic analysis

Additionally, apart from the energy and exergy analyses presented, the study was completed with a sensitivity analysis, where a basic economic evaluation, considering both capital investment of the tank and the natural gas and electricity flows of the micro-CHP, is carried out.

The economic feasibility is evaluated through the Net Present Value (NPV), so relating the corresponding incomes and outcomes existing through the life-time of the installation to the initial investment, as presented in Equation 3.3. As the TES volume is only changed from one simulation to another, a comparative NPV is considered. Thus, departing from the configuration with no accumulation capacity, to which NPV=0 is assigned, variations in the tank investment, as well as natural gas input and electricity output of the micro-CHP device values are evaluated, with respect to the aforementioned case.

$$NPV = -\Delta Inv + \sum_{n=0}^{n=LT} \left[ \frac{\Delta NS}{(1+r)^n} \right]$$

Equation 3.3

where $\Delta Inv$ is the differential cost of the storage tank with respect to the one in the reference case, $LT$ is the lifetime of the plant, $r$ is the rate of discount, and $\Delta NS$ responds to the annual cash flows generated with respect to the reference case, which were calculated as detailed in Equation 3.4.

$$\Delta NS = \sum_{j=1}^{j=YT} \left( \Delta I_e + \Delta I_f \right)_j$$

Equation 3.4

where $\Delta I_e$ stands for the differential incomes associated to the electricity produced by the installation (taking into consideration specific retributions, as well as both sales and avoided costs due to self-consumption), $\Delta I_f$ is the differential income due to avoided natural gas consumption, and $YT$ is the full-year time in the corresponding time-basis.

# 4. Case study

This Chapter deals with the implementation of TES within Stirling engine-based micro-CHP installations in single family dwellings. Thereby, once defined how TES can be integrated in this kind of plants, according to the configurations previously presented, together with the evaluation methodology introduced, the next step is to apply this methodology to assess a case study which enables fulfilling the target objectives.

The case study analysed is a recently built detached house sited in a rural area close to Vitoria-Gasteiz, Basque Country (Northern Spain). The dwelling, which was geometrically modelled using Google Sketch Up along with the TRNSYS 3d plug-in as extensively explained in Appendix D (Figure 3.9), is a typical single-family dwelling in the north-side, built early in the current decade, with 198.43 m² of thermally conditioned surface distributed among three floors (basement, ground floor and first floor).



Figure 3.9 – Sketch of the building modelled.

Each of the main elements of the envelope was defined for fulfilling its respective referential transmittance value established by the CTE in force at the moment of the execution of the project for both new and refurbished buildings sited in the aforementioned climatic zone. The main features of the envelope, which are described in detail in Appendix D, are summarized in Table 3.3.

Except for ventilation rates, which were based on those values required by the Indoor Air Quality document of the CTE (2013c), the main use patterns of the building, i.e. occupancy profiles, internal gains, infiltration rates and heating set-point temperatures – 17 °C from 11 p.m. to 7 a.m. and 20 °C the rest of the day – were based on the schedules given by IDAE (2009).

Table 3.3 – Actual transmittances of the constructive elements and the maximum values permitted when the project was executed.

| Component | U-value (W/K·m$^{-2}$) | |
| --- | --- | --- |
| | Real | Maximum |
| Exterior wall : Type 1 | 0.44 | |
| Exterior wall : Type 2 | 0.40 | 0.86 |
| Exterior wall : Type 3 | 0.37 | |
| Roof | 0.22 | |
| Ceilings | 0.44 | 0.49 |
| Floors | 0.42 | 0.64 |
| Windows | 1.24 | 3.50 |

Concerning DHW, demand values estimated in Appendix D, being representative of hourly total consumption of DHW in the dwelling, do not match accurately the real instantaneous nature of DHW consumption characterized by sharp instantaneous peaks. Thus, when sizing the generation devices of the thermal plant, a security margin must be considered in order to deal with these greater peaks. Otherwise, as later on used throughout the simulations, 1-minute profiles can be generated with the profile generation tool developed within the IEA Task 26 context (Jordan and Vajen, 2001).

Bearing all the described parameters of the household in mind, i.e. the thermal features of its envelope, together with its shape and geometry, as well as its total net surface and usage patterns, the selected building is susceptible of being considered as a representative detached dwelling for Spanish cold climatic zones. Furthermore, it also

represents refurbished detached dwellings, as once a deep renovation on a housing is assessed, those requirements for new constructed buildings must also be fulfilled.
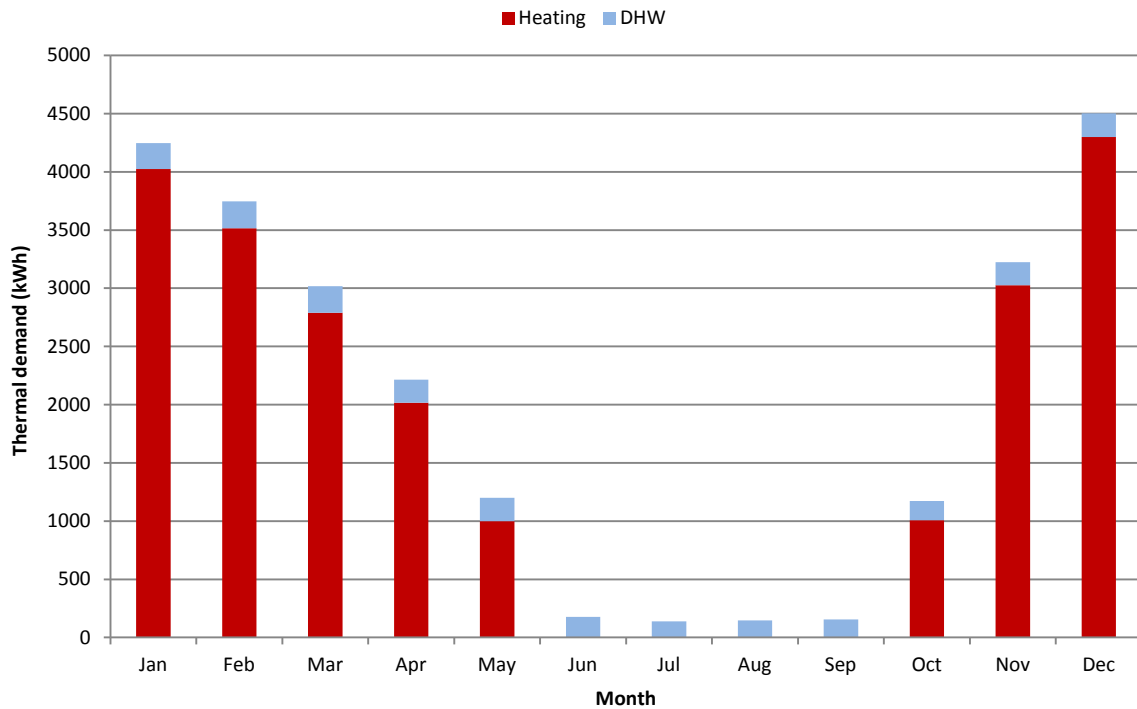


Figure 3.10 – Monthly distribution of the annual thermal demand.
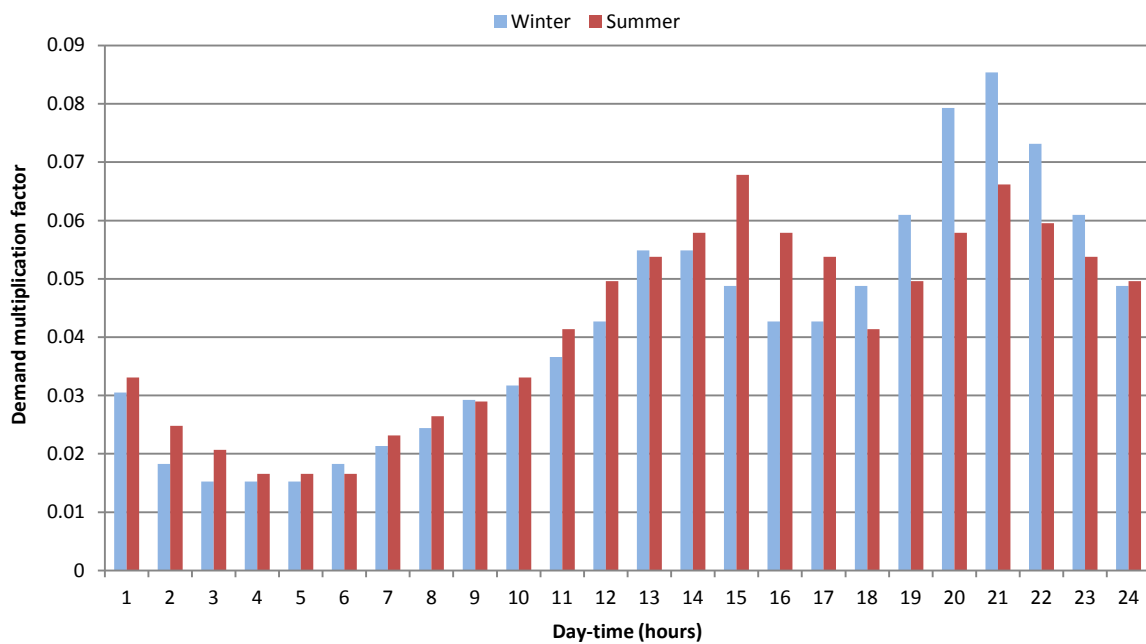


Figure 3.11 – Daily electricity multiplication factors.

According to the usage patterns given by the Spanish standards, which are described in detail in Appendix D, the heating demand of this dwelling on a one-minute basis comes to 22.2 MWh/a, with a power peak of 16.5 kW, while the DHW demand comes to 2368 kWh/a, both distributed throughout the year as represented in Figure 3.10.
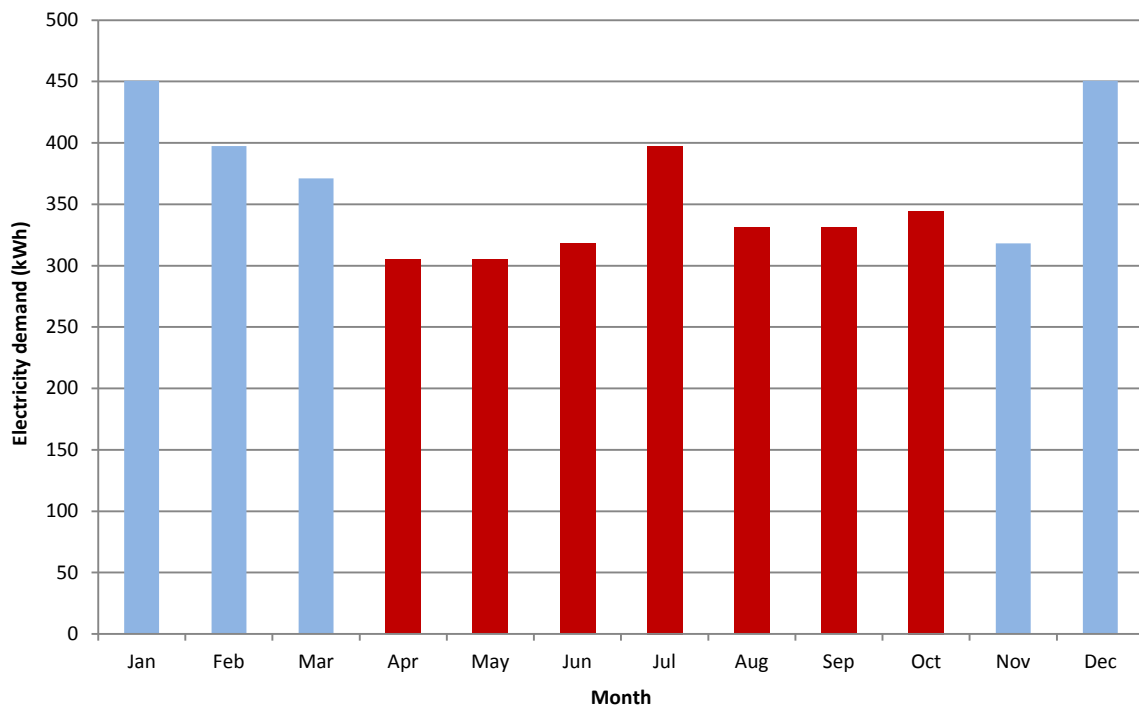


Figure 3.12 – Monthly distribution of the annual electricity demand.

Finally, regarding the electricity demand, it was assumed that the mean demand of a single family dwelling in Spain is 4320 kWh (IDAE, 2011b). Daily electricity consumption profiles were obtained taking into consideration the hourly multiplication values, shown in Figure 3.11, where summer and winter day-profiles are distinguished, and the monthly values shown in Figure 3.12, both provided by the Spanish operator of the electricity grid (REE, 2010).

## 4.1. Selection of the micro-CHP unit

There are several criteria for sizing a micro-CHP module, amongst which the most commons are based on maximizing the contribution of the micro-CHP to the thermal

demand of the final user. For that purpose, the global demand (space heating and DHW) over a year must be determined, hourly as far as possible.

Thereby, once obtained the hourly-basis demand obtained for the reference dwelling, the annual monotonic heat demand curve is built. This curve is a very important tool when sizing micro-CHP modules, as it gives information on the number of hours each demand value is required.

Once built this curve, there are two main criteria for selecting the size of the micro-CHP device:

i. The micro-CHP nominal output remains between the 10% and the 30% (20% recommended) of the peak thermal demand value.

ii. The micro-CHP nominal output is that power value which allows generating the maximum amount of useful thermal energy at full load.

Even though the second criterion is the most widespread one, it is desirable to fulfil both criteria at the same time, since the first one is focused on avoiding successive warm-up and shut-down periods of the unit which may damage the unit at the long run and reduce its useful life considerably (Fenercom, 2012).

Following these premises, the aforementioned design thermal power is obtained by inscribing the rectangle of maximum area in the monotonic heat demand curve (Haeseldonckx et al., 2007), as depicted in Figure 3.13 (a).

Consequently, a 4.65 kW thermal power value was obtained as the optimum (corresponding to the 26% of the peak thermal demand), corresponding to 2311 hours per year running at full load, which turns into covering an energy demand of roughly 10.7 MWh per year.

This sizing method, nevertheless, can sometimes present the drawback that the maximum thermal production corresponds to a high thermal power and a low number of running hours. Amongst the multiple possibilities mentioned by Voorspools and D'haeseleer (2006) and detailed by Pérez-Iribarren (2016) existing to solve this fact, thermal storage – the study of which is the aim of this chapter – and partial load

operation, as depicted in Figure 3.13 (c) and (b), respectively, are the key in small residential applications.
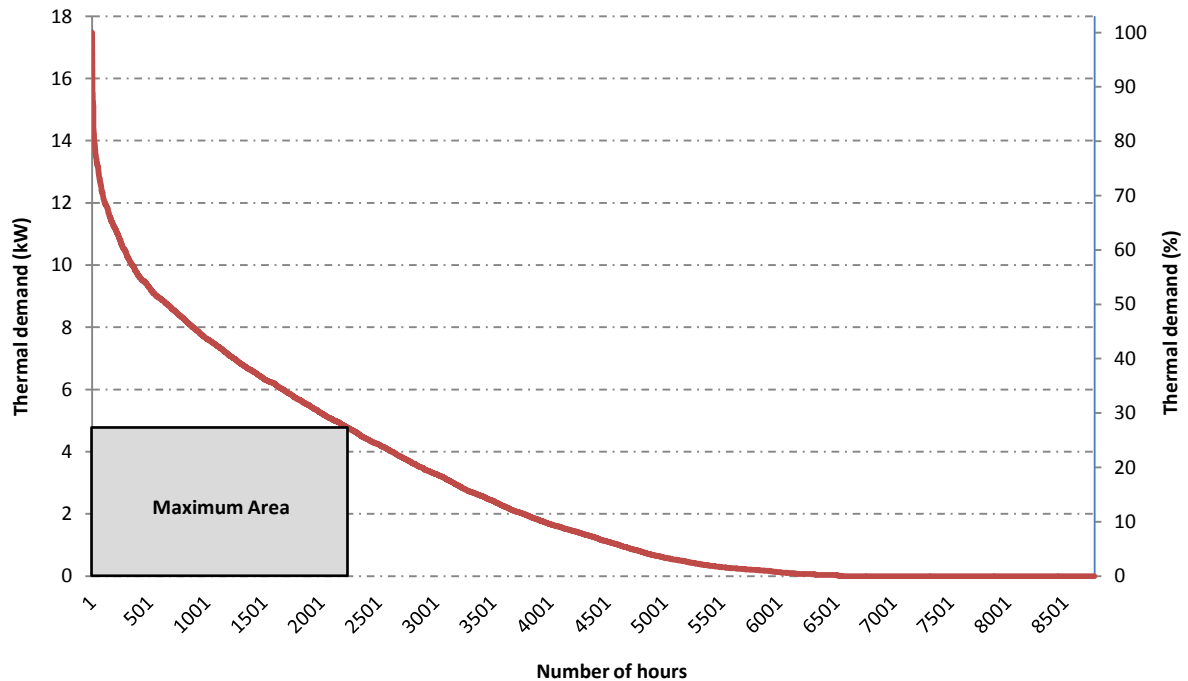


(a)
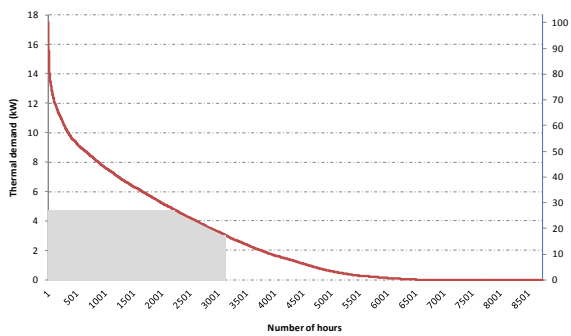


(b)
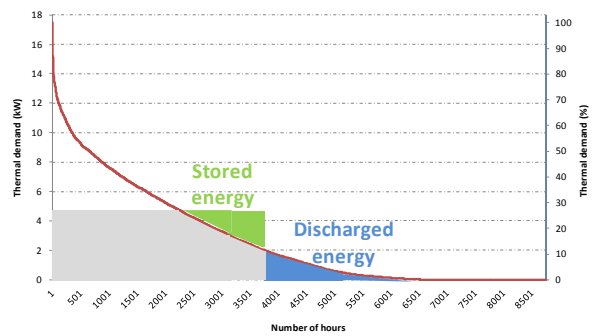


(c)

Figure 3.13 – Maximal area method applied to the monotonic heat demand curve (a) and solutions for incrementing the number of hours of operation: part-load operation (b) and thermal energy storage (c).

Accordingly, a micro-CHP unit among the commercially available with a nominal thermal power output immediately below the calculated value, which may regulate its thermal load if possible, must be chosen.

In Table 3.4 some of the commercially available Stirling units, with thermal outputs of 10 kW and below are summarized. Taking into consideration the design value of the thermal power and the market power range availability, the Remeha eVita engine might seem to be the one that fits best.

Table 3.4– Available small Stirling micro-CHP units.

| Manufacturer | Engine type | Fuel | Input Power (kW) | Electric Power (kW) | Thermal Power (kW) |
|---|---|---|---|---|---|
| Qnergy QB-3500 | Linear free piston | Natural gas Propane Wood pellet Biogas | 15 | 3.5 | 10 |
| Whispergen EU1 | Alpha | Natural gas | 9.5 | 1 | 8.3 |
| Baxi Ecogen | Linear free piston | Natural gas Biogas | 7.4 | 1 | 6 |
| Senertec Dachs Stirling | Linear free piston | Natural gas LPG | 7.5 | 1 | 5.8 |
| De Dietrich Hybris Power | Linear free piston | Natural gas | 7.3 | 1 | 5.8 |
| Viessmann Witowin 350-F | Linear free piston | Natural gas | 6.5 | 1 | 5.3 |
| Remeha eVita | Linear free piston | Natural gas LPG | 6.3 | 1 | 5 |

Even though the thermal power indicated in the specification of the Remeha eVita device (around 5 kW) is above the design value obtained, a field test presented by Lipp (2013) showed that this Stirling engine produced about 4 kW$_t$ when reached steady-state status. Likewise, in laboratory tests carried out and presented in Chapter 2, it was checked that, depending on the return temperature of the cooling water, the thermal output of the engine in steady state varies from 4.5 to 5.2 kW, being around 4.6 kW when working with those typical outlet temperatures of conventional radiators. This power value makes this unit match the requirements of this application. Additionally, when working with radiators, the unit is able to modulate its power output down to

$3.2\ kW_t$ approximately, so increasing substantially the theoretical yearly hours of operation of the engine up to 3066 and achieving a mean coverage of about 56% of the thermal demand without considering any heat storage.

The Remeha eVita micro-CHP device, as detailed in Chapter 2, is based on a linear free-piston Stirling engine developed by Microgen Engine Corporation (MEC) which produces around $1\ kW_e$ (Microgen Engine Corporation, 2015). Furthermore, the unit also contains a supplementary burner that allows covering peak demands up to 23 kW, which, being the peak demand of the building around 18 kW on an hourly basis, makes no additional generation device necessary. Concerning to its installation, its design and dimensions make of it a suitable device for wall-mounting, as conventional condensing boilers are.

Thus, all these facts exposed above make of the Remeha eVita the most appropriate Stirling-based boiler for the case-study and in more global terms, due to the representativeness of the dwelling assessed, for any detached house in the northern half of Spain.

## 4.2.  Operative and normative conditions

Before running the TRNSYS 17 simulation of the different cases contemplated, some assumptions on the operative parameters of the models employed have to be made. In this sense, concerning the generation unit, the Remeha eVita micro-CHP unit is equipped with a control that enables varying the generation set-point temperature from 30 up to 85 °C. Taking into consideration that in those cases where DHW is produced through a hot water tank, and that the terminal units considered for the building are those traditionally employed, i.e., high-temperature radiators, the production temperature of the unit was set to 70 °C.  The micro-CHP units is externally governed by a controller that aims to maintain the temperature of the water delivered to the demand side above 65 °C. This control provides the installation with a hysteresis that avoids repeated on-off cycles of the generation unit. Thus, once the unit is switched off, it will not be switched on again until the bottom temperature of the tank or the hydraulic compensator drops below 60 °C. This helps to get a smoother operation of the Stirling engine.

Hot water tanks employed in the cases previously set out and summarized in Table 3.1 have a volume of 200 and 500 liters for DHW and TES, respectively, while, in those cases when DHW is produced instantaneously, and the total storage volume is to be maintained, due to market-availability reasons, the capacity of the combined buffer tank is 750 litres. These tanks, as well as the hydraulic compensators which have a capacity of 15 liters, have a heat loss coefficient of 0.25 W/(m²·K). Additionally, when utilizing the model of these deposits, 10 temperature levels have been considered.

Concerning the demand side of the installation, the heating control employed is performed with a thermostatic valve which maintains the control room temperature between 17 and 18 °C from 11 p.m. to 7 a.m. and between 20 and 21 °C during the day. With respect to the heat exchanger responsible of instantaneously or tank-through producing DHW, a constant effectiveness of 90% was assumed.

On the other hand, in order to be able to assess the suitability of the TES with respect to the evaluation criteria exposed in Section 3, the different configurations implemented and modelled in the TRNSYS 17 simulation environment, were simulated for a year with a time-step of 1 minute, so that important transient effects in the plant, such as start-up and shut-down processes of the Stirling engine and filling of the hot water tanks, could be taken into consideration and, in turn, avoid convergence problems (Hendron et al., 2010). From these simulations, flow rates, temperatures and energy flows were obtained, so enabling the annual evaluation of each configuration.

Concerning the energy analysis, when calculating the PES value according to Equation 3.1, references parameters for separate heat and electricity productions ($RefH_\eta$ and $RefE_\eta$), according to the EED, acquire values of 0.9 and 0.45, respectively.

Regarding GHG emissions, the emission factor considered for the combustion of natural gas was 0.252 kg $CO_2$-eq per kWh, while that due to the production of a kWh of electricity, according to the energy mix shown in Figure 3.14, was 0.331 kg $CO_2$-eq per kWh (IDAE, 2016).
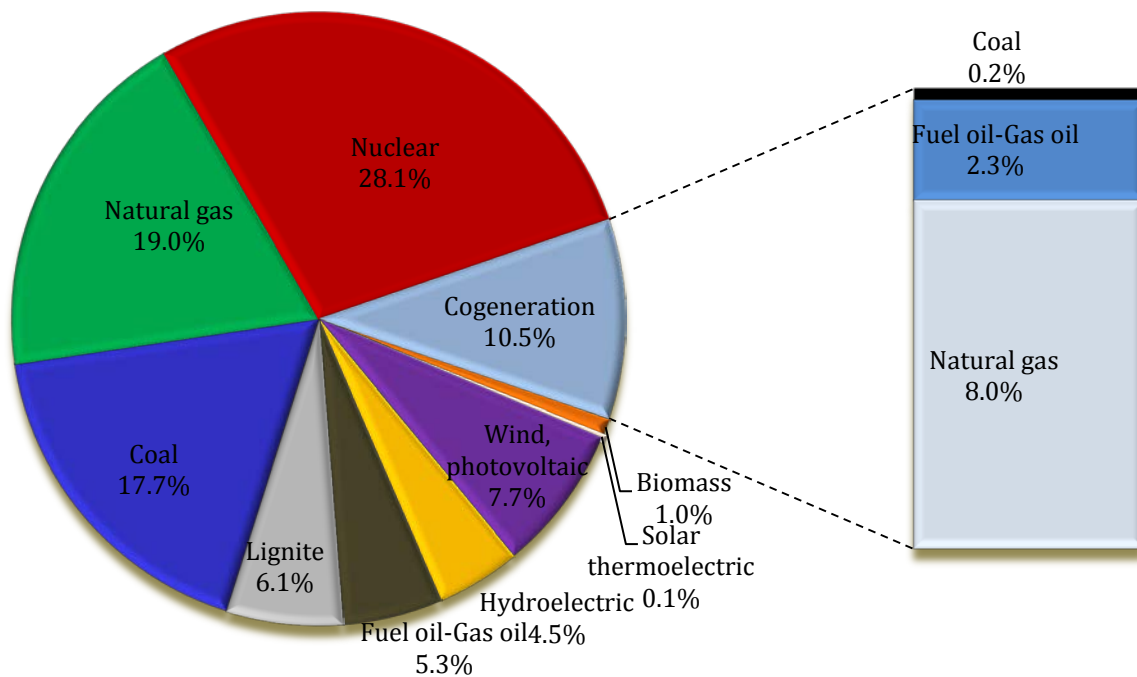
Figure 3.14 – Spanish energy mix.

When assessing the economic evaluation in terms of NPV, a discount rate of 5% is lately considered for this kind of projects to represent faithfully the available bank products under the current economic situation (IDAE, 2014; European Commission, 2014).

Additionally, for determining the differential incomes associated to the electricity produced by the installation, the Spanish electricity prices and specific retribution were considered. Thus, this term used in Equation 3.4 was calculated as indicated in Equation 3.5:

$$\Delta I_e = R_{inv} + R_o + i_e \hspace{3cm} \text{Equation 3.5}$$

where $R_{inv}$ and $R_o$ are the retribution to investment and the retribution to operation of the micro-CHP unit, respectively (as explained in Chapter 4), and $i_e$ is the income due to sold and self-consumed electricity.

In the current work, $R_{inv}$ was neglected since this complement is just attributed to the purchase of the micro-CHP device, while when dealing with electricity and fuel consumptions, only the variable terms are considered, as the fixed terms are common

for every case. Therefore, according to RD 413/2014, which regulates the electricity production activity based on renewable energies, cogeneration and waste in Spain (Ministerio de Industria, Energía y Turismo, 2014c), the incentive to operation $R_o$ corresponding to the selected micro-CHP unit is 78.05 € per MWh$_e$ poured into the grid. Additionally, whilst natural purchase-price is 5.04 c€/kWh (Ministerio de Industria, Energía y Turismo, 2014d), tariff corresponding to purchased electricity, according to the most common taxation modality, is 12.41 c€ (Ministerio de Industria, Energía y Turismo, 2014e), while no income corresponding to sold electricity was considered since no guaranteed payment is nowadays established.
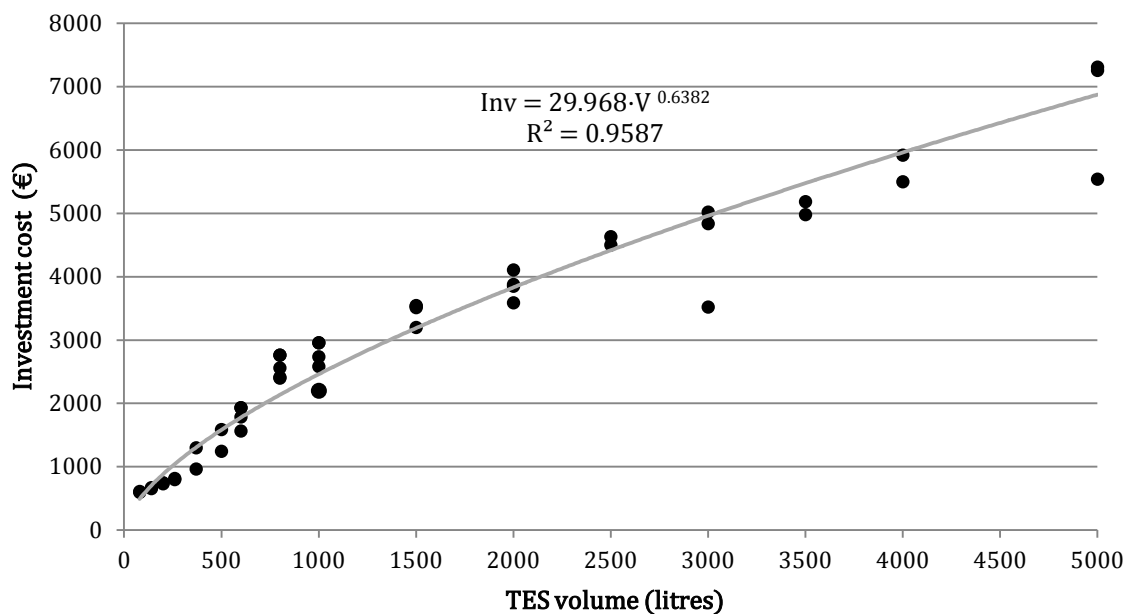


Figure 3.15 – Investment cost-to-volume relation for vertical cylindrical hot water tanks.

Finally, for taking into consideration investment costs of the tanks, based on various databases and commercial catalogues, an expression relating investment costs ($Inv_{TES}$), in €, to the volume of hot water tanks ($V_{TES}$), in litres, was obtained (Equation 3.6), by means of a regression as depicted in Figure 3.15.

$$Inv_{TES} = 29.968 \cdot V_{TES}^{0.6382}$$
<div style="text-align: right">Equation 3.6</div>

# 5. Results and discussion

Applying the methodology exposed in Section 3 to the case study, together with the assumptions set in Section 4, results summarized in Table 3.5 were obtained for each configuration simulated. Results corresponding to the second type of control (i.e. that which switches valves configuration between top-bottom when charging to bottom-top when discharging) for configurations 3 and 4 have been excluded, since it does not report any improvement with respect to the other control type but more complexity and higher cost.

Table 3.5– Summary of the annual behaviour of the micro-CHP plant.

| Case | ON/OFF cycles | Hours of operation | | Net electricity (kWh) | Net thermal energy (kWh) | | Fuel consumption (kWh) | | η (%) | PES (%) | ψ (%) |
|------|------|-------|-----------|------|---------|-------------|---------|---------------|------|------|------|
| | | Total | Part-load | | SE | Aux. burner | SE | Aux. burner | | | |
| PP500.200 | 666 | 3503 | 310 | 2859.1 | 13870.3 | 8444.9 | 20135.9 | 10630.3 | 81.5 | 7.5 | 12.1 |
| PS500.200 | 866 | 3174 | 486 | 2560.2 | 12390.5 | 9962.7 | 18079.3 | 12524.4 | 81.1 | 7.1 | 11.3 |
| PP500.000 | 647 | 3489 | 286 | 2837.4 | 13804.0 | 8327.2 | 20067.8 | 10490.3 | 82.2 | 7.3 | 12.7 |
| PS500.000 | 922 | 3173 | 487 | 2537.1 | 12305.8 | 9866.0 | 18051.8 | 12428.5 | 81.6 | 6.5 | 11.9 |
| PP750.000 | 520 | 3720 | 331 | 3043.3 | 14597.9 | 7520.0 | 21338.1 | 9534.5 | 82.1 | 7.2 | 13.2 |
| PS750.000 | 720 | 3420 | 517 | 2804.5 | 13250.2 | 8933.0 | 19439.9 | 11335.3 | 81.5 | 7.2 | 12.4 |
| SP500.200 | 627 | 3372 | 103 | 2726.1 | 13802.7 | 9318.9 | 19629.2 | 11521.9 | 79.7 | 8.2 | 11.5 |
| SS500.200 | 613 | 3530 | 157 | 2844.2 | 14462.3 | 8128.1 | 20480.8 | 10098.1 | 82.0 | 8.5 | 12.2 |
| SP500.000 | 530 | 3428 | 189 | 2745.4 | 13397.5 | 9192.9 | 19832.7 | 11353.3 | 80.0 | 5.5 | 12.1 |
| SS500.000 | 494 | 3517 | 175 | 2827.4 | 14368.4 | 8422.5 | 20375.8 | 10473.1 | 81.4 | 8.4 | 12.6 |
| SP750.000 | 446 | 3653 | 241 | 2914.8 | 14265.2 | 8384.4 | 21061.4 | 10349.3 | 80.0 | 5.7 | 12.5 |
| SS750.000 | 420 | 3760 | 208 | 3017.0 | 15346.2 | 7571.8 | 21738.4 | 9382.6 | 81.3 | 8.5 | 13.1 |

First of all, when analyzing results corresponding to the parallel arrangement of the TES, it can be appreciated that, when dispensing with the DHW tank, better results are obtained in general terms, even when the global storage volume is smaller. In this sense, under a similar total volume of accumulation, while both overall efficiency and PES values remain virtually constant, the total operation time of the engine and the running-hours per on-off cycle, i.e. the mean length of the operation periods, increase substantially.

Concerning the consumption-side configuration, widely better results are obtained with parallel distribution. This fact is directly related to the mass flow of the cold-side of the

TES. Since the generation device is controlled with the low-side temperature of the tank and, and the return temperature to the tank is lower as a consequence of pumping fewer mass flow, the return temperature to the tank is consequently lower, and when mixed at the bottom of the tank, makes this control temperature reduce and so increase the need for switching generation on and make it work at high-load to reach the limits imposed.

In brief, within the parallel arrangement of the TES, according to the efficiency indicators established, cases PP500.000 and PP750.000 would be the most suitable, depending on if it is the TES or the global volume, respectively, to be maintained. Even if the net energy provided by the SE in case PP500.000 is slightly smaller than in case PP500.200, being the global storage volume nearly 30% smaller (so avoiding investment costs in the DHW tank and the pump of the secondary loop of the heat exchanger), the number of hours of operation per on-off cycle is virtually equal.

Regarding to the series layout of the TES, similar conclusions to the parallel arrangement can be drawn, except for the distribution loop, which is just the opposite. In this case, parallel connection of the two consumption loops allows achieving better efficiency results. Additionally, although the yearly running-time of the SE is in some cases slightly smaller than that of the parallel distribution, so happens to the number of on-off cycles of the engine, thereby having longer operation periods and avoiding efficiency losses that repetition of the start-up and shut-down periods give raise to. Consequently, within the series layout of the TES, distribution in series and instantaneous DHW production would be the most efficient solution.

Finally, when comparing both TES arrangements to each other (cases PP500.000 and SS500.000), it can be highlighted that, in general terms, installing TES in series provides slightly better results than doing it in parallel. In this sense, this series arrangement enables substantially increasing the annual hours of operation while also drastically decreasing on-off cycles of the unit, so getting longer and smoother operational cycles. This fact turns into a considerable increment of both the percentage of thermal demand covered by the SE (64.7 % versus 61.7 %) and the PES value, while both global energy and exergy efficiencies are slightly higher in the parallel arrangement. This latter fact is induced by a quite better performance of the tank itself. In this sense, even though the

series arrangement enables getting higher maximum amounts of energy stored per litre of capacity (1.11 versus 1.13), it is also noteworthy that the efficiency of the tank is notably lower (94.6% versus 97.5%), since charging-discharging processes do not occur simultaneously as it sometimes happens in the parallel configuration and, consequently, energy losses are more noteworthy. Focusing on the capacity of storing exergy of the TES when arranged in parallel and in series, it turned out annual exergy destructions of 220 kWh and 348 kWh, turning into efficiencies of 94.4 % and 78.7 %, respectively, so demonstrating a better performance of the tank when arranged in parallel. This fact is mainly due to the layout of the inlet-outlet pipes of the tanks since, in parallel, hot and cold flows are always top and bottom-connected, respectively, so maintaining and taking advantage of the different temperature levels reached within the tank. Providing TES with a top-bottom connection when charging and a bottom-top layout when discharging would substantially improve the exergy performance of the TES when arranged in series but, as previously discussed, it would turn into a quite complex and expensive control for such a housing.

Taking all the above-exposed considerations, apart from the instantaneous DHW water production and the corresponding distribution design determined for each case, it cannot be categorically stated that the optimum operation of this kind of installations would be achieved by arranging a heat buffer in series or in parallel. Consequently, a parametric analysis is presented next, for determining both the optimum configuration and size of the TES, where economic aspects are also introduced.

## 5.1. Parametric analysis

According to the results summarized in Table 3.5, it is evident that the sizing of the TES system is a crucial aspect when designing this sort of installation. Thus, for finally defining the optimal configuration, a heuristic sensibility analysis based on some parameters influenced by the size of the tank was also assessed. Likewise, apart from the energy and exergy analyses presented in Section 3, the study was completed with the basic economic evaluation introduced in the aforementioned section.

For determining the optimum storage capacity, technical and economic issues separately, as well as jointly (techno-economic optimization) were assessed for each of the two cases previously selected in Section 5 (PP500.000 and SS500.000).

First, the operational parameters were analyzed. In this sense, results show that, for both series and parallel arrangements, the sharpest reduction of the number of on-off cycles of the engine per unit of volume of the TES occurs when increasing the tank capacity up to 100 liters approximately, afterwards continuing that reduction substantially up to 350 liters, turning into mean operation periods of roughly 5 hours. Such effect gets almost mitigated with volumes bigger than 400-450 liters. Furthermore, when compared, it was obtained that, averagely, the engine switches on every 4.1 and 5.6 hours, respectively, for cases PP350.000 and SS3500.000, becoming into almost 40 % on-off cycles less for the series case.
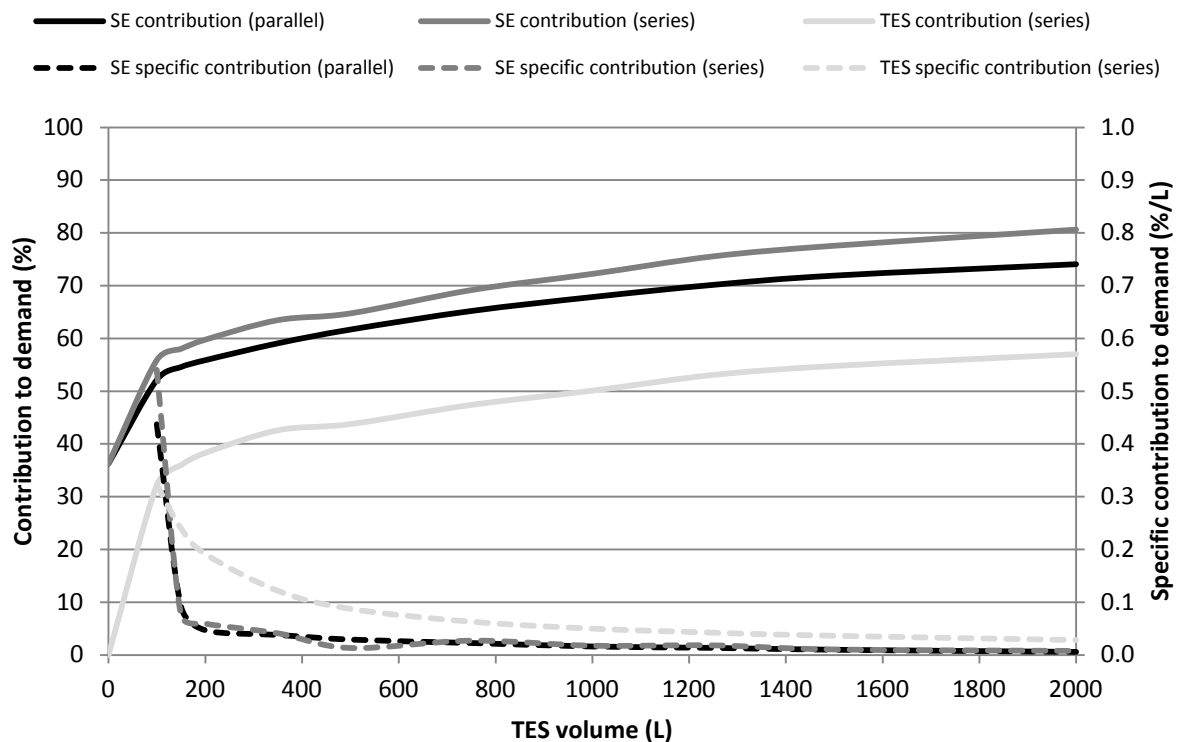


Figure 3.16 – Variation of the contribution of the SE and the TES to the demand in function of the volume of storage.

Concerning energy terms, the percentages of demand covered by both the SE and the TES (in the series case) undergo important augmentations as long as the tank gets

bigger. However, when analyzed these two facts per unit of volume, it is observed that the bigger the tank gets, the lower this contribution gets. As shown in Figure 3.16, the greatest agreement between both the absolute and the specific contributions corresponds to an accumulation capacity of around 105 liters while, if what it is to be optimized is just the percentage of coverage but still keeping an eye on the specific reduction, storage volumes close to 160 liters would be the most suitable. Additionally, it can also be observed that series arrangement does always allow the engine to deliver substantially more thermal energy than the parallel case does.

Something similar happens to the PES. In this case, the best agreement between the absolute and the specific values is reached at 130 liters, even though the optimum PES value for the series case is achieved at a slightly higher value. Meanwhile, for volumes above 450 litres the PES growth lessens due to the higher specific weight of heat losses, up to the point that for big volumes it trends to reduce. Comparing both configurations, PES shows an evolution where two sections can be distinguished: first, up to volumes of 250 liters, parallel arrangement presents slightly better PES values while, from that point on, this trend is reverted and, moreover, parallel connection shows a negative slope. This fact is due to the weight losses in the hydraulic compensator disposed in the series case has on the efficiency of the plant when working with low storage volumes.

On the other hand, concerning GHG emissions, it was detected that emitted $CO_2$-eq is quite similar in both cases. Besides, even though emissions per unit of volume keep on reducing as the volume of the tank gets increased, the most pronounced reduction occurs during the 0-150 interval, afterwards keeping relatively flat.

With regards to exergy, even though it is true that overall irreversibilities in the plant get reduced as the size of the tank increases – irreversibilities due to heat losses through the walls of the tank increase, but irreversibilities due to mixture of the water decrease to a greater extent –, these reductions respect to variations on the tank volume are very limited for volumes higher than 150-200 liters, as highlighted in Figure 3.17. Furthermore, it is noteworthy that, opposite to the PES trend, the exergy efficiency of the plant is slightly better with series arrangements for small storage volumes (up to 300 liters) and, subsequently, the parallel configuration is to reach better results.
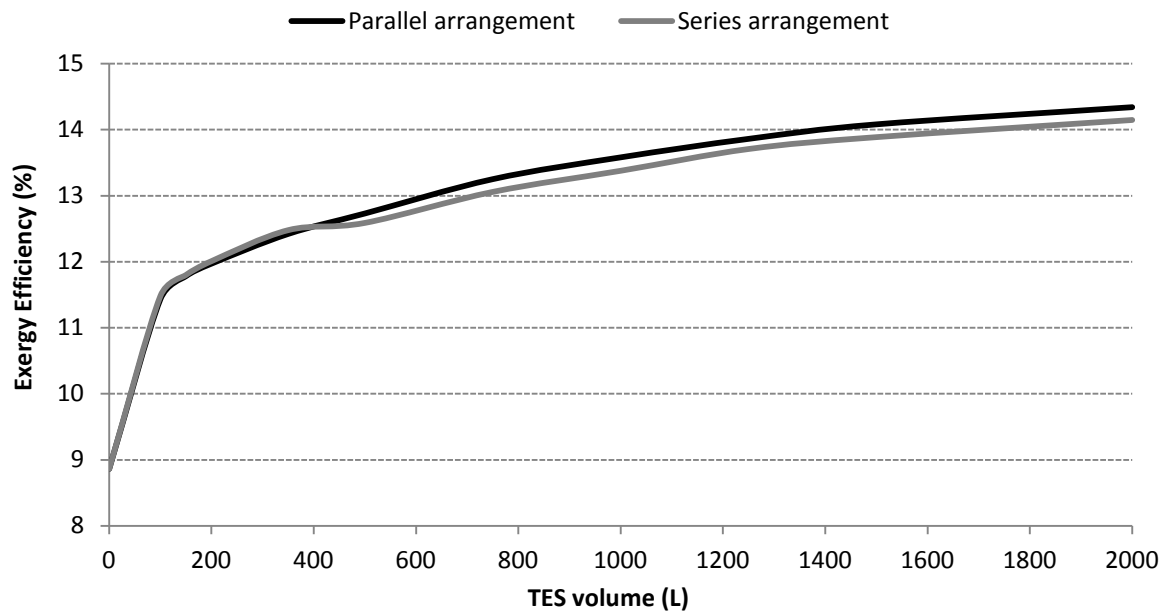
Figure 3.17 – Overall exergy efficiency of the installation with respect to the TES volume.

Additionally, from the economic point of view, it was observed that the optimum volume is far from those traditionally installed, being the most appropriate around 120 and 150 liters for the parallel and the series arrangements, respectively, for the case-study, as plotted in Figure 3.18. In any case, the NPV value of the parallel arrangement of the TES is virtually always slightly higher than that of the series one.
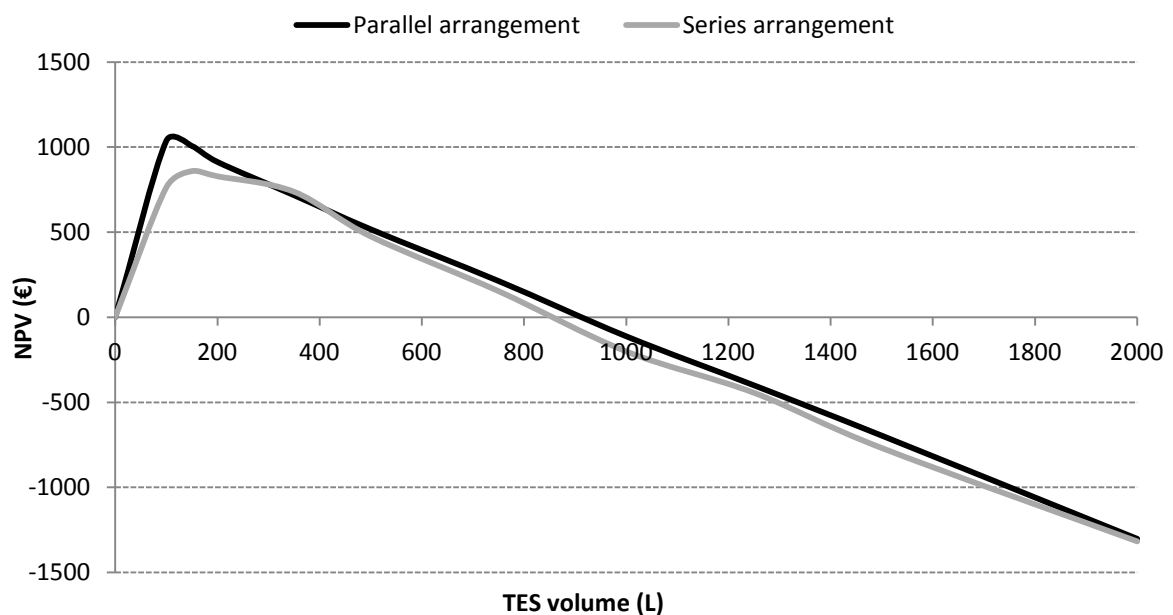


Figure 3.18 – Net Present Value (year 15) of the tank investment with respect to its volume.

Taking into consideration all the aforementioned issues, it can be stated that, in general, for small accumulation volumes, proved to be the most suitable for applications like the one of the current case study, installing thermal storage in parallel with both the generation and the demand provides better global results. Even though operational, energy and exergy results are slightly worse, since no significant differences are got between both arrangements in this sense, it is the economic criterion, which is given by the quasi-linear dependence of the TES price with its volume, the only that unequivocally sets the best design.

Thus, it is concluded that the optimum TES system for such an installation should be installed in parallel, with a storage capacity of 120 liters, corresponding to an accumulation factor of approximately 25 liters of TES per nominal thermal power of the SE.

Finally, it must be pointed out that, if larger volumes are to be employed in order to augment the number of hours of operation of the engine while diminishing the number of on-off cycles, so that the integrity of the engine can be preserved to a greater extent, results show that series connection of the TES will provide much better overall results for accumulation volumes above 300 liters.

# 6. Conclusions

Small-scale residential Stirling cogeneration systems, recognized as an efficient technology with great economic, energy and environmental potential, have lately appeared as an agent to keep in mind for contributing to the attainment of EU's objectives on energy efficiency and pollutant emissions, as pointed out in both the EPBD and the EED. Nevertheless, due to the low electric efficiency of these devices, a good thermal performance of them is indispensable. Therefore, improving the behaviour of this technology, both individually and integrated within a residential thermal installation, possesses vital importance. In this sense, a suitable coupling of the SE with thermal energy storage plays a key role for maximizing its aforementioned strong points.

Thus, this chapter focuses on the importance of the correct sizing and design of a micro-CHP residential installation and the vital role TES plays on it. For that purpose, based on previous works and experiences, key aspects of the installation design are highlighted and different configurations are presented.

This way, how TES should be arranged within the plant is first considered: parallel arrangement, fully decoupling demand and generation sides, or series arrangement, which presents in turn upstream and downstream potential integrations. Additionally, together with the TES, the need of DHW accumulation is also assessed. Finally, these two facts are lately combined with the way thermal energy is distributed through the thermal loads – series or parallel –, thus giving raise to the variety of configurations contemplated.

For deepening on the analysis of the different designs set out, a complete evaluation methodology is introduced. The energy performance, in accordance with the EED, is partially evaluated with the primary energy savings achieved in each case with respect to the separate production of heat and electricity, without overlooking the overall efficiency of the whole installation, as well as the its environmental impact. Additionally, focusing on preserving the integrity of the generator, the number of on-off cycles and hours of operation of the engine are taken into consideration. Finally, the performance of the Stirling engine is not only assessed, but the performance of the TES itself is also analysed, in terms of energy and exergy, so that the effectiveness of the charge and discharge processes can be maximised.

On the other hand, the analysis is complemented with the economic yield each solution provides, evaluated in terms of NPV at the end of the lifetime of the micro-CHP unit. This analysis is applied to a case study previously defined, with a micro-CHP properly size for its integration in the considered dwelling.

Results show that, in small installations suitable for this kind of detached houses, where simplicity is a factor that must be kept in mind, it is preferable to directly produce DHW instead of using a tank, as no significant improvement is achieved but efficiency deterioration. Additionally, it is also proved that the layout of the distribution loop has an importance on the final performance of the plant that must be kept in mind.

The chapter is finally completed through a heuristic analysis of the influence the size of thermal energy storage has on both the performances of the tank itself and the SE and the global functioning of the plant, so that its size can be optimised. Results extracted from this sensibility analysis containing operational as well as energy, exergy and economic indicators, show that TES systems coupled with small-scale micro-CHP engines are traditionally oversized, which allow slightly incrementing the number of hours of operation of the generation unit at the expense of an important worsening of the economic viability. For such big storage capacities, with respect to the TES arrangement within the plant, installing TES in series seems to be the optimum configuration. However, for those accumulation-volume intervals suitable for installations in single family dwellings, it is observed that, even though it is complicated to categorically state the optimum configuration, parallel arrangement of the TES requires slightly lower accumulation values, achieving an optimum size of the tank that allows obtaining better economic results while keeping virtually equal the technical indicators when compared to the optimum series arrangement, and, consequently, from a multi-objective point of view.

Finally, it must be remarked that, even though in the current case study, which can be considered as representative of those detached houses with strong thermal requirements, parallel connections turns out to be the most suitable arrangement, the performance of any thermal plant is heavily dependent on both the thermal demand profile and the type of control that governs the operation of it. Consequently, for those conditions that may not be represented by the current case study, a customized analysis should be tackled.

# CHAPTER 4

## TECHNO-ECONOMIC FEASIBILITY OF STIRLING ENGINE-BASED RESIDENTIAL MICRO-CHP INSTALLATIONS

# 1. Introduction and objectives

There is an emerging interest in using Stirling engine-based micro-CHP systems in residential applications due to their potential for achieving all the benefits mentioned so far when supplying heating, DHW and electric power.

As described in Chapter 1, over the years, Stirling engines for micro-CHP have been researched from different perspectives, some of which are out of the scope of this thesis and others related to which have been previously assessed in Chapters 2 and 3.

In this chapter the techno-economic feasibility of Stirling engine-based micro-CHP installations in residential buildings is assessed, from a comparative point of view. For this purpose, taking into consideration energy requirements of the detached house defined in Annex D, and considering the optimum size and configuration of the micro-CHP plant previously obtained in Chapter 3, two different energy plants for energy supply to the dwelling are approached. Thus, the overall feasibility of the Stirling engine-run plant is addressed, that is, the energy, environmental and economic performance of the micro-CHP plant with respect to the reference scenario, in order to identify the pros and cons of each technology for the target application of this thesis.

Additionally, the work also aims to deepen in the economic aspect of the implementation of SE in housing applications, focusing on analysing how the latest modifications in the Spanish micro-CHP and renewable energy regulation affect the viability of this

technology. This includes taking into consideration what results could be achieved if the policy support mechanisms in Spain were like those in other European countries where the use this kind of equipment is more extended. Definitely, a study that constitutes an estimation of how the support mechanisms of each country influence the economic feasibility of these small-scale Stirling micro-cogeneration devices is assessed, focusing on the regulation governing the electric side of the micro-CHP and the incentives existing for this sort of equipment in Spain, Germany and the United Kingdom.

The chapter is organised in five main blocks. Once introduced the chapter, Section 2 is dedicated to introducing the evolution of the normative and economic framework for cogeneration in Spain, as well as a brief description of German and British support mechanisms and regulations in force where the work was carried out. Then, Section 3 provides a step by step description of the methodology to assess the technical, environmental and economic viability of a micro-CHP installation. Thus, since this kind of study should be, as mentioned, approached from a comparative point of view, i.e. with respect to that technology the micro-CHP aims to compete with, the first step was to define the reference installation and optimise its design. Section 4 is focused on a case-study where the methodology previously defined is used for analysing the techno-economic feasibility of such an installation for a detached dwelling in Spain. In Section 5 the main techno-economic results obtained for the defined case study are presented and commented. The work is completed with a sensitivity analysis which is presented in Section 0, where different future scenarios of the economic variables taking part in the techno-economic analysis are assessed, emphasizing the influence regulatory conditions have on final results. Finally, Section 7 sums up the main conclusions obtained throughout the chapter.

The chapter corresponds to an extended and adapted version of articles *Parametric study of the operational and economic feasibility of Stirling micro-cogeneration devices in Spain, Applied Thermal Engineering, 71 (2014) 821-829* and *Influence of the regulation framework on the feasibility of a Stirling engine-based residential micro-CHP installation, Energy, 84 (2015) 575-588.*

# 2. Economic and regulation frameworks

As explained in Chapter 1, electricity generation based on renewable and high efficiency energy sources constitutes the basis for achieving the objectives of GHG emissions reduction, so guaranteeing the security of energy supply. Over the last twenty years, the significant development undergone by renewable energies, cogeneration and waste-based technologies have given rise to great modifications in the regulation framework.

## 2.1. Spain

High efficiency and renewable energy-based technologies were first regularised and developed in the 1980s, with Law 82/1980 on energy conservation (Jefatura del Estado, 1981). This law was created in order to tackle the oil crisis and reduce the external dependency, as well as to improve energy efficiency of the industrial sector, so promoting auto-generation and mini-hydraulic generation. Based on it, Royal Decree 907/82 on the promotion of electric energy auto-generation was redacted (Ministerio de Industria y Energía, 1982).

Afterwards, in the next decade, the National Energy Plan 1991-2000 was developed, where an incentive program for cogeneration and renewable-based production was established. Likewise, Law 40/1994 of the national electric system was approved as well; thereafter the especial regime term was consolidated (Jefatura del Estado, 1994). Based on that law, Royal Decree 2366/1994 on the regulation of the electricity generation under especial regime was published, where electricity production through hydraulic installations, cogeneration, and renewable and waste-based installations with power outputs below 100 MVA were included (Ministerio de Industria y Energía, 1994).

Law 54/1997 of the Electrical Sector also differentiates the production under ordinary regime from that under special regime, and identifies the retributive economic framework for each of these two models of generation (Jefatura del Estado, 1997). The special regime activity includes installations with power outputs under 50 MW utilising renewable or waste-based primary energy, as well as high efficiency technologies such as cogeneration.

Royal Decree 2818/1998, on the electricity production through installations using renewable sources, waste and cogeneration, established the retribution for energy sold under especial regime, and had to be updated yearly and revised every four years (Ministerio de Industria y Energía, 1998). However, the lack of participation especial regime installations had on the market under this latter Royal Decree gave rise to Royal Decree-Law 6/2000 (Jefatura del Estado, 2000), which took urgent measures for intensifying the competitiveness on the goods and services market, encouraging the participation of especial regime installations in the market and establishing the possibility of arranging electricity sales contracts with marketers. These goals were subsequently developed in Royal Decree 841/2002 (Ministerio de Economía, 2002).

In 2004 Royal Decree 2818/1998 was derogated, through the approval of Royal Decree 436/2004, where a methodology for the update and systematization of the legal and economic regime of the electric energy production under especial regime was established (Ministerio de Economía, 2004). The owner of the installation could sell the production at a regulated tariff or, on the contrary, sell electricity in the free market, receiving an incentive and a bonus for taking part in it.

Additionally, in 2004 Directive 2004/8/EC on the promotion of cogeneration based on a useful heat demand in the internal energy market was approved. As mentioned in Chapter 1, its objective was to increment energy efficiency and improve the energy supply through the creation of a new framework for the development, taking into consideration particularities of each Member States (mainly economic and climatic), of high efficiency cogeneration, based upon useful heat demand and primary energy savings. According to this normative, legislative actuations should eliminate the obligation of electrical self-consumption, incentive or bonus not only the electricity surplus but the whole electricity production, establish an economic regime which prioritizes the primary energy savings and separate the figure of the promoter of the project of the cogeneration installation for the final user of the thermal energy.

This Directive was transposed to the Spanish regulatory framework in 2007, through the approval of Royal Decree 661/2007, which regulated the economic activity of electricity production under special regime (Ministerio de Industria, Turismo y

Comercio, 2007). This Royal Decree, which substituted Royal Decree 436/2004 but maintaining its basic scheme, regulated both renewable and cogeneration based electric energy productions, giving feed-in priority and ensuring a reasonable payment to owner for their investments to get feasible. This way, the double retribution option was maintained; the owner of the plant could pour electricity into the grid at a regulated tariff or sell its production in the free market perceiving a bonus, but the incentive for taking part in the market was eliminated. However, small-scale cogeneration plants did only have the possibility to sell electricity at a regulated tariff, which depended on the installed power and the fuel used.

Electricity fed into the grid could receive not only a regulated feed-in tariff, but also complements for reactive power and efficiency, as well as an optional complement for rewarding delivery in on-peak, as summarized in Equation 4.1:

$$i_e = Rt_e + C_{eff} + C_{reac} + C_{dh}$$

<div align="right">Equation 4.1</div>

where $i_e$ is the incomes due to electricity sales, $Rt_e$ the regulated tariff, and $C_{eff}$, $C_{reac}$ and $C_{dh}$ the complements for efficiency, reactive power and hourly discrimination, respectively. An accurate summary of this normative, where each term contained in Equation 4.1 is defined, was presented by Campos-Celador et al. (2011).

Likewise, RD 661/2007 defined the efficiency of a cogeneration plant through the equivalent electric efficiency (REE), as defined in Equation 4.2. This REE compares electricity generated by a CHP with that obtained by a plant whose unique product is electricity. RD 661/2007 established that for a natural gas fed small size (<1MW$_e$) reciprocating engine-based CHP plant to be considered a high efficiency producer, the annual REE of the cogeneration plant had to be over 0.45.

$$REE = \frac{E_{CHP}}{F_{CHP} - \left(\dfrac{Q_{CHP}}{RefH_\eta}\right)}$$

<div align="right">Equation 4.2</div>

where $E_{CHP}$, $F_{CHP}$ and $Q_{CHP}$ are the annual electricity production, fuel consumption and heat production of the cogeneration plant, respectively, while $RefH_\eta$ is the harmonised efficiency for heat production.

However, the publication of Royal Decree-Law 1/2012 on the suspension of retributive procedures and omission of economic incentives for electricity-production new cogeneration and renewable installations revoked all the aforementioned remunerative complements (Jefatura del Estado, 2012b), so limiting development possibilities of cogeneration.

Later on in 2012, a new Law on fiscal measures for energetic sustainability (Law 15/2012) was approved (Jefatura del Estado, 2012a), where new taxes with purely collecting purposes for facing and reducing the so-called electrical-tax deficit were created. A new 7% tax for electric energy producers taking part in the different engagement modalities of the electric energy production market was established. Together with this Law the so-called green-cent was created, a new tax for each GJ of natural gas consumed.

During 2013, cogeneration in Spain suffered substantial cutbacks concerning retribution, which joined the aforementioned moratorium and the repeal of the regulation framework of the activity. In this sense, in February RDL 2/2013 was approved (Jefatura del Estado, 2013b), eliminating bonuses when selling electricity produced in the free market, and forcing special-regime producers to make a choice between free market and regulated tariff for the whole life of the plant.

In July 2013, complements for efficiency and reactive power were abolished through RDL 9/2013 (Jefatura del Estado, 2013c). Later that year, Law 24/2013 was published, regulating the electric sector for the electric supply to be guaranteed with the required quality levels and the lowest cost, and ensuring economic and financial sustainability of the system (Jefatura del Estado, 2013a). This Law solved the existing uncertainty for those CHP plants affected by the onset of the electrical reform, since it assumed one of the fundamental principles set in the original Law 54/1997, which states that retributive regimes must let installations under special regime cover the necessary costs to be able

to compete in the market on an equal level with the rest of technologies and obtain a reasonable profitability on the whole project.

Despite all the aforementioned regulations, it was not until June 2014 when the baffling situation in which cogeneration was submerged was partially solved, when the new legislation substituting the previous complement-based regulation and developing the new Law on the Electric Sector was published. RD 413/2014, currently in force, establishes a new retribution framework for renewable energy, cogeneration and waste-based electricity production installations, both new and existing (Ministerio de Industria, Energía y Turismo, 2014c).

According to this normative, retribution is only applied to those installations which cannot reach a reasonable feasibility with existing market prices, provided that they fulfil the high efficiency conditions defined in RD 661/2007. This new retributive framework distinguishes between some fix costs (investment, operation and fix maintenance) and other variable costs (fuel, operation and variable maintenance).

In consequence, the payment is divided into two main groups: electricity sales at market price and specific retribution. This second term, in turn, is split into two categories: retribution to investment ($R_{inv}$), which stands for the investment costs of the reference installation that cannot be recovered just with electricity sales during each year, and retribution to operation ($R_o$), which is set as the difference between the ideal operative costs and the estimated incomes of the installation, which is obtained by multiplying the stipulated value and the sold electricity.

$$Rinv_{j,a} = C_{j,a} \cdot VNA_{j,a} \cdot \frac{t_j \cdot (1 + t_j)^{VR_j}}{(1 + t_j)^{VR_j} - 1}$$

Equation 4.3

where $Rinv_{j,a}$ is the annual retribution to investment per power unit (in €/MW) corresponding to the type installation with exploitation authorization in year $a$, each year of the $j$ period, $C_{t,a}$ is an adjustment coefficient representing the investment costs of the reference installation which cannot be recovered just with electricity sales during

each year $a$ of the period $j$, $VNA_{j,a}$ represents the net value of the active per power unit at the beginning of the regulation period $j$ (which is tabulated in function of power ranges, primary mover and fuel and the age of the installation), $t_j$ is the updating rate whose value is that reasonable feasibility established for period $j$, and $VR_j$ is the residual lifetime at the beginning of the $j$ regulation period.

On the other hand, retribution to operation is set as the difference between the ideal operative costs and the estimated incomes of the installation, which is obtained by multiplying the stipulated value and the sold electricity.

Both retributive parameters, which are determined in Order IET/1045/2014 (Ministerio de Industria, Energía y Turismo, 2014a) and may be modified in periods of three or six years, are tabulated and sorted out by categories depending on the fuel, power range and technology of the plant and its year of installation, which subsequently stand for different reference cases. The methodology for updating the retribution to operation is established in Order IET/1045/2015 (Ministerio de Industria, Energía y Turismo, 2015).

Figure 4.1 summarizes the evolution of the legislative framework of cogeneration in Spain.
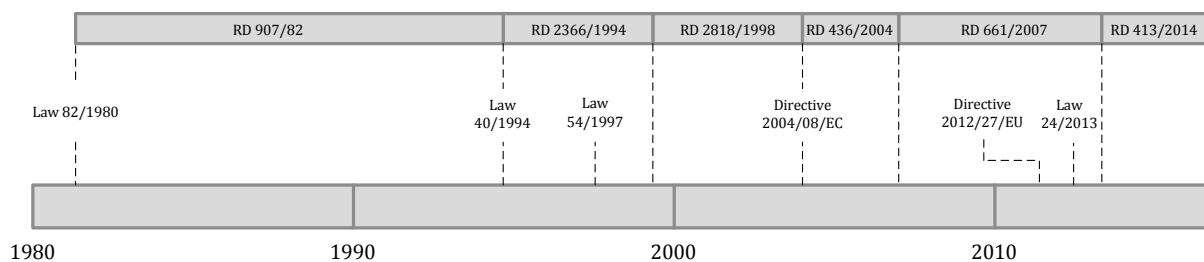


Figure 4.1 – Legislative framework of cogeneration in Spain.

## 2.2. Germany

As described more in detail in the Annex 54 of the International Energy Agency (IEA) on the Integration of micro-generation and related energy technologies in buildings (A. Hawkes et al., 2014), in Germany, a law to support cogeneration was approved in 2002,

which was revised in July 2014[1] (Deutscher Bundestag, 2002). This law grants access to the electrical network and gives priority for the feed-in of the electricity generation. For each kWh of electricity generated with a CHP system with an output capacity below 50 $kW_e$, a generation premium of 5.41 c€/$kWh_e$ is paid to the generator, regardless of if the electricity is delivered to the net or self-consumed. These generation premiums are paid until 30,000 hours of full load operation are reached, or, alternatively for operators of systems with a capacity below 50 $kW_e$, over a period of 10 years instead. Furthermore, as the premium is paid on approved amounts of generated electricity, operators of systems up to 2 $kW_e$ can decide whether to get the payment of the whole bonus in advance or not. Additionally, there is a remuneration for electricity fed-in to the grid, valued at 3.35 c€/kWh.

Furthermore, there is a tax refund related to consumed natural gas, receiving back 0.55 c€ per each kWh of natural gas feeding the micro-CHP unit. Similarly, there is a refund on the grid charges, normally between 0.5-1.5 c€/kWh, related to electricity fed-in to the grid, due to avoided grid charges for distribution companies.

Finally, for micro-generation systems with capacities below 20 $kW_e$, an investment subsidy can be obtained through a support program (Bundesministerium für Umwelt, Naturschutz, Bau und Reaktorsicherheit, 2014), provided that some requirements are met. This grant, which is dependent on the size of the system as detailed in Table 4.1, can be complemented with two supplements: bonus for thermal efficiency, valued at 25% of the investment subsidy, and bonus for electric efficiency, valued at 60% of the investment subsidy.

Table 4.1 – Investment subsidy for mini-CHP units in Germany.

| Minimum power [$kW_e$] | Maximum power [$kW_e$] | Grant quantity [€/$kW_e$] |
|:---:|:---:|:---:|
| 0 | <=1 | 1900 |
| >1 | <=4 | 300 |
| >4 | <=10 | 100 |
| >10 | <=20 | 10 |

[1] This law was last updated in July 2017. However, all the calculations were carried out according to conditions in force in 2015.

## 2.3.  United Kingdom

As summarized by Hawkes (2013; 2014), in the UK there is a feed-in tariff mechanism available for electricity generated with micro-CHP devices with power outputs below 2 kW$_e$. Each generator receives two different payments: a generation reward and an export reward.

While the generation reward is applied to every kWh$_e$ the system produces during the first 10 years of operation of the plant (15.93 c€/kWh$_e$), regardless of if it is poured into the grid or self-consumed, the export reward is applied to every kWh$_e$ exported to the grid (5.73 c€/kWh$_e$). This way, being the electricity tariff (17.62 c€/kWh$_e$) notably higher than the export reward, self-consumption of the electricity produced within the micro-CHP plant is stimulated. The values of the tariffs were results of converting £ to € at the moment of developing this work.

# 3.  Methodology

Traditional performance assessment methodologies normally include energy, environmental and economic analyses. They compare, generally on an annual basis, primary energy consumption, operating costs and $CO_2$ emissions of an alternative system with those of a conventional or reference system that produces, separately, the same amount of useful energy in terms of thermal and electric demand. The reference system is normally based on traditional and widely used technologies, i.e. condensing gas boilers for providing thermal energy in terms of heating and DHW and electricity supply from the global power system through the electricity grid (Dorer and Weber, 2007). However, there may exist country-dependant specific constraints that must be taken into consideration.

## 3.1.  Definition of the reference installation

The first stage when facing a techno-economic assessment consists of defining and implementing the installations to be analysed and compared. Thus, the procedure of design and modelling in TRNSYS of the reference installation is first addressed in this

chapter, while that run with the Stirling engine is that already defined in Chapter 3 and depicted in Figure 4.2. Then, the main output indicators of the simulation are presented, which, combined with some other factors defined throughout this chapter, constitute the energy, environmental and economic analyses.
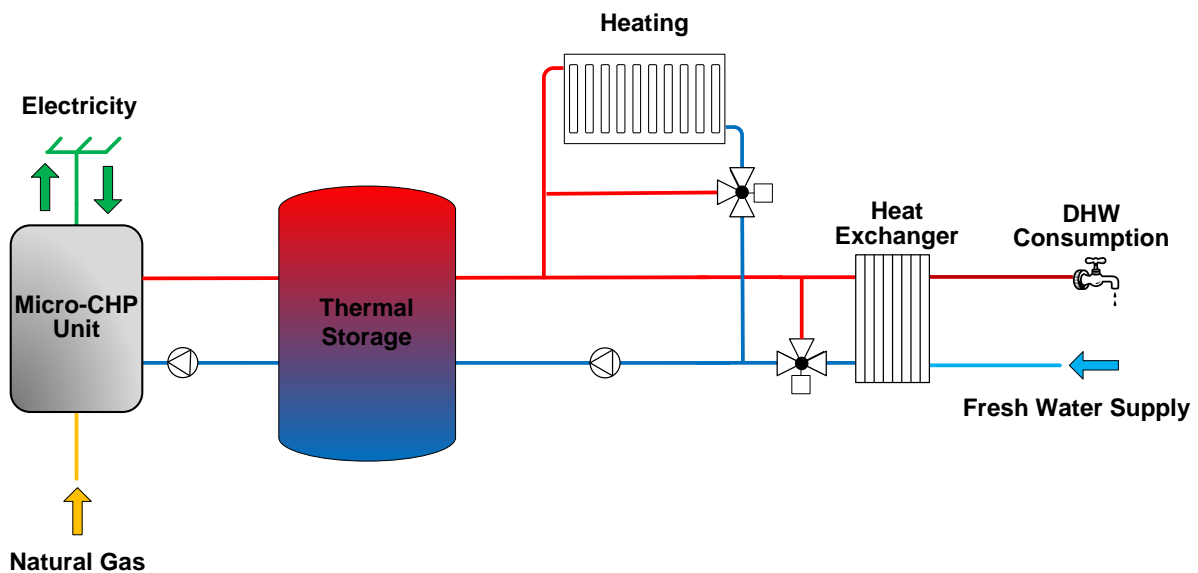


Figure 4.2 – Schematic diagram of the SE-based micro-CHP installation.

Since the CTE became effective in 2007, endorsed with the updated versions of 2013 and 2017, in addition to the main thermal energy source for space heating and DHW, there is a minimum percentage of the DHW demand that must be covered by solar thermal or other renewable sources or cogeneration (CTE, 2013b). Among the existing alternatives in Spain and most European countries, the most common generation installation for space heating and DHW in dwellings has been the natural gas-run condensing boiler, lately supported by solar thermal panels for base DHW production. Thus, the reference scenario is constituted by such an installation.

As required by the CTE, both solar and conventional productions must be independent, i.e. no backup source can be connected to the solar storage tank. Thus, if DHW accumulation is to be installed, two tanks must be disposed, one for the solar circuit and another one for the DHW production, as depicted in Figure 4.3. Both tanks are normally connected in series; therefore, the domestic cold water is preheated first in the solar

tank, and subsequently flows into the DHW tank. There, if required, additional heat is
supplied by the boiler through a flat-plate heat exchanger to maintain the DHW
temperature over 60°C as established by the regulation to avoid the appearance of
legionellosis (Ministerio de Sanidad y Consumo, 2003).
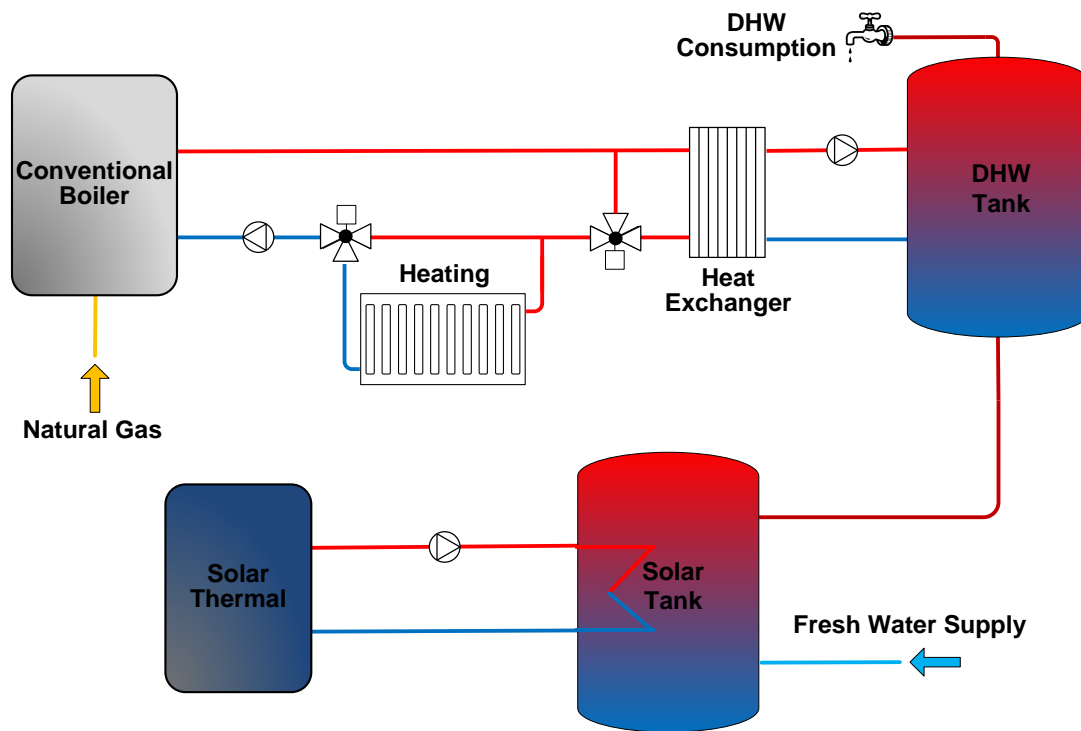


Figure 4.3 – Schematic diagram of the reference installation with DHW accumulation.

Otherwise, cold water from the mains can be previously preheated in the solar tank and
afterwards sent through the boiler to elevate its temperature above 55 °C to avoid
legionellosis, as depicted in Figure 4.4.

In this chapter, taking into consideration conclusions concerning DHW accumulation
extracted from Chapter 3, where installing DHW storage in installations of such size was
evinced not to be viable either from an economic point of view or energetically, the
second option was proposed. This way, additionally, when assessing the subsequent
economic comparative analysis with the micro-CHP installation, both plants can be
similarly approached due to the absence of DHW accumulation.
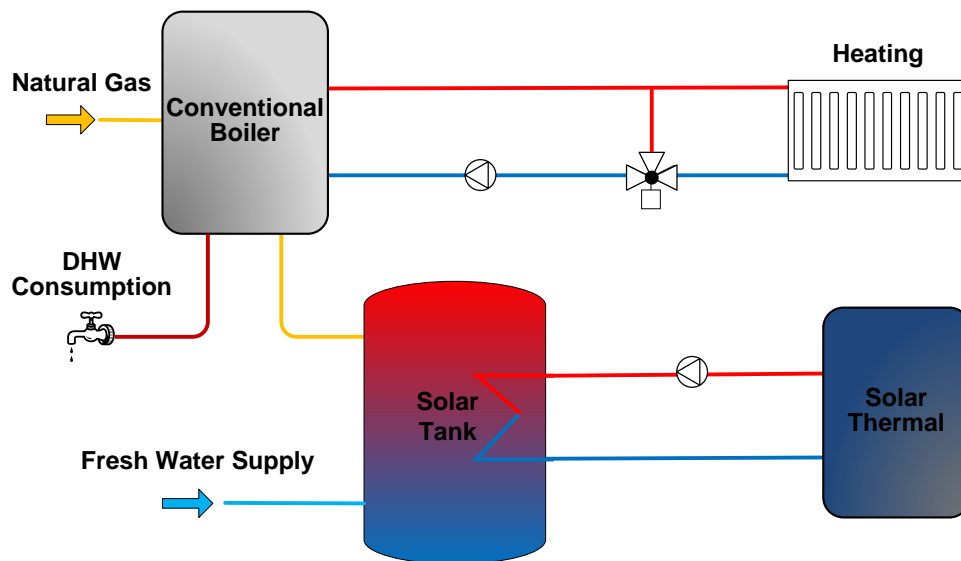
Figure 4.4 – Schematic diagram of the reference installation with instanteanous DHW production.

Assessing a correct sizing of the solar collection surface and the accumulation volume are two crucial aspects to guarantee the feasibility of the installation. According to the cited regulation, the ratio between the solar tank volume and solar collector surface must be between 50 and 180 litres per square meter (CTE, 2013b).

For this purpose, the F-Chart method was applied to the DHW demand obtained for the reference dwelling defined in Appendix D and previously used in Chapter 3. The F-Chart method, also known as the f-curves method, is a tool that enables estimating the mean long-term performance of a solar thermal system (Beckman et al., 1977). It is based on identifying the dimensionless variables of the solar system and utilizing the equation of the solar energy absorbed by a panel.

First, for setting the storage capacity, a 2 m² constant surface of south-oriented and 43° sloped generic solar thermal collectors was considered (optical efficiency factor: 0.727; heat loss coefficient: 3.002 W/m²·K), for the climatic conditions of Vitoria-Gasteiz, varying the volume-to-area rate (V/A) from the minimum to the maximum permitted and so calculating the obtained relative savings with respect to the cost of producing the same DHW amount with a condensing boiler of a considered seasonal efficiency of 90%, as suggested by the EED. Natural gas purchase-price was set at 5.04 c€/kWh (Ministerio de Industria, Energía y Turismo, 2014d). Investment and maintenance costs of the solar installation were calculated according to correlations proposed by Pérez-Iribarren

(2016), presented through Equation 4.4 and Equation 4.5, while the cost of the solar tank was estimated through Equation 3.6 introduced in Chapter 3.

$$Inv_{sol} = 1420.6 \cdot A_{sol}^{-0.125}$$

Equation 4.4

$$Maint_{sol} = 73.246 \cdot A_{sol}^{-0.127}$$

Equation 4.5
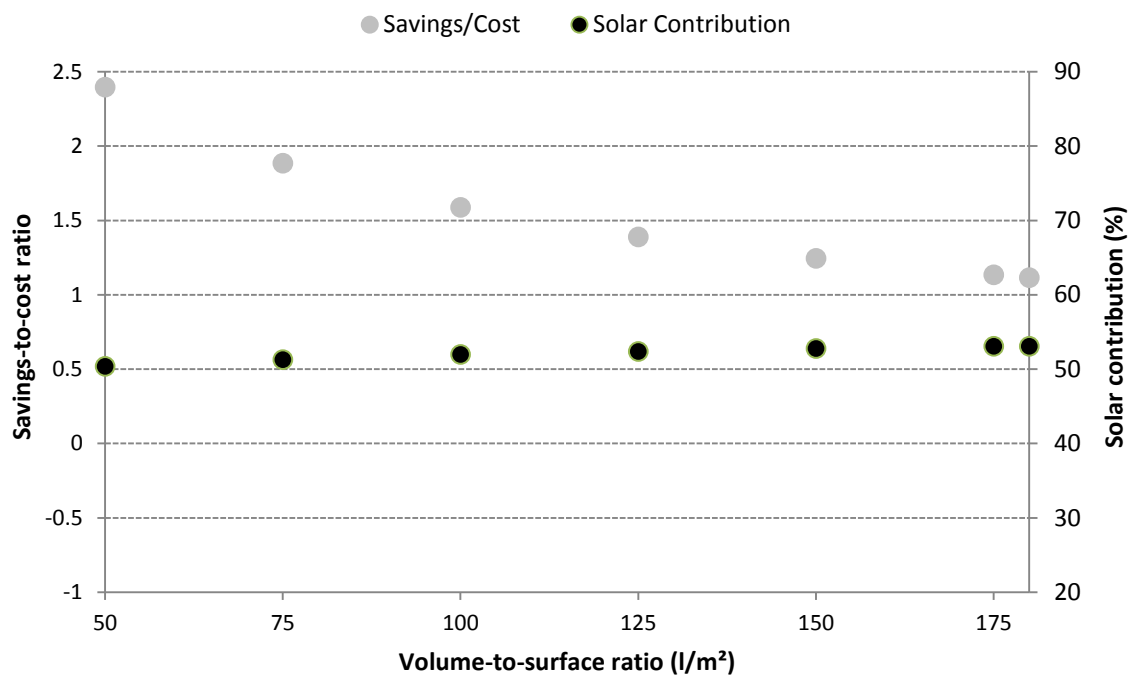


Figure 4.5 – Variation of the savings-to-cost ratio and solar contribution with the solar tank size.

In Figure 4.5 it can be observed that increasing significantly the tank volume does not report an important augmentation on the solar contribution. On the contrary, increasing the tank volume makes the economic feasibility more difficult, since the difference between the investment cost and the achieved fuel savings associated to the solar production gets bigger and bigger as the tank volume gets higher.

Thus, as long as the economic factor is only considered, the minimum tank volume should be the choice when designing an installation. However, for preventing the storage water from reaching high temperatures which may damage the materials of the tank during a sunny day with low or null demand, a 1.5 security coefficient is applied to

the tank volume for better absorbing and softening this thermal impact, so giving rise to a V/A value of 75. This conclusion is therefore in line with the V/A value recommended by Atecyr (2013).

On the other hand, the influence of the installed solar surface on the solar contribution and the costs and savings was also analysed, keeping the V/A ratio constant at 75. In this way, and contrary to the case of the thermal storage capacity augmentation, increasing the solar surface turns into a much higher solar contribution, although, as it can be observed in Figure 4.6, the relationship between additional costs and savings attributable to such costs, which is always negative as there are no positive net savings, gets worse at the same time.
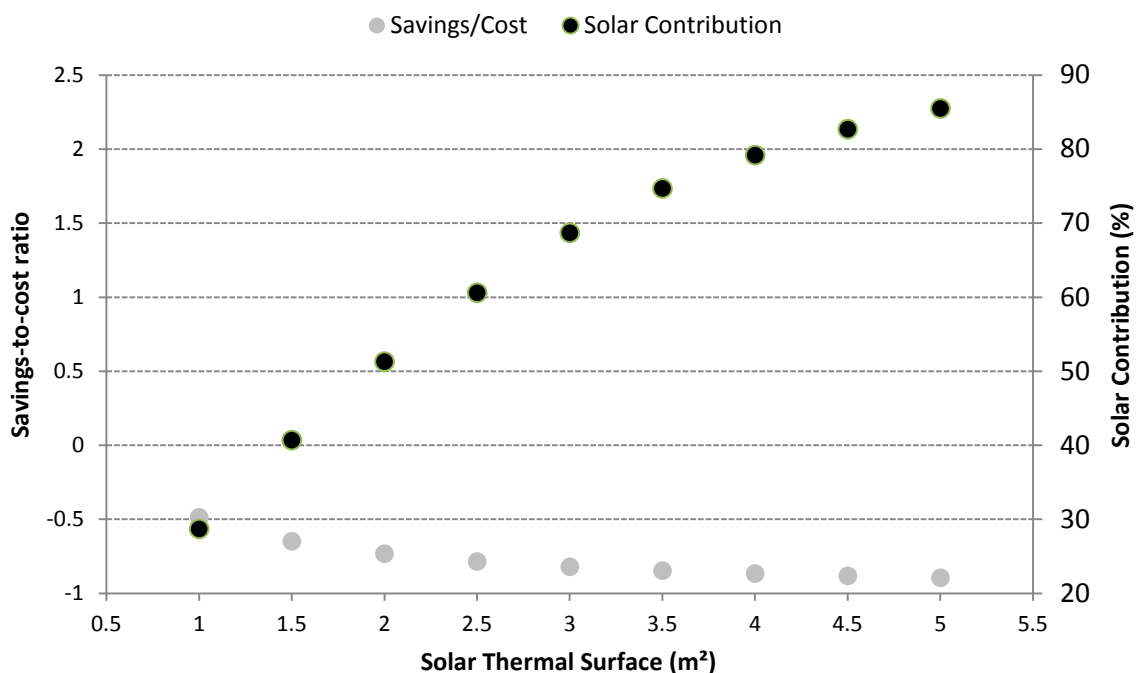


Figure 4.6 – Variation of the savings-to-cost ratio and solar contribution with the installed solar thermal surface.

This way, it is advisable that, from an economic point of view, the net installed surface should be that minimum value which allows meeting the DHW percentage coverage requirements. Even though, as reflected in Equation 4.4 and Equation 4.5 respectively, investment and maintenance costs per square meter of solar panel decrease with the augmentation of the installed area, such reduction is not so pronounced for typical

surface ranges affordable in low demand buildings such as detached dwellings (generally up to 4 m²), so the cost of increasing the disposed solar surface is hardly recoverable with the yearly incomes obtained due to natural gas savings.

Finally, it must be remarked that, for the case under consideration, an installed surface bigger than 3 m² makes the installation not fulfil the requirement of not reaching a solar fraction higher than 100% in three consecutive months. Exceeding this limit makes a counteracting measure necessary, which may turn into extra costs.

For selecting the installed surface for reaching the 30% annual solar fraction required for the location where the reference building is, a survey of the commercial availability surfaces of panels between 1 and 2 m² was carried out. Afterwards, the same procedure was repeated for choosing the storage volume.

As summarized in Annex E, most of the commercially available solar flat collectors with surfaces in the range between 1 and 2 m² have absorption surfaces from 1.85 to 2 m²; therefore, attending to market availability, a 2 m² net surface could be considered as representative for the current scenario. Taking into consideration such surface and a V/A ratio of 75, as well as the available deposit volumes, the solar storage volume was set to 150 litres.

One final remarkable aspect concerning the design of the conventional installation is that, instead of a tank with an external heat exchanger and an additional pumping unit, the employment of an inter-accumulator was considered to be more appropriate. This is mainly because, besides avoiding the necessity of installing an extra pump, a small solar installation, with low energy exchanges and the consequent low flows, as it is the case, must be as simple as possible. Additionally, inter-accumulators are typically provided with a thermostat which enables activating the external back-up source if necessary.

## 3.2. Climatic conditions

One of the main objectives of this chapter is to analyze how Stirling micro-CHP devices can work under different conditions of thermal solicitations. For this purpose, the analysis was propounded for different representative climatic zones of Spain, chosen in

function of their climatic severity (CS). These weather data were obtained from the Meteonorm database (Remund and Kunz, 1997).

The climatic severity of a place, as indicated in the HE1 Section of the Energy Savings Document of the CTE (2013a), is defined as the quotient between the energy demand of any building in that zone and that corresponding to the same building in the reference zone, i.e. Madrid for the case of Spain. Two climatic severities are distinguished: one for summer and another one for winter. This way, as depicted in Figure 4.7 and Figure 4.8, climatic zones are defined according to the climatic severities in winter (α, A, B, C, D, E) and summer (1, 2, 3, 4).



Figure 4.7 – Different climatic zones in Spain.
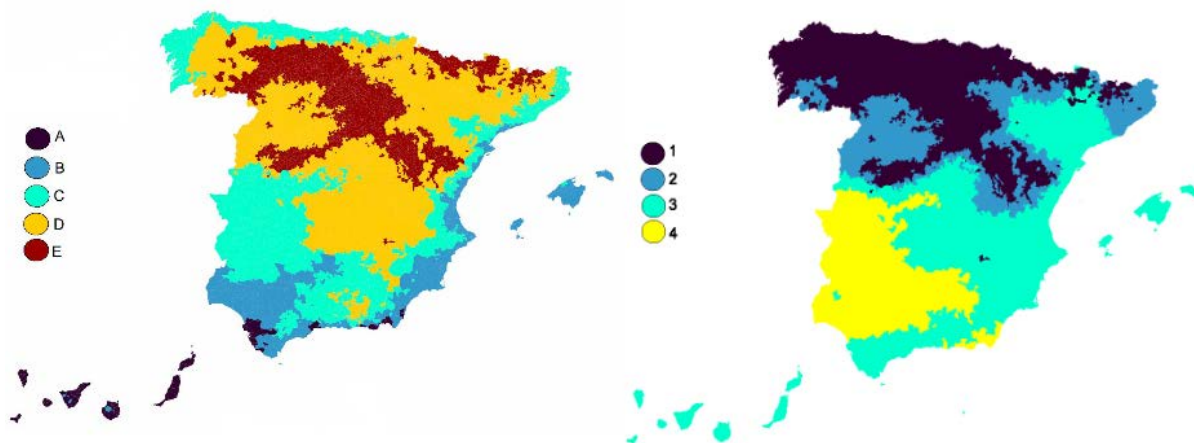


Figure 4.8 – Winter (left) and summer (right) severity map of Spain (Álvarez and Molina, 2016).

Climatic severity combines degree-days and solar radiation of a locality, so that when two places have the same winter climatic severity the heating demand of a building sited in both locations is quite the same.

In order to cover the various climatic conditions exposed, three representative climatic zones were chosen: zone A4, which is characterized by hot summers and warm winters, zone E1, which includes locations with very cold winters and warm summers, and zone D3, which has cold winters and very hot summers.

## 3.3. Modelling and simulation

Both thermal installations – the micro-CHP and the reference conventional installation – were implemented in TRNSYS simulation environment. All the main Types employed in the simulations, summarized in Table 4.2, were described in Chapter 3.

Table 4.2 – Main components employed in TRNSYS simulations.

| Component | Model | Source |
|---|---|---|
| Conventional boiler | Type 700 | TESS |
| Solar thermal collectors | Type 1b | Standard |
| Micro-CHP boiler | Type 159 | Self-tailored |
| Hydraulic compensator | Type 4 | Standard |
| Constant flow pumps | Type 114 | TESS |
| Storage tanks | Type 4 | Standard |
| Flow diverters | Type 11f | Standard |
| Flow mixers | Type 11h | Standard |
| Differential controller | Type 2 | Standard |
| Heat exchanger | Type 91 | Standard |
| Radiators | Type 211 | Self-tailored |

For simulating the reference installation, two additional Types were employed with respect to Chapter 3: Type 700 and Type 1b. Type 700, included within the TESS libraries, models a condensing boiler, defined by its overall efficiency and by its combustion efficiency. Meanwhile, Type 1b models the thermal performance of a flat-plate solar collector from user-provided information: efficiency of the collector versus a ratio of fluid inlet temperature minus ambient temperature, and tested flow rate. This Type uses a second order quadratic function to compute the effects of off-normal solar incidence in terms of incidence angle modifier (IAM), whose coefficients are determined following an ASHRAE or equivalent tests, as usually supplied by manufacturers.

## 3.4. Performance indicators

The performance of the micro-CHP installation must be evaluated by means of a series of energy, environmental and economic indicators.

First, since micro-cogeneration generators in general and Stirling engines in particular are not designed to work sporadically or intermittently, in order to be able to guarantee that the engine is properly used, its annual operating hours and the number of on-off cycle were obtained.

Additionally, different vectors associated to energy inputs and outputs of both installations were extracted from the simulations every minute to perform the operational study:

- Natural gas consumed by the auxiliary burner, $F_{ab}$
- Natural gas consumed by the main burner of the Stirling engine, $F_{CHP}$
- Heat produced by the auxiliary burner, $Q_{ab}$
- Heat produced by the engine, $Q_{CHP}$
- Electricity produced by the alternator of the engine, $E_{CHP}$
- Electricity consumed within the micro-CHP installation, $E_{plant_{CHP}}$
- Natural gas consumed by the conventional boiler, $F_{boiler}$
- Heat produced by the conventional boiler, $Q_{boiler}$
- Heat produced by the solar thermal collector, $Q_{sol}$
- Electricity consumed by the conventional boiler, $E_{boiler}$
- Electricity consumed by the conventional plant, $E_{plant_{ref}}$

With these data, energy, environmental and economic analyses, subsequently introduced, were assessed.

### 3.4.1. Energy and environmental indicators

The energy analysis was first assessed in terms of PES, defined in the EED, and REE, calculated according to Equation 4.2. Both indicators, which compare the heat and electricity generation of the micro-CHP with the separate production of both by-

products by conventional means, are focused on determining whether a CHP system can be considered as a high efficiency system. In the case of the REE, it is related to economic incentives analyzed later on.

However, since the aim of a techno-economic assessment is to compare the primary energy consumption of the alternative system with respect to a reference system which may not fulfil the approach proposed by the EED, another indicator was introduced in order to distinguish between the technical analysis and regulatory constraints.

For that purpose, PES expressed in absolute terms was utilized, introducing some modifications with respect to traditional approaches, as proposed in Equation 4.8. This indicator allows comparing primary energy savings of the two plants under consideration, and so express overall primary energy savings achievable with the micro-CHP installation, taking into consideration electricity consumption and/or renewable heat production which take place in the reference plant:

$$PES\ (MWh) = PES_{CHP} - PES_{ref}$$

Equation 4.6

$$PES_{CHP} = \frac{Q_{CHP}}{RefH_\eta} + \frac{E_{CHP}}{RefE_\eta} - F_{CHP}$$

Equation 4.7

$$PES_{ref} = \frac{Q_{SOLAR}}{RefH_\eta} - \frac{E_{sol} + E_{boiler}}{RefE_\eta}$$

Equation 4.8

Primary energy savings calculated in terms of energy enables the comparison of the non-renewable primary energy consumption of both micro-CHP and reference installations.

Additionally, another indicator was introduced in order to distinguish between the technical analysis and European regulatory constraints. In this sense, as done in the Annex 54 on integration of micro-generation and related energy technologies in buildings (Sasso et al., 2014), the primary energy saving ratio (PESR), according to Feng et al. (1998), was used:

$$PESR = \frac{PE_{ref} - PE_{CHP}}{PE_{ref}}$$

Equation 4.9

where $PE_{ref}$ and $PE_{CHP}$ are the primary energy inputs of the reference and the micro-CHP systems, respectively.

$$PE_{ref} = PE_{ref}^{f} + PE_{ref}^{e}$$

Equation 4.10

$$PE_{CHP} = PE_{CHP}^{f} - PE_{CHP}^{e}$$

Equation 4.11

where $PE_{CHP}^{f}$ accounts for the natural gas consumed by both the main and the auxiliary burners of the micro-CHP device.

Contrary to most traditional approaches, in the indicators used in this thesis the electric consumption of the conventional boiler, as well as that of the solar circuit, is taken into consideration when calculating the primary energy associated to the conventional production.

Primary energy associated to both natural gas and electricity can be obtained through final-to-primary energy conversion coefficients extracted given by IDAE. In the same way, $CO_2$-eq emissions are related to primary and final energy consumption. This way, when assessing and environmental comparative analysis of a micro-CHP plant with respect to the separate production of heat and electricity by conventional means, $CO_2$-eq emissions can be calculated taking into consideration the corresponding emission factor of each energy resource utilized.

$$\Delta m_{CO_2-eq}(\%) = \frac{m_{CO_2-eq}^{ref} - m_{CO_2-eq}^{CHP}}{m_{CO_2-eq}^{ref}} \cdot 100$$

Equation 4.12

where $m_{CO_2-eq}$, the pollutant mass of each plant, can be disaggregated into the different energy sources which take place and be calculated as follows:

$$m_{CO_2-eq} = \mu_f \cdot F + \mu_e \cdot E \qquad \text{Equation 4.13}$$

where $\mu_f$ and $\mu_e$ are the specific $CO_2$ emission factor of natural gas and electricity, respectively. In the current case, 0.331 kg $CO_2$/ kWh$_{final}$ for electricity and 0.252 kg $CO_2$/ kWh$_{final}$ for natural gas were adopted (IDAE, 2016). These values were calculated in accordance to the energy mix of the electric system at that moment, averaged for the 2005 – 2011 period, whose primary energy-based distribution is presented in Figure 3.14.

Likewise, an hourly-based electricity balance was carried out, so that the contribution of the μCHP plant to the demand of the building could be evaluated, and so enabling the performance of the economic assessment afterwards. For analysing the electric performance, three indicators were introduced for each of the cases: self-consumed electricity ($SC_e$), net electricity coverage ($NC_e$), and relative electricity coverage ($RC_e$).

Whilst $SC_e$ stands for that electricity produced in the micro-CHP unit that is self-consumed within the building at the moment of its generation, the term $NC_e$ attends to the electric energy supply with net balance, i.e. the net production of the plant with respect to the total consumption of the dwelling. On the other hand, since the consumption of the plant itself must be deduced from its power output, if the net balance was applied to the conventional plant, owing to the consumption of the auxiliaries of the plant, a negative contribution would be obtained. To take into consideration this effect, the $RC_e$ was introduced, so considering the net balance of the micro-CHP plant with respect to that of the conventional installation by means of its electricity consumption, which is discounted. The three indicators are calculated according to that defined in Equation 4.14, Equation 4.15 and Equation 4.16, respectively:

$$SC_e(\%) = \left(\frac{E_{CHP} - E_{grid}}{E_{CHP}}\right) \cdot 100$$

Equation 4.14

$$NC_e(\%) = \left(\frac{E_{CHP} - E_{plant_{CHP}}}{E_{demand}}\right) \cdot 100$$

Equation 4.15

$$RC_e(\%) = \left[\frac{E_{CHP} - \left(E_{plant_{CHP}} - E_{plant_{ref}}\right)}{E_{demand}}\right] \cdot 100$$

Equation 4.16

where $E_{demand}$ is the electricity demand of the building, excluding that corresponding to the thermal installation.

### 3.4.2.  Economic indicators

Concerning the economics, as indicated by Hawkes (2011), when assessing any economic discussion of a micro-CHP system, the relation between prices of electricity and fuel must be regarded. This relationship is expressed by means of the spark spread (SS), which is, in general terms, a measure of the gross economic value a generator can expect to obtain when selling one unit of electricity after consuming the fuel necessary to produce such electricity. When dealing with micro-CHP, where two products are obtained, the SS concept has to be adapted to take into consideration the economic value of the heat output. Thus, assuming that the value of a heat unit is that corresponding to the cost of producing it in a conventional boiler, the relationship presented in Equation 4.17 is obtained:

$$SS = EP - \frac{FP}{\eta_e} + \left(\frac{\eta_g}{\eta_e} - 1\right) \cdot \left(\frac{FP}{\eta_0}\right)$$

Equation 4.17

where $EP$ and $FP$ are the respective unitary prices of electricity and fuel, $\eta_e$ and $\eta_g$ are the electric and overall efficiencies of the micro-CHP, respectively, and $\eta_0$ is the reference thermal efficiency, i.e. of the conventional boiler the micro-CHP competes with.

Based on the spark spread concept, the spark gap (SG) can also be defined. In the case where both the overall efficiency of the micro-CHP and that of the reference boiler are approximately the same ($\eta_g \approx \eta_0$) and close to 1, SS reduces to the SG, as indicated in Equation 4.18:

$$SG = EP - FP$$ 

<div align="right">Equation 4.18</div>

Even though the spark gap does not take into account all the necessary information about the economics and other limiting aspects of a micro-CHP, it is a quite reliable measure to have a first impression of the competitiveness of a micro-CHP unit, since as its value increases the profitability of the micro-CHP improves.

Once observed that the SG was positive, so there is a positive cash-flow regarding energy input and outputs, the economics of the micro-CHP installation was approached by broadening the basic economic analysis set out in Chapter 3.

Thus, in addition to the NPV, which is slightly modified with respect to that stated in Chapter 3, the Pay-back period was also utilized to evaluate the investment of the micro-CHP installation. As mentioned, the NPV considers all incomes and outcomes in the economic lifetime of the plant in relation to the initial capital investment, whilst the discounted Pay-back period, which contrary to the simple payback takes into account the time value of the money, represents that moment when the investment gets recovered.

Assuming that the whole investment is made in the beginning of the project, the NPV value can be obtained through Equation 4.19:

$$NPV = -Inv + \sum_{n=1}^{n=LT} \left[ \frac{NS}{(1+r)^n} \right]$$

<div align="right">Equation 4.19</div>

where $Inv$ is the relative investment of the project, deducing the hypothetical investment costs of the conventional plant – avoided costs – , $LT$ is the number of years

to consider the investment, $r$ is the rate of discount, and $NS$ represents the annual cash flows generated, which were calculated using the variables obtained in the energetic performance study by means of Equation 4.20. For this kind of projects, a lifetime of 15 years is typically assumed, and a rate of discount of 5% is lately considered to represent faithfully the available bank products (IDAE, 2014; European Commission, 2014).

$$NS = \sum_{i=1}^{i=8760} \left( Inc + I_e + I_{ac} - C_f - C_m \right)_i \qquad \text{Equation 4.20}$$

where $Inc$ are the applicable incentives and complements in each case, $I_e$ are the avoided costs owed to sales and self-consumption of the electricity generated in the μCHP, $I_{ac}$ are the avoided costs related to the fuel consumed in the conventional plant, $C_f$ are the costs related to the natural gas consumed in the current cogeneration plant, and $C_m$ represents the difference between maintenance costs of the micro-CHP and the conventional plant.

Within this context, $I_e$ is obtained by multiplying each value of the self-consumed and sold electricity vectors by the stipulated price. Avoided natural gas costs ($I_{ac}$) are obtained by multiplying the total consumption of the previous installation by the current natural gas tariff, while costs related to the fuel consumed in the current installation ($C_f$) are calculated by multiplying natural gas consumption of both the micro-CHP device and the auxiliary boiler to the current natural gas supply price. Maintenance costs ($C_m$) are obtained by subtracting the maintenance costs associated to the solar thermal panels and the conventional boiler to those corresponding to the micro-cogeneration boiler, as the remaining maintenance costs exist for both the conventional and the μCHP plants.

For evaluating the economic investment of the different components of the plants, two possibilities were contemplated: consider specific products with their corresponding prices, or, based on catalogue data of manufacturers, relate investment costs with the power supplied by that category of product general prices, as done by Pérez-Iribarren (2016). While the second approach was selected for the solar installation, as

previously presented in Section 3.1, in order to make investments as comparable as possible due to the wide range of wall-mounted condensing boilers available, it was considered that the first criterion was more appropriated for evaluating the investment of the conventional boiler. This way, if the micro-CHP unit does not incorporate an auxiliary source, the conventional boiler and that backing up the micro-CHP unit should be the same. On the other hand, if, as usual, the micro-CHP engine is integrated within a wall mounted boiler, the conventional boiler selected should be one similar to that one of the system where the micro-CHP is integrated.

# 4. Case study

The building selected as case study is that previously used in Chapter 3 and, as mentioned, defined in Annex D. This building, taking into consideration its year of execution and the corresponding design requirements with respect to thermal demand, must fulfil two reference climatic-zone dependant transmittance values. The first one, named *single* in Table 4.3, states that each individual element of the envelope must not exceed the maximum value established for the category where it is included; the second one, named *joint* in Table 4.3, establishes that the global transmittance of a category when all the individual elements of such category are put together must not exceed the transmittance value specified.

Since one of the parameters taken into consideration in the analysis is the climatic severity, aside from Vitoria-Gasteiz where the defined building stands, three other cities, with representative weather conditions, were chosen: Almería, Burgos and Madrid. According to that previously exposed in Section 3.2 and as shown in Figure 4.7 and Figure 4.8 in Section 3.2 and Figure 4.9, where the classification of the different climatic zones and the average monthly outdoor temperatures of the four cities under study are depicted, respectively, Almería (A4 zone) has extremely hot summers and warm winters; Burgos (E1 zone) has very cold winters and warm summers; Madrid (D3 zone) has cold winters and very hot summers. Meanwhile, Vitoria-Gasteiz (D1 zone) has cold winters and warm summers.
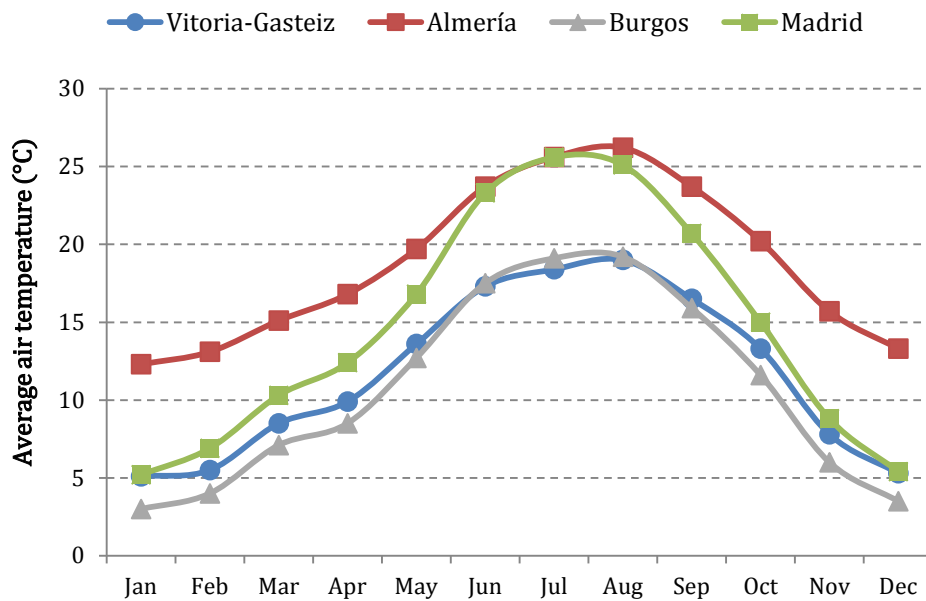
Figure 4.9 – Monthly average ambient temperatures of the different locations considered.

In accordance with these premises, the main features of the envelope and the corresponding maximum values achievable for the different climatic zones considered in the parametric analysis are summarized in Table 4.3.

Table 4.3 – Actual transmittances of the constructive elements and the maximum values permitted when the project was executed for different climatic zones.

| Component | U-value (W/K·m⁻²) | | | | | | | | | |
|---|---|---|---|---|---|---|---|---|---|---|
| | Real | | Maximum | | | | | | | |
| | | | Zone A4 | | Zone C3 | | Zone D1 | | Zone E1 | |
| | Single | Joint | Single | Joint | Single | Joint | Single | Joint | Single | Joint |
| Ext. wall T1 | 0.44 | | | | | | | | | |
| Ext. wall T2 | 0.40 | 0.39 | 1.22 | 0.94 | 0.95 | 0.73 | 0.86 | 0.66 | 0.74 | 0.57 |
| Ext. wall T3 | 0.37 | | | | | | | | | |
| Roof | 0.22 | 0.25 | 0.65 | 0.50 | 0.53 | 0.41 | 0.49 | 0.38 | 0.46 | 0.35 |
| Ceilings | 0.44 | | | | | | | | | |
| Floors | 0.42 | 0.42 | 0.69 | 0.53 | 0.65 | 0.50 | 0.64 | 0.49 | 0.62 | 0.48 |
| Windows | 1.24 | 1.24 | 5.70 | 5.70 | 4.40 | 4.40 | 3.50 | 3.50 | 3.10 | 3.10 |

## 4.1. Energy demands

Taking into consideration the climatic premises established, the different energy demands were calculated, similarly to those defined in Appendix D for Vitoria-Gasteiz. Considering both heating and DHW, respective annual demands obtained for Almería, Burgos and Madrid were 4.32 MWh, 29.77 MWh and 17.54 MWh, while cooling demands were not considered.

In the heat demand graph presented in Figure 4.10, where the annual thermal energy demand of each case study is depicted, broken down into heating and DHW, a strong need for heating during almost all the heating season long can be appreciated for Burgos, while in Almería DHW is the most significant demand throughout most part of the year.

With respect to electricity, demands for every case are those calculated in Annex D and previously used in Chapter 3.
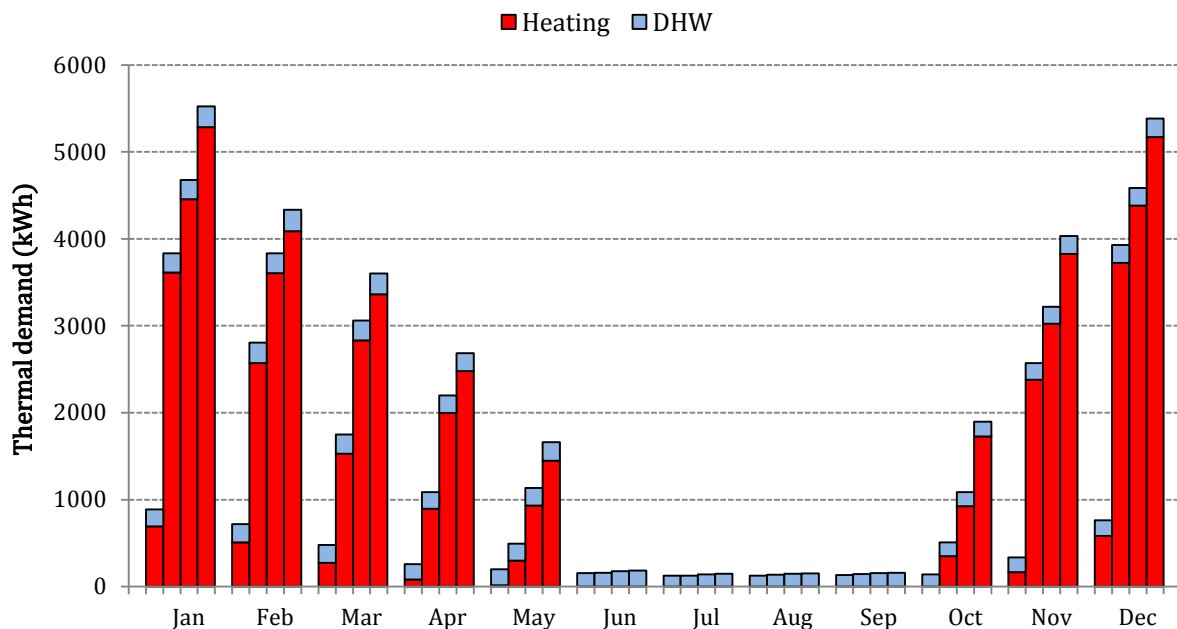


Figure 4.10 – Annual total thermal demand (from left to right: Almería, Madrid, Vitoria-Gasteiz, Burgos).

## 4.2.   Reference installation: modelling and operation

While the micro-CHP installation follows the same operation already defined in Chapter 3, some insights should be made regarding the reference installation prior to continuing with the analysis.

As stated, the prime mover of the installation is a condensing boiler, modelled in TRNSYS through Type 700 and a mean seasonal efficiency equal to 83 %. This efficiency responds to the high temperature installation (50 - 70 °C) where the boiler is integrated – nominal efficiency of boilers decrease considerably when working in temperature ranges above 50 °C since no latent heat recovery takes place –, as well as to the fact that, due to the comparative nature of the techno-economic assessment, it was considered that the boiler ought to have similar features to that where the SE is integrated. The conventional boiler operates whenever there is need for space heating.

On the other hand, the control-logic of the DHW supply is designed to meet two requirements. Since DHW is firstly preheated by the solar system, the boiler should only act whenever the DHW supply temperature is below 45 °C. Additionally, if DHW and heating demands coexist simultaneously, and the power provided to the DHW is not sufficient to achieve the temperature defined, the heating supply will be cut off and the whole production of the boiler will be dedicated to fulfil DHW necessities.

Concerning the solar installation, applying the methodology described in Section 3 for the house sited in Vitoria-Gasteiz, the main design of the solar installation was also solved for each of the three representative climatic conditions, thus determining the solar surface and the solar storage capacity. Beyond radiation conditions of the climates considered, as well as the solar fractions required for each one, results reached corroborate conclusions presented in the mentioned section of the current chapter: it is desirable that the solar surface is the minimum that enables reaching the contribution requirements, and the V/A relationship should be 75 in order to guarantee security and economic savings. In order to better compare every installation, the same solar collecting surface was employed for all the climatic zones. For this purpose, the total

absorption surface was set to 2 m², so that the most restrictive contribution percentage could be reached.

Table 4.4 – Main parameters of the solar thermal collector TRNSYS Type 1b.

| Parameter | Value | Units |
|---|---|---|
| Collector area | 2 | m² |
| Tested flow rate | 40 | kg/(h·m²) |
| Intercept efficiency | 0.801 | - |
| Efficiency slope | 3.93 | W/( m²·K) |
| Efficiency curvature | 0.026 | W/( m²·K²) |
| First order IAM | 0.34 | - |
| Second order IAM | 0 | - |

The main parameters used in the simulation of the solar thermal collector are those summarized in Table 4.4. In order to maximise the absorption of solar radiation, the panel is south-oriented with a slope equal to the latitude where the installation is placed. On the other hand, to ensure the proper operation of the system and maximize the exploitation of the solar energy, the control system of the shunt pump is differential. That is, the shunt pump activates when the difference between the outlet temperature of the solar collectors and that of the solar tank is greater than 7 ℃, while it will get switched of when that temperature difference is below 2 ℃ (CTE, 2013b).

## 4.3. Economic framework

Regarding legislative conditions that influence the economic analysis in the Spanish context, previously exposed in Section 1, for the current case-study, a natural gas-fired engine with a power output below 0.5 MW, and installed in 2014 (at the moment of carrying out the analysis), $R_{inv}$ and $R_o$ acquired values of 163,121 €/MW and 78.05 €/MWh per year, respectively.

Concerning gas and electricity, natural gas acquisition prices are determined by the Ministry of Industry, Energy and Tourism, through tariffs called TUR. Tariffs are updated quarterly, provided that there is a variation in the cost of the raw material greater than ±2% (Ministerio de Industria, Turismo y Comercio, 2009b). In the case of electricity,

electricity tariffs worked in a similar way to those of the natural gas – called TUR as well – until July 1st 2014 (Ministerio de Industria, Turismo y Comercio, 2009a), when all the procedures for establishing the electricity prices were updated (Ministerio de Industria, Energía y Turismo, 2014b). However, the main commercial companies, apart from the new tariffs where prices are estimated daily or even hourly, still offer the previous pricing modalities, equivalent to TUR tariffs, now available for periods of no less than a year.

Prices of both products are divided into 2 terms: fixed and variable. In the case of the natural gas, the fixed term is not dependent on any factor. In the electricity case, the fix-term depends on the consumption peak power, which may be contracted according to some preset power ranges. For the variable term, 3 tariff typologies are available:

i) without time discrimination: the price of the variable term stays constant during the whole day.

ii) with 2-period discrimination: two different prices are applied depending on the period of the day.

iii) supervalley: three different pricing periods are distinguished throughout the day.

Whilst natural purchase-price was 5.04 c€/kWh as previously set in Section 3 (Ministerio de Industria, Energía y Turismo, 2014d), tariffs corresponding to purchased electricity are those summarized in Table 4.5 (Ministerio de Industria, Energía y Turismo, 2014e).

As far as electricity sales are concerned, currently no payment is mandatorily assigned to this concept in Spain. In this context, two different scenarios were considered: in the first scenario no electricity retribution was considered (NR) while, in the second, a hypothetical retribution equal to the pool price was considered (PR). Specifically, the latter considers the hourly value at which commercial companies acquire electricity in the energy market. As shown in Table 4.5, pool hourly values were averaged for time intervals corresponding to those applied to electricity-purchase tariffs. In both cases, in order to increase the SG and, consequently, the economic viability, it is desirable to maximize the self-consumed electricity produced instead of selling it.

Table 4.5 – Pricing periods and costs of the different electricity-purchase tariff modes.

| Tariff | | Electricity cost [c€/kWh] | | | | | | |
|---|---|---|---|---|---|---|---|---|
| | | 0-1 h | 1-7 h | 7-12 h | 12-13 h | 13-22 h | 22-23 h | 23-24 h |
| No discrimination | | 12.4107 | 12.4107 | 12.4107 | 12.4107 | 12.4107 | 12.4107 | 12.4107 |
| 2-periods discrimination | Summer | 5.7995 | 5.7995 | 5.7995 | 5.7995 | 14.8832 | 14.8832 | 5.7995 |
| | Winter | 5.7995 | 5.7995 | 5.7995 | 14.8832 | 14.8832 | 5.7995 | 5.7995 |
| Supervalley | | 7.1879 | 4.4146 | 7.1879 | 7.1879 | 15.0812 | 15.0812 | 7.1879 |
| Pool | Summer | 4.5222 | 3.7542 | 4.8460 | 5.0322 | 4.8039 | 5.2655 | 4.7759 |
| | Winter | 3.5107 | 2.2540 | 3.8418 | 4.0728 | 4.3309 | 4.6083 | 4.2105 |
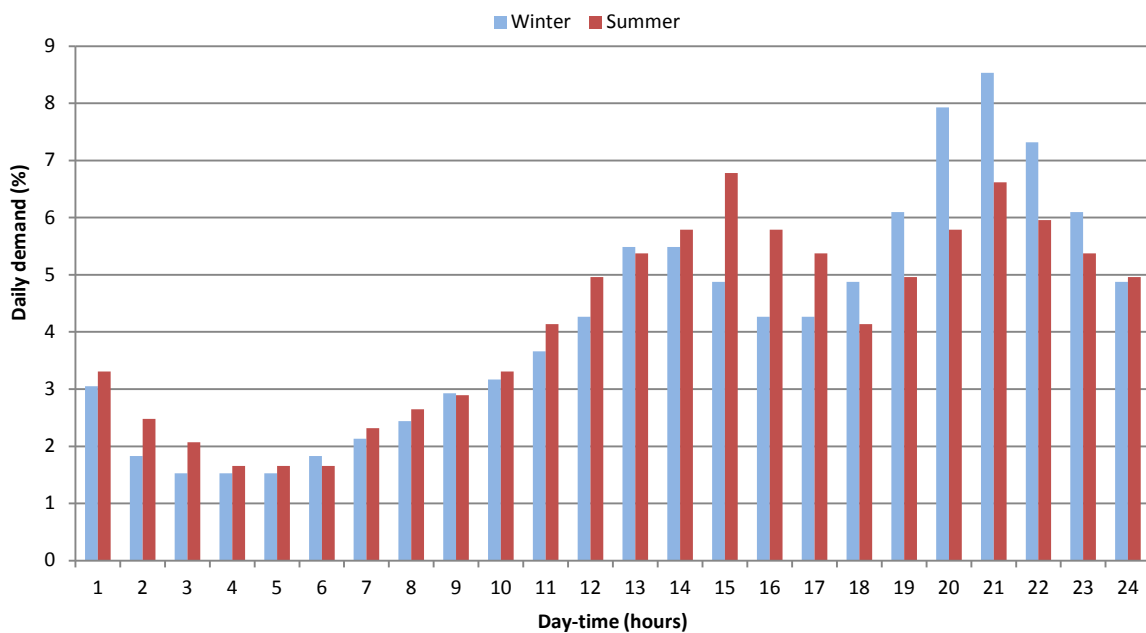


Figure 4.11 – Daily electricity consumption profile.

While electricity tariffs considered are those summarized in Table 4.5, the peak power-based fix-term was neglected. This is due to the fact that, although the peak consumption of the dwelling on an hourly basis in the case of the micro-CHP installation is slightly lower (up to 17% in the most favourable conditions), the contracted power must be the same for both cases. Since the economic analysis was made from a comparative point of

view, no fixed term was either considered for natural gas supply, as it is common for both installations.

## 4.4. Investment and maintenance costs

When tackling the economic analysis, initial investment and the annual savings achieved through that investment are compared. Investment costs must account for the initial cost of the micro-CHP unit, as well as its corresponding connection to the low voltage network (estimated at a 5% of the total cost of disposing the device (Sedigas, 2012)), together with the cost of acquiring and installing all other components that take part in the plant.

Table 4.6 – Main components of each thermal installation.

| Component | Micro-CHP plant | Conventional plant |
|---|:---:|:---:|
| Micro-CHP unit | √ | - |
| Condensing boiler | - | √ |
| Solar panels | - | √ |
| Piping & valves | √ | √ |
| Pump 1 | √ | √ |
| Pump 2 | √ | √ |
| TES + Heat exchanger | √ | √ |

Nevertheless, since the analysis was formulated in comparative terms, hydraulic components were considered to have the same cost for both installations, so they were not taken into account. Additionally, the cost of the TES and the external heat exchanger for DHW of the micro-CHP installation was equated to that of the inter-accumulator of the solar circuit. In Table 4.6 the main components of each thermal installation are summed up.

As long as investment in the main components of the plant is concerned, while solar investment, as previously presented in Section 3.1, can be determined through Equation 4.4, as argued late in Section 3.4, a conventional boiler similar to that where the Stirling engine is integrated was selected for the reference installation, raising its cost up to

2065 €. The thermal power of this boiler by Remeha is 23.5 kW$_t$ when working at low temperatures, and its characteristics, as well as its cost, are similar to mid-range combi boilers from other manufacturers. With respect to the micro-CHP device, its cost was 12,000 € when it was purchased for its installation in the experimental plant of the LCCE.

Thus, when determining the initial investment, $Inv$, the price of the condensing wall-mounted boiler, as well as that corresponding to the solar thermal panels must be discounted to the initial investment due to micro-CHP unit:

$$Inv = Inv_{CHP} - (Inv_{boiler} + Inv_{sol})$$
<div align="right">Equation 4.21</div>

With respect to maintenance costs, since LFPSE integrated within wall-mounted condensing boilers, as it is the case of Remeha eVita, only require the same maintenance tasks as conventional boilers, only maintenance costs associated to the solar thermal installation were accounted. According to the selected surface, 2 m², and Equation 4.5, the solar installation requires 67 €/year in maintenance concept.

# 5. Results

Once defined every main aspect taking part in the techno-economic assessment of the micro-CHP installation, the performance and viability study was carried out for the three representative climatic regions, as well as the primary location of the case-study building.

Operational results of the conventional plant, which are collected in Table 4.7, show that, in the four considered cases, the established solar surface is enough for fulfilling the Spanish CTE, as the required 60%, 50% and 30% for Almería, Madrid, and Burgos and Vitoria-Gasteiz, respectively, are thoroughly exceeded in some cases by the 60%, 52%, and 43% and 44% obtained.

Table 4.7 – Annual operational results of the reference installation.

| | Almería | Burgos | Madrid | Vitoria-Gasteiz |
|---|---|---|---|---|
| $Q_{sol}$ (kWh) | 1306 | 1103 | 1243 | 1086 |
| Contribution to DHW (%) | 60.07 | 42.89 | 52.32 | 44.50 |
| $Q_{boiler}$ (kWh) | 2385 | 25759 | 14161 | 21004 |
| $F_{boiler}$ (kWh) | 2873 | 31033 | 17060 | 25308 |
| Heating supply (kWh) | 1747 | 24821 | 13443 | 20091 |
| DHW supply (kWh) | 2001 | 2366 | 2176 | 2306 |
| $m_{CO2-eq}$ (kg CO2-eq) | 1007 | 8163 | 4613 | 6705 |

Concerning the micro-CHP installation, its main annual operation indicators are presented in Table 4.8. It can be appreciated that the number of hours of operation of the Stirling engine is extremely short for the case of Almería, increasing but being still low for the case of Madrid, and getting up to almost a half of the year for the case of Burgos and Vitoria-Gasteiz, which is a reasonable number of working hours. Meanwhile, if not only the thermal needs of the predefined heating season established by the CTE were covered, but also those necessary during the non-heating season, which are 1946 MWh and 1071 MWh respectively for Burgos and Vitoria-Gasteiz, the respective number of hours of operation would be 3700 and 3104[2]. For the two cases of hot summers, no significant variations were appreciated in this sense.

Furthermore, a very high overall efficiency is achieved for the whole plant, which indicates that primary energy is used in an efficient way. In this sense, PES results remark that primary energy savings with respect to the separate production of both thermal and electrical energy increase as the running time of the Stirling engine augments. This is due to the fact that operation periods are longer, with less warm-up and cool-down periods where the efficiency of generators decreases. Results of the three cities, except for the one which is subject to warm conditions, far exceed the minimum value of primary energy savings requested by the Energy Efficiency 2012/27/EU

---

[2] The number of hours of operation at full load got when sizing the micro-CHP unit for the housing in Chapter 3, with no heat storage nor part-load operation, was 2311 hours.

Directive. So happens to the REE, exceeding the 45% value established by the Spanish normative in order to be considered as high efficiency cogeneration.

Table 4.8 – Annual operational results of the micro-CHP installation.

| | Almería | Burgos | Madrid | Vitoria-Gasteiz |
|---|---|---|---|---|
| Number of on/off cycles of the μCHP | 1121 | 1538 | 1392 | 1517 |
| Number of hours of operation of the μCHP | 741 | 3450 | 2182 | 2962 |
| Number of hours of operation per on/off cycle | 0.7 | 2.2 | 1.6 | 2.0 |
| $Q_{CHP}$ (kWh) | 2705 | 13908 | 8667 | 11898 |
| $E_{CHP}$ (kWh) | 494 | 2797 | 1720 | 2381 |
| $F_{CHP}$ (kWh) | 4242 | 20066 | 12631 | 17200 |
| PES (%) | -3.3 | 7.4 | 6.1 | 7.1 |
| REE (%) | 40.0 | 60.6 | 57.3 | 59.8 |
| $Q_{ab}$ (kWh) | 870 | 12999 | 6702 | 10197 |
| $F_{ab}$ (kWh) | 1134 | 16219 | 8423 | 12747 |
| $\eta_{plant,CHP}$ (%) | 75.6 | 81.8 | 81.2 | 81.7 |
| $m_{CO2\text{-}eq}$ (kg $CO_2$-eq) | 1217 | 8325 | 4801 | 6204 |
| Heating supply (kWh) | 1743 | 24739 | 13415 | 19992 |
| DHW supply (kWh) | 2004 | 2380 | 2182 | 2322 |

Analyzing PES in terms of energy, results in Table 4.9 show that, except for hot climates, where no primary energy savings are got with the micro-CHP installation with respect to the separate production of both byproducts, non-renewable primary energy savings in the micro-CHP plant range from 2 to over 6 times the savings in the conventional plant, depending on the winter severity of the place where the housing is placed.

With respect to PESR, results of Almería follow the same dynamic shown by PES. The other representative climatic zones achieve PESR values above 0, which evidence that, under actual operative conditions of each plant, primary energy is saved when installing the Stirling engine-based micro-CHP device instead of disposing of traditional solar collecting surface on the roof of the dwelling.

Table 4.9 – Comparative results of both installations.

|  |  | Almería | Burgos | Madrid | Vitoria-Gasteiz |
|---|---|---|---|---|---|
| PES (kWh/a) | $PES_{ref}$ | 442 | 305 | 403 | 295 |
|  | $PES_{CHP}$ | -138 | 1603 | 822 | 1311 |
| PESR (%) |  | 0.3 | 5.2 | 4.8 | 15.9 |
| $\Delta m_{CO2\text{-}eq}$ (%) |  | -20.9 | -2.0 | -4.1 | 7.5 |

Regarding GHG emissions, results remark that slightly better environmental results are usually achieved with the solar installation. It can be underlined that GHG emissions are closely related to non-renewable primary energy savings, getting lower as the PES gets increased. However, this tendency is not maintained in the results presented. In this sense, it must be remarked that emissions calculations are heavily dependent on the emission factors considered for natural gas and electricity, and these have suffered a noteworthy variation over the last years. As an example, for the values given by IDAE, the emission factor of natural gas has risen a 19%, while that corresponding to electricity has dropped to almost half the value it had in 2015.

Additionally, it must be taken into consideration that this variation in the emissions has been calculated with respect to a reference installation composed of a conventional boiler and a solar thermal circuit. If the environmental impact of the micro-CHP installation is compared to that resultant of producing the same amount of heat and electricity as specified in the EED, i.e. a dispensing with the solar installation, $\Delta m_{CO2\text{-}eq}$ would be virtually zero except for the warmest climatic conditions and those who are already positive.

On the other hand, Table 4.10 outlines data obtained from the annual electricity study of the micro-CHP plant. Analyzing the hourly balance of the plant, results show that almost 80% of the electricity produced with the Stirling engine is self-consumed in all of the cases assessed. Moreover, as the winter climatic severity raises, the net electricity coverage of the Stirling device, i.e. the electricity production-to-consumption rate, grows significantly, from about 10% in the case of Almería up to over 58% in the case of the coldest region. This fact means that in the latter case, although only 75% of the

electricity produced in-situ is directly consumed, the production coming from the alternator of the Stirling engine exceeds half the total demand value. Concerning the relative electricity coverage to the demand of the dwelling, results show that in the cold climates around four fifths of the electric consumption of the dwelling is provided by the micro-CHP unit.

Table 4.10 – Annual electricity balance of the micro-CHP plant.

|  | Almería | Burgos | Madrid | Vitoria-Gasteiz |
|---|---|---|---|---|
| $E_{demand}$ (kWh) | 4200 | 4200 | 4200 | 4200 |
| $E_{CHP} - E_{plant,CHP}$ (kWh) | 415 | 2475 | 1525 | 2116 |
| $E_{purchase}$ (kWh) | 3875 | 2423 | 3027 | 2637 |
| $E_{grid}$ (kWh) | 90 | 698 | 352 | 552 |
| $SC_e$ (%) | 84.5 | 75.4 | 80.2 | 77.3 |
| $NC_e$ (%) | 9.9 | 58.9 | 36.3 | 50.4 |
| $RC_e$ (%) | 30.2 | 83.6 | 58.8 | 73.9 |

Finally, looking at the economic aspect, as previously mentioned, two different scenarios were considered:

- Scenario 1: no income due to electricity sales (NR)
- Scenario 2: electricity sales at pool price (PR)

Additionally, since the most common electricity tariff in Spain is that with constant prices all over the day, results achievable with the tariff with no discrimination were first assessed. Then the influence of changing to the tariff with two discrimination periods was also analyzed.

As summarized in Table 4.11, it can be seen that after the 15 years lifetime of the micro-CHP device, the initial extra investment with respect to conventional reference generators is not recovered in any of the cases. Taking into account that the initial investment difference between the micro-cogeneration plant and the reference one raises to 9,000 € approximately, the percentages of recovery in that instant 29%, 36%

40% and 41% for Almería, Madrid, Vitoria-Gasteiz and Burgos, respectively. In the case of warm climate overall annual cash flows are insignificant with respect to the conventional plant, except for maintenance costs and retribution to investment.

Table 4.11 – Economic results of the micro-CHP plant: tariff with no discrimination.

| | | Almería | Burgos | Madrid | Vitoria-Gasteiz |
|---|---|---|---|---|---|
| Inv (€) | | 9264.00 | 9264.00 | 9264.00 | 9264.00 |
| NS (€) | Scenario 1 (NR) | 257.33 | 368.94 | 319.35 | 356.05 |
| | Scenario 2 (PR) | 260.97 | 393.69 | 332.35 | 376.06 |
| NPV (€) (year 15) | Scenario 1 (NR) | -6592.90 | -5434.44 | -5949.13 | -5568.17 |
| | Scenario 2 (PR) | -6555.12 | -5177.50 | -5814.20 | -5360.47 |

For the most favorable case, that is, that corresponding to the coldest climatic zone (Burgos), the payback period would be greater than the lifetime of the plant even if this was 30 years. Therefore, under current conditions, Stirling engine-run micro-cogeneration devices are completely unprofitable for detached houses in Spain.

Attending to overall annual savings, the difference between the NR and the PR cases, which lies in the retribution for sold electricity, confirms that this retribution does not report any significant benefit, so confirming that it is desirable to self-consume as much electricity as possible. In this sense, it should be considered that the mean cost of a self-consumed kWh is more than 3 times higher than that poured into the grid at pool price.

Table 4.12 – Economic results of the micro-CHP plant: tariff with two discrimination-periods.

| | | Almería | Burgos | Madrid | Vitoria-Gasteiz |
|---|---|---|---|---|---|
| Inv (€) | | 9264.00 | 9264.00 | 9264.00 | 9264.00 |
| NS (€) | Scenario 1 (NR) | 232.26 | 315.95 | 277.96 | 308.08 |
| | Scenario 2 (PR) | 235.90 | 340.71 | 290.96 | 328.09 |
| NPV (€) (year 15) | Scenario 1 (NR) | -6853.11 | -5984.40 | -6378.078 | -6066.16 |
| | Scenario 2 (PR) | -6815.33 | -5727.46 | -6243.85 | -5858.46 |

Amongst the different modalities available for the acquisition of electrical energy presented in Section 4.2, taking into consideration the combination of electric consumption profiles generated in Appendix D and depicted in Figure 4.11 and pricings defined in Table 4.5, the tariff with two discrimination-periods turned out to be the most advantageous one for providing the house with electric energy. Nevertheless, as it can be appreciated when comparing results presented in Table 4.11 with those in Table 4.12, economic comparative results between both installations are widely better if the tariff with no discrimination is chosen. This occurs since the conventional installation is penalized to a greater extent due to its higher electric consumption during the central hours of the day – which mainly lies in the functioning of the solar installation – and, therefore, annual savings are more significant.

In this latter case, the discounted pay-back period for all the climatic zones considered gets increased by 30% approximately with respect to the case with the electric tariff with no discrimination.

# 6. Sensitivity analysis

The previous viability calculations were done under a concrete and steady technical and economic situation. Because the feasibility of this kind of investments depends heavily on some economic factors such as the prices of natural gas and electricity, as well as the inflation rate, a sensitivity analysis was carried out in order to study how these variables influence final economic results. Additionally, taking into consideration results obtained in the previous case, variations of the cost of the micro-CHP device were also considered.

## 6.1. Influence of costs

Firstly, concerning the influence of energy prices on the final economic results for the toughest climatic conditions (Burgos), different SG scenarios were considered, as a consequence of different annual price variations for both electricity and natural gas. For the sake of clarity, and taking into consideration that the amelioration that a tariff with discrimination provides depends heavily on the electricity consumption patterns, variations of electricity prices were carried out taking into consideration the tariff

without hourly discrimination; i.e. constant price throughout the whole day, which is the most usual tariff in Spanish households.
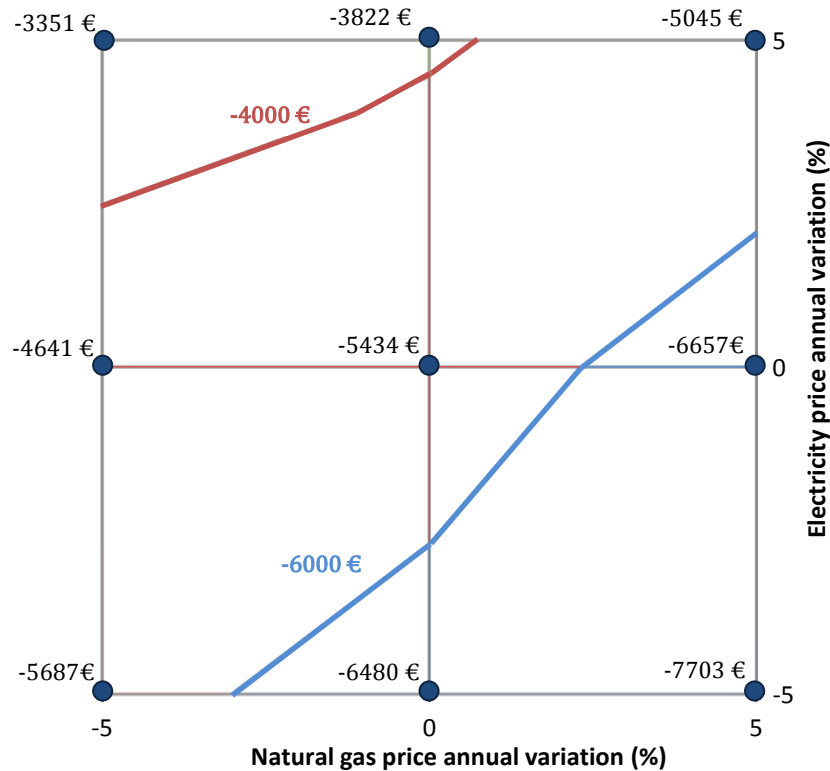


Figure 4.12 – NPV results depending on the evolution of energy prices.

As depicted in Figure 4.12, it is observed that, as expected, annual updating in terms of augmentations in electricity prices and decreases in fuel prices, i.e. increments in the SG, favour annual savings. However, the weight of the electricity percentage variation in the annual cash flows is 30 % higher than the influence of the natural gas tariffs. Thus, if a 5% annual decrease in the natural gas price happened every year, together with a 5% decrease in the electricity price, NPV after year 15 would be considerably lower than that in the no-variation scenario (ΔNPV=-253 €). On the contrary, if a 5% annual augmentation in the prices of both products took place, i.e. the SG was incremented in a 5%, the NPV final result would get improved in 389 €. Finally, it must be highlighted that, even for the most optimistic variation tendency considered, i.e. the unlikely case where the price of electricity is successively incremented and that of natural gas is reduced at the same time, no positive NPV was achieved.

Secondly, three different stages of augmentations of the spark gap were considered: increment of the electricity cost, decrement of the natural gas price, and a joint variation of both previous scenarios. In this case price variations considered in each case were constantly applied to the economic analysis of the whole lifetime of the plant, that is, no annual price updates were considered.
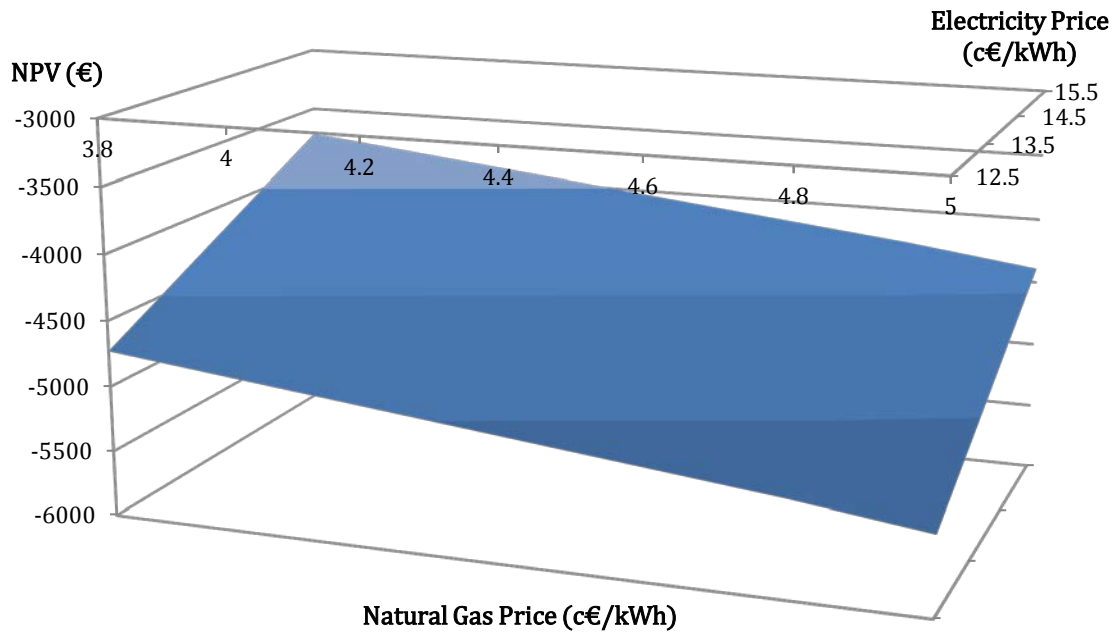


Figure 4.13– NPV as a function of different combinations of natural gas and electricity prices for the coldest climatic zone (Burgos).

Within this context, the most optimistic case is only highlighted, that is, a 25% increase of the electricity prices and 25% reduction in that of the natural gas. In this context, economic results improve considerably, but the Stirling-based micro-CHP unit still remains highly unfeasible regardless of the climatic conditions. Therefore, any possible and realistic change in prices of both products will not consequently vary the viability of the installation by themselves, even though they could satisfactorily contribute in combination with changes in other parameters, as depicted in Figure 4.13 for the most favorable case under study. In the case of the increase considered for the price of electricity, it must be noted that this augmentation is completely possible, as it was until few years ago, when the regulation of the complements for electricity produced through cogeneration were still in force.

On the other hand, the effect of the rate of discount, initially set at 5%, was also studied. For this purpose, three additional values to the initial one were considered (4%, 3% and 2%), with no fully satisfactory results in the viability, as shown in Table 4.13.

Finally, considering that the initial price of the micro-cogeneration device could get lower if a consolidated implantation of the device happened in the global market, amongst other factors, the price below which the investment would get viable was determined for each of the four cases. Thereby, it was regarded that there is no possible viability for warm climates even though the unit cost was below 5500 €, as annual cash flows would make the investment unfeasible after its 15 years lifetime. For the other cases, Vitoria-Gasteiz, Madrid and Burgos, limit prices of the device obtained were 6432 €, 6051 € and 6565 € respectively for the plants to be feasible under current conditions.

Table 4.13– Main economic results of the sensibility analysis.

| NPV (15 years) | | Almería | Burgos | Madrid | Vitoria-Gasteiz |
|---|---|---|---|---|---|
| ΔEP | +25% | -6197 | -4392 | -5199 | -4639 |
| ΔEP ΔGP | +25% -25% | -5875 | -3716 | -4684 | -4042 |
| r | 4% | -6403 | -5162 | -5713 | -5305 |
| | 3% | -6192 | -4860 | -5451 | -5013 |
| | 2% | -5957 | -4523 | -5160 | -4689 |
| Inv$_{CHP}$ [€] | 10,000 | -4593 | -3435 | -3949 | -3568 |
| | 8000 | -2593 | -1435 | -1949 | -1568 |
| | 6000 | -593 | 565 | 51 | 432 |
| | 5000 | 407 | 1565 | 1051 | 1432 |

Variations of the different aforementioned factors affecting the feasibility study of the plant are summarized in Table 4.13.

Thereby, it can be concluded that this kind of equipment could get feasible for supplying heating and DHW in single-family dwellings for extremely cold climates in Spain, provided that commercial prices decrease considerably. For intermediate climates such as the one at Madrid, with cold winters and hot summers, there is a need to increase the number of hours of operation of the engine, in order to achieve savings attached to the energy supply with cogeneration. This could be achieved, for instance, by covering the

cooling demand through thermally activated chillers, but its economic assessment is out of the scope of this PhD Thesis.

On the other hand, as mentioned in previous sections, complements for cogeneration electricity sold to the net were abolished, so decreasing the income due to sales or even making them zero, since no obligatory to pay for it is nowadays established. Moreover, since electricity tariff in Spain suffers from a concept known as structural deficit, costs of producing electricity in conventional plants is about 20% more expensive that prices established by the PVPC (previously called TUR) tariffs. This fact, together with the above-mentioned, penalizes seriously viability of micro-CHP.
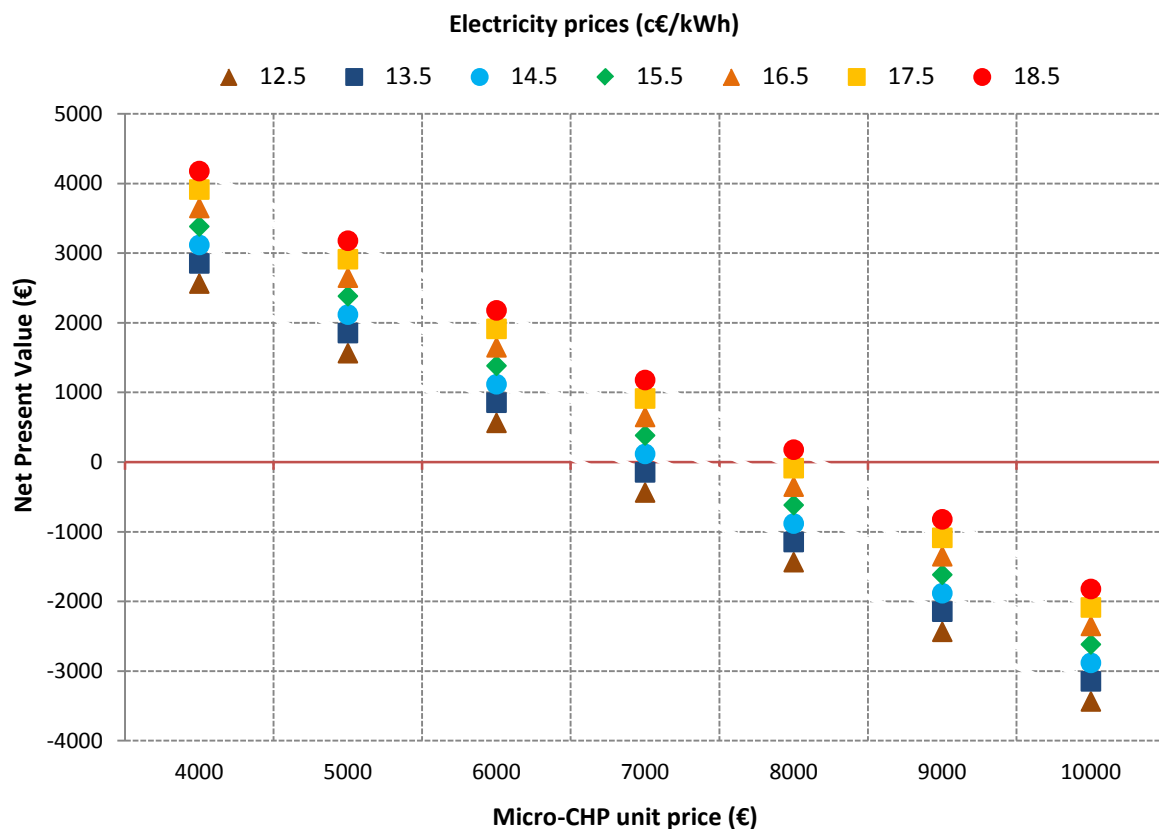


Figure 4.14– NPV (year 15) as a function of different combinations of investment costs of the Remeha eVita and electricity prices for the most favourable case (Burgos).

Figure 4.14 shows how NPV varies with the Stirling engine price for seven different electricity prices[3]. According to the exposed, there may exist possibilities of having both

---

[3] The constant tariff with no discrimination offered by two of the most important electricity marketers in Spain during 2018 was of 15.4 and 15.7 c€/kWh, respectively.

electricity remuneration substantially increased and initial cost of the cogeneration device decreased, which could make economic viability more feasible. Results show that having a 45% decrease in the investment cost of the unit, current conditions make the micro-CHP feasible. Additionally, if the electricity remuneration got increased on a 15%, a 40% drop in the unit cost would make installing this device economically viable. Finally, data also reflects that less than a 30% decline in the micro-cogeneration price makes any realistic increase of the price of electricity generated insufficient for viability.

## 6.2. Influence of the regulation framework

Following the methodology explained in Section 3 and 4, the economic study was complemented for the most favourable climatic zone, i.e. Burgos, taking into consideration those regulative constraints, exposed in Section 2, applicable to Spain, Germany and the UK.

Table 4.14– Main economic flows of the two plants under the current Spanish situation.

| Concept | Cost (€/a) | |
|---|---|---|
| | Conventional plant | Micro-CHP plant |
| Specific Investment | 3368 | 12632 |
| Natural Gas | 1564 | 1829 |
| Electricity [4] | 650 | 246 |
| Specific Maintenance | 67 | 0 |

First, main intermediate results for the current Spanish regulation with constant energy prices, summarized in Table 4.14, show that being the initial investment much higher for the micro-CHP case, within the framework described, savings with respect to the reference scenario are very low compared to that extra cost, being the positive relative income mainly related to electricity, which accounts for the sales (if a payment is considered) and the self-consumption, as well as the incentives to investment and operation.

---

[4] The value of the electricity cost associated to the case with the micro-CHP plant includes the deduction corresponding to retribution to investment and operation.

As so, according to data corresponding to the coldest climatic zone shown in Table 4.15, around a 41% recovery of the initial investment is only reached after the 15-years lifetime considered. Even though when comparing these results with those obtained during the in-pass situation which took place between January 2012 and June 2014, when no incentive was applied (Table 4.15), an obvious amelioration of the feasibility is observed (2259€), feasibility is far from being achieved.

Table 4.15 – Main economic results of the micro-CHP for Spain.

| Normative scenario | Electricity savings (€/a) | NPV (year 15) (€) | Payback (years) |
|---|---|---|---|
| No-incentives | 349 | -7693 | No payback |
| Previous regulation | 648 | -4593 | No payback |
| Current regulation | 404 | -5434 | No payback |

On the other hand, calculating results that would be achieved applying the regulation in force until late 2011 (RD 661/2007), with current fuel and electricity pricings and without considering any complement due to reactive power ($C_{reac}$), payback would not either be reached after the lifetime of the plant is passed by. Comparison between these two economic results shows a final difference in the net present value of almost 900 € after 15 years of operation, out of a relative investment of roughly 9000 €. This fact constitutes a great step back for the implantation of this efficient technology.

Besides the exposed difference between the two scenarios, which lies in the elimination of the incentives for high efficiency generators and the implementation of the new regulation, the trend of fuel and electricity prices in the last few years in Spain is also negatively affecting the feasibility of this technology. As shown in Figure 4.15 for the so-called TUR tariffs, while the natural gas price has increased by 34% in the period considered, composed by 13% and 35% raises in the fixed and the consumption terms respectively, the electricity tariff increment has almost reached 17%, which comes from a respective augmentation of 104% and 5% of the power and the variable terms.

In the case of electricity, the increase of the price, which is expected to keep on rising progressively in the coming years in order to deal with the so-called tariff-deficit, has mainly led to a huge augmentation of the term corresponding to the contracted power

instead of the consumption term. Given that the power term contract works with prearranged and stepped values, and the achievable peak power demand reduction is not enough to shift from one step to a lower one, no savings are possible in this sense. This fact constitutes a very noteworthy drawback for the economic feasibility of micro-CHP, since savings due to self-consumed electricity do not rise even though electricity gets more expensive.
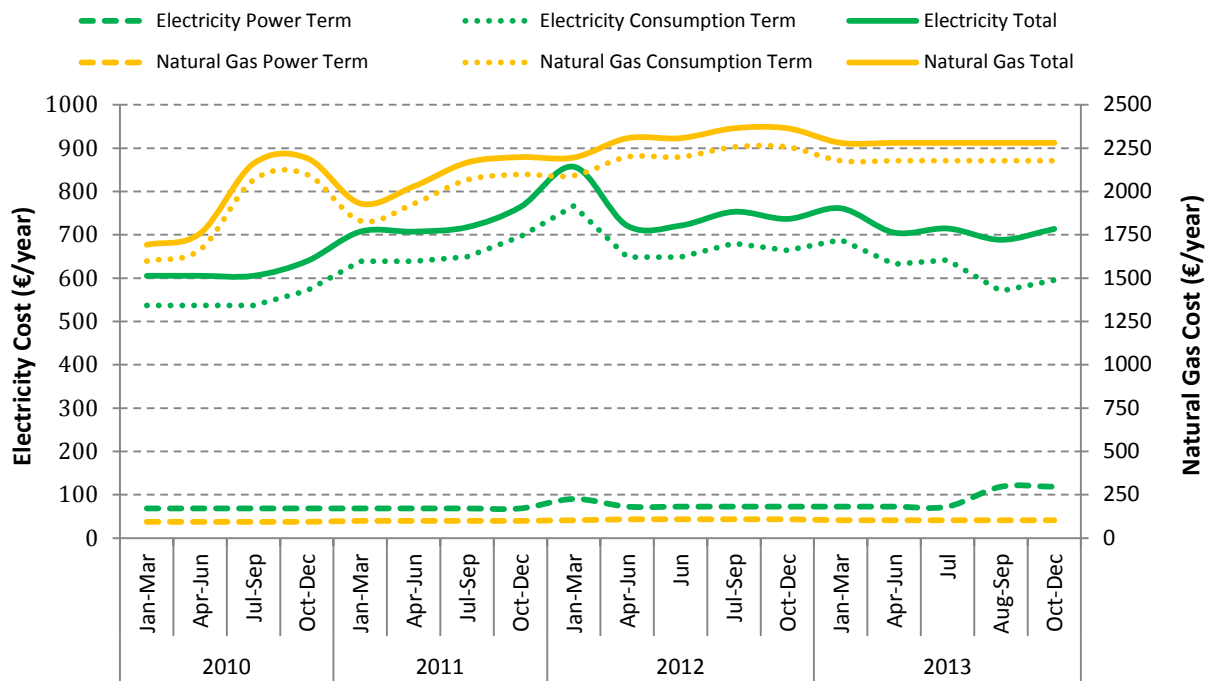


Figure 4.15 – Evolution of natural gas and electricity prices in Spain applied to the reference scenario.

When comparing results obtained in Spain with those achievable under the Germany and United Kingdom economic framework, with and without considering the incentives existing in those countries, a vast difference is detected. Seven cases were considered in order to perform the comparative analysis, as presented in Figure 4.16. The letters correspond to the code of each country (ES: Spain, DE: Germany, UK: United Kingdom), while numbers 1 and 2 indicate if there is not any incentive or if complements are considered, respectively. In the case of Spain, while ES1 does not include any complement, ES2.1 and ES2.2 make reference to previous (RD 661/2007) and current (RD 413/2014) incentives, respectively.
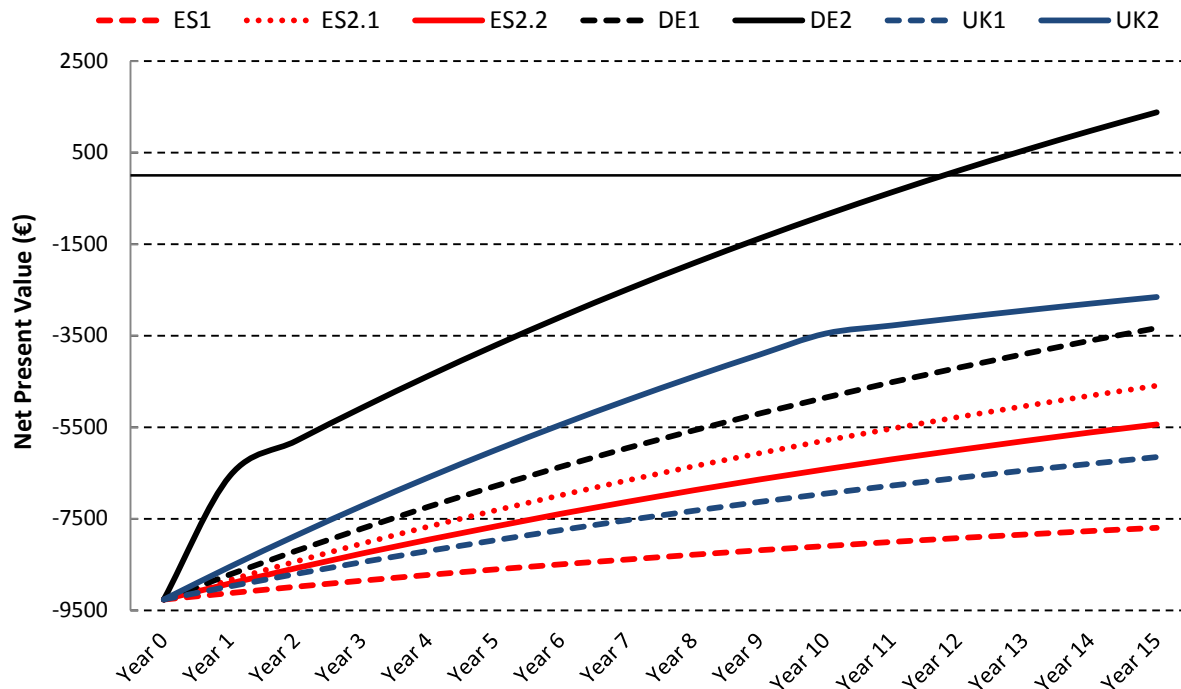
Figure 4.16 – NPV in the end of the lifetime of the micro-CHP plant for different cases.

Under the German framework, results achieved when the considered lifetime of the plant is completed, even neglecting economic incentives (DE1), net present value is smoothly above that obtained in Spain when applying previous economic bonuses (ES2.1). This fact is partially explained with the electricity-to-natural gas price ratio. In Spain, this value has decreased from 3.16 to 2.46 in the last 4 years, while it is 5.09 for Germany. Thus, when generating a kWh of electricity for self-consumption, economic savings got in Germany are twice those achieved in Spain. Meanwhile, after the 15th year of operation, while payback is not even reached with any Spanish regulation, NPV under the current German framework (DE2) shows profits of almost 1500 € out of an initial extra investment of slightly more than 9000 €, resulting in an absolute NPV difference with respect to the RD 413/2014 case (ES2.2) slightly higher than 6800 €. Consequently, aside from the mentioned ratio, it is obvious that support mechanisms in Germany, even not considering bonus but only the investment subsidy, are broadly more effective than those which have ever existed in Spain. For this case (DE2), a payback period of 11.8 years is achieved, which is considered to be a reasonable value for such investment to get attractive when analysed not only taking into consideration economic aspects but also environmental.

On the other hand, taking a look at the results obtained with the conditions in force in the United Kingdom, the effectiveness of the support mechanisms applicable can be highlighted. While no payback is possible without considering any incentive (UK1), nearly achieving a 34 % recovery of the initial investment after 15 years, a 71 % recovery percentage is obtained under the current legislation (UK2), with a final NPV of -2656 €. Comparing the ratio relating electricity and natural gas prices for the UK with that obtained for Germany, a large difference is also observed, being the British value 1.8 times lower. Considering this difference and that the relation of the final NPV of cases DE2 and UK2, it can be concluded that economic support in force in the UK also rewards suitably benefits provided by micro-CHP.

When comparing results obtained under the conditions of the UK and those existing in Spain under both the RD 661/2007 previously and the RD 413/2014 currently, it can be observed that applying the prices and incentives in force in the UK allows a final money recovery with respect to the initial investment around 21% higher than the value for the conditions established in the aforementioned revoked Spanish Royal Decree. This fact allows reaching a final NPV under the UK framework almost 2800 € higher than the one currently in Spain. Since the electricity-to-natural gas price ratio for both countries is similar, this difference on the final economic indicators can be attributed exclusively to the effectiveness of the support mechanisms adopted in each country.

All these results show that there is still a long way to go in the regulation matter in Spain. Analysing how current incentives work, two main aspects, related to each other, can be highlighted. On the one hand, the incentive to operation is not applied to the whole electricity generated by the micro-CHP but to that amount which is sold. Considering this bonus for all the electricity produced, the pay-back period would be reached after 41 years, that is, after a period of 2.7 times the lifetime of the plant. On the other hand, retribution related to the investment of the device is calculated with relation to a much lower amount to that necessary to acquire the Stirling unit. This is partially due to the high cost of this small-scale technology, which may decrease with improvements in the regulation framework which could make feasibility possible and so turn into a major introduction of this technology. However, it is also noteworthy that using a linear relationship between the nominal power and the initial cost of the CHP for

a very large power range is not appropriate, as it is obvious that features of a 1 kW$_e$ and a 500 kW$_e$ CHP differ hugely. Furthermore, it must be remarked that these incentives are calculated and applicable taking a lifetime of 25 years as a reference, even though the typical useful life of this kind of installations is 15 years.

This way, an appropriate basis for the determination of the investment incentive, combined with the previously mentioned assumption of the operation retribution, could make feasibility possible, and so progressively boost other economic facts affecting profitability.

# 7. Conclusions

Residential micro-cogeneration systems in general, and those based on Stirling engines in particular, have lately emerged as efficient systems with great potential to provide economic, energy and environmental savings. However, there is need for further research to better characterize the behaviour of this technology, so that it can be progressively introduced in the market. In the case of Spain, where they are not commercially available, little research has been done in this issue. Thus, this chapter deals with a techno-economic assessment of the performance of this technology when implemented into a micro-CHP plant for satisfying heating, DHW and electric demands in a detached reference Spanish housing, analysing how different climatic conditions and regulations and economic frameworks influence viability of such devices.

Once thermal and electric profiles are calculated, performance data of two energy plants, constituting the reference and the Stirling micro-cogeneration scenarios, are obtained from dynamic simulations. From these simulations, an economic analysis is carried out, taking into account present economic conditions and regulatory framework.

It is concluded that there is no possible economic viability for any of the three representative climatic zones. Additionally, it is also observed that implanting this technology for covering DHW and heating demands in warm climates is not worth either from the economic or operational and environmental points of view, while for the case of Madrid, although both PES and PESR values and environmental results are good

enough, running-hours are quite low, so an increase in the number of hours with demand would be necessary to increase the number of hours of operation.

On the other hand, a sensibility analysis is carried out, varying electricity and natural gas prices, the investment cost of the Stirling engine, and the rate of discount. Results reflect that improvements in the conditions of both electricity and natural gas prices and the rate of discount themselves do not represent a sufficient amelioration in the economic results, even for the most optimistic cases considered. However, decreasing the price of the µCHP device to a reasonable amount, which could be achieved by a major introduction of this equipment in the global market, allows the plant to be feasible for the coldest climatic zone.

Following the techno-economic methodology described, the economic analysis is extended taking both the previous and the current regulations for cogeneration in Spain. Likewise, results achievable with the regulatory frameworks existing in Germany and the UK are also calculated, and the influence of their support mechanisms is also analysed.

It is concluded that, even though technical results achieved confirm the benefits micro-CHP and in particular the Stirling technology can offer, the current situation for cogeneration in Spain is still untenable. Being the initial investment quite elevated, the money recovery is extremely low when the lifetime of the plant is passed by - not much better than when omitting incentives -, nearly achieving pay-back with the previous regulatory framework. This confirms that there is much to improve in regulation matters in Spain for this efficient technology to get competitive and thus get the benefits it provides.

On the other hand, comparison between results obtained for Spain and those achievable in Germany and United Kingdom show that feed-in tariffs and support policies in force in these latter countries allow obtaining attractive payback periods in some cases, getting improvements in relation to the no-incentive cases more than twice than in the case of Spain.

It is important to highlight that, although nowadays there is no possible economic viability in Stirling micro-cogeneration installations for new and retrofitted single-family dwellings in Spain, feasibility in medium-term could be reached in cold climatic zones by regulating the electricity market and the cogeneration policies and by spreading out the use of this equipment for manufacturing costs to get cheaper. In case of older homes with no possibility of thermal retrofitting, with worse envelopes that turn into higher thermal demands, reaching viability could be considerably more achievable.

Finally, it must be remarked that besides the unfavourable framework lately approved in Spain, one of the main drawbacks for installing micro-CHP devices lies in the uncertainty existing on the regulation and prices related to the field of cogeneration and renewable energies, which result detrimental when attempting to invest on this technology. Thus, taking into account the obvious potential this technology can offer for reaching the energy challenges existing, and the weight regulation has on its feasibility itself and in other parameters directly related to feasibility, some steps forward should be taken for promoting such efficient units, which, evidently, bring numerous benefits.

# CHAPTER 5

## CONCLUSIONS AND CLOSING REMARKS

# 1. Introduction

In this chapter the main conclusions and contributions of this PhD Thesis to the Stirling engine-based residential micro-CHP technology research are summarized. Additionally, future research lines and further works are also identified, together with the means to proceed with them. All this is accompanied by the scientific plan, that is, the list of publications related to the work carried out throughout the development of the thesis, some of which are currently available and others under preparation.

# 2. Contributions

The main objective of this PhD Thesis was to develop a full procedure for the energy, environmental and economic evaluation of residential micro-CHP Stirling engines with the aim of analyzing its potential in the Spanish household sector and so contribute to improving its acceptation and participation in the energy transition. According to that objective, the goals reached within this thesis are summarized next.

## 2.1. Modelling of a Stirling engine-based micro-CHP unit

In Chapter 2 **a dynamic model of a Stirling** engine-based **micro-CHP unit has been developed** (**O1.2**), taking into consideration the engine itself and the auxiliary burner which is normally integrated within the same casing by boilers manufacturers. Due to its

potential application in dynamic energy simulation environments, a **grex-box empirical modelling** approach was selected as the best cost-effective option. The model **contemplates** all the possible modes presented by the engine during its operation: standby, warm-up, normal operation – both full load and **part load operation** – and shut-down. Equations for all operation modes have been developed, presenting, each of them, their specific equations for determining fuel, thermal and electric exchanges. This model is consistent with the energy conservation equations of the three control volumes proposed for determining the transient response of the engine and, consequently, allows estimating its dynamic thermal and electricity output.

Additionally, fulfilling another objective of the thesis (**O2.2**), **a pilot experimental installation** where forthcoming energy generation technologies for buildings can be tested **has been developed**. The test facility has been **modular**ly **design**ed so that individual technologies can be characterized by fixing different preset working conditions and, additionally, these technologies can be integrated with others so giving raise to hybrid installations where, together with the possibility of communicating this plant with energy simulation tools, **the plant can be submitted to work under realistic conditions** of any building.

This chapter also possesses an important experimental component, since an exhaustive experimental routine was followed in order to **characterize the performance of** the Remeha eVita **Stirling engine-based natural gas-run combi-boiler** (**O1.3**). These tests, carried out under different cooling water conditions, have been divided into steady-state tests, considering different load rates, cold and hot warm-up tests, depending on whether the device was in thermal equilibrium with the air contained within the room where the device was installed, as well as shut-down tests. Except for the exhaustiveness in the warm-up process, the same routine has been followed for characterizing **both the prime and the auxiliary movers**. This experimental part also includes an **uncertainty analysis** in order to identify the main uncertainty sources and determine how uncertainty is propagated in indirect measurements.

**The model** has been programmed in Fortran language and by means of Intel Visual Fortran and Microsoft Visual Studio it **has been implemented** as a self-tailored Type 159

in the **TRNSYS Simulation Studio** Libraries, as pretended in **O1.4**. This Type, prior to its utilization, was calibrated and validated. The calibration was carried out following three different procedures, finally choosing that based on an optimization process with genetic algorithms. Calibration results were the result of reducing the simultaneous error between data predicted by the model and those measured in three different data-sets collected in the laboratory. Once calibrated, **the model was validated by comparison with an experimental** full **test** which contemplated the real functioning of the engine, both considering the transient warm-up and shut-down phases as well as full and part load operation. Additionally**, the model was** also **compared to** the previously **validated** Annex 42 **model**.

## 2.2. Analysis of TES integration within micro-CHP plants

In Chapter 3 **a methodology for analysing** the importance of the correct **sizing and design of a micro-CHP** residential installation **and** the vital role **TES** plays on it has been presented (**O2.3**). Different arrangements and TES sizes have been assessed and, by means of transient simulations utilizing the previously developed model to a representative case study, they have been analysed using diverse criteria and the design of the plant has been optimised. The case study is based on a reference dwelling, representative of the kind of building where micro-CHP can be suitable for meeting its energy needs.

The **energy performance** has been evaluated with the primary energy savings achieved in each case with respect to the separate production of heat and electricity, the overall efficiency of the whole installation, as well as the its **environmental impact**. Additionally, focusing on preserving the integrity of the generator, the number of on-off cycles and hours of operation of the engine are taken into consideration. Finally, the performance of the Stirling engine is not only assessed, but the **performance of** the **TES** itself **is** also **analysed, in terms of energy and exergy**, so that the effectiveness of the charge and discharge processes can be maximised.

On the other hand, the **analysis** has been complemented with **the economic yield** each solution provides, evaluated in terms of NPV at the end of the lifetime of the micro-CHP

unit. This analysis has been applied to a case study previously defined, with a micro-CHP properly size for its integration in the considered dwelling.

Chapter 3 has been finally completed through a **heuristic analysis of the influence of the TES size** on both the performances of the tank itself and the SE and the global functioning of the plant, so that its size can be optimised. Results extracted from this sensibility analysis containing operational as well as energy, exergy and economic indicators, show that **TES systems** coupled with small-scale micro-CHP engines **are traditionally oversized**, which allow slightly incrementing the number of hours of operation of the generation unit at the expense of an important worsening of the economic viability. For accumulation-volume intervals suitable for installations in single family dwellings, it is observed that, even if the series arrangement allows obtaining slightly better technical results, parallel arrangement of the TES requires slightly lower accumulation values and leads to better results from a multi-objective point of view.

## 2.3. Techno-economic evaluation of micro-CHP plants

In Chapter 4, based on outcomes of previous chapters, **a** complete **methodology for assessing the technical, environmental and economic performances** of Stirling engine-based units in particular, and micro-CHP units in general, has been introduced (**O1.1**). On it, key aspects such as climatic conditions or proper sizing of the main generator have not been overlooked.

The **techno-economic feasibility** of the micro-CHP installation has been assessed **with respect to** a reference scenario constituted by **a conventional installation**. Once the design of the installation has been previously optimized in Chapter 3, the **criteria** taken into consideration **for designing and optimizing** the **reference installation,** constituted by a condensing wall-mounted boiler and solar thermal support, have been exposed.

**Economic results are put down to hypothetical variations** in the main economic parameters, so constituting the sensibility analysis through which the **long-term performance** of the installation can be kept in mind.

Additionally, in relationship with objective **O2.4**, Chapter 4 also deepens on analyzing

how normative and economic frameworks influence the economic profitability of micro-CHP installations in general and those based on Stirling engines in particular, due to the higher cost they normally have. For this purpose, **the evolution of normative conditions** regulating micro-CHP **in Spain has been overviewed** and translated to economic terms by means of a case study. These economic results have been **compared to** those achievable in **countries pioneering** introduction of **micro-CHP** in residential applications. In short, the reality of the micro-CHP and renewable energies in Spain has been deeply analysed and the main obstacles to overcome have been discussed.

# 3. Conclusions

Conclusions of the thesis have been partially presented along each chapter which constitutes this thesis. For that reason, in this section the main conclusions are summarized and the most significant are only highlighted.

Related to the modelling and experimental characterization of a Stirling engine-based micro-CHP unit, the following is concluded:

- The model is only adapted to gas-fired applications.
- Tests for three water flow levels and return temperatures from 30 to 70 °C have been carried out and hence the validity of the model is limited to these values.
- Uncertainty associated to the fuel input can distort the energy performance of the micro-CHP unit and, ultimately, predictions made by the model developed.
- Special care must be taken when selecting initial values when optimization techniques are used when calibrating these sorts of models, since local optimums can be obtained as a solution instead of global ones.
- The model has been validated by comparison with experimental results of a unique Stirling engine, but also by comparison with an already validated model.

With respect to the TES integration in a micro-CHP plant, both considering its sizing and configuration, conclusions obtained are summarized next:

- In small micro-CHP installations it is preferable to directly produce DHW instead of using a tank, as no significant improvement is achieved but efficiency deterioration.

- The layout of the distribution loop has an importance on the final performance of the plant that must be kept in mind.

- TES systems coupled with small-scale micro-CHP engines are traditionally oversized, which allow slightly incrementing the number of hours of operation of the generation unit at the expense of an important worsening of the economic viability.

- For accumulation-volume intervals suitable for installations in single family dwellings, it is observed that, optimum size of the tank when installed in parallel provides better results form a multi-objective point of view and requires slightly lower accumulation values, while if operational constraints are prioritised series arrangement should be chosen.

Finally, concerning the techno-economic profitability of Stirling engine-based micro-CHP units in Spain, the following conclusions were achieved:

- Technical results achieved confirm the benefits micro-CHP and in particular the Stirling technology can offer.

- Under current conditions, i.e. normative conditions and prices of energetic and economic resources, there is no possible economic viability for any climatic zone in Spain.

- Implanting this technology for covering DHW and heating demands in warm climates is not worth either economically or technically, i.e. from operational and environmental points.

- Improvements in the conditions of both electricity and natural gas prices and the rate of discount themselves do not represent a sufficient amelioration in economic results.

- Decreasing the initial cost of the µCHP device to a reasonable amount, which could be achieved by a major introduction of this equipment in the global market, could make the plant feasible for the coldest climatic zones.

- Current situation for cogeneration in Spain is untenable and, as expected, there is much to improve in regulation matters in Spain for this efficient technology to get competitive.

- Comparison between results obtained for Spain and those achievable in other countries show that feed-in tariffs and support policies in force in these other countries allow obtaining very attractive payback periods.

- It has been ascertained that one of the main drawbacks for installing micro-CHP devices lies in the uncertainty existing on the regulation and prices related to the field of cogeneration and renewable energies, which result detrimental when attempting to invest on this technology.

# 4. Scientific production

Even though some results of this research have been already published, the diffusion of the results is still in process at the time of writing these lines. The main relevant contributions to the dissemination of the results are subsequently listed, some of which are not explicitly part of the work presented in this thesis but are somehow related to it.

## 4.1. International Journals

- J. Terés-Zubiaga, A. Campos-Celador, I. González-Pino, G. Diarce, The role of the design and operation of individual heating systems for the energy retrofits of residential buildings, *Energy Conversion and Management*, 126 (2016) 736-747.
- I. González-Pino, E. Pérez-Iribarren, A. Campos-Celador, J. Las-Heras-Casas, J.M. Sala, Influence of the regulation framework on the feasibility of a Stirling engine-based residential micro-CHP installation, *Energy*, 84 (2015) 575-588.
- I. González-Pino, A. Campos-Celador, E. Pérez-Iribarren, J. Terés-Zubiaga, J.M. Sala, Parametric study of the operational and economic feasibility of Stirling micro-cogeneration devices in Spain, *Applied Thermal Engineering*, 71 (2014) 821-829.

## 4.2. International Conferences

- Ana Picallo Perez, José Mª Sala Lizarraga, Estíbaliz Perez Iribarren, Iker González Pino, Jesús las Heras Casas. "Testing and analysis of the results of a condensing boiler and solar collectors hybrid installation for heating and DHW." *VI European Conference on Energy Efficiency and Sustainability in Architecture and Planning.* San Sebastian, 2015.

- Álvaro Campos-Celador, Iker González-Pino, Tatyana Bandos, Luis María López-González. "Simulation of a latent heat thermal storage system within a Stirling based microCHP residential installation." *16th International Stirling Engine Conference*. Bilbao, 2014.

- I. González-Pino, A. Campos-Celador, E. Pérez-Iribarren, J. Terés-Zubiaga, J.M. Sala. "Parametric study of the operational and economic feasibility of Stirling microcogeneration devices in Spain." *The 3rd International Conference on Microgeneration and Related Technologies*. Naples, 2013.

- E. Pérez-Iribarren, I. González-Pino, A. Campos-Celador, J.M. Sala. "Economic optimal selection between solar thermal and cogeneration for covering domestic hot water demand in a residential building in Spain." *The 3rd International Conference on Microgeneration and Related Technologies*. Naples, 2013.

- Iker González Pino, Álvaro Campos Celador, Estíbaliz Pérez Iribarren, Edorta Carrascal Lecumberri, José María Sala Lizarraga. "Experimental test-bench for energy conversion technologies in buildings." *III European Conference on Energy Efficiency and Sustainability in Architecture and Planning*. San Sebastian, 2012.

## 4.3. National Conferences

- A. Picallo-Pérez, E. Pérez-Iribarren, I. González-Pino, A. Campos-Celador, J.M. Sala, J. Las-Heras-Casas, L.M. López-González. "Planta experimental para ensayos de instalaciones térmicas híbridas." *Foroclima Jornadas Técnicas*. Madrid, 2015.

- Iker González Pino, Estibaliz Pérez Iribarren, Alvaro Campos Celador, Víctor de la Peña Aranguren, José María Sala Lizarraga. "Modelado de un motor Stirling para microcogeneración y validación a partir de datos experimentales." *VIII Congreso Nacional de Ingeniería Termodinámica*. Burgos, 2013.

- Estíbaliz Pérez Iribarren, Zaloa Azkorra Larrinaga, Jon Terés Zubiaga, Iker González Pino, Luis Alfonso Del Portillo Valdés. "Análisis comparativo de las tecnologías solar térmica y microcogeneración aplicadas a la producción de agua caliente sanitaria en edificios residenciales." *VIII Congreso Nacional de Ingeniería Termodinámica*. Burgos, 2013.

## 4.4. Other contributions

- Edorta Carrascal Lecumberri, Izaskun Garrido Hernández, Iker González Pino, José María Sala Lizarraga. "Pilot plant control of heating systems using NI LabVIEW and NI CompactRIO." National Instruments Case Study, 2012.

# 5. Future research lines

Even though this PhD Thesis finishes here, the research work is still in progress. Different directions have been identified to carry on with it.

Firstly, related to the modelling of the Stirling engine, during the process of development of the model presented in Chapter 2, it was detected that modelling some heat transfer processes taking into consideration a deeper analysis of the combustion gases instead of using equivalent UA values could turn into more precise predictions, while maintaining the simplicity of the model.

In order to face this new modelling approach, new experimental data-sets should be obtained. These data sets should include more intensive data acquisition at low water return temperatures where condensing of the flue gases occur and at high water temperatures where an internal control limits the fuel input, as well as wider surface measurements in order to better characterize heat losses through the casing of the device. Furthermore, in order to reduce uncertainty associated to measurements and so improve their quality, more precise information about the fuel composition, pressure and temperature results indispensable.

Additionally, it would result interesting to be able to validate the model for other micro-CHP Stirling units, and face the validation by comparison with models previously validated by other authors.

Likewise, in a near future, the model is to be completed with the inclusion of the internal pump this kind of engine is normally provided with and the control that governs the functioning of the additional burner. This way, together with another future research which consists of using optimization algorithms which enable optimizing the operation

of the device when integrated within an energy plant, a comparison of both controls can be assessed, and so determine the mode of operation that maximises the benefits this technology can provide.

In relation with Chapter 3, where the influence of TES sizing and arrangement within a micro-CHP plant was analysed, in order to take a step forward, optimization algorithms, such as GenOpt, in order to, once optimised the sizing and arrangement of the TES, the global operation of the plant can be improved taking into consideration energy, environmental and/or economic criteria. The scope of this objective could be expanded to physical installations in real buildings with the help of the semi-virtual platform developed within the experimental installation of the LCCE and model calibration methods, as already proposed in the coordinated project entitled "Implementación de técnicas de calibración y optimización multiobjetivo automatizados aplicado a simulación de modelos energéticos en edificios monitorizados energéticamente", funded by the "Ministerio de Economía y Competitividad" of the Spanish Government.

Additionally, in the context of the Enedi Research Group, where LHTES solutions are also investigated, solutions based on Stirling engine micro-CHP devices and LHTES for detached, semi-detached and multifamily dwellings are presented as a future research.

On the other hand, due to energy and environmental challenges to face during the forthcoming years, it could be interesting to use the techno-economic methodology presented in Chapter 4 in order to compare other alternatives, such as internal combustion engine-based micro-CHP units, heat pumps, or biomass fuelled boilers or Stirling engines of similar thermal power ranges and, analogously, compare these new solutions to those based in conventional sources. Furthermore, in order to improve mid and long-term predictions, it seems to be indispensable to deepen in analysing the evolution of the regulation framework, prices and other factors which have been identified to be of vital transcendence on the profitability of this technology and hence on the role it can play in the energy transition.

Finally, it could also be interesting to develop a methodology which allows analysing all the facts contained within Chapters 3 and 4 of this thesis without having the necessity to define and model a specific building but in function of a set of variables representative of

the climatic conditions and the physics of the buildings where the studied device is to be implemented.

# APPENDICES

# Appendix A. Model parameters

In this annex the main parameters, inputs and outputs of the model developed in Chapter 2 are listed.

Table A.1 (a) – Main parameters of the proposed model.

| Number | Parameter | Description | Units |
|--------|-----------|-------------|-------|
| 1 | $T_{cw,o}^{max}$ | Maximum cooling water outlet temperature | °C |
| 2 | $T_{cw,o}^{sp}$ | Cooling water set-point temperature | °C |
| 3 | $\Delta T$ | On-off temperature hysteresis | °C |
| 4 | $[MC]_{head}$ | Thermal mass of the head control volume | J/K |
| 5 | $[MC]_{eng}$ | Thermal mass of the engine control volume | J/K |
| 6 | $[MC]_{HX}$ | Thermal mass of the heat exchanger control volume | J/K |
| 7 | $[UA]_{eng,normal}$ | Effective heat transfer coefficient of the engine during warm-up and normal operation | W/K |
| 8 | $[UA]_{eng,shutdown}$ | Effective heat transfer coefficient of the engine during shut-down | W/K |
| 9 | $[UA]_{eng,standby}$ | Effective heat transfer coefficient of the engine during stand-by | W/K |
| 10 | $[UA]_{HX,normal}$ | Effective heat recovery coefficient during warm-up and normal operation | W/K |
| 11 | $[UA]_{HX,shutdown}$ | Effective heat recovery coefficient during shut-down | W/K |
| 12 | $[UA]_{HX,standby}$ | Effective heat recovery coefficient during stand-by | W/K |
| 13 | $[UA]_{loss,normal}^{se}$ | Effective heat loss coefficient during warm-up and normal operation | W/K |
| 14 | $[UA]_{loss,shutdown}^{se}$ | Effective heat loss coefficient during shut-down | W/K |
| 15 | $[UA]_{loss,standby}^{se}$ | Effective heat loss coefficient during stand-by | W/K |
| 16 | $[UA]_{loss}^{ab}$ | Effective heat loss coefficient of the auxiliary burner | W/K |
| 17 | $T_{head,nom}^{start}$ | Head nominal temperature for fuel overshooting during warm-up | °C |
| 18 | $T_{stop}^{e}$ | Head temperature at which electricity production gives up during shut-down | °C |
| 19 | $T_{stop}^{q}$ | Head temperature at which the shut-down period ends | °C |
| 20 | $T_{eng,nom}$ | Engine nominal temperature | °C |
| 21 | $k_f$ | Sensitivity of the fuel power to the head temperature | - |
| 22 | $k_{f,max}$ | Fuel overshooting factor during warm-up | - |
| 23 | $k_{e,1}$ | Sensitivity of the net electric power to the engine temperature during warm-up 1 | - |
| 24 | $k_{e,2}$ | Sensitivity of the net electric power to the engine temperature during warm-up 2 | - |
| 25 | $k_{e,3}$ | Sensitivity of the gross electric power to the head temperature during shut-down | - |
| 26 | $\dot{E}_{standby}$ | Electric power consumed in stand-by mode | W |

### Table A.1 (b) – Main parameters of the proposed model.

| Number | Parameter | Description | Units |
|---|---|---|---|
| 26 | $\alpha_{t,min}^{ab}$ | Minimum firing rate of the auxiliary burner | - |
| 27 | $T_{cw,i}^{ref}$ | Reference inlet cooling water temperature | °C |
| 28 | $\dot{m}_{cw}^{ref}$ | Reference cooling water mass flow rate | kg/s |
| 29 | $\eta_{e,ref}^{se}$ | Reference fuel power | W |
| 30 | $\eta_{comb}^{ref}$ | Combustion efficiency reference value | - |
| 31 | $\dot{E}_{net}^{ref}$ | Net electric power reference value | W |
| 32 | $a_1^{se}$ | Sensitivity factor of the maximum heat output to the cooling water inlet temperature | - |
| 33 | $b_1^{se}$ | Sensitivity factor of the power input to the cooling water inlet temperature | - |
| 34 | $b_2^{se}$ | Sensitivity factor of the power to the cooling water flow rate | - |
| 35 | $c_1^{se}$ | Sensitivity factor of the combustion efficiency to the cooling water inlet temperature | - |
| 36 | $c_2^{se}$ | Sensitivity factor of the combustion efficiency to the cooling water flow rate | - |
| 37 | $d^{se}$ | Coefficient of the firing rate correlation | - |
| 38 | $e_1^{se}$ | Sensitivity factor of the net electric power to the head temperature | - |
| 39 | $e_2^{se}$ | Sensitivity factor of the net electric power to the cooling water inlet temperature | - |
| 40 | $c_1^{ab}$ | Sensitivity factor of the combustion efficiency to the cooling water inlet temperature | - |
| 41 | $c_2^{ab}$ | Sensitivity factor of the combustion efficiency to the cooling water flow rate | - |
| 42 | $d_1^{ab}$ | Sensitivity factor of the thermal efficiency to the cooling water inlet temperature | - |
| 43 | $d_2^{ab}$ | Sensitivity factor of the thermal efficiency to the cooling water flow rate | - |
| 44 | $e^{ab}$ | Coefficient of the firing rate correlation | - |
| 45 | $LHV_f^{\circ}$ | Fuel lower heating value | kWh/Nm³ |
| 46 | $\rho_0$ | Fuel relative density | - |
| 47 | $y_{N_2}$ | Volumetric content of nitrogen | % |
| 48 | $y_{CO_2}$ | Volumetric content of carbon dioxide | % |
| 49 | $y_{CH_4}$ | Volumetric content of methane | % |
| 50 | $y_{C_2H_6}$ | Volumetric content of ethane | % |
| 51 | $y_{C_3H_8}$ | Volumetric content of propane | % |
| 52 | $y_{iC_4H_{10}}$ | Volumetric content of isobutane | % |
| 53 | $y_{nC_4H_{10}}$ | Volumetric content of n-butane | % |
| 54 | $y_{iC_5H_{12}}$ | Volumetric content of isopentane | % |
| 55 | $y_{nC_5H_{12}}$ | Volumetric content of n-pentane | % |
| 56 | $y_{C_6H_{14}}$ | Volumetric content of hexane | % |

Table A.2 – Inputs of the proposed model.

| Number | Variable name | Description | Units |
|:------:|:-------------:|-------------|:-----:|
| 1 | $State$ | Control signal | - |
| 2 | $T_{cw,i}$ | Cooling water inlet temperature | °C |
| 3 | $\dot{m}_{cw}$ | Cooling water mass flow rate | kg/h |
| 4 | $T_{air}$ | Boiler-room temperature | °C |

Table A.3 – Outputs of the proposed model.

| Number | Variable name | Description | Units |
|:------:|:-------------:|-------------|:-----:|
| 1 | $T_{head}$ | Temperature of the head control volume | °C |
| 2 | $T_{eng}$ | Temperature of the engine control volume | °C |
| 3 | $T_{cw,o}^{se}$ | Outlet temperature of the cooling water for the SE | °C |
| 4 | $T_{cw,o}^{ab}$ | Outlet temperature of the cooling water for the AB | °C |
| 5 | $\dot{F}^{se}$ | Fuel power input of the SE | W |
| 6 | $\dot{E}_{net}$ | Net electrical power output of the SE | W |
| 7 | $\dot{Q}_{net}^{se}$ | Net heat power output of the SE | W |
| 8 | $\dot{F}^{se}$ | Fuel power input of the AB | W |
| 9 | $\dot{Q}_{net}^{ab}$ | Net heat power output of the AB | W |
| 10 | $\dot{V}_f$ | Fuel volumetric flow | m³/h |
| 11 | $LHV_f^{\circ}$ | Lower heating value of the fuel | kWh/Nm³ |

# Appendix B. Technical data of the Remeha eVita micro-CHP boiler

In this annex manufacturer-provided technical information of the Remeha eVita micro-CHP boiler modelled and tested in Chapter 2 and used in subsequent chapters is presented, distributed from Table A.4 to Table A.9.

Table A.4 – General data of the Remeha eVita.

| Boiler type | eVita | | 25s | 28c |
|---|---|---|---|---|
| Flow rate setting | | | Modulating | |
| Nominal output (Pn) Heating System (80 / 60 °C) | minimum – maximum Factory setting | kW | 3.7 – 24.9 24.9 | 3.7 – 24.9 24.9 |
| Nominal output (Pn) Heating System (50 / 30 °C) | minimum – maximum Factory setting | kW | 4.1 – 27.4 27.4 | 4.1 – 27.4 27.4 |
| Nominal output (Pn) DHW System | minimum – maximum Factory setting | kW | - - | 6.1 – 27.4 27.4 |
| Nominal input (Qn) Heating System (Hi) | minimum – maximum Factory setting | kW | 3.8 – 25.5 25.5 | 3.8 – 25.5 25.5 |
| Nominal input (Qn) Heating System (Hs) | minimum – maximum Factory setting | kW | 4.2 – 28.3 28.3 | 4.2 – 28.3 28.3 |
| Nominal input (Qnw) Heating System (Hi) | minimum – maximum Factory setting | kW | - - | 6.5 – 29.2 29.2 |
| Nominal input (Qnw) Heating System (Hs) | minimum – maximum Factory setting | kW | - - | 7.2 – 32.4 32.4 |
| Maximum boiler input (Qnw) DHW System (Hi) | maximum | kW | - | 35.0 |
| Maximum boiler input (Qn) Heating System (Hi) | maximum | kW | 25.5 | - |
| Heating efficiency under full load (Hi) (80 / 60 °C) | - | % | 97.7 | |
| Heating efficiency under full load (Hi) (50 / 30 °C) | - | % | 107.4 | |
| HRe efficiency (high efficiency electricity) | - | % | 139.9 | |

Table A.5 – Data on the gases and combustion gases.

| Boiler type | eVita | | | 25s | 28c |
|---|---|---|---|---|---|
| Gas categories | | - | | $I_{2L}$ , $I_{2H}$ | |
| Gas inlet pressure G20 (Gas H) | minimum – maximum | mbar | | 17 – 30 | |
| Gas consumption G20 (Gas H) | minimum – maximum | m³/h | | 0.4 – 2.7 | 0.4 – 3.7 |
| $NO_x$ emission per year (n=1) | | ppm | | 19 | |
| | | mg/kWh | | 33 | |
| CO emission per year (n=1) | | ppm | | 31 | |
| | | mg/kWh | | 33 | |
| Mass flue gas flow rate | minimum – maximum | kg/h | | 9 – 43 | 9 – 59 |
| Flue gas temperature | minimum – maximum | °C | | 35 – 65 | 35 – 70 |
| Maximum counter pressure | | Pa | | 115 | |

Table A.6 – Data on the characteristics of the heating circuit.

| Boiler type | eVita | | 25s | 28c |
|---|---|---|---|---|
| Water content | | l | 3.6 | |
| Water operating pressure | minimum | bar | 0.8 | |
| Water operating pressure (PMS) | maximum | bar | 3.0 | |
| Water temperature | maximum | °C | 110 | |
| Operating temperature | maximum | °C | 85 | |
| | Factory setting | | 80 | |
| Manometric height central heating circuit (ΔT = 20 K) | | mbar | 150 | |

Table A.7 – Data on the characteristics of the domestic hot water circuit.

| Boiler type | eVita | | 25s | 28c |
|---|---|---|---|---|
| Specific hot water flow (60 °C) | | l/min | - | 7.5 |
| Specific hot water flow (40 °C) | | l/min | - | 12 |
| Domestic water resistance | | mbar | - | 715 |
| Flow rate threshold | minimum | l/min | - | 1.2 |
| Water content | | l | - | 0.3 |
| Operating pressure (Pmw) | maximum | bar | - | 8 |
| Annual operational efficiency for domestic water | | % | - | 80 |

Table A.8 – Data on the electrical characteristics.

| Boiler type | eVita | | | 25s | 28c |
|---|---|---|---|---|---|
| Power supply voltage | | $V_{AC}$ | | 230 | |
| Power consumption Full Load | maximum | W | | 165 | 175 |
| Power consumption Part Load | maximum | W | | 95 | |
| Power consumption Standby | maximum | W | | 16 | |
| Delivered power **Pe** [1] | maximum | kW | | 1.0 | |
| Electricity / heating ratio | Full load | | | 0.175 | |
| | Part load | | | 0.168 | |
| Electrical protection index | | IP | | X4D | |

[1] Return temperature 60 °C. For a 1 °C thermal increase in return temperature above 60 °C, Pe falls by approximately 20 W.

Table A.9 – Other characteristics.

| Boiler type | eVita | | 25s | 28c |
|---|---|---|---|---|
| Dimensions | Height | | 913.5 | |
| | Width | mm | 493 | |
| | Depth | | 472 | |
| Weight (empty) | | kg | 133.5 | 135.5 |
| Acoustic level at 1 meter | | dB (A) | 46 ($\pm$ 2 dBA) | 175 |
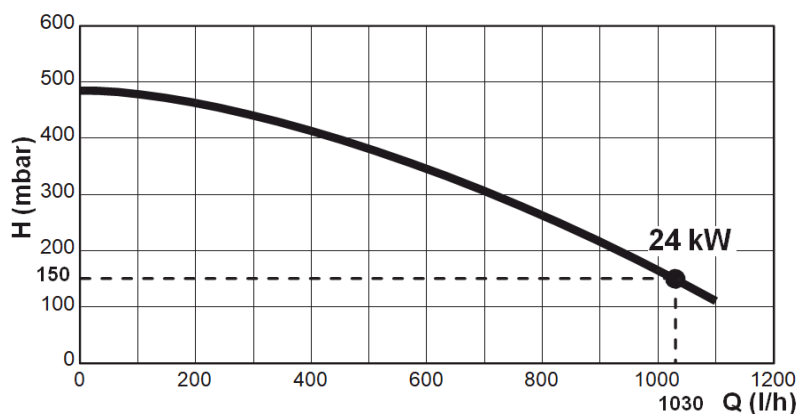


Figure A.1 – Characteristic curve of the internal pump.

Additionally, the boiler is fitted with a 3 level Grundfos UPR 15-60 type internal pump, whose characteristic curve is presented in Figure A.1 (where H is the manometric height of the heating circuit and Q is the water flow). In central heating mode, the controller regulates the flow at an appropriate level by automatically switching between the 3

pumping levels disposed. Meanwhile, in domestic hot water mode (only available in 28c model) the controller ensures that the pump turns at the highest speed.

# Appendix C. Description of the experimental plant

In this annex the full experimental installation developed within the context of this PhD Thesis is presented. As mentioned in Chapter 2, the experimental facility is sited at the Laboratory for the Quality Control in Buildings (LCCE) of the Basque Government (Departamento de Medio Ambiente, Planificación Territorial y Vivienda, 2018).

## 1. Background

In 2005, a collaboration agreement for developing the Thermal Area of the LCCE was signed between the so-called Office of Housing and Social Affairs of the Basque Government and the University of the Basque Country. Within the scope of this agreement, an experimental micro-CHP test-bench has been set up, in order to test forthcoming energy conversion technologies for buildings, so that valuable information to be used by the companies in this field can be obtained. In short, this test-bench allows acquiring performance data of various systems working under different operating strategies, which will enable assessing the most efficient technologies, their integration, as well as the working modes that reduce the energy consumption.

## 2. Main goals of the test bench

The LCCE experimental test-bench was designed in order to achieve the following goals:

- Evaluation tests of different operation modes.

- Calibration tests for developed energy systems models.

- Certification tests of the energy performance of different systems.

The test bench is designed for the evaluation of systems in the small-scale range of powers, up to 10 $kW_e$ and 25 $kW_t$.

# 3. Description of the installation

## 3.1. Main components of the installation

The energy conversion technologies considered and included in the experimental plant are basically grouped into the following modules, as depicted in Figure A.2:

A) High temperature production module

B) Low temperature production module

C) Distribution module

D) Thermal storage module

E) Consumption module

F) Solar thermal energy module

G) Electrical storage module

H) Acquisition and control system
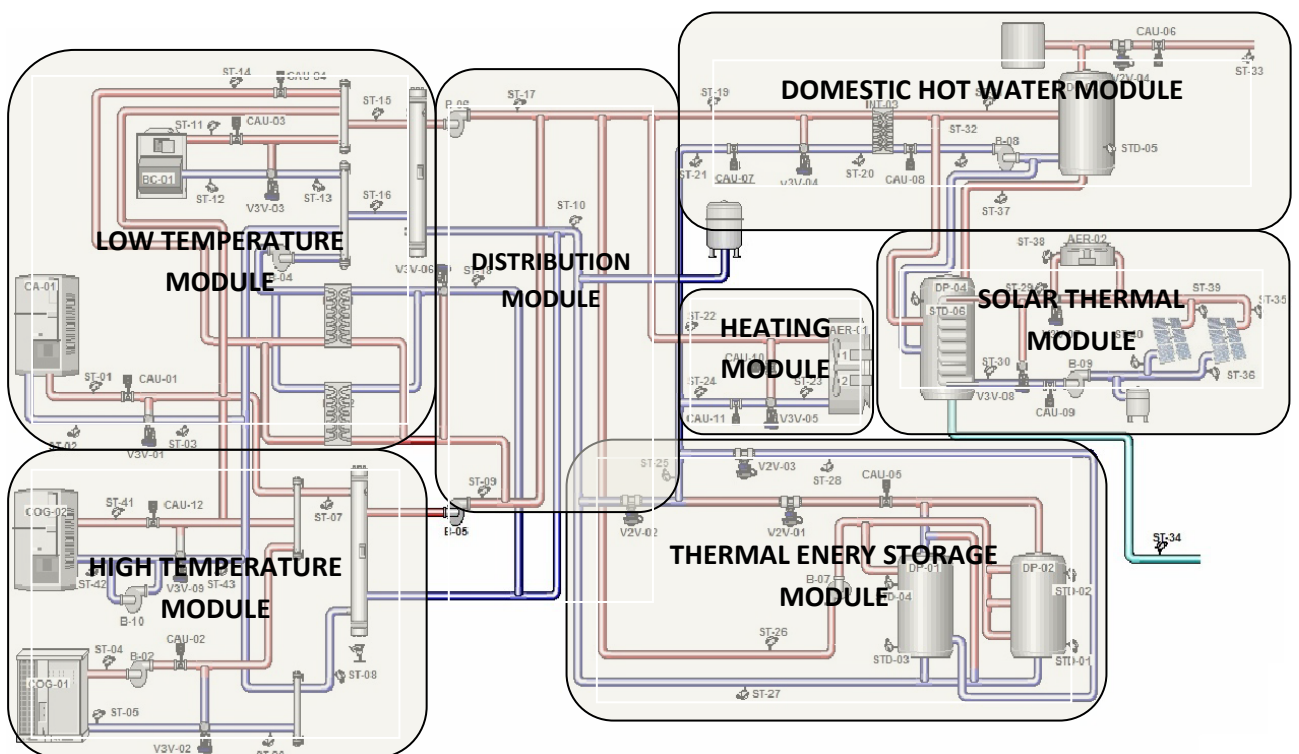


Figure A.2– Simplified diagram of the modular experimental test-bench of the LCCE.

The modular structure of the test-rig leaves the door open to expanding the installation in a simple manner, so that emerging technologies can get progressively included.

A) High Temperature Production Module

The high temperature production module encompasses those technologies working at temperatures up to 85 °C. Thus, apart from the Stirling engine-based micro-cogeneration unit described in Chapter 2, it comprises another reciprocating engine-based micro-CHP system, based on an internal combustion engine (ICE), and a conventional wall-mounted condensing boiler (Figure A.3).

_Conventional boiler_

The conventional boiler consists of a BaxiRoca BIOS 24/28F condensing boiler, which can work at both high and low temperatures. Its nominal thermal power outputs are 24 kW when working at high temperature, and 26 kW when operating at low temperature, with thermal efficiencies in the order of 97 and 107% respectively.



Figure A.3 – Wall-mounted condensing boiler (left) and ICE-based micro-CHP unit (right).

*Internal combustion engine based micro-cogeneration unit*

The ICE based micro-CHP unit is a Dachs module by Baxi Senertec. This is a mini-combined heat and power supplier for electricity, heating and DHW, capable of producing 5.5 $kW_e$ gross electrical output and 12.5 $kW_t$ heat output.

Specifically, the system consists of the Dachs CHP unit itself and a condensing kit for recovering the latent heat of the exhaust gases when the returning temperature is low enough. It also has a water cooled asynchronous generator, a heat exchanger for the exhaust gas pipe, and a complete electronic regulation system which ensures a proper performance of the unit.

The overall efficiency of the system reaches 90%, being able to achieve up to 98% through condensation of the exhaust gases, increasing this way the thermal output in 2.5 kW.

B) Low Temperature Production Module

This module is suitable for those generation devices with outlet temperatures of 40-50 °C, such as heat pumps or condensing devices. Accordingly, it is mainly composed of a heat pump, even though, as mentioned before, both the conventional boiler and the Stirling micro-CHP unit, as condensing units they are, can operate at low temperature as well. The hydraulic design also provides the possibility of working with the conventional and the micro-CHP boilers through two heat exchangers arranged in parallel.

There are two air-to-water heat pumps (see Figure A.4). The Txaey-117-P1 by Sedical, is a multipurpose ecological system, with air condensation and fan coils. The thermal power output working under normal operating conditions (outlet temperature equal to 45 °C) is 17.9 kW, and presents a COP of 2.95.

On the other hand, the Vaillant aroTHERM VWL 55/2 A presents a nominal heat output of 4.4 kW and a COP of 4.7 when working with radiant floor at 35 °C with an outdoor temperature of 7 °C.

Figure A.4– Air-to-water heat pumps: Sedical Txaey (left) and Vaillant aroTHERM (right).

C) Distribution Module

The distribution module, as shown in Figure A.5, is made of the drive pumps corresponding to the high temperature (B-05[1]) and the low temperature (B-06) modules. Furthermore, there are two plate heat exchangers that allow heat exchanges between the high and the low temperature modules, so enabling degrading heat (INT-01/INT-02 + B-04).



Figure A.5 – Core of the distribution loop.

[1] Nomenclature according to the SCADA and the hydraulic principle diagram presented in Figure A.11 and Figure A.13, respectively.

D) Thermal Storage Module

The test-bench's thermal storage module consists of three inertial storage tanks: a 200 litres tank by Vaillant, and two 1000 litres Lapesa G-1000-l inertial storage tanks. These latter are made of carbon steel, with a 950 millimetres diameter and 2.25 metres height.

Additionally, a latent heat thermal energy storage (LHTES) prototype, developed by Campos-Celador (2012) and Diarce (2017) is also disposed, as shown in Figure A.6.



Figure A.6 – Thermal Storage Module: hot water tanks (left) and LHTES (right).

E) Consumption Module

The consumption module emulates the different thermal consumptions. It comprises the systems associated to the DHW and the heating production (Figure A.7).

For this purpose, a 1000 litres Lapesa CV-1000-RB storage tank (and another inter-accumulator tank associated with the Solar Thermal Energy Module), made of vitrified steel, with the same dimensions as the inertial tanks, and a convective heat release system were installed, respectively, so that both demands can be simulated.

The heating module is composed of a three-way valve and a Sedical-Rhoss Yardi HP 5R250 and 2 pipe system fan-coil unit, with a nominal maximum thermal output of 24.9

kW when a 50 °C inlet temperature, and 42.8 kW when flow water temperature goes up to 70 °C. This system can operate at three different rates of velocity.
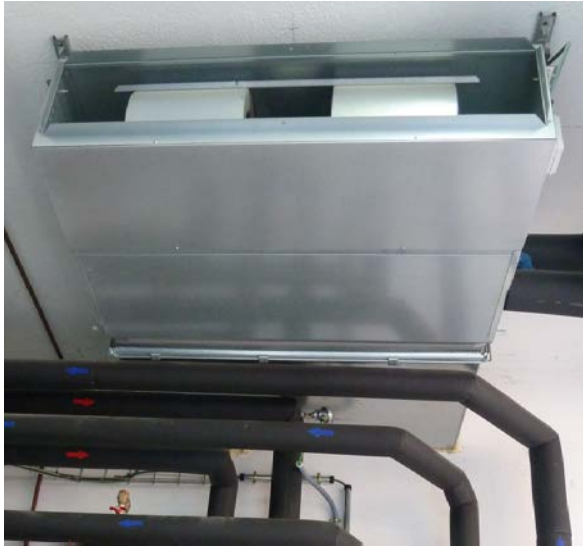


Figure A.7 – Consumption module.

F) Solar Thermal Energy Module

The solar thermal energy module, shown in Figure A.8, consists of two sets of two serial connected panels each, a heat sink and an inter-accumulator tank.



Figure A.8 – Solar Thermal Energy Module.

Both sets of panels are connected in parallel with each other, also providing the possibility of connecting them in series in order to get a single set of four serial connected panels.

The heat rejection system, a Roca UL-210 one of up to 17 kW, is used to remove the heat surplus produced by the panels during a test, so that the requirements of testing standards can be fulfilled. In the same way, to be able to achieve the strict certainty in the solar panels' return temperature measurements required by the standards, a storage tank is used, in order to provide inertia to the circuit and help the return temperature stay constant. It is an enamelled accumulation tank, model Roca 500-E, with a 500 litres capacity, and equipped with a 2.8 kW electrical resistance.

G) Electrical Storage Module

The electrical storage module is composed of 18 Zigor 12LDA134 batteries, made of watertight lead, of 12 V and a 134 Ah rated capacity. This module allows the heat pump work with the electricity generated by the micro-CHP units, by storing the produced electricity instead of pouring it to the electrical mains of the LCCE.



Figure A.9 – Electrical Storage Module.

H) Control and data acquisition system

The test-bench comprises more than 120 signals, in order to control and monitor the desired variables, so that detailed information can be obtained, and the good functioning

of the plant is guaranteed. This way, 55 high precision Pt 100 1/10 temperature sensors have been installed (47 in pipes and 8 in storage tanks), as well as 11 Siemens SITRANS F M (MAG 3100 and 5100 W sensors and MAG 6000 transmitters) and 2 Magflux 7100 electromagnetic flow-meters with an uncertainty below 0.1%. Furthermore, there are ambient temperature, humidity and pressure sensors inside and outside the laboratory room, gas meters for measuring gas consumption in the boiler and CHP units, as well as electricity meters to account the electrical energy produced by cogenerations and the consumption of the heat pumps.
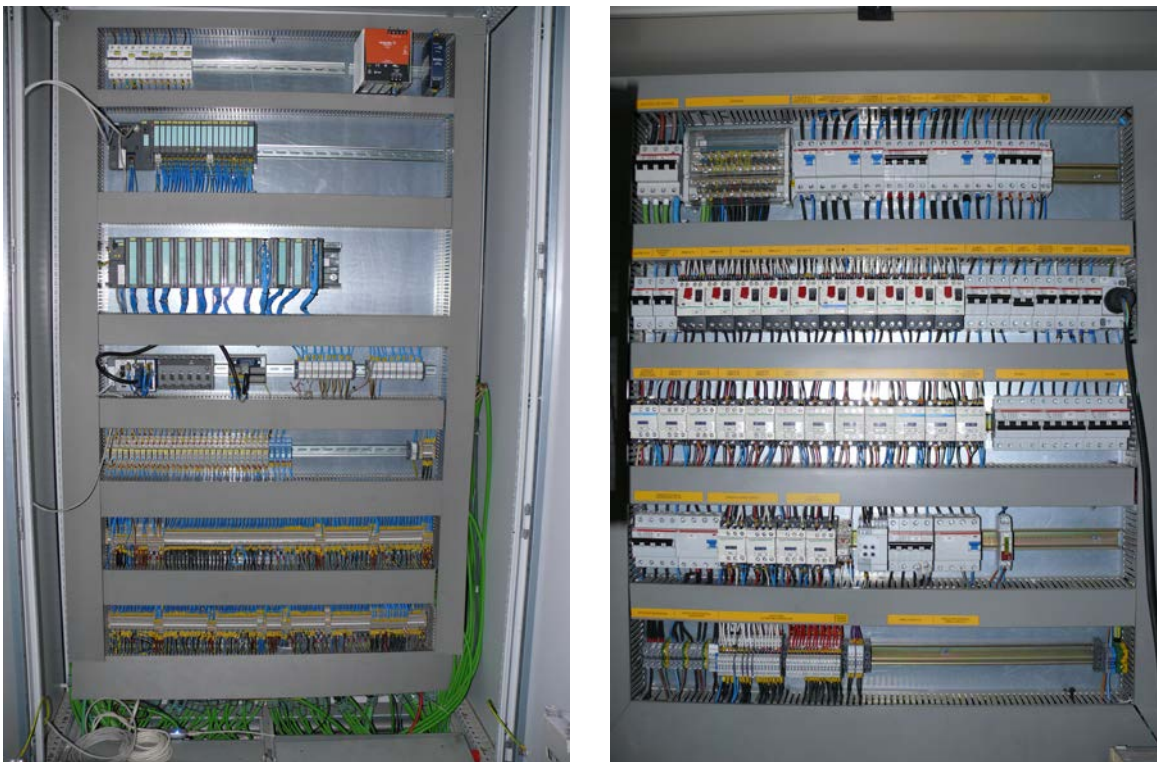


Figure A.10 – Control box (left) and distribution board (right).

The test-bench control is driven by a Siemens IM 151-8 PN/DP CPU programmable logic controller (PLC) and an expansion module, as well as the corresponding signals cards, connected via Ethernet to a personal computer with the interface the plant is operated through and where data is acquired. Additionally, by transferring signals gathered by the PLC through the NI OPC Server, the installation can also be controlled by means of LabVIEW and CompactRIO by National Instruments (NI).

Figure A.10 and Figure A.11 show the control box where both controllers are integrated and the supervisory control and data acquisition (SCADA) interface, respectively.
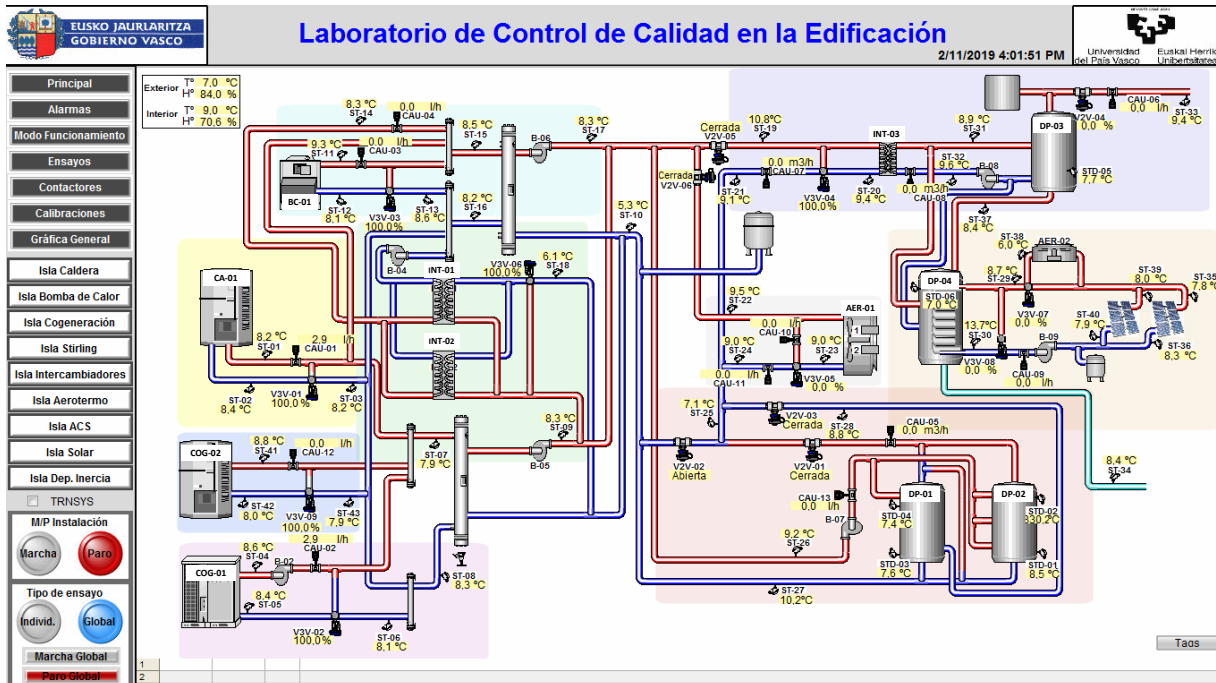


Figure A.11 – SIMATIC WinCC SCADA of the experimental plant.

## 3.2. General approach of the installation

The installation is constituted by several islands independently programmed, that do not recognize the existence of the other islands or the way they operate. For instance, the Stirling engine produces hot water at a certain temperature but is not aware if another device is working in parallel, its position within a cascade operation, where its hot water flows…

The concept of island responds to an ensemble of devices that are necessary to carry out some operation, i.e. a system that is made up of different elements that are put together following a series of premises, together with external boundary or variables that affect the operations that must be completed.

For example, the Stirling engine forms an island together with the pump, the three-way valve and the temperature and flow sensors, attached to the control loop and internal instructions of the device itself, as shown in the SCADA screenshot of Figure A.12.
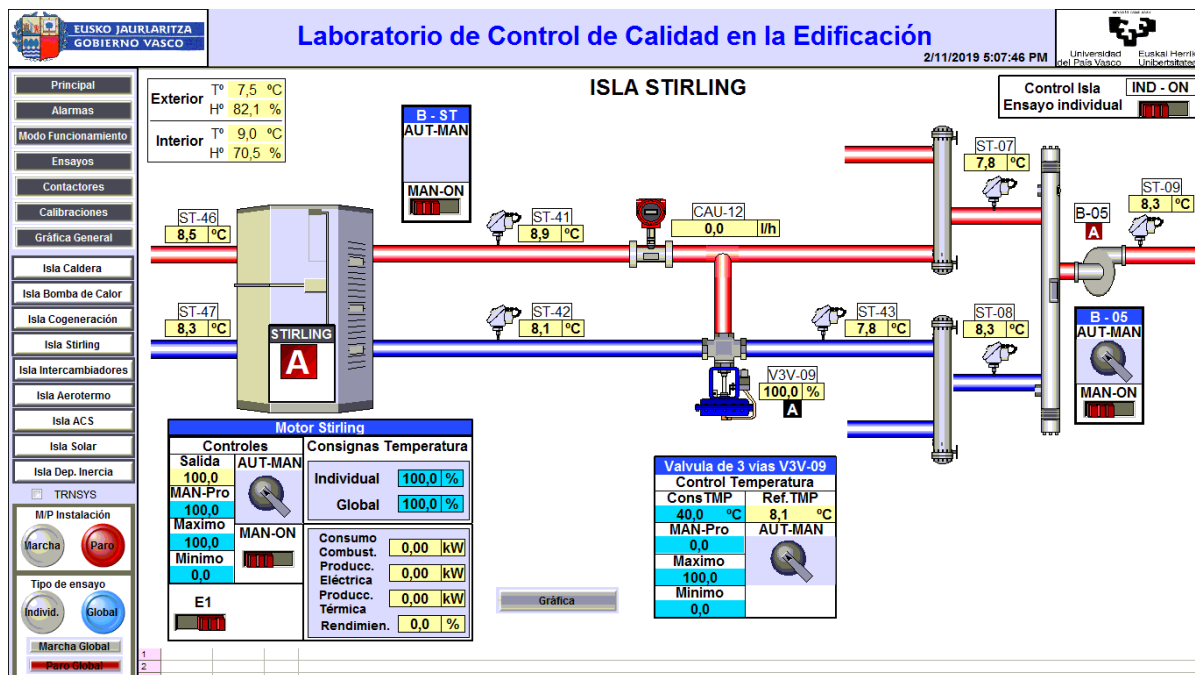
Figure A.12 – Island of the SE-based micro-CHP boiler.

The list of islands that make up the installation, named according to the main device contained, is the following:

- Wall-mounted natural gas-run condensing boiler (CA-01)
- ICE-based micro-CHP engine (COG-01 + B-02)
- SE-based micro-CHP boiler (COG-02 + B-03)
- Air-to-water heat pump (BC-01)
- High-to-low temperature plate heat exchangers (INT-01/INT-02 + B-04)
- Inertial storage system (DP-1/DP-02 + B-07)
- DHW generation and demand system (DP-03 + INT-03 + B-08)
- Heating demand system (AER-01)
- High temperature flow pump (B-05)
- Low temperature flow pump (B-06)
- Solar thermal system (Collectors + DP-04 + B-09 + AER-02)

In Figure A.13 the detailed hydraulic scheme of the whole experimental plant is presented.
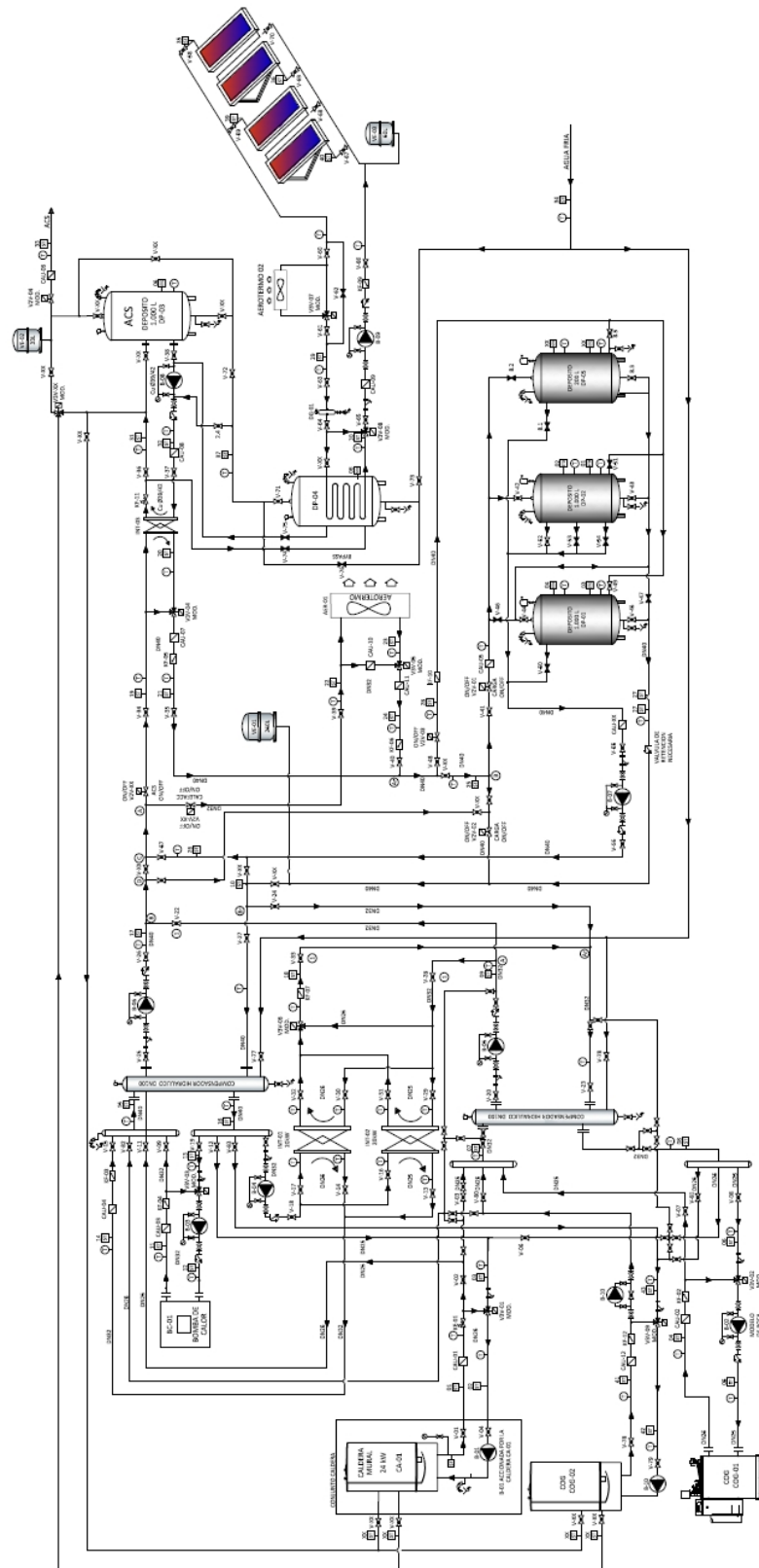
**Figure A.13 – Detailed hydraulic scheme of the experimental plant.**

# 4. Operating principle of the installation

One of the main goals of the test-bench is to evaluate the individual and collective performance of different energy production systems submitted to different working strategies, in order to evaluate the most efficient technologies, their integration, as well as the working modes that reduce the energy consumption.

Individual tests consist of making an energy production system work under some predefined conditions, and register the values of its main parameters, so that the system can be characterized. In this kind of tests, priority is to maintain the working conditions of the specific units, while rejecting the so produced heat. Meanwhile, in combined operating modes and strategies tests, operating strategies of the whole test-bench are defined, establishing priorities and working conditions for each module, both internally and in association with other systems.

One key aspect of the operation of the plant is to simulate thermal demands through the programmed operating philosophy. In each case, this is got for heating and DHW respectively by rejecting heat in the fan-coil and by an instantaneous flow of water flowing through the DHW tank or straightaway through the DHW heat exchanger.

For simulating virtual heating demands, hot water is provided to the heat rejection unit and, by activating the fan and the modulation, the heat quantity required is rejected. When tests are carried out for studying individual systems, the fan-coil unit rejects heat so that the return temperature stays constant. When combined performance strategies tests, two alternatives are available. First, using a previously defined discrete virtual power demand curve, which is continuously compared to energy data obtained with temperature sensors and flow-meters associated to the system. Secondly, by utilizing the semi-virtual platform, which enables a bidirectional real-time connection of the experimental plant with dynamic building simulation software where the dwelling whose demand is to be covered with such plant is implemented (see Figure A.14).

Meanwhile, the DHW module, whose performance is based on reading flow-rate values corresponding to a discretized demand curve, consists of an open cold and domestic hot water circuit which is composed of a flat plate heat exchanger responsible of avoiding mixture of the heat transfer fluid with the consumption water and a DHW tank, if required.
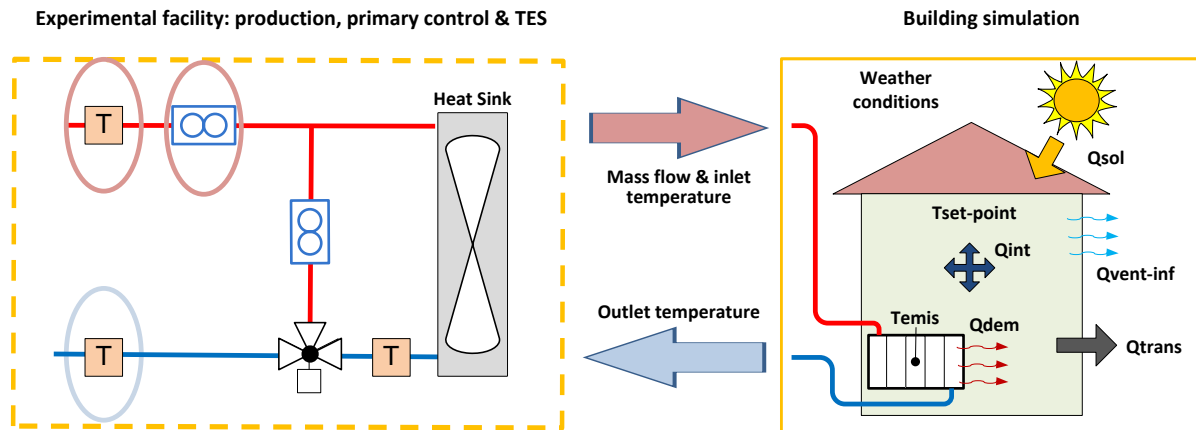


Figure A.14 – Simplified diagram of the principle of operation of the semi-virtual platform.

The charging and discharging of the inertial storage tanks is activated when indicated by the programmed operating philosophy. Generally, storage can be carried out both simultaneously with the heating and DHW demands, simply meeting the demand curves and circulating the return water of these systems through the tanks, and also by just storing the whole heat produced, when there is no demand. Discharge is activated when, simultaneously, the tank temperature is higher than a default value and the programmed scheduling enables discharging.

Another goal of the LCCE test-bench is to certify the energetic performance of individual systems, that is, their power outputs and efficiencies. To achieve this objective, the test conditions and methods have to be those required in the current standards, having installed the required instrumentation for this purpose.

# Appendix D. Definition of the reference dwelling

In this annex a representative detached dwelling is defined and, based on the main usage patterns and profiles commented, its TRNSYS model is developed and described. The model is employed along the PhD Thesis together with the models of the different thermal installations assessed.

## 1. TRNSYS modelling of the dwelling

The reference dwelling used in this PhD Thesis is a recently built two-floor single-family house (Figure A.15) sited in a rural area close to Vitoria-Gasteiz, the capital city of the Basque Country (Northern Spain). Thus, according to the climatic severity defined in the Section on Energy Demand Limitation of the HE Basic Document of the Spanish Technical Building Code (CTE, 2013a), which is explained in Section 3 of Chapter 4 of this PhD Thesis, the house is located in the D1 climatic zone, which is characterised by cold winters and warm summers.



Figure A.15 – Single family dwelling defined.

For modelling and simulating the reference detached house TRNSYS dynamic energy simulation tool was chosen. The building, as depicted in Figure A.16, was geometrically defined using Google Sketch Up through the utilization of the Trnsys3d plug-in available with the TRNSYS 17 version. The geometrical and construction data was provided by the architect who designed the dwelling.



Figure A.16 – Sketch of the building modelled.
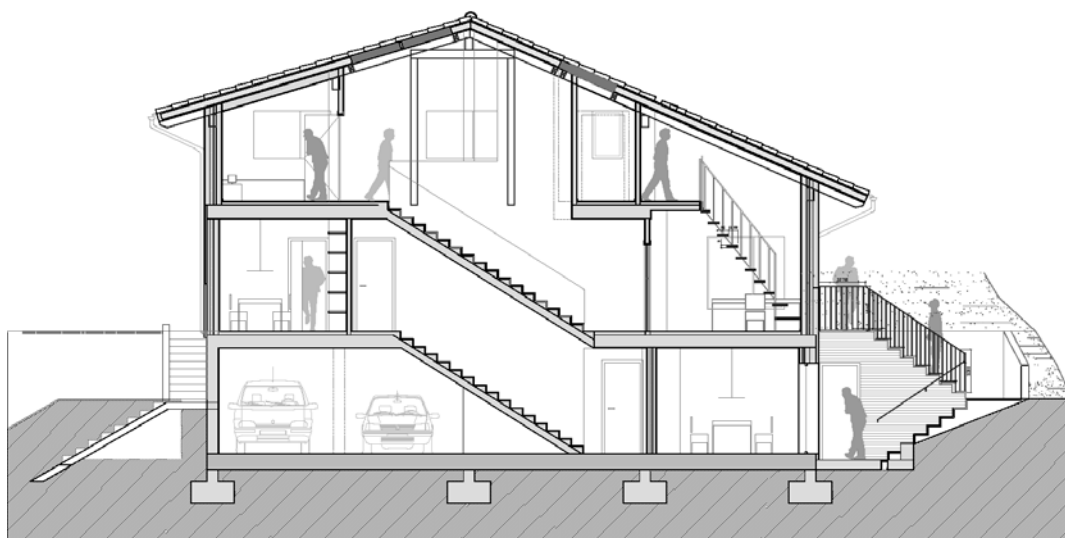


Figure A.17 – Type section of the dwelling.

## 1.1. Geometrical and construction data

The building, as shown in Figure A.17, is divided into 3 main floors: basement, ground floor and first floor. The net thermally conditioned area of the dwelling is 211.74 m².

When modelling, special care must be taken when defining each stage of the housing (University of Illinois, University of California, 2013). Thus, as detailed in Table A.10, each of the three floors was split into different thermal areas or air nodes (see Figure A.18). This zoning was carried out taking into consideration both thermal conditions and the zones' convexity requirement of TRNSYS 3d plug-in for Sketch Up.

Table A.10 – Correspondence and characteristics of simulation zones.

| Floor | | Zone | Net Area m² | Volume m³ |
|---|---|---|---|---|
| BASEMENT | 01 | Garage (Part 1) | 35.87 | 101.87 |
| | 02 | Garage (Part 2) | 10.31 | 22.29 |
| | 03 | Garage (Part 3) & Engine room | 44.30 | 125.81 |
| | 04 | Stairs | 4.92 | 14.43 |
| | 05 | Bathroom & Corridor | 7.77 | 22.07 |
| | 06 | Storehouse | 3.94 | 11.19 |
| | 07 | Dining room | 24.41 | 69.32 |
| | 08 | Warehouse | 6.23 | 17.69 |
| GROUND FLOOR | 09 | Living room | 42.02 | 126.90 |
| | 10 | Kitchen (Part 1) | 15.39 | 46.48 |
| | 11 | Kitchen (Part 2) | 5.39 | 16.28 |
| | 12 | Hall | 6.76 | 20.42 |
| | 13 | Stairs | 4.92 | 7.44 |
| | 14 | Bathroom & Corridor | 5.56 | 16.79 |
| | 15 | Studio | 14.55 | 68.02 |
| FIRST FLOOR | 16 | Bedroom No. 2 (Part 1) | 12.00 | 35.47 |
| | 17 | Bedroom No. 2 (Part 2) | 4.22 | 15.14 |
| | 18 | Bedroom No. 3 | 10.86 | 32.09 |
| | 19 | Bathroom No. 2 | 5.24 | 21.18 |
| | 20 | Corridor | 3.47 | 13.33 |
| | 21 | Living room | 19.43 | 74.61 |
| | 22 | Bedroom No. 1 (Part 1) | 17.09 | 58.11 |
| | 23 | Bedroom No. 1 (Part 2) | 2.46 | 7.26 |
| | 24 | Bathroom No. 1 | 5.28 | 15.58 |
| | 25 | Box room | 16.08 | 26.63 |
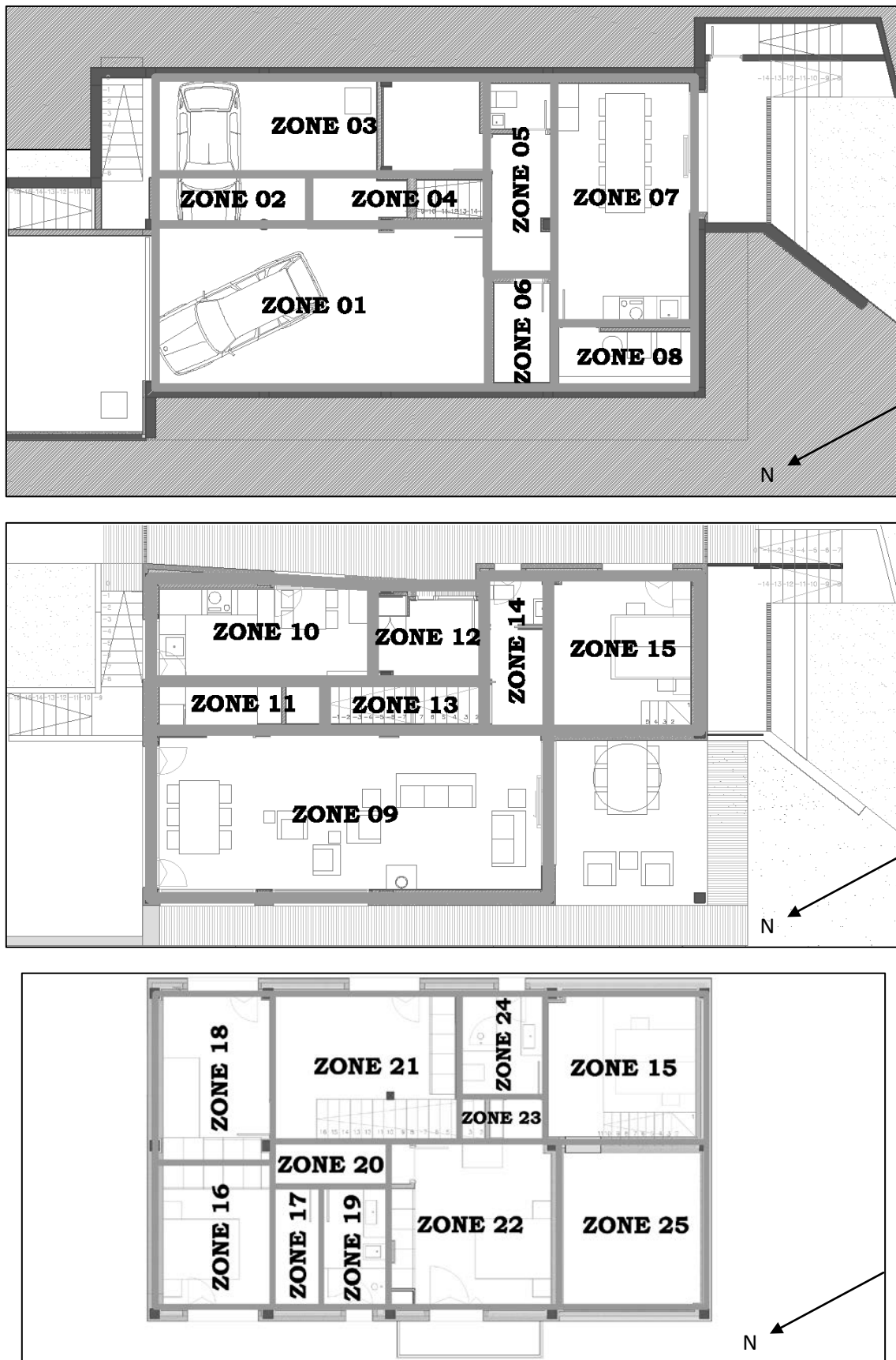
Figure A.18 – Plan of the dwelling an its zoning: basement, ground floor and first floor.

Concerning constructive characteristics, north-east and south-west façades of the basement are in contact with the ground, and so are defined in TRNSYS 3d. Physical properties of the building envelope components are presented in Table A.11. These elements, both internal and external, were defined for fulfilling their respective individual transmittance requirements established by the CTE in force at the moment of executing the project, valid for both new and refurbished buildings sited in the aforementioned climatic zone.

Table A.11 (a) – Thermal properties of constructive elements.
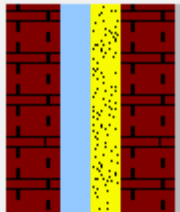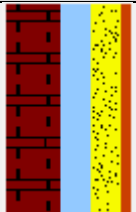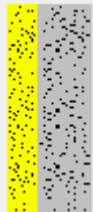
| Material | w (cm) | λ (W/m·K) | ρ (kg/m³) | C_p (J/kg·K) | R (m²·K/W) | U-value (W/m²·K) | Section |
|---|---|---|---|---|---|---|---|
| **FAÇADE: FIRST FLOOR** | | | | | | | |
| Gypsum plaster | 1.5 | 0.180 | 600 | 1000 | - | | |
| Double hollow brick | 9 | 0.490 | 1200 | 900 | - | | |
| Air chamber | - | - | - | - | 0.047 | 0.368 | |
| Projected polyurethane | 5 | 0.026 | 45 | 1800 | - | | |
| Double hollow brick | 9 | 0.490 | 1200 | 900 | - | | |
| Cement mortar | 1.5 | 1.400 | 2000 | 1100 | - | | |
| **FAÇADE: GROUND FLOOR AND EXTERNAL BASEMENT** | | | | | | | |
| Gypsum plaster | 1.5 | 0.180 | 600 | 1000 | - | | |
| Double hollow brick | 9 | 0.490 | 1200 | 900 | - | | |
| Air chamber | - | - | - | - | 0.047 | 0.396 | |
| Projected polyurethane | 5 | 0.026 | 45 | 1800 | - | | |
| Stone cladding | 2 | 2.800 | 2600 | 1100 | - | | |
| **FAÇADE: BASEMENT IN CONTACT WITH GROUND** | | | | | | | |
| Gypsum plaster | 1.5 | 0.180 | 600 | 1000 | - | | |
| Projected polyurethane | 5 | 0.026 | 45 | 1800 | - | 0.443 | |
| Concrete | 9 | 2.300 | 2300 | 1000 | - | | |

### Table A.11 (b) – Thermal properties of constructive elements.
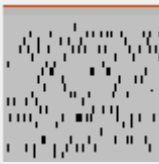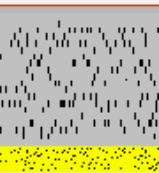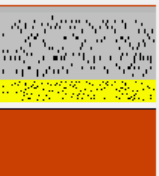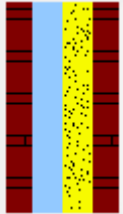
| Material | w (cm) | λ (W/m·K) | ρ (kg/m³) | $C_p$ (J/kg·K) | R (m²·K/W) | U-value (W/m²·K) | Section |
|---|---|---|---|---|---|---|---|
| **HORIZONTAL PARTITIONS BETWEEN THERMALLY CONDITIONED ZONES** | | | | | | | |
| Ceramic pavement | 0.5 | 1.050 | 2000 | 1200 | - | | |
| Screed mortar | 1.5 | 1.400 | 2000 | 1100 | - | 2.649 | |
| Reinforced concrete | 25 | 2.300 | 2300 | 1000 | - | | |
| Gypsum plaster | 1.5 | 0.180 | 600 | 1000 | - | | |
| **HORIZONTAL PARTITIONS BETWEEN CONDITIONED & NON CONDITIONED ZONES** | | | | | | | |
| Ceramic pavement | 0.5 | 1.050 | 2000 | 1200 | - | | |
| Screed mortar | 1.5 | 1.400 | 2000 | 1100 | - | | |
| Reinforced concrete | 25 | 2.300 | 2300 | 1000 | - | 0.436 | |
| Projected polyurethane | 5 | 0.026 | 45 | 1800 | - | | |
| Gypsum plaster | 1.5 | 0.180 | 600 | 1000 | - | | |
| **BASEMENT GROUND (HABITABLE)** | | | | | | | |
| Ceramic pavement | 0.5 | 1.050 | 2000 | 1200 | - | | |
| Screed mortar | 1.5 | 1.400 | 2000 | 1100 | - | | |
| Concrete slab | 15 | 2.300 | 2300 | 1000 | - | 0.423 | |
| Projected polyurethane | 5 | 0.026 | 45 | 1800 | - | | |
| Polyethylene sheet | 0.5 | 0.330 | 920 | 2200 | - | | |
| Crushed stone | 15 | 0.810 | 1700 | 900 | - | | |
| **BASEMENT GROUND (NON HABITABLE)** | | | | | | | |
| Screed mortar | 1.5 | 1.400 | 2000 | 1100 | - | | |
| Concrete slab | 15 | 2.300 | 2300 | 1000 | - | | |
| Projected polyurethane | 5 | 0.026 | 45 | 1800 | - | 0.424 | |
| Polyethylene sheet | 0.5 | 0.330 | 920 | 2200 | - | | |
| Crushed stone | 15 | 0.810 | 1700 | 900 | - | | |
| **ROOF** | | | | | | | |
| Beam | - | - | - | - | - | | |
| Fir terrace | 3 | 0.130 | 500 | 1600 | - | | |
| Rockwool | 12 | 0.030 | 50 | 1000 | - | | |
| Waterproof membrane | 0.7 | 0.17 | 1050 | 1000 | - | 0.218 | |
| Wooden double rails & counter rails | - | - | - | - | - | | |
| Roman tile | 0.5 | 1.000 | 2000 | 800 | - | | |

Table A.11 (c) – Thermal properties of constructive elements.

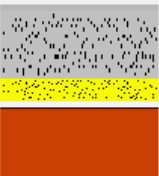| Material | w (cm) | λ (W/m·K) | ρ (kg/m³) | $C_p$ (J/kg·K) | R (m²·K/W) | U-value (W/m²·K) | Section |
|---|---|---|---|---|---|---|---|
| **VERTICAL PARTITIONS BETWEEN THERMALLY CONDITIONED ZONES** | | | | | | | |
| Gypsum plaster | 1.5 | 0.180 | 600 | 1000 | - | | |
| Hollow brick | 7 | 0.490 | 1200 | 900 | - | 2.085 | |
| Gypsum plaster | 1.5 | 0.180 | 600 | 1000 | - | | |
| **VERTICAL PARTITIONS BETWEEN CONDITIONED & NON CONDITIONED ZONES** | | | | | | | |
| Gypsum plaster | 1.5 | 0.180 | 600 | 1000 | - | | |
| Hollow brick | 4.5 | 0.490 | 1200 | 900 | - | | |
| Air chamber | - | - | - | - | 0.047 | | |
| Projected polyurethane | 5 | 0.026 | 45 | 1800 | - | 0.384 | |
| Hollow brick | 4.5 | 0.490 | 1200 | 900 | - | | |
| Gypsum plaster | 1.5 | 0.180 | 600 | 1000 | - | | |

Transmittance values of the different components of the envelope are summarized and compared to the reference values in Table A.12. Types 1, 2 and 3 specified in the façades stand for first floor, ground floor and external basement, and basement in contact with the ground, respectively.

Additionally, apart from the individual requirements, each type of enclosure must meet the global requirements. Thus, for the façade ensemble, the global transmittance value must be below 0.660 W/(m²·K), 0.570 W/(m²·K), 0.730 W/(m²·K), and 0.940 W/(m²·K) for D1, E1, C3 and A4 climatic zones, respectively, while the one obtained in reality is 0.402.

Table A.12 – Transmittances of constructive elements of the envelope and reference values.

| U-value [W/(m²·K)] | | Envelope component | | | | | |
|---|---|---|---|---|---|---|---|
| | | Façade type 1 | Façade type 2 | Façade type 3 | Roof | Ground basement | Windows |
| Real | | 0.368 | 0.396 | 0.443 | 0.218 | 0.423 | 1.240 |
| Limit | Zone D1 | 0.860 | 0.860 | 0.860 | 0.380 | 0.490 | 3.500 |
| | Zone E1 | 0.740 | 0.740 | 0.740 | 0.350 | 0.480 | 3.100 |
| | Zone C3 | 0.950 | 0.950 | 0.950 | 0.410 | 0.500 | 4.400 |
| | Zone A4 | 1.220 | 1.220 | 1.220 | 0.500 | 0.530 | 5.700 |

## 1.2. Operational conditions of the dwelling

In this section the operational conditions assumed for simulating the energy demand of the building are presented. These conditions – set-point temperature, ventilation and infiltration rates, internal gains, electricity and DHW demands – were defined according to existing bibliography, normative requirements and/or guides and recommendations.

## 1.2.1. Air infiltration and ventilation

Concerning to air infiltration due to sealing defects of envelope components, the Institute for Energy Diversification and Saving (IDAE) determines that it is equivalent to a constant value of 0.3 renovations per hour in habitable zones of single family dwellings, while it is assumed to be 1 for non-habitable spaces which are likely to have sealing defects in their envelopes (IDAE, 2009).

On the other hand, the necessary ventilation of the dwelling was calculated according to the requirements established in the Indoor Air Quality document of the CTE (2013c). Those reference values are summarized in Table A.13:

Table A.13 – Required minimum ventilation flows.

| | Minimum ventilation flow ($q_v$) in l/s | | |
| --- | --- | --- | --- |
| | Per person | Per net m² | Other parameters |
| Bedroom | 5 | - | - |
| Living & Dining rooms | 3 | - | - |
| Toilet & Bathroom | - | - | 15 per room |
| Kitchen | - | 2 | - |
| Store room | - | 0.7 | - |
| Garage | - | - | 120 per parking space |

The aforementioned minimum requirements lead to the following values for the reference detached dwelling, as shown in detail in Table A.14, with a global renovation value for the whole house of 1.84 renovations per hour, while for summertime, as a consequence of opening the windows, 4 renovations per hour must be considered from 1 to 8 a.m..

Table A.14 – Ventilation values of the reference dwelling according to the CTE.

| Floor | | Zone | VENTILATION | | |
| | | | CTE requirements | | ZHV |
| | | | l/s | m³/h | Vol/h |
|---|---|---|---|---|---|
| BASEMENT | 01 | Garage (Part 1) | 97.81 | 352.10 | 3.46 |
| | 02 | Garage (Part 2) | 21.40 | 77.04 | 3.46 |
| | 03 | Garage (Part 3) & Engine room | 120.79 | 434.85 | 3.46 |
| | 04 | Stairs | - | - | - |
| | 05 | Bathroom & Corridor | 15.00 | 54.00 | 2.45 |
| | 06 | Storehouse | 2.76 | 9.93 | 0.89 |
| | 07 | Dining room | 48.82 | 175.75 | 2.54 |
| | 08 | Warehouse | 4.36 | 15.70 | 0.89 |
| GROUND FLOOR | 09 | Living room | 12.00 | 43.20 | 0.34 |
| | 10 | Kitchen (Part 1) | 30.78 | 110.81 | 2.38 |
| | 11 | Kitchen (Part 2) | 10.78 | 38.81 | 2.38 |
| | 12 | Hall | - | - | - |
| | 13 | Stairs | - | - | - |
| | 14 | Bathroom & Corridor | 15.00 | 54.00 | 3.22 |
| | 15 | Studio | 12.00 | 43.20 | 0.64 |
| FIRST FLOOR | 16 | Bedroom No. 2 (Part 1) | 14.80 | 53.27 | 1.50 |
| | 17 | Bedroom No. 2 (Part 2) | 5.20 | 18.73 | 1.24 |
| | 18 | Bedroom No. 3 | 20.00 | 72.00 | 2.24 |
| | 19 | Bathroom No. 2 | 15.00 | 54.00 | 2.55 |
| | 20 | Corridor | - | - | - |
| | 21 | Living room | 12.00 | 43.20 | 0.58 |
| | 22 | Bedroom No. 1 (Part 1) | 17.48 | 62.94 | 1.08 |
| | 23 | Bedroom No. 1 (Part 2) | 2.52 | 9.06 | 1.25 |
| | 24 | Bathroom No. 1 | 15.00 | 54.00 | 3.47 |
| | 25 | Box room | 11.26 | 40.52 | 1.52 |

## 1.2.2.  Internal gains

Internal gains profiles for the simulated dwelling, which are split into three main categories – occupation, artificial lighting and appliances gains – , are based on the hourly schedules proposed by the CTE, as described in the present section. All these values are summarized in Table A.15.

### Occupation gains

Occupation gains are divided into sensible and latent gains, as shown in Table A.15. According to the IDAE, 40% of the sensible part of these occupational gains are

considered to be convective gains, while the remaining fraction is assigned to radiative gains. Latent gains are taken into account in terms of humidity gains (IDAE, 2009).

Table A.15 – Internal gains reference values according to the CTE.

| [W/m²] | Day-time period | | | | | | | |
|---|---|---|---|---|---|---|---|---|
| | 0-7 h | | 7-15 h | | 15-23 h | | 23-24 h | |
| **Occupation gains** | | | | | | | | |
| | Sensible | Latent | Sensible | Latent | Sensible | Latent | Sensible | Latent |
| Working day | 2.15 | 1.36 | 0.54 | 0.34 | 1.08 | 0.68 | 2.15 | 1.36 |
| Weekend | 2.15 | 1.36 | 2.15 | 1.36 | 2.15 | 1.36 | 2.15 | 1.36 |
| **Artificial lighting gains** | | | | | | | | |
| Daily | 0.44 | | 1.32 | | 1.32 | | 2.2 | |
| **Appliances gains** | | | | | | | | |
| Daily | 0.44 | | 1.32 | | 1.32 | | 2.2 | |

## *Artificial lighting gains*

In the case of gains due to artificial lighting, IDAE establishes that a fraction of 0.2 is related to convective gains.
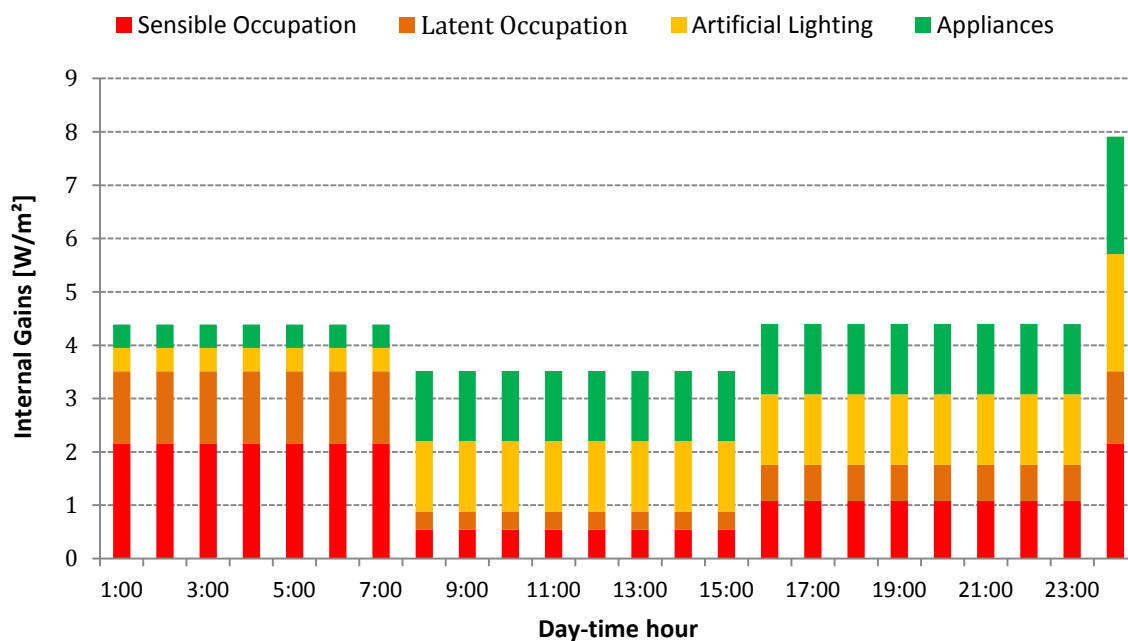


Figure A.19 – Working-day schedule for internal gains.

*Appliances gains*

Internal gains due to appliances in houses are to be reassigned according to the following fraction: 0.3 for convective gains and the remaining 0.7 for radiative gains.

Daily profiles of all these internal gains during working days are gathered and depicted in Figure A.19.

## Input for the TRNSYS Reference Model

For introducing all this information in TRNBuild, internal gains must be classified in three types of energy gains, calculated according to the fractions specified above: convective gains, radiative gains, and gains due to humidity absorption. These values per square meter surface are summarized in Table A.16.

Table A.16 – Total internal gains introduced in the TRNSYS model of the dwelling.

|  | Type of energy gain | 0-7 h | 8-15 h | 15-23 h | 23-24 h |
|---|---|---|---|---|---|
| | Convective (W/m²) | 0.32 | 0.95 | 0.95 | 1.58 |
| Work day | Radiative (W/m²) | 10.59 | 10.50 | 12.44 | 22.00 |
| | Humidity (kg/h·m²) | 0.002 | 0.0005 | 0.001 | 0.002 |
| | Convective (W/m²) | 0.32 | 0.95 | 0.95 | 1.58 |
| Weekend | Radiative (W/m²) | 10.59 | 16.29 | 16.29 | 22.00 |
| | Humidity (kg/h·m²) | 0.002 | 0.002 | 0.002 | 0.002 |

# 2. Thermal demand

## 2.1. Domestic hot water demand

Two criteria were taken into consideration when defining DHW consumption profiles. The first one, according to Spanish standards, consists of combining the requirements established in the CTE and the profiles published by IDAE.

According to the CTE, the daily demand at 60 °C in a single-family dwelling rises up to 112 litres per day (CTE, 2013b). In case the DHW supply temperature is different from 60 °C, the corresponding demand of water must be calculated as follows:

$$D(T) = D(60°C) \cdot \frac{60 - T_c}{T - T_c}$$

Equation A.1

where $D(T)$ is the DHW demand at the selected $T$ temperature, $D(60°C)$ is de DHW demand at 60 °C, and $T_c$ is the network cold water temperature, established by the CTE and reflected in Table A.17.

Table A.17 – Monthly average temperature of the network cold water.

| City | Water temperature (°C) | | | | | | | | | | | |
|---|---|---|---|---|---|---|---|---|---|---|---|---|
| | Jan | Feb | Mar | Apr | May | Jun | Jul | Aug | Sep | Oct | Nov | Dec |
| Vitoria-Gasteiz | 7 | 7 | 8 | 10 | 12 | 14 | 16 | 16 | 14 | 12 | 8 | 7 |

Thus, total yearly DHW demand, in terms of energy, reaches 2334.15 kWh. Daily demand is calculated afterwards taking into consideration hourly (Figure A.20) and monthly (Figure A.21) multiplication factors provided by IDAE (2011a).
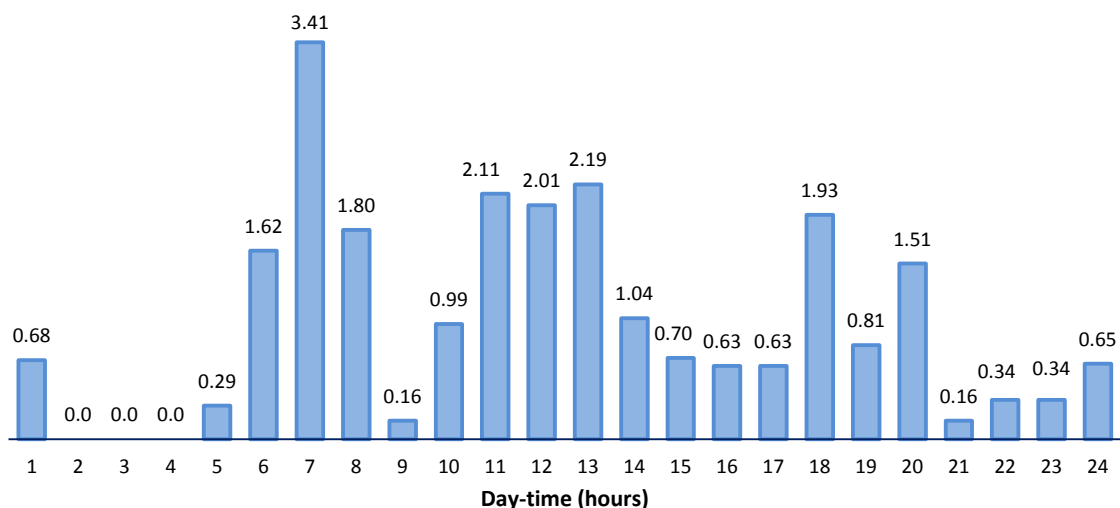


Figure A.20 – DHW hourly multiplication factors.

However, due to the instantaneous nature of the DHW consumption and the importance it has on the size of the thermal generator when no DHW accumulation is used, these latter profiles were modified in order to get distributions in lower time-steps.
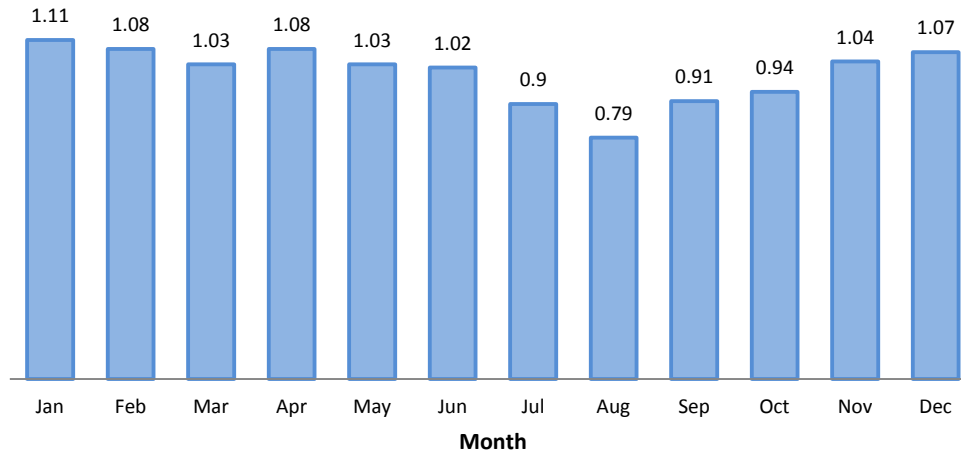


Figure A.21 – DHW monthly multiplication factors.

For this purpose, profiles developed within the scope of the Task 26 of the Solar Heating and Cooling Program of the International Energy Agency (Jordan and Vajen, 2001) were also utilized. These profiles, calculated through the DHWcalc tool (Jordan and Vajen, 2005), are developed with statistical means according to a probability function, so generating sets of load profiles with DHW flow rates during a whole year.

Three kinds of parameter settings must be defined: i) General parameters, ii) Draw-offs parameters and iii) statistical parameters. Main general parameters consist of defining the number of draw-off categories for flow rates, the time-step period (from 1 to 60 min) and the total daily consumption. This way, in combination with daily total consumption reference values set by the CTE for Spanish dwellings, fairly realistic conditions are taken into account, since the one-minute time step allows covering all the transient effects that take place.

Flow-rates associated to each draw-off category, summarized in Table A.18, as well as the maximum flow rate after superposition of the different draw-offs, were set according to IDAE (2010), considering the default draw-off duration for each category.

Table A.18 – Unitary DHW flows associated to the different apparatus.

| Appliance | DHW flow (l/s) |
|---|---|
| Sink | 0.1 |
| Washing machine | 0.15 |
| Dishwasher | 0.1 |
| Bathtub | 0.2 |
| Bath sink | 0.065 |
| Bidet | 0.065 |
| Shower | 0.1 |

Finally, statistical parameters associated to the probability distributions of the DHW during the day, were defined according to the multiplication factors previously defined.

## 2.2. Heating demand

Heating demand of the detached dwelling is obtained of the hourly simulation carried out in TRNSYS, where all the aforementioned information which defines the performance of the housing was introduced.
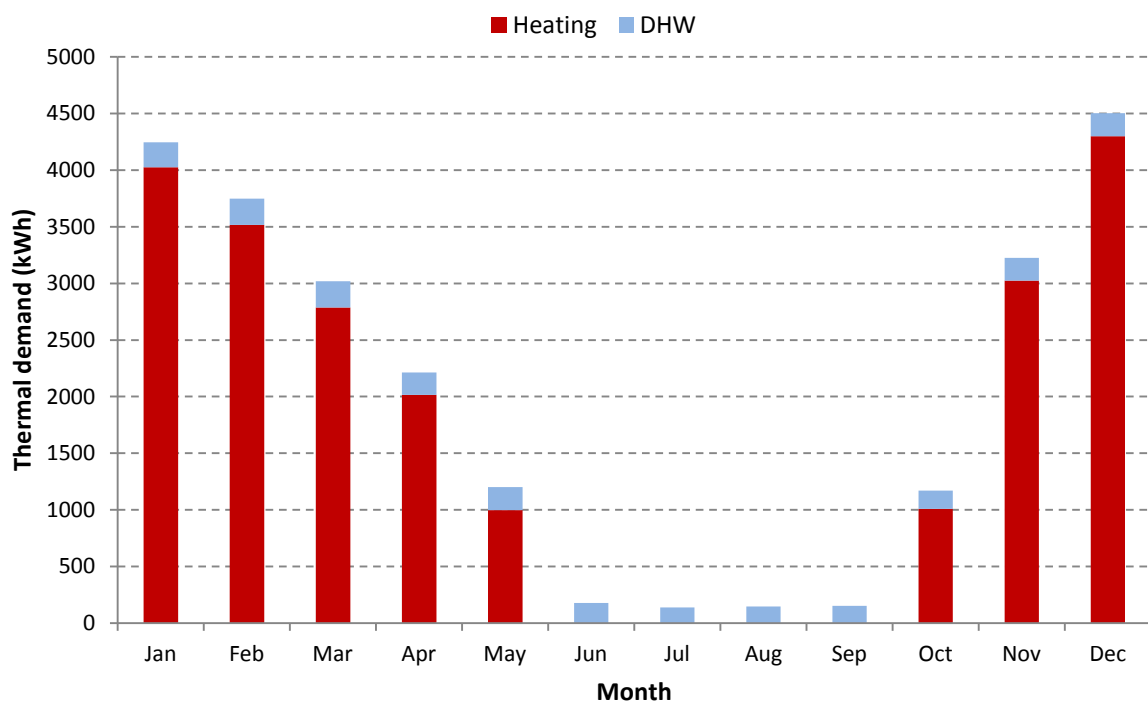


Figure A.22 – Monthly thermal demand.

Additionally, concerning the weather conditions, due to the propinquity of the town where the house is and Vitoria-Gasteiz, as well as the environmental similarities, weather data of this latter geographic position was utilized. To that effect, weather conditions were extracted from the Meteornorm database (Remund and Kunz, 1997).

With all these considerations, the total annual heating demand raises to 25.57 MWh. In Figure A.22 monthly total thermal demand (both including heating and DHW) is depicted. Concerning heating, it can be appreciated that no heating requirements exist from June to September, as established by the CTE. The remaining heating demands are those corresponding to temperature set-points inside the dwelling of 20 °C from 8 a.m. to 11 p.m. and 17 °C for the rest of the day.

# 3. Electricity demand

Two criteria were considered in order to assess the electricity demand of the housing:

i)      Internal Gains Criterion

ii)     Load profiles

### *Internal Gains Criterion*

This criterion given by IDAE considers that all the internal gains, except those related to occupation, are a consequence of electricity consumption, that is, all the electricity consumption is converted into artificial lighting and appliances internal gains afterwards. According to the exposed, the electricity demand profile calculation turns into the following profiles:

Table A.19 – Daily electricity demand of the dwelling (Internal Gains Criterion).

| Schedule | Electricity demand | | |
|---|---|---|---|
| | W/m² | W | Total period kWh |
| 0-7 h | 0.88 | 186.33 | 1.30 |
| 7-15 h | 2.64 | 558.99 | 4.47 |
| 15-23 h | 2.64 | 558.99 | 4.47 |
| 23-24 h | 4.4 | 931.66 | 0.93 |
| | | Daily Total (kWh) | 11.17 |

This calculation criterion leads to a 4080 kWh electricity demand for the whole year, distributed daily as depicted in Figure A.23.
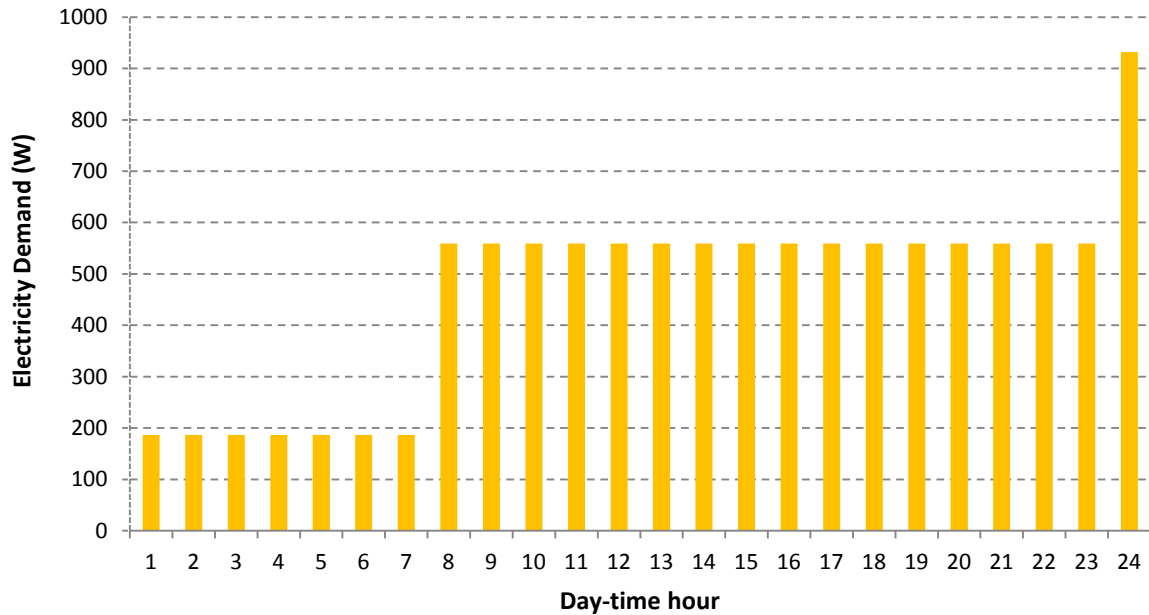


Figure A.23 – Electricity demand daily profile.
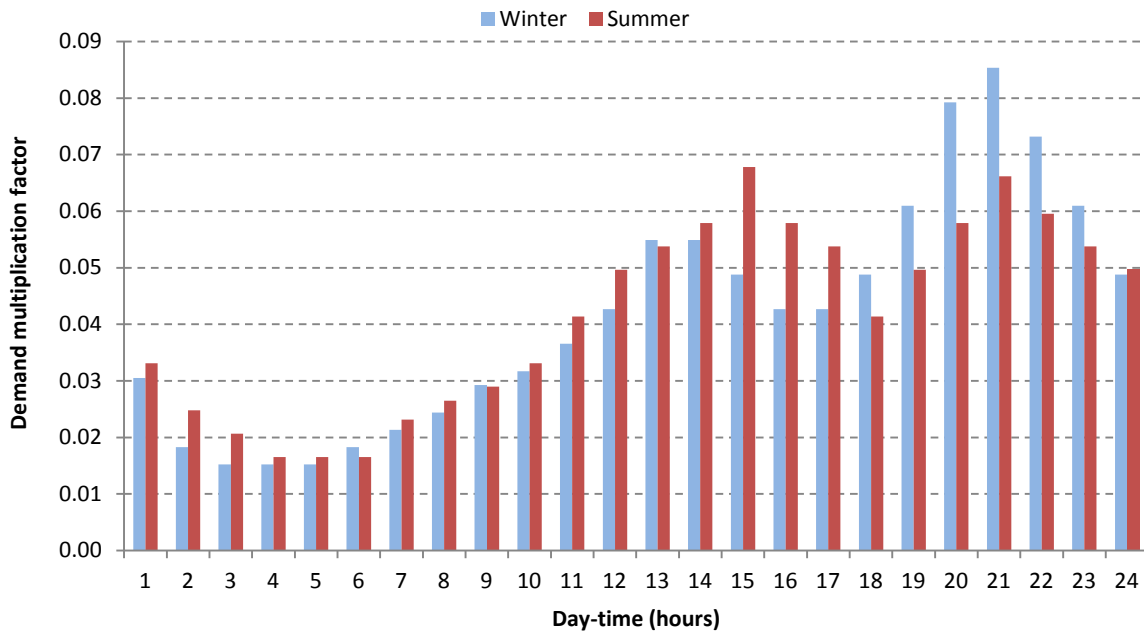


Figure A.24 – Daily electricity multiplication factors: (left) Winter period, (right) Summer period.

## Load profiles Criterion

This criterion establishes the total annual demand of the dwelling according to the SECH-SPAHOUSEC project carried out by IDAE, where an analysis of the electricity consumption of the housing sector in Spain was carried out (IDAE, 2011b). This report determines that the mean electricity demand of a detached dwelling in Spain reaches 4200 kWh.

Daily demand profiles, based on REE data, were obtained from the product of hourly multiplication factors given in the daily profiles (Figure A.24) and monthly consumption values depicted in Figure A.25. As shown in Figure A.24, two daily demand profiles are distinguished: winter-time and summer-time.
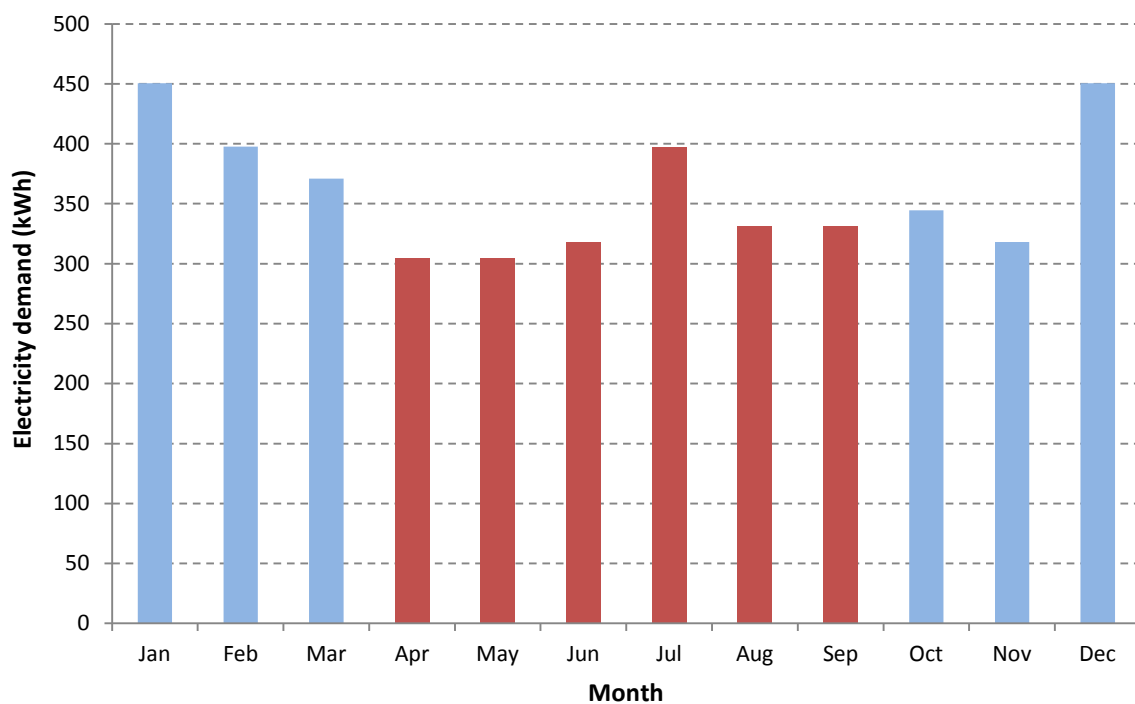


Figure A.25 – Annual profile of electricity demand.

Due to its more realistic hourly distribution, amongst the two criteria presented, for the current work the second one was chosen.

# Appendix E. Commercial solar thermal panels

In this annex a survey of the absorption surfaces of commercially available flat-plate solar collectors in the range between 1 and 2 m² is presented.

Table A.20 – Commercially available surfaces of solar thermal panels.

| Manufacturer | Model | Absorption surface (m²) |
|---|---|---|
| Adisa | Adisol Blue 2.00A | 1.79 |
| | Adisol 2.00P | 1.81 |
| | Adisol 2.30 | 2.00 |
| Ariston | Kairos CF 2.0 | 1.76 |
| Buderus | Logasol CKN 2.0-S | 1.92 |
| Cointra | Icaro 2.0 VF | 1.87 |
| | Icaro 2.3 VF | 1.87 |
| De Dietrich | Inisol DB 200H | 1.88 |
| Domusa | DS Class V3 | 1.89 |
| Fagor | Nature 2.0 | 1.92 |
| | Nature 2.0 S | 1.92 |
| Fercofloor | FC 2.0 | 1.86 |
| | FC 2.2 M | 2.00 |
| | FH 2.2 M | 2.00 |
| Junkers | Classic FCB-2 S | 1.92 |
| | Comfort FCC-2 S | 1.92 |
| Pasanqui | Titanio V1-K | 1.88 |
| | PSS.100.S | 1.89 |
| Roth | Heliostar 218 S4 Steck | 1.95 |
| Salvador Escoda | RKM2001 | 1.85 |
| Wolf | F3-1 | 2.00 |
| | CFK-1 | 2.00 |

# REFERENCES

A. T. D. Perera, M. P. G. Sirimanna, 2014. A novel simulation based evolutionary algorithm to optimize building envelope for energy efficient buildings, In: 7th International Conference on Information and Automation for Sustainability, pp. 1-6.

Abd Alla, G.H., 2002. Computer simulation of a four stroke spark ignition engine. Energy Conversion and Management, 43, 1043-1061.

Alanne, K., Söderholm, N., Sirén, K., Beausoleil-Morrison, I., 2010. Techno-economic assessment and optimization of Stirling engine micro-cogeneration systems in residential buildings. Energy Conversion and Management, 51, 2635-2646.

Álvarez, S., Molina, J.L., 2016. Ventilative cooling issues in Mediterranean regions (the Spanish case). QUALICHECK.

Andlauer, B., 2011. Optimisation systémique de micro-cogénérateurs intégrés au bâtiment.

ASHRAE, 1996. Chapter 7: Cogeneration Systems and Engine and Turbine Drives, in: ASHRAE Handbook: HVAC Systems and Equipment, Atlanta, USA.

Atecyr, 2013. DTIE 18.03: Integración de energías renovables en la rehabilitación energética de los edificios. Asociación Técnica Española de Climatización y Refrigeración.

Babaelahi, M., Sayyaadi, H., 2014. Simple-II: A new numerical thermal model for predicting thermal performance of Stirling engines. Energy, 69, 873-890.

Barbieri, E.S., Melino, F., Morini, M., 2012. Influence of the thermal energy storage on the profitability of micro-CHP systems for residential building applications. Applied Energy, 97, 714-722.

Barbieri, E.S., Spina, P.R., Venturini, M., 2012. Analysis of innovative micro-CHP systems to meet household energy demands. Applied Energy, 97, 723-733.

Baxi, 2010. Baxi Ecogen. http://www.baxi.com, 2014.

Beausoleil-Morrison, I., 2007. Experimental investigation of residential cogeneration devices and calibration of Annex 42 Models. IEA/ECBCS Annex, 42.

Beckman, W.A., Klein, S.A., Duffie, J.A., 1977. Solar heating design, by the f-chart method. NASA STI/Recon Technical Report A, 78.

Bejan, A., 1982. Second-Law Analysis in Heat Transfer and Thermal Design. Advances in Heat Transfer, 15, 1-58.

Bogdan, Ž, Kopjar, D., 2006. Improvement of the cogeneration plant economy by using heat accumulator. Energy, 31, 2285-2292.

Bosch Thermotechnik, 2010. Der Stirling-Motor in der Heizungstechnik. http://www.stromerzeugende-heizung.de, 2017.

Bouvenot, J.-., Andlauer, B., Stabat, P., Marchio, D., Flament, B., Latour, B., et al., 2014. Gas Stirling engine µCHP boiler experimental data driven model for building energy simulation. Energy and Buildings, 84, 117-131.

Bowman, L., 1993. A Technical Introduction to Free-Piston Stirling Cycle Machines: Engines, Coolers, and Heat Pumps. technical papers, Sunpower, Inc.

Bundesministerium für Umwelt, Naturschutz, Bau und Reaktorsicherheit, 2014. Richtlinie zur Förderung von KWK-Anlagen bis 20 kWel (Mini-KWK-Richtlinie).

Bureau International des Poids et Mesures, Commission électrotechnique internationale, Organisation internationale de normalisation, 1995. Guide to the Expression of Uncertainty in Measurement, International Organization for Standardization.

Cacabelos, A., Eguía, P., Míguez, J.L., Rey, G., Arce, M.E., 2014. Development of an improved dynamic model of a Stirling engine and a performance analysis of a cogeneration plant. Applied Thermal Engineering, 73, 608-621.

Campos Celador, A., Erkoreka, A., Martin Escudero, K., Sala, J.M., 2011. Feasibility of small-scale gas engine-based residential cogeneration in Spain. Energy Policy, 39, 3813-3821.

Campos Celador, A., Odriozola, M., Sala, J.M., 2011. Implications of the modelling of stratified hot water storage tanks in the simulation of CHP plants. Energy Conversion and Management, 52, 3018-3026.

Campos-Celador, A., González-Pino, I., Bandos, T., López-González, L.M., 2014. Simulation of a latent heat thermal storage system within a Stirling based microCHP residential installation, In: Proceedings of the 16th International Stirling Engine Conference, Centro Stirling (Ed.), Bilbao, 24-26 September.

Campos-Celador, A., 2012. Integration of latent thermal energy storage systems in the design and operation of cogeneration plants.

Campos-Celador, A., Pérez-Iribarren, E., Sala, J.M., del Portillo-Valdés, L.A., 2012. Thermoeconomic analysis of a micro-CHP installation in a tertiary sector building through dynamic simulation. Energy, 45, 228-236.

Carlsen, H., Fentz, J., 2004. Development of a 9 kW Stirling engine, Vancouver, Canada ed. In: Proc. of International Gas Research Conference (IGRC 2004), 2-4 November.

Carotenuto, A., Giovinco, G., Viglietti, B., Vanoli, L., 2005. A new procedure for the determination of calibration curves for a gas chromatograph used in natural gas analysis. Chemometrics and Intelligent Laboratory Systems, 75, 209-217.

Chen, N.C.J., Griffin, F.P., 1983. A review of Stirling engine mathematical models. Oak Ridge National Laboratory.

Cleanergy, 2014. Stirling CHP systems. www.cleanergy.com, 2014.

COGEN Europe, 2013. Micro-CHP: A cost-effective solution to save energy, reduce GHG emissions and partner with intermitten renewables. http://www.cogeneurope.com/.

Conroy, G., Duffy, A., Ayompe, L.M., 2014. Economic, energy and GHG emissions performance evaluation of a WhisperGen Mk IV Stirling engine μ-CHP unit in a domestic dwelling. Energy Conversion and Management, 81, 465-474.

Conroy, G., Duffy, A., Ayompe, L.M., 2013. Validated dynamic energy model for a Stirling engine μ-CHP unit using field trial data from a domestic dwelling. Energy and Buildings, 62, 18-26.

Costa, S., Tutar, M., Barreno, I., Esnaola, J., Barrutia, H., García, D., et al., 2014. Experimental and numerical flow investigation of Stirling engine regenerator. Energy, 72, 800-812.

CTE, 2013a. Código Técnico de la Edificación, Documento Básico HE Ahorro de Energía, Sección HE1: Limitación de la demanda energética. Ministerio de Fomento, Gobierno de España.

CTE, 2013b. Código Técnico de la Edificación, Documento Básico HE Ahorro de Energía, Sección HE4: Contribución solar mínima de agua caliente sanitaria. Ministerio de Fomento, Gobierno de España.

CTE, 2013c. Código Técnico de la Edificación, Documento Básico HS Salubridad, Sección HS3: Calidad del aire interior. Ministerio de Fomento, Gobierno de España.

Darcovich, K., Entchev, E., 2014. An International Survey of Electrical and DHW Load Profiles for Use in Simulating the Performance of Residential Micro-cogeneration Systems. published by Technische Universität München, Germany, 10.

De Paepe, M., D'Herdt, P., Mertens, D., 2006. Micro-CHP systems for residential applications. Energy Conversion and Management, 47, 3435-3446.

de Wit, J., 2007a. Heat storage for CHP plants. Cogeneration and On-Site Power Production, PennWell Ed., ISSN, 1469-0349.

de Wit, J., 2007b. Heat storages for CHP optimisation, In: Proceedings of the Power Gen Europe.

Dentice d'Accadia, M., Musto, M., 2011. Engineering analysis of uncertainties in the performance evaluation of CHP systems. Applied Energy, 88, 4927-4935.

Departamento de Medio Ambiente, Planificación Territorial y Vivienda, 2018. Laboratorio de Control de Calidad en la Edificación. Gobierno Vasco, http://www.euskadi.eus/lcce, 2017.

Deutscher Bundestag, 2002. Gesetz für die Erhaltung, die Modernisierung und den Ausbau der Kraft-Wärme-Kopplung (Kraft-Wärme-Kopplungsgesetz KWK-G). Bundesgesetzblatt, 1092-1096.

Diarce, G., 2017. Development of new eutectic phase change materials and plate-based latent heat thermal energy storage systems for domestic cogeneration applications.

Dincer, I., Rosen, M., 2002. Thermal energy storage: systems and applications, John Wiley & Sons,.

Dochat, G., 1993. SPDE/SPRE final summary report. SPDE/SPRE Final Summary Report, 187086.

Dorer, V., Weber, A., 2007. Methodologies for the performance assessment of residential cogeneration systems. A Report of Subtask C of FC COGEN-SIM The Simulation of Building-Integrated Fuel Cell and Other Cogeneration Systems. Annex, 42.

EHE, 2008. Whispergen EU1. Efficient Home Energy S.L., 2012.

EPRI, 2002. Stirling Engine Assessment., 1007317.

EU Commission, 2011. Energy Roadmap 2050. COM (2011), 885.

European Commission, 2014. Guide to cost-benefit analysis of investment projects for cohesion policy 2014-2020.

Eurostat, 2012. Statistics Database - Energy statistics - Supply, transformation, consumption.

EVE, 2013. Claves energéticas del sector doméstico en Euskadi. Ente Vasco de la Energía, Departamento de Desarrollo Económico e Infraestructuras, Gobierno Vasco.

Fenercom, 2012. Guía Básica. Microcogeneración. Fundación de la Energía de la Comunidad de Madrid, Consejería de Economía y Hacienda, Comunidad de Madrid.

Feng, X., Cai, Y., Qian, L., 1998. A new performance criterion for cogeneration system. Energy Conversion and Management, 39, 1607-1609.

Fernández, M., Eguía, P., Granada, E., Febrero, L., 2017. Sensitivity analysis of a vertical geothermal heat exchanger dynamic simulation: Calibration and error determination. Geothermics, 70, 249-259.

Fragaki, A., Andersen, A.N., Toke, D., 2008. Exploration of economical sizing of gas engine and thermal store for combined heat and power plants in the UK. Energy, 33, 1659-1670.

Gustafsson, S., Karlsson, B.G., 1992. Heat accumulators in CHP networks. Energy Conversion and Management, 33, 1051-1061.

Gutschker, O., 2008. Parameter identification with the software package LORD. Building and Environment, 43, 163-169.

Haeseldonckx, D., Peeters, L., Helsen, L., D'haeseleer, W., 2007. The impact of thermal storage on the operational behaviour of residential CHP facilities and the overall CO2 emissions. Renewable and Sustainable Energy Reviews, 11, 1227-1243.

Harrison, J., 2013. micro combined heat & power: Stirling engine; http://www.microchap.info/, 2014.

Harrison, J., E.ON, 2011. 8 - Stirling engine systems for small and micro combined heat and power (CHP) applications, in: Small and Micro Combined Heat and Power (CHP) Systems, Beith, R. (Ed.), Woodhead Publishing, pp. 179-205.

Hawkes, A., 2013. Comparative review of policy support mechanism for microgeneration: Proceedings of the 3rd edition of the International Conference on Microgeneration and Related Technologies, 15—17 April, 2013. Naples, Italy.

Hawkes, A., Brandoni, C., Tzscheutschler, P., 2014. A comparative review of microgeneration policy instruments in OECD countries.

Hawkes, A.D., 2011. 2 - Techno-economic assessment of small and micro combined heat and power (CHP) systems, in: Small and Micro Combined Heat and Power (CHP) Systems, Beith, R. (Ed.), Woodhead Publishing, pp. 17-41.

Hendron, B., Burch, J., Barker, G., 2010. Tool for generating realistic residential hot water event schedules. IBPSA-USA Journal, 4, 328-335.

Heywood, J.B., 1998. Internal Combustion Engine Fundamentals, McGraw-Hill, inc., New York, USA.

Horlock, J., 1997. Cogeneration-Combined Heat and Power (CHP): Thermodynamics and Economics. Malabar, FL: Krieger Publishing.

Ibáñez, A.S., Linares, J.I., Cledera, M.M., Moratilla, B.Y., 2014. Sizing of thermal energy storage devices for micro-cogeneration systems for the supply of domestic hot water. Sustainable Energy Technologies and Assessments, 5, 37-43.

IDAE, 2017. Boletín de Estadísticas Energéticas de la Cogeneración para el año 2015. Instituto para la Diversificación y Ahorro de la Energía, Ministerio de Industria, Turismo y Comercio, Gobierno de España.

IDAE, 2016. Factores de emisión de CO2 y coeficientes de paso a energía primaria de diferentes fuentes de energía final consumidas en el sector de edificios de España. Instituto para la Diversificación y Ahorro de la Energía, Ministerio de Industria, Energía y Turismo, Gobierno de España.

IDAE, 2014. Guía de elegibilidad de proyectos con cargo al fondo JESSICA F.I.D.A.E. Instituto para la Diversificación y Ahorro de la Energía, Ministerio de Industria, Turismo y Comercio, Gobierno de España.

IDAE, 2011a. Evaluación del potencial de climatización con energía solar térmica en edificios. Estudio técnico PER 2011-2020. Instituto para la Diversificación y Ahorro de la Energía, Ministerio de Industria, Turismo y Comercio, Gobierno de España.

IDAE, 2011b. Proyecto Sech-Spahousec: Análisis del consumo energético del sector residencial en España. Informe Final. Instituto para la Diversificación y Ahorro de la Energía, Ministerio de Industria, Turismo y Comercio, Gobierno de España.

IDAE, 2010. Guía técnica de agua caliente sanitaria central. Instituto para la Diversificación y Ahorro de la Energía, Ministerio de Industria, Turismo y Comercio, Gobierno de España.

IDAE, 2009. Condiciones de aceptación de procedimientos alternativos a Lider y Calener. Anexos. Instituto para la Diversificación y Ahorro de la Energía, Ministerio de Industria, Turismo y Comercio, Gobierno de España.

IDAE, 2005. Análisis del potencial de cogeneración de alta eficiencia en España 2010-2015-2020. Instituto para la Diversificación y Ahorro de la Energía, Ministerio de Industria, Turismo y Comercio, Gobierno de España.

INE, 2011. Censo de población y viviendas 2011. Instituto Nacional de Estadística, http://www.ine.es/, 2015.

Inspirit Energy, 2016. The Inspirit Charger. http://www.inspirit-energy.com/, 2017.

Jefatura del Estado, 2013a. Ley 24/2013, de 26 de diciembre, del Sector Eléctrico. BOE n. 310.

Jefatura del Estado, 2013b. Real Decreto-ley 2/2013, de 1 de febrero, de medidas urgentes en el sistema eléctrico y en el sector financiero. BOE n. 29.

Jefatura del Estado, 2013c. Real Decreto-ley 9/2013, de 12 de julio, por el que se adoptan medidas urgentes para garantizar la estabilidad financiera del sistema eléctrico. BOE n. 167.

Jefatura del Estado, 2012a. Ley 15/2012, de 27 de diciembre, de medidas fiscales para la sostenibilidad energética. BOE n. 312.

Jefatura del Estado, 2012b. Real Decreto-ley 1/2012, de 27 de enero, por el que se procede a la suspensión de los procedimientos de preasignación de retribución y a la supresión de los incentivos económicos para nuevas instalaciones de producción de energía eléctrica a partir de cogeneración, fuentes de energía renovable y residuos. BOE n. 24.

Jefatura del Estado, 2000. Real Decreto-ley 6/2000, de 23 de junio, de Medidas Urgentes de Intensificación de la Competencia en Mercados de Bienes y Servicios. BOE n. 151.

Jefatura del Estado, 1997. Ley 54/1997, de 27 de noviembre, del Sector Eléctrico. BOE n. 285.

Jefatura del Estado, 1994. Ley 40/1994, de 30 de diciembre, de ordenación del Sistema Eléctrico Nacional. BOE n. 313.

Jefatura del Estado, 1981. Ley 82/1980, de 30 de diciembre, sobre conservación de energía. BOE n. 23.

Jordan, U., Vajen, K., 2005. DHWcalc: Program to generate domestic hot water profiles with statistical means for user defined conditions, In: ISES Solar World Congress, pp. 1-6.

Jordan, U., Vajen, K., 2001. Realistic domestic hot-water profiles in different time scales.

Katulić, S., Čehil, M., Bogdan, Ž, 2014. A novel method for finding the optimal heat storage tank capacity for a cogeneration power plant. Applied Thermal Engineering, 65, 530-538.

Kawajiri, K., Fujiwara, M., Suganami, T., 1989. Analysis of Stirling engine performance, In: Energy Conversion Engineering Conference, 1989. IECEC-89., Proceedings of the 24th Intersociety, pp. 2341-2346 vol.5.

Kelly N., B., I., 2007. Specifications for modelling fuel cell and combustion-based residential cogeneration devices within whole-building simulation programs. IEA/ECBCS Annex 42.

Kelly, N.J., 1998. Towards a design environment for building-integrated energy systems: the integration of electrical power flow modelling with building simulation.

Khan, K., Rasul, M., Khan, M.M.K., 2004. Energy conservation in buildings: cogeneration and cogeneration coupled with thermal energy storage. Applied Energy, 77, 15-34.

Klein, S., 2012. TRNSYS 17-a TRaNsient SYstem Simulation program, Volume 4 - Mathematical Reference.

Klein, S.A., Alvarado, F., 1992. EES: Engineering equation solver for the Microsoft Windows operating system, F-Chart Software.

Klein, S.A., Beckman, W., Duffie, J., 1976. A design procedure for solar heating systems. Solar Energy, 18, 113-127.

Kongtragool, B., Wongwises, S., 2006. Thermodynamic analysis of a Stirling engine including dead volumes of hot space, cold space and regenerator. Renewable Energy, 31, 345-359.

Kongtragool, B., Wongwises, S., 2003. A review of solar-powered Stirling engines and low temperature differential Stirling engines. Renewable and Sustainable Energy Reviews, 7, 131-154.

Kuhn, V., Klemeš, J., Bulatov, I., 2008. MicroCHP: Overview of selected technologies, products and field test results. Applied Thermal Engineering, 28, 2039-2048.

Lipp, J., 2013. Field test with Stirling engine micro-combined heat and power units in residential buildings. Proceedings of the Institution of Mechanical Engineers, Part A: Journal of Power and Energy, 227, 43-52.

Lombardi, K., Ugursal, V.I., Beausoleil-Morrison, I., 2010. Proposed improvements to a model for characterizing the electrical and thermal energy performance of Stirling engine micro-cogeneration devices based upon experimental observations. Applied Energy, 87, 3271-3282.

Lozano, M.A., Ramos, J.C., Serra, L.M., 2010. Cost optimization of the design of CHCP (combined heat, cooling and power) systems under legal constraints. Energy, 35, 794-805.

Lund, H., Hvelplund, F., Østergaard, P.A., Möller, B., Mathiesen, B.V., Karnøe, P., et al., 2013. System and market integration of wind power in Denmark. Energy Strategy Reviews, 1, 143-156.

Machairas, V., Tsangrassoulis, A., Axarli, K., 2014. Algorithms for optimization of building design: A review. Renewable and Sustainable Energy Reviews, 31, 101-112.

Magri, G., Di Perna, C., Serenelli, G., 2012. Analysis of electric and thermal seasonal performances of a residential microCHP unit. Applied Thermal Engineering, 36, 193-201.

McBride, B.J., Gordon, S., Reno, M.A., 1993. Coefficients for calculating thermodynamic and transport properties of individual species.

McCrorie, K.A.B., Underwood, W.B., le Feuvre, R.F., 1996. Small-scale combined heat and power simulations: development of a dynamic spark-ignition engine model. Building Services Engineering Research and Technology, 17, 153-159.

Microgen Engine Corporation, 2015. http://www.microgen-engine.com/, 2015.

Mikalsen, R., 2011. 6 - Internal combustion and reciprocating engine systems for small and micro combined heat and power (CHP) applications, in: Small and Micro Combined Heat and Power (CHP) Systems, Beith, R. (Ed.), Woodhead Publishing, pp. 125-146.

Ministerio de Economía, 2004. Real Decreto 436/2004, de 12 de marzo, por el que se establece la metodología para la actualización y sistematización del régimen jurídico y económico de la actividad de producción de energía eléctrica en régimen especial. BOE n. 75.

Ministerio de Economía, 2002. Real Decreto 841/2002, de 2 de agosto, por el que se regula para las instalaciones de producción de energía eléctrica en régimen especial su incentivación en la participación en el mercado de producción, determinadas obligaciones de información de sus previsiones de producción, y la adquisición por los comercializadores de su energía eléctrica producida. BOE n. 210.

Ministerio de Industria y Energía, 1998. Real Decreto 2818/1998, de 23 de diciembre, sobre producción de energía eléctrica por instalaciones abastecidas por recursos o fuentes de energía renovables, residuos y cogeneración . BOE núm. 312.

Ministerio de Industria y Energía, 1994. Real Decreto 2366/1994, de 9 de diciembre, sobre producción de energía eléctrica por instalaciones hidráulicas, de cogeneración y otras abastecidas por recursos o fuentes de energía renovables . BOE núm. 313.

Ministerio de Industria y Energía, 1982. Real Decreto 907/1982, de 2 de abril, sobre fomento de la autogeneración de energía eléctrica. BOE núm. 111.

Ministerio de Industria, Energía y Turismo, 2016. Real Decreto 56/2016, de 12 de febrero, por el que se transpone la Directiva 2012/27/UE del Parlamento Europeo y del Consejo, de 25 de octubre de 2012, relativa a la eficiencia energética, en lo referente a auditorías energéticas, acreditación de proveedores de servicios y auditores energéticos y promoción del suministro de energía. BOE núm. 38.

Ministerio de Industria, Energía y Turismo, 2015. Orden IET/1345/2015, de 2 de julio, por la que se establece la metodología de actualización de la retribución a la operación de las instalaciones con régimen retributivo específico. BOE n. 161.

Ministerio de Industria, Energía y Turismo, 2014a. Orden IET/1045/2014, de 16 de junio, por la que se aprueban los parámetros retributivos de las instalaciones tipo aplicables a determinadas instalaciones de producción de energía eléctrica a partir de fuentes de energía renovables, cogeneración y residuos. BOE n. 150.

Ministerio de Industria, Energía y Turismo, 2014b. Real Decreto 216/2014, de 28 de marzo, por el que se establece la metodología de cálculo de los precios voluntarios para el pequeño consumidor de energía eléctrica y su régimen jurídico de contratación. BOE núm. 77.

Ministerio de Industria, Energía y Turismo, 2014c. Real Decreto 413/2014, de 6 de junio, por el que se regula la actividad de producción de energía eléctrica a partir de fuentes de energía renovables, cogeneración y residuos. BOE n. 140.

Ministerio de Industria, Energía y Turismo, 2014d. Resolución de 28 de enero de 2014, de la Dirección General de Política Energética y Minas, por la que se corrigen errores en la de 26 de diciembrede 2013, por la que se publica la tarifa de último recurso de gas natural. BOE n. 26.

Ministerio de Industria, Energía y Turismo, 2014e. Resolución de 31 de enero de 2014, de la Dirección General de Política Energética y Minas, por la que se revisa el coste de producción de energía eléctrica y los precios voluntarios para el pequeño consumidor. BOE n. 28.

Ministerio de Industria, Turismo y Comercio, 2009a. Orden ITC/1659/2009, de 22 de junio, por la que se establece el mecanismo de traspaso de clientes del mercado a tarifa al suministro de último recurso de energía eléctrica y el procedimiento de cálculo y estructura de las tarifas de último recurso de energía eléctrica. BOE n. 151.

Ministerio de Industria, Turismo y Comercio, 2009b. Orden ITC/1660/2009, de 22 de junio, por la que se establece la metodología de cálculo de la tarifa de último recurso de gas natural. BOE n. 151.

Ministerio de Industria, Turismo y Comercio, 2007. Real Decreto 661/2007, de 25 de mayo, por el que se regula la actividad de producción de energía eléctrica en régimen especial. BOE núm. 126.

Ministerio de Sanidad y Consumo, 2003. Real Decreto 865/2003, de 4 de julio, por el que se establecen los criterios higiénico-sanitarios para la prevención y control de la legionelosis. BOE n. 171.

Mongibello, L., Capezzuto, M., Graditi, G., 2013. Technical and cost analyses of two different heat storage systems for residential micro-CHP plants. Applied Thermal Engineering, 71, 636-642.

Official Journal of the European Communities, 2002. DIRECTIVE 2002/91/EC of the European Parliament and of the Council of 16 December 2002 on the energy performance of buildings.

Official Journal of the European Union, 2012. DIRECTIVE 2012/27/UE of the European Parliament and of the Council of 25 October 2012 on the energy efficiency, amending Directives 2009/125/EC and 2010/30/EU and repealing Directives 2004/8/EC and 2006/32/EC.

Official Journal of the European Union, 2010. DIRECTIVE 2010/31/UE of the European Parliament and of the Council of 19 May 2010 on the energy performance of buildings .

Official Journal of the European Union, 2004. DIRECTIVE 2004/8/EC of the European Parliament and of the Council of 11 February 2004 on the promotion of cogeneration based on a useful heat demand in the internal energy market and amending Directive 92/42/EEC.

ÖkoFEN International, 2015. Microgen Stirling Engine. http://www.okofen-e.com/en/engine/, 2017.

Organ, A.J., 1987. Thermodynamic Design of Stirling Cycle Machines. Proceedings of the Institution of Mechanical Engineers, Part C: Journal of Mechanical Engineering Science, 201, 107-116.

Peacock, A.D., Newborough, M., 2005. Impact of micro-CHP systems on domestic sector CO2 emissions. Applied Thermal Engineering, 25, 2653-2676.

Pearce, J.M., Al Zahawi, B.A.T., Auckland, D.W., Starr, F., 1996. Electricity generation in the home: evaluation of single-house domestic combined heat and power. Science, Measurement and Technology, IEE Proceedings, 143, 345-350.

Pearce, J.M., Al Zahawi, B.A.T., Shuttleworth, R., 2001. Electricity generation in the home: modelling of single-house domestic combined heat and power. Science, Measurement and Technology, IEE Proceedings, 148, 197-203.

Pehnt, M., 2006. Micro cogeneration technology, in: Micro Cogeneration, Springer, pp. 1-18.

Pérez-Iribarren, E., Campos-Celador, A., Sala Lizarraga, J.M., del Portillo Valdés, L.A., 2011. Exergoenvironmental analysis of a residential micro-CHP installation, In: Proceedings of the 2nd International Conference on Microgeneration and Related Technologies (MICROGEN II), Glasgow, Scotland, UK, pp. e6.

Pérez-Iribarren, E., 2016. Optimización en la operación y el diseño de plantas de microcogeneración para edificios de viviendas.

Petchers, N., 2003. Combined heating, cooling & power handbook: Technologies & applications: An integrated approach to energy resource optimization, Lilburn, GA: The Fairmont Press.

Pfannstiel, D., 2010. Der Stirling-Motor gibt Gas! HLH, 61, 40-44.

Qiu, G., Liu, H., Riffat, S., 2011. Expanders for micro-CHP systems with organic Rankine cycle. Applied Thermal Engineering, 31, 3301-3307.

Qnergy, 2013. http://www.qnergy.com/, 2014.

Qvale, E.B., Smith, J.L., 1968. A mathematical model for steady operation of Stirling-type engines.

E. B. Qvale and J. L. Smith, Jr. , "A Mathematical Model for Steady Operation of Stirling-Type Engines", Transactions of ASME, J. of Engineering for Power, pp. 45-50, January 1968. Journal of Engineering for Power - Transactions of ASME, 45-50.

REE, 2010. Guía de consumo inteligente. Red Eléctrica de España. http://www.ree.es, 2013.

Remeha, 2010. Micro-CHP. http://www.remeha.com/, 2016.

Remund, J., Kunz, S., 1997. METEONORM: Global meteorological database for solar energy and applied climatology, Meteotest.

Ren, H., Gao, W., 2010. Economic and environmental evaluation of micro CHP systems with different operating modes for residential buildings in Japan. Energy and Buildings, 42, 853-861.

Rogdakis, E.D., Antonakos, G.D., Koronaki, I.P., 2012. Thermodynamic analysis and experimental investigation of a Solo V161 Stirling cogeneration unit. Energy, 45, 503-511.

Roncato, J., Macchi, E., 2000. 'Report of Study Group 7.2: Comparison of Medium or Large Scale CHP and Combined Cycles, in Various Countries, In: Woc7 Report, Proc. of World Gas Conference, pp. 55-82.

Rosato, A., Sibilio, S., 2013. Energy performance of a micro-cogeneration device during transient and steady-state operation: experiments and simulations. Applied Thermal Engineering, 52, 478-491.

Rosato, A., Sibilio, S., Ciampi, G., 2013. Energy, environmental and economic dynamic performance assessment of different micro-cogeneration systems in a residential application. Applied Thermal Engineering, 59, 599-617.

Roselli, C., Sasso, M., Sibilio, S., Tzscheutschler, P., 2011. Experimental analysis of microcogenerators based on different prime movers. Energy and Buildings, 43, 796-804.

Sala, J.M., 2015. 20 - Thermal energy storage (TES) systems for cogeneration and trigeneration systems, in: Advances in Thermal Energy Storage Systems, Cabeza, L.F. (Ed.), Woodhead Publishing, pp. 493-509.

Sasso, M., Angrisani, G., Roselli, C., 2014. Methodologies for the Performance Assessment of Micro Hybrid Polygeneration Systems. published by Technische Universität München, Germany, 10, 3-3.

SAVE, E., 2002. Micro-Map: Mini and Micro CHP-Market Assessment and Development Plan: Summary Report. London, UK.

Schulz, S., Schwendig, F., 1996. A General Simulation Model for Stirling Cycles. Journal of Engineering for Gas Turbines and Power, 118, 1-7.

Sedigas, 2012. Soluciones tecnológicas eficientes que utilizan combustibles gaseosos. In: Contribución del gas para una edificación sostenible, 4 December, 2012. Vitoria - Gasteiz, Spain.

Senft JR., 1993. Ringbom Stirling engines, Oxford University Press, New York.

Six, D., Vekemans, G., Dexters, A., 2009. Market opportunities for micro-CHP in Flanders (Belgium), In: Energy Market, 2009. EEM 2009. 6th International Conference on the European, IEEE, pp. 1-6.

Soares, C., 2007. Microturbines: Applications for Distributed Energy Systems, Elsevier Inc.

Sousa, J., 2012. Energy simulation software for buildings: review and comparison, In: International Workshop on Information Technology for Energy Applicatons-IT4Energy, Lisabon.

Stirling Robert, 1816. Stirling air engine and the heat regenerator.

Streckienė, G., Martinaitis, V., Andersen, A.N., Katz, J., 2009. Feasibility of CHP-plants with thermal stores in the German spot market. Applied Energy, 86, 2308-2316.

Sunmachine, 2009. Wood Pellet Stirling CHP. http://www.sunmachine.com/, 2009.

Terés-Zubiaga, J., Campos-Celador, A., González-Pino, I., Diarce, G., 2016. The role of the design and operation of individual heating systems for the energy retrofits of residential buildings. Energy Conversion and Management, 126, 736-747.

TeymouriHamzehkolaei, F., Sattari, S., 2011. Technical and economic feasibility study of using Micro CHP in the different climate zones of Iran. Energy, 36, 4790-4798.

Thiers, S., Aoun, B., Peuportier, B., 2010. Experimental characterization, modeling and simulation of a wood pellet micro-combined heat and power unit used as a heat source for a residential building. Energy and Buildings, 42, 896-903.

Thomas, B., 2008. Benchmark testing of Micro-CHP units. Applied Thermal Engineering, 28, 2049-2054.

Thomas, B., 2014. Experimental determination of efficiency factors for different Micro-CHP units according to the standard DIN 4709. Applied Thermal Engineering, 71, 721-728.

Thombare, D.G., Verma, S.K., 2008. Technological development in the Stirling cycle engines. Renewable and Sustainable Energy Reviews, 12, 1-38.

Thombarse, D.G., 2008. Stirling Engine: Micro-CHP System for Residential Application, in: Encyclopedia of Materials: Science and Technology (Second Edition), Buschow, K.H.J.,

Cahn, R.W., Flemings, M.C., Ilschner, B., Kramer, E.J., Mahajan, S., et al (Eds.), Elsevier, Oxford, pp. 1-8.

Ulloa, C., Míguez, J.L., Porteiro, J., Eguía, P., Cacabelos, A., 2013a. Development of a transient model of a stirling-based CHP system. Energies, 6, 3115-3133.

Ulloa, C., Porteiro, J., Eguía, P., Pousada-Carballo, J.M., 2013b. Application model for a stirling engine micro-generation system in caravans in different European locations. Energies, 6, 717-732.

Ulloa, C., Eguía, P., Miguez, J.L., Porteiro, J., Pousada-Carballo, J.M., Cacabelos, A., 2013c. Feasibility of using a Stirling engine-based micro-CHP to provide heat and electricity to a recreational sailing boat in different European ports. Applied Thermal Engineering, 59, 414-424.

University of Illinois, University of California, 2013. Energy Plus. Getting started.

Urieli, I., Berchowitz, D., 1984. Stirling cycle engine analysis, Adam Hilger Ltd., Bristol, UK.

Valenti, G., Silva, P., Fergnani, N., Di Marcoberardino, G., Campanari, S., Macchi, E., 2014. Experimental and Numerical Study of a Micro-cogeneration Stirling Engine for Residential Applications. Energy Procedia, 45, 1235-1244.

Van Bael, J., Six, D., Vanhoudt, D., Desmedt, J., 2011. Feasibility and potential of micro combined heat and power in Flanders, In: Proceedings of the 2nd International Conference on Microgeneration and Related Technologies (MICROGEN II), Glasgow, UK, 4-6 April 2011,.

Verda, V., Colella, F., 2011. Primary energy savings through thermal storage in district heating networks. Energy, 36, 4278-4286.

Viessmann, 2011. Vitotwin 300-W. http://www.viessmann.com, 2015.

Voorspools, K.R., D'haeseleer, W.D., 2006. Reinventing hot water? Applied Thermal Engineering, 26, 1972-1981.

Walker G., 1980. Stirling engines, Clarendon Press, Oxford.

West CD., 1988. A historical perspective on Stirling engine performance, American Society of Mechanical Engineers, Denver,.